The Dissertation Committee for Wipawee Dechapanya Certifies that this is the approved version of the following dissertation:

Kinetic and Physic Models of Secondary Organic Aerosol Formation and their Application to Houston Conditions

Committee:

David T. Allen

David T. Allen, Supervisor

Gary Rochelle

Gary Rochelle

Charles Mullins

Charles Mullins

Richard C.

Richard Corsi

Elena McDonald-Buller

Elena McDonold Buller

Kinetic and Physic Models of Secondary Organic Aerosol Formation and their Application to Houston Conditions

by

Wipawee Dechapanya, M.S.

Dissertation

Presented to the Faculty of the Graduate School of

the University of Texas at Austin

in Partial Fulfillment

of the Requirements

for the Degree of

Doctor of Philosophy

The University of Texas at Austin

December 2002

I would like to dedicate this dissertation to Raweewan Dechapanya, my mother.

ACKNOWLEDGMENTS

I would like to thank my advisor, Prof. David T Allen, for his support, guidance and patience throughout this research project. I also would like to thank my committee: Dr Elena McDonald Buller and Dr. Richard Corsi of the Department of Civil and Environmental Engineering, and Dr. Gary Rochelle and Dr. Buddy Mullins of the Department of Chemical Engineering, for their continued support and advice. Thanks also to Dr. Alexandra Eusebi for assisting me the guidance, knowledge, and mental support.

A very special thank to Dr. Yosuke Kimura, this work would not have been done without his help and patience. I also would like to thank my friends at center for energy and environmental resources (CEER).

I am deeply indebted to the Royal Thai Government who provides me with the financial support throughout my studies in the United States.

I would like to express my gratitude to my mother; Raweewan, my sister; Wipada, my cats; Nu-Meaw and especially Midas, and all my friends in Thailand for their love and greatest support. Finally, a very special thank you to my dearest husband, Attaso Khamwichit, for his continued encouragement, support, and love.

Kinetic and Physic Models of Secondary Organic Aerosol Formation and their Application to Houston Conditions

Publication No._____

Wipawee Dechapanya, Ph.D.

The University of Texas at Austin, 2002

Supervisor: David T Allen

Atmospheric reactions of volatile organic compounds can produce low volatility species that condense onto atmospheric particles (secondary organic aerosol), and these particles have significant impact on public health. This work develops quantitative kinetic and physical phase partitioning models of secondary organic aerosol (SOA) formation. These mechanisms were integrated into a state of the art mechanism for gas phase reactions (SAPRC). Using the resulting model, a series of sensitivity analyses were performed. Analyses of the sensitivity of SOA formation to several parameters (e.g., VOC/NOx ratio, rate parameters) were performed. Results indicated that aerosol yield (SOA formed per amount of hydrocarbons reacted) depends on the extent of conversion of parent hydrocarbons, partitioning coefficient (*Kom*), initial aerosol mass concentration (M_{int}), and rate

parameters. Based on the sensitivity studies, empirical models for SOA yield were developed for both individual and lumped hydrocarbon species.

The models were used to examine a number of case studies relevant to the formation of SOA in Houston. In general, the analyses indicated that strategies effective in reducing ozone concentrations will also be effective in reducing SOA. Emission reductions that reduce ozone mixing ratios by O.1 ppm reduces SOA concentration by approximately 2.5 $\mu g/m^3$.

The models developed in this study are effective prognostic tools for analyzing SOA production under a variety of conditions, and these models can be readily implemented into 3D air quality models, and modified easily if more experimental data on SOA formation become available.

Table of Contents

List of Tables

List of Figures

Chapter 1 Introduction

1.1Background and Motivation

New National Ambient Air Quality Standards (NAAQS) for fine airborne particles smaller than 2.5 μm, were issued in July 1997 by the administrator of the U.S. Environmental Protection Agency (EPA). This legislation was brought about due to recent epidemiological evidence that indicates a strong relationship between elevated concentrations of fine particulate matter and increased mortality (Schwartz, 1996). Studies from EPA (1999) indicate that approximately 76 million people (29% of the total U.S. population) lived in areas in 1996 where long term ambient $PM_{2.5}$ levels were predicted to be at or above 16 $\mu g/m^3$, the low end of the range of long term average $PM_{2.5}$ concentrations which may cause serious health effects. Reducing $PM_{2.5}$ concentrations to meet the new standards is likely to require substantial reductions in emissions leading to fine particulate matter, and therefore a thorough understanding of fine particulate matter sources has become necessary.

Airborne particulate matter may be liquid or solid and can contain acids, salts, heavy metals, organics, and biological or biogenic material. Sources of ambient particles that are emitted directly to the atmosphere include forest fires, wind erosion, agricultural activities, fossil fuel combustion, industrial manufacturing, and construction of buildings and roads. These particles emitted directly into atmosphere

are referred to as "primary" particulate matter. In contrast, some particulate matter is formed as a result of reactions that occur in the atmosphere, and are referred to as "secondary" particulate matter. This secondary particulate matter includes sulfate produced by the reactions of SO_2 emissions, nitrates produced as a result of the reactions of NOx, and low volatility organics produced as a result of the reactions of hydrocarbons.

Ambient particulate matter is made up of both inorganic and organic, primary and secondary particles. The chemical and physical compositions of ambient particulate matter vary depending on geographical location, time of year, and weather. While the sources and formation pathways for inorganic aerosols are reasonably well known, very little is understood concerning the sources and chemistry of secondary organic aerosol (SOA). Previous investigators (e.g., Seinfeld 1992) presented several approaches to understanding the compositions and sources of particulate matter, yet it is not entirely clear what fraction of atmospheric organic aerosol is secondary, and more detailed studies are required to investigate their sources.

Currently the most commonly employed methodology for estimating SOA formation is to assume that gas phase hydrocarbons react, in the gas phase, to form products that condense into the particle phase. The selectivity of gas phase reactions to SOA is assumed to be constant, and fixed fractional aerosol coefficients (FACs), which were developed based on smog chamber experiments and expert judgment, are employed (Grosjean and Seinfeld, 1989). The concept of incremental ozone

reactivities (described in more detail in Chapter 2), which reveal that different hydrocarbons lead to different rates of ozone production in the atmosphere, suggests that FAC will not be constant, and that FAC will be a function of the concentrations of hydrocarbons, concentrations of NOx, and other parameters.

This study extends the concept of incremental ozone reactivities to PM formation. Quantitative mechanistic models of SOA formation were developed based on data from smog chamber experiments. The sensitivity of SOA formation to changes of NOx, changes in the mixture of hydrocarbon precursors, and other parameters were investigated. This work will be one of the first attempts to quantitatively model SOA formation using data from chamber experiments, and one of the first attempts to incorporate chemical mechanisms of SOA formation into a comprehensive gas phase photochemical model.

1.2 Research objective

The overall objectives of this study were to develop quantitative models of SOA formation, and to use these models to characterize SOA formation in Houston. The specific objectives were to:

- Use data available from previous chamber experiments to develop quantitative photochemical mechanistic models for individual and lumped aromatic hydrocarbons.

- Use a phase partitioning model from the literature to estimate the partitioning of individual compounds and lumped species between gas and aerosol phases.
- Incorporate chemical and physical models into a detailed gas phase photochemical mechanism developed by the Statewide Air Pollution Research Center (SAPRC).
- Apply the modified SAPRC mechanisms to characterize the pathways important for SOA formation in Houston, and to investigate the sensitivity of SOA formation in Houston to changes in NOx concentrations, and other parameters.

1.3 Dissertation overview

This dissertation discusses the development of quantitative mechanistic models of SOA, for individual and lumped species, and application of these models to characterize SOA formation in Houston. A literature review is provided in Chapter 2. Chapter 3 discusses the methodology and procedure used to develop quantitative photochemical mechanistic models for individual aromatic hydrocarbons. This chapter also includes the procedure and methodology employed to describe partitioning between gas and particle phases. Chapter 4 discusses lumping procedures and development of chemical models and partitioning models for lumped aromatic species. Chapter 5 addresses application of models developed in Chapter 4

to Houston conditions, and describes the sensitivity of SOA formation to the changes of NOx emissions and other parameters. Summaries and conclusions are presented in chapter 6.

Chapter 2 Literature Review

2.1 Organic Particulate Matter

Atmospheric aerosols have significant impacts on our health and quality of life. While many studies have focused on role of inorganic species in atmospheric aerosol, new interest has been given to the organic portion. The organic component of PM is hypothesized to cause adverse health effects (Schwartz, 1996), and organics may be particularly important because approximately 95% of organics present in urban aerosols are found in particles with diameters less than 3 microns, which can be deposited deeply into the human respiratory system (Isidorov, 1990). Because of their optical characteristics, organic aerosols also are a major cause of reductions in visibility (EPA, 1997). In addition, as will be demonstrated in this thesis, SOA formation is associated with the photochemical reactions leading to ozone production. Further, deposition of particles containing organic acid species may change the nutrient balance and acidity of land, plant, or water bodies. Finally, organic PM may change the chemical, optical, and hygroscopic behavior of inorganic aerosols (Saxena et al., 1995).

Legislation has been placed in effect to reduce the amount of fine particles that are emitted directly into atmosphere, and control the emissions of gases that are precursors of condensable gases that lead to PM formation (secondary PM). National

Ambient Air Quality Standards (NAQQS) for particulate matter were issued by U.S. EPA in 1997. These include standards or proposed standards for both fine particulate matter smaller than 10 microns in diameter (PM_{10}), and fine particulate matter smaller than 2.5 microns in diameter ($PM_{2.5}$). These standards are:

A PM_{10} annual average standard of 50 $\mu g/m^3$.

A PM_{10} 24-hour average standard of 150 $\mu g/m^3$.

A proposed $PM_{2.5}$ annual average standard of 15 $\mu g/m^3$.

A proposed $PM_{2.5}$ 24-hour average standard of 65 $\mu g/m^3$.

For the 24-hour standard, the concentrations measured during a year are rank ordered. If the concentration at the 98^{th} percentile is greater than the 24 hour standard, a region is designated non-attainment. For an annual standard, concentrations measured throughout a year are averaged. To determine whether an area meets the annual standard, samples are collected on a regular basis (daily, every third day or 6^{th} day) over a 24-hour period. Samples are collected using a filter-based sampler with an inlet that removes large particles. The filters are weighted and using the airflow rate through the filter, a concentration is determined.

Developing effective strategies to reduce concentrations of PM to meet these standards will require a better understanding of PM sources, including the mechanisms responsible for their production.

2.1.1 Sources of atmospheric PM

The sources of particulate matter are summarized in Figure 2.1. Figure 2.1 indicates that approximately two-thirds of the mass of atmospheric particles is inorganic. The composition and sources of these inorganic species are reasonably well understood. In contrast to the inorganics, the composition and sources of carbonaceous species, which are significant contributors to total particle mass, are poorly understood.

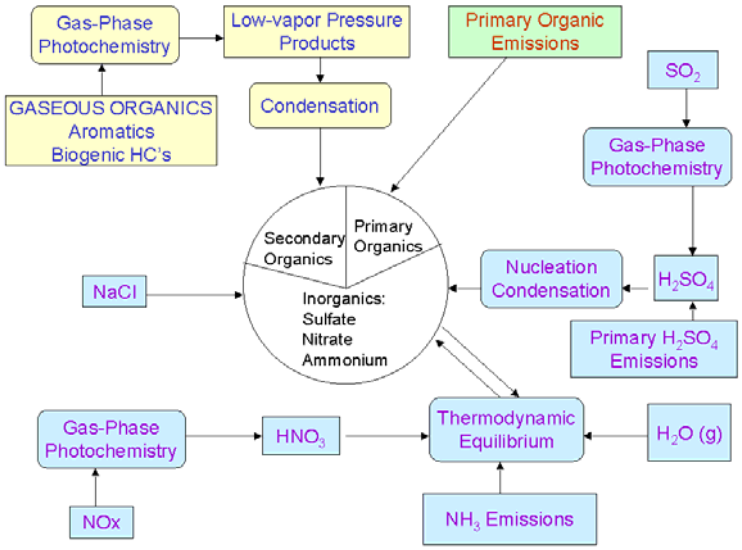

Figure 2.1: Sources of atmospheric particulate matter (Seinfeld, et al., 1994)

The distribution of ambient particulate matter in Figure 2.1 is specific to Southern California. This distribution can vary depending on geographical location, time of year, and meteorology. Figure 2.2 illustrates the distribution of ambient PM

that is found in several locations in Texas (Tropp et al., 1998). These distributions were identified during a Texas PM2.5 sampling and analysis study performed between 03/11/97 and 03/12/98. While the distributions shown in Figure 2.2 do not explicitly indicate the relative percent of secondary versus primary species, they do show the relative contribution of inorganic and organic compounds present in ambient aerosol. The results from the Texas $PM_{2.5}$ study indicate slightly different ratios of organic to inorganic species than those noted in Southern California. In Southern California organic species contribute roughly 33 % of ambient aerosol. In Texas organic species were found to range between 25 % and 50 % in the study locations. Organics contribute approximately 25 % of airborne loadings in San Antonio and Corpus Christi. In contrast, roughly 40 % of ambient PM in Houston and Dallas are organics, and up to 50 % of PM-2.5 in El Paso is organic.

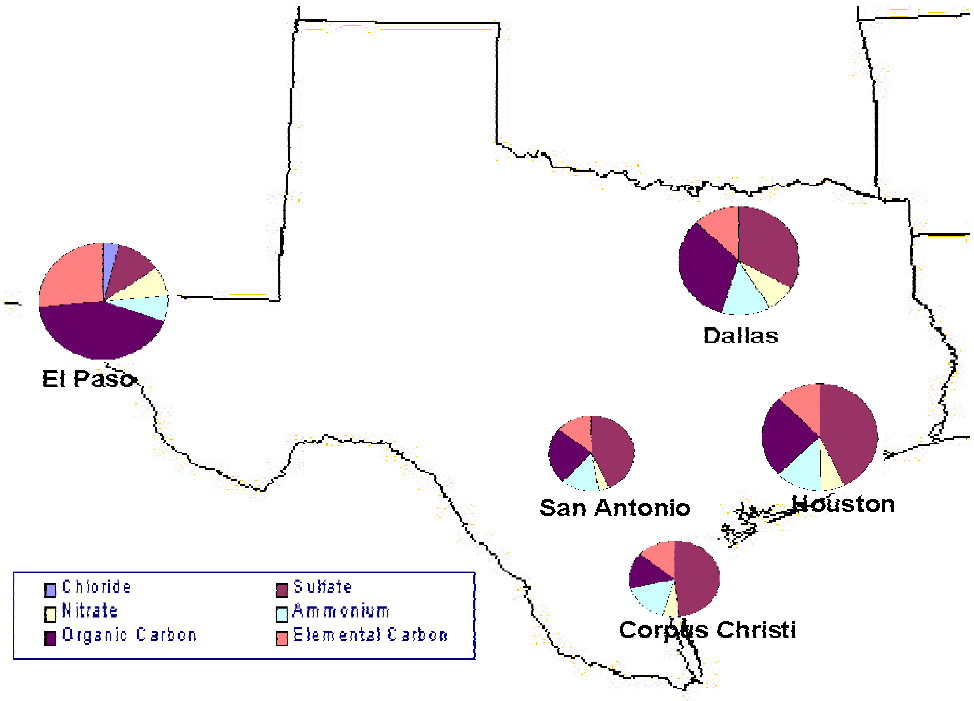

Figure 2.2: Spatial distribution of major chemical components during the Texas PM2.5 Sampling and Analysis Study between 03/11/97 and 03/12/98

2.1.2 Organic PM Formation

Organic particulate matter is both primary and secondary in nature. Sources of primary organic aerosol include combustion processes, forest fires, and agricultural activities. Secondary organic aerosols (SOA) are produced by the gas-phase photochemical oxidation reactions of volatile organic compounds (VOCs). These reactions produce low volatility products which partition into the aerosol phase. VOCs are emitted from a variety of sources, and include alkanes, alkenes, aromatics, aldehydes, terpenes, and oxygenated species. Although photooxidation reactions to form SOA may proceed via reactions of VOCs with NO_3 and ozone, OH radicals

initiate the majority of the reactions. It is not entirely clear what fraction of atmospheric organic aerosol is secondary; however, in most urban areas, secondary organic aerosol is believed to dominate total organic loadings.

2.1.3 Composition and Sources of Secondary Organic Aerosol

Several previous investigations have attempted to determine the compositions and sources of secondary organic aerosol. Most have relied on measurements of the fraction of volatile carbon (also called organic carbon, OC) and non-volatile carbon (also called graphitic or elemental carbon, EC) in the particulate matter. In these studies, it is assumed that all EC is primary in origin and that all primary emissions will have a characteristic organic (volatile) carbon to elemental carbon ratio (OC/EC).

$$OC_{secondary} = OC_{total} - OC_{primary} \qquad \textbf{Equation 1}$$

$$OC_{primary} = EC^{*} (OC/EC)_{primary} \qquad \textbf{Equation 2}$$

Turpin and Huntzicker (1991), among others, have examined the ratios of elemental and organic carbon in aerosol to estimate the extent of primary and secondary aerosol. They calculated secondary organic carbon concentrations in Southern California using primary OC/EC ratios between 1.4 and 2.9, and by assuming that only primary organic carbon is present in the morning. Based on these assumptions, the authors could determine what fraction of OC in the afternoon was secondary. Correlations based on Turpin and Huntzicker's estimates of SOA indicate that the concentration of secondary organic aerosol depends on the O_3, NOx, and

organic precursor concentrations. It was estimated that approximately 30-50 % of the carbon present in aerosol during August in Los Angeles is secondary. More recent studies by Allen and co-workers (Pickle et al., 1990; Mylonas et al., 1991; Eusebi 1996) have utilized infrared spectroscopy to characterize the chemical structure and compound classes present in organic aerosols, as a function of particle size. Results from these studies show a good correlation between carbonyls and organonitrates with ozone concentrations; therefore, it can be concluded that the carbonyls and organic nitrates in atmospheric aerosol are mainly the results of atmospheric reactions. Statistical analysis indicated that approximately 95 % of aerosol carbonyl loadings in Los Angeles are secondary (Pickle et al, 1990). The limitations of these studies are that no individual organic molecules, only compound classes can be identified in ambient aerosol, and that distinguishing between primary and secondary organics based on these profiles is difficult.

An alternative approach to understanding the composition and sources of SOA is to predict the extent and composition of secondary aerosol based on the estimated yields of products resulting from atmospheric reactions. Grosjean and Seinfeld (1989) and Grosjean (1992) predicted average aerosol composition by using emission inventories and their knowledge of the photochemistry of gas-phase hydrocarbon emissions.

Using this approach, the formation rate for a single condensable organic product formed in the oxidation of one hydrocarbon precursor with hydroxyl radical is assumed to be given by:

$$d[SOA]/dt = ad[P]/dt = -a*\alpha d[VOC]/dt = a*\alpha k_{OH}[OH][VOC] \quad \textbf{Equation 3}$$

where:

k_{OH} = rate constant of oxidation reaction of VOC by OH radicals

[P] = concentration of reaction product

[SOA] = concentration of SOA produced by oxidation reaction

[OH] = concentration of OH radicals in the reaction

α = fraction of VOC reacted that produced product P

a = fraction of the product that is present in the condensed phase

Currently the most commonly employed methodology for estimating SOA formation is to assume the selectivity to SOA (parameters "a and α" in Equation 3) are constant and to employ a fractional aerosol coefficient. The fractional aerosol coefficient (FAC) is the fraction of SOA that would result from the emissions of a particular gas phase hydrocarbon (VOC).

$$FAC = [SOA] / [VOC]_0 * \text{Fraction of VOC reacted} \quad \textbf{Equation 4}$$

Where:

[SOA] = concentration of SOA ($\mu g/m^3$)

$[VOC]_0$ = initial concentration of VOC ($\mu g/m^3$)

The estimation of FAC is based on the assumption that the oxidation reactions of each VOC lead to a fixed fraction of secondary organic aerosol product. For example, the data in Table 2.1 indicate that 2.9 % of the products formed from the reaction of 1,3,5-trimethybenzene with OH radicals will be SOA (Grosjean, 1992).

Table 2.1 displays the typical amount of individual organic species emitted into the atmosphere in the Los Angeles area on a kilogram per day basis. Grosjean (1992) estimated FAC of each organic species and the amount of each species that is transformed to secondary aerosol. Examination of Table 2.1 provides a rough characterization of the roles of various hydrocarbon compound classes in the formation of secondary aerosol.

Table 2.1: VOC Emissions Inventory and Secondary Aerosol Yields (Grosjean, 1992)

Hydrocarbon Precursors	Amount of VOC emitted** (kg / day)	Fractional aerosol coefficient (%)	Fraction of VOC reacted	Amount of aerosol produced (kg / day)
Olefins				
Alkenes:				
1-Heptene	2,891	2.0	0.52	30.2
C7 terminal alkenes	7,259	1.0	0.52	38.0
1-Octene	3,619	1.0	0.55	19.9
C8 terminal alkenes	381	1.0	0.55	2.2
Cis-2-octene	131	2.0	0.64	1.9
2,4,4-trimethyl-1-pentene	159	4.9	0.64	5.1
Methyl heptene	272	2.0	0.59	3.0
1-Nonene	1,024	6.0	0.57	34.8
C9 terminal alkenes	7,076	3.0	0.57	120.8
Ethyl heptene	492	60	0.57	16.5
1-Decene	1,712	9.0	0.57	87.8
1-Undecene	153	12.0	0.57	10.3
C11 terminal alkenes	5,477	6.0	0.57	187.5
Trimethyldecene	517	15.0	0.57	49.9
Cyclic Olefins:				
Cyclopentene	412	4.0	0.94	15.4
1-Methylcyclopentene	165	5.0	0.95	7.8
3-Methylcyclopentene	412	5.0	0.95	19.6
Cyclohexene	824	7.0	0.79	45.6
1-Methylcyclohexene	459	10.6	0.76	37.0
3-Methylcyclohexene	494	3.1	0.53	8.1
4-Methylcyclohexene	494	3.1	0.65	10.0
Aromatics				
Toluene	105,480	5.4	0.12	683.5
o-Xylene	19,614	5.0	0.26	255.0
m-Xylene	12,186	4.7	0.4	229.1
p-Xylene	12,057	1.6	0.28	54.0
Ethylbenzene	8,481	5.4	0.15	68.7
1,3,5-Trimethylbenzene	4,667	2.9	0.74	100.1
1,2,4-Trimethylbenzene	7,029	2.0	0.58	81.5
1,2,3-Trimethylbenzene	4,133	3.6	0.51	75.9
n-Propylbenzene	591	1.6	0.12	1.1
Isopropyl benzene	208	4.0	0.13	1.1
o-Ethyltoluene	1,282	5.6	0.23	16.5
m-Ethyltoluene	4,126	6.3	0.31	80.6
p-Ethyltoluene	1,345	2.5	0.21	7.1
n-Butylbenzene	174	2.6	0.18	0.9
Sec-butylbenzene	174	2.6	0.19	1.0
Tert-butylbenzene	1,631	2.6	0.19	8.0
1,3-Diethylbenzene	558	6.3	0.47	16.4
1,4-Diethylbenzene	168	6.3	0.47	5.2
1,2-Diethylbenzene	168	6.3	0.47	5.2
Tetra methylbenzene	1,373	6.3	0.58	49.9
Substituted benzenes: tri, C10	11,380	6.3	0.47	337.0
mono, C11	1,100	7.5	0.47	38.5
di, C11	10,180	7.5	0.47	358.6
tri, C11	10,180	7.5	0.47	358.6
di, C12	2,850	8.5	0.47	113.7
tri, C12	2,850	8.5	0.47	113.7
Miscellaneous				

Table 2.1 (continued)

Hydrocarbon Precursors	Amount of VOC emitted** (kg / day)	Fractional aerosol coefficient (%)	Fraction of VOC reacted	Amount of aerosol produced (kg / day)
β-Pinene	630	30.0	1.0	189.0
α-Pinene	487	30.0	1.0	146.0
Parafins				
Alkanes:				
n-Heptane	27,233	0.06	0.14	2.3
n-Octane	10,284	0.06	0.17	1.0
3-Methylheptane	5,791	0.5	0.1	2.9
2-Methylheptane	3,540	0.5	0.1	1.8
2,4,4-Trimethylpentane	4,719	0.73	0.16	5.4
n-Nonane	10,975	1.5	0.2	33.0
3,5,5-Trimethylhexane	6,927	0.5	0.19	6.6
2,2,5-Trimethylhexane	5,928	0.5	0.19	5.7
2,6-Dimethylheptane	5,626	0.65	0.16	5.8
n-Decane	25,840	0.2	0.22	113.8
Branched C10 alkanes	17,500	2.0	0.22	77.0
n-Undecane	3,016	2.5	0.25	18.7
Branched C11 alkanes	7,700	2.5	0.25	48.0
n-Dodecane	1,932	3.0	0.26	15.1
Branched C12 alkanes	1,950	3.0	0.26	15.1
n-Tridecane	1,101	3.5	0.28	10.6
n-Tetradecane	431	4.0	0.28	4.8
n-Pentadecane	0	5.0	0.28	0.0
Cycloalkanes:				
Methylcyclopentane	5,024	0.17	0.10	0.8
Cyclohexane	12,370	0.17	0.14	2.9
Methylcyclopentane	8,695	2.7	0.20	46.9
Ethylcyclopentane	1,558	2.7	0.12	5.0
Trimethylcyclopentane	307	2.7	0.12	1.0
Dimethylcyclohexane	2,488	2.7	0.10	6.7
Ethylcyclohexane	2,016	2.7	0.12	6.5
Trimethylcyclohexane	1,157	3.0	0.12	4.2
n-Propyl cyclohexane	815	3.0	0.12	2.9
Diethylcyclohexane	1,734	4.0	0.12	8.3
n-Butylcyclohexane	776	4.0	0.12	3.7
n-Pentylcyclohexane	769	5.0	0.12	4.6
n-Hexylcyclohexane	287	6.0	0.12	2.0
Oxygenated aliphatics				
2-Methyl 3 hexanone	3,990	0.12	0.26	1.3
C8 aldehyde	2,034	0.24	0.47	2.3
Heptanone	881	0.12	0.26	0.3
C4 subst. cyclohexanone	219	0.17	0.19	0.1
Propyl cyclohexanone	156	0.17	0.19	0.1
Dibutyl ether	36	0.65	0.26	0.1
2-Butyl tetrahydrofuran	23	0.65	0.19	0.1
Miscellaneous compounds				
2-Methylnaphthalene	939	5.0	0.68	32.0
Naphthalene	667	4.0	0.32	8.3
Indan	427	2.5	0.19	2.1
Ethyl indan	1,032	2.5	0.19	4.9
Phenol	417	5.0	0.46	9.7
Decalin	0	3.0	0.35	0.0
Ethyl decalin	362	4.0	0.38	5.3
Carvomethol	166	30.0	0.35	17.5

Table 2.1 (continued)

Hydrocarbon Precursors	Amount of VOC emitted** (kg / day)	Fractional aerosol coefficient (%)	Fraction of VOC reacted	Amount of aerosol produced (kg / day)
Carvone	166	30.0	0.35	17.5
Indene	30	10.0	1.0	3.0
Isopulegone	299	30.0	0.35	24.1
$\alpha + \gamma$ terpinene	970	30.0	1.0	291.0
Total	450827	522.76	37.75	5030.1

Using these fraction aerosol coefficients, studies by previous investigators (Pandis et al., 1992; Grosjean and Seinfeld, 1989) have concluded that certain hydrocarbon classes contribute much more substantially to secondary organic aerosol formation than other compound classes. Pandis et al., (1992) found aromatic precursors contribute 65 % of the SOA in Los Angeles, while biogenics, alkanes, and alkenes contribute 16 %, 15 %, and 4 % respectively. Grosjean and Seinfeld (1989) suggested that individual hydrocarbons within these compound classes can dominate overall secondary organic aerosol formation as displayed in Table 2.1. For example, the photooxidation reaction of toluene leads to over 600 kg/day of SOA, accounting for 13.6% of the total SOA yield

Currently, the best available estimates of fractional aerosol coefficients are the fixed values, listed in Table 2.1. The problem associated with this approach is that FACs are not constant, and can vary based on the conditions of the reacting mixture. Therefore, the estimates of SOA formation assuming FACs are constant can result in inaccuracies in estimating SOA. To understand the variability in SOA as a function of hydrocarbon mixture effects and other variables, it is useful to examine a related concept: incremental ozone reactivity.

2.1.4 Incremental Ozone Reactivity

Carter (1994) has used a detailed photochemical model to examine how changes in hydrocarbon emissions influence ozone formation. He defined the concept of incremental ozone reactivity as

$$IRi = \Delta[O_3\}/\Delta[VOCi] \qquad \textbf{Equation 5}$$

Where Δ[O3] are grams of additional ozone formed per gram of hydrocarbon added to a reacting mixture (Δ[VOC]). Carter (1993,1994) developed 18 separate reactivities scales using a detailed gas phase mechanism in a single-cell trajectory model. Three of these 18 scales are commonly used in quantifying the reactivities of a variety of VOCs. The first scale is the maximum incremental reactivity (MIR). MIR is the additional grams of ozone formed per gram of hydrocarbon added to a mixture with an initial ratio of VOC to NOx that generates the largest average incremental reactivity. For this scenario, ozone formation is inclined to effect greatly by emissions of VOC. As a result, this generally occurs at a low VOC to NOx ratio. MIR is mathematically expressed as

$$MIR_i = \left\{ MAX\left[\frac{\partial[O_3]}{\partial[VOC_i]} \right] \right\}$$

Where MIR_i is maximum incremental reactivity of species i.

Carter estimated the MIR_i by fixing the VOC concentrations and adjusting the NOx until the reactivity for specific model run was maximized.

The second scale is the maximum ozone reactivity (MOIR). MOIR are grams of ozone formed per gram of hydrocarbon added to a mixture with an initial ratio of VOC to NOx that generates the maximum amount of ozone. This commonly represents conditions in which the VOC to NOx ratio is moderate (transition region between VOC limitation and NOx limitation). MOIR for compound i is given by

$$MOIR_i = \left\{ \left[\frac{\partial [O_3]}{\partial [VOC_i]} \right]_{for [O_3] \max imized} \right\}$$

MOIR was evaluated by setting the NOx concentration in the trajectory to give the maximum ozone formation, and then assessing the sensitivity of the ozone for individual VOCs.

The third scale is the equal benefit incremental reactivity (EBIR), which are grams ozone per gram of hydrocarbon added to a mixture in which both NOx and VOC levels limit ozone formation. EBIR scale is determined for conditions that are midway between VOC limitation and NOx limitation. The National Research Council (1999) reviewed the major characteristics of these three scales as detailed in Table 2.2.

Table 2.2: Summary of Major Characteristics of the Primary Carter Reactivity Scale

Scale	**Type of Scenarios Used**	**Derivation of Scale from Individual Scenario Reactivity**	**Ozone Quantification**	**Reflects Effect of VOC on**
Maximum incremental reactivity (MIR)	Low VOC to NOx ratio conditions in which ozone is most sensitive to VOC changes	Average of incremental reactivities in the MIR scenarios	Maximum ozone	Ozone formation rates
Maximum ozone reactivity (MOR)	Moderate VOC to NOx ratio condition in which highest ozone yield are formed	Average of incremental reactivities in the MOR scenarios	Maximum ozone	Ultimate ozone yields
Equal benefit incremental reactivity (EBIR)	Higher VOC to NOx ratio conditions in which VOC an NOx control are equally effective in reducing ozone	Average of incremental reactivities in the EBIR scenarios	Maximum ozone	Ultimate ozone yields

Three incremental reactivity scales for selected hydrocarbons evaluated by Carter (1994) are listed in Table 2.3.

Table 2.3: Incremental ozone reactivities for selected hydrocarbons, evaluated using three different initial mixtures of air pollutants (Carter, 1994)

Hydrocarbon	Maximum Incremental Reactivity	Incremental reactivity at maximum ozone levels	Incremental reactivity for nitrogen oxide limited Chemistry
Octane	0.19	0.34	0.33
Octene	0.85	0.90	0.89
Toluene	0.88	0.53	-0.023
o-Xylene	2.11	1.60	1.26
Benzadehyde	-0.18	-1.08	-2.7
Isoprene	2.9	2.9	3.3
α-Pinene	1.04	1.08	1.23

It is evident from Table 2.3 (more incremental reactivities are available from Carter, 1994) that incremental ozone reactivities are different between compounds and can vary for any given compound, or even change in sign based on the initial conditions of the reacting mixture. This principle should also extend to incremental particle formation since SOA formation, like ozone formation, is controlled by OH radical reactions. The goal of this thesis was to develop quantitative mechanistic models and fractional aerosol yield models for a variety of hydrocarbon precursors, accounting for this phenomenon.

2.2 PM modeling

2.2.1 Background

For decades, researchers have been developing modeling tools that are used to simulate particulate matter concentrations in the atmosphere. Modeling systems required for simulating particulate matter formation includes an air quality model, a PM module incorporated in the air quality model, and a meteorological model. The major inputs for an air quality PM model are represented in Figure 2.3.

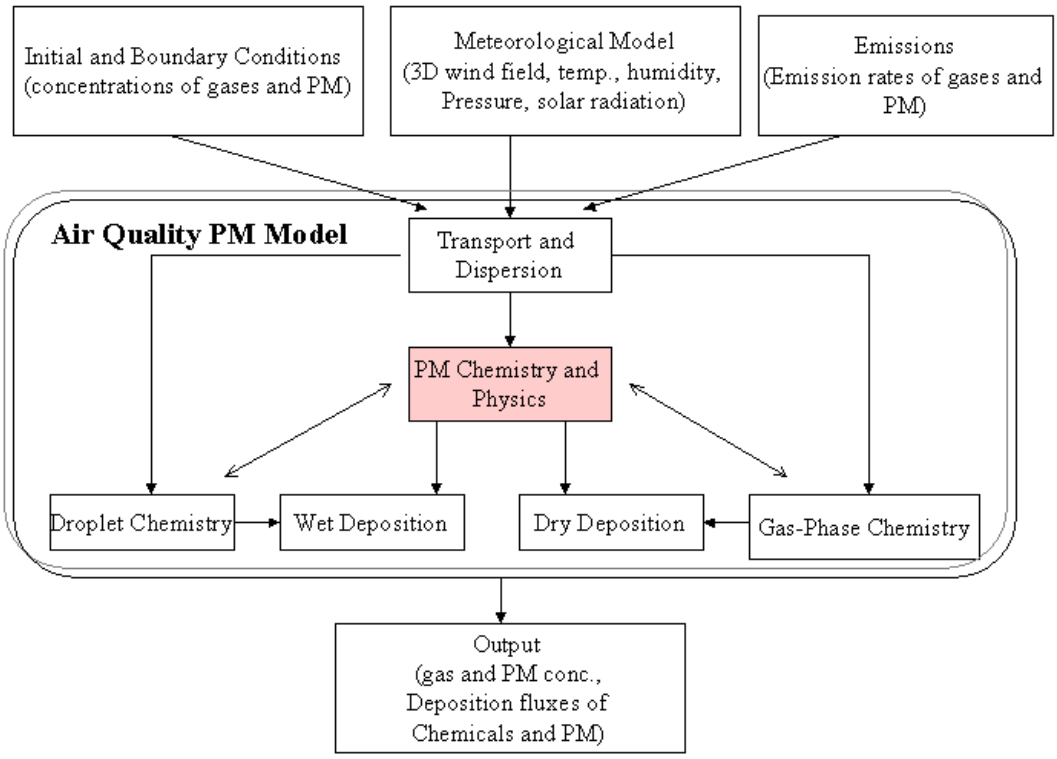

Figure 2.3: Schematic Representation of a PM Source Model (Seigneur, 1997)

As shown in Figure 2.3, there are three major components required to simulate atmospheric PM concentrations. The first component identifies initial and boundary conditions such as concentrations of gases and PM. The second component is meteorological data, e.g., wind field and temperature. Emissions from point and area sources are also required. In addition to these input components are understanding of gas phase chemistry and PM chemistry and physics, i.e., chemical mechanisms and deposition rates are required. This thesis focuses on the integration of gas phase chemistry with PM chemistry and physics.

2.2.2 PM Models

PM models can be categorized into two groups: Lagrangian models, and Eulerian three-dimensional gridded models. Lagrangian models simulate the formation of PM in a parcel of air that is convected along a mean wind trajectory. The several types of Langrangian models can further be separated into plume models and trajectory models. Although these two model categories are similar in their formulation, which is based on the Langragian framework, plume models (e.g., the Industrial source complex model, ISC (EPA, 1992)) focus on the simulation of PM formation from a single source plume emission. On the other hand, trajectory models focus on the input of all emission sources along the air parcel trajectory. This thesis will utilize primarily trajectory models.

Eulerian models simulate PM formation in a three-dimensional gridded domain. The simulation of PM formation for Eulerian models is based on the solution of the mass continuity equation. Major components required to run Eulerian simulations include: initial and boundary conditions of chemical species in model, emission rates of these chemical species, meteorological data, physiographic information, and time and date of the scenario being simulated. Results from simulations include the concentrations of specific chemical species as a function of time and location.

Eulerian models are able to simulate the evolution of PM in a three-dimensional domain. Eulerian models can further be grouped into two major

categories: episodic, and long-term models. Episodic models include a detailed mechanism of atmospheric chemistry. These models are generally limited in their application to a short period of simulation time (e.g., a few days) because of their computational cost. More long-term models can simulate longer time periods, but required simplified mechanism for atmospheric chemistry. Seigneur (1997) identified eight Eulerian episodic PM air quality models.

- The CIT model, developed at the California Institute of Technology.
- The Denver Air Quality Model (DAQM), developed by the State University of New York at Albany and Science & Policy Associates for the Denver Air Quality Council.
- The Gas, Aerosol, Transport, and Radiation model (GATOR), developed at the University of California at Los Angeles and at Stanford University.
- The Regional Particulate Model (RPM), developed at the U.S. EPA office of Research and Development (ORD) as a postprocessor to the Regional Acid Deposition Model (RADM) framework.
- The SAPMAP Air Quality Model with aerosols (SAQM-AERO) developed at the State University of New York at Albany and modified for PM by the California Institute of Technology, Sonoma Technology, Inc. and others for the California Air Resources Board.

- The Urban Airshed Model version IV with aerosols (UAM-AERO), using UAM-IV as the host air quality model, developed by the California Institute of Technology, Sonoma Technology, Inc. and others for the California South Coast Air Quality Management District and the California Air Resources Board.
- The Urban Airshed Model version IV with an aerosol module based on the Aerosol Inorganic Model (UAM-AIM), using UAM-IV as the host air quality model, developed at the University of Delaware.
- The Comprehensive Air Quality Model with Extensions (CAMx) version III, developed by Environ International Cooperation.

Table 2.4 presents a list of PM episodic models along with their host air quality model, the meteorological models used, and the geographical areas where these models have been applied.

Table 2.4: Host Air Quality Model, Meteorological Model and Applications to Date of Episodic PM Models (Seigneur, 1997)

PM Model	**Air Quality Model**	**Meteorological Model**	**Applications to Date**
CIT	CIT	Diagnostic model	Los Angeles Basin, CA
DAQM	RADM	MM4*	Denver, CO
GATOR	GATOR	MMTD	Los Angeles Basin, CA
PRM	RADM	MM4*	Eastern North America
SAQM-AERO	SAQM	MM5	San Joaquin Valley, CA
UAM-AERO	UAM-IV	Various models	Los Angeles Basin and San Joaquin Valley, CA

PM Model	**Air Quality Model**	**Meteorological Model**	**Applications to Date**
UAM-AIM	UAM-IV	Various models	Los Angeles Basin
CAMx	CAMx	MM5, SAIMM, RAMS	Eastern Texas

* Further applications are planned with MM5

From Table 2.4, two PM models use UAM-IV as host air quality model, the other two models use RADM, and the rest use the CIT, GATOR, CAMx, and SAQM, respectively. There are several meteorological models employed for these PM models, the most commonly used model is MM4. This model, however, will be replaced by MM5.

2.2.3 Treatment of SOA in PM models

Since this research focuses on developing a mechanistic model of SOA formation, this section discusses the current treatment of SOA in PM models. The current PM models use various methods to predict and treat SOA formation. Four gas phase mechanisms are used among the seven episodic PM models. These mechanisms are the Statewide Air Pollution Research Center (SAPRC) gas phase chemistry model developed by Carter (1990, 1995), the Carbon-Bond Mechanism version IV (CBM-IV) of Gery et al., (1989), the RADM mechanism version 2 (RADM2) developed by Stockwell et al., (1990), and a mechanism developed

explicitly for GATOR (Jacobson, 1994). Table 2.5 details current treatment of SOA formation in PM models.

Table 2.5: Treatment of SOA formation in PM models (Seigneur, 1997)

PM Model	SOA Treatment		Reference
	Gas Phase Chemical Mechanism	SOA formation	
CIT	Extended LCC	Absorption mechanism with mass transfer	Odum et al., 1996; Meng et al., 1997
DAQM	RADM2	Lumped aerosol yields of Pandis et al., 1992	Moucheron and Milford, 1996
GATOR	GATOR	Solubility	Jacobson, 1997
RPM	RADM2	Lumped aerosol yields of Pandis et al., 1992	Binkowski and Shankar, 1995
SAQM-AERO	CBM-IV and SAPRC	Lumped aerosol yields of Pandis et al., 1992	NA
UAM-AERO	CBM-IV and SAPRC	Lumped aerosol yields of Pandis et al., 1992	Kumar et al., 1996
UAM-AIM	CBM-IV and SAPRC	Lumped aerosol yields of Pandis et al., 1992	Sun and Wexler, 1997
VISHWA	Condensed chemistry (7 reactions and 7 species)	2-component approach with aromatic and terpene lumped aerosol yields of Pandis et al., 1992 adjusted downward to match ambient observations	Venkatram et al., 1997
CAMx	CBM-IV and SAPRC	Simplified parameterized aerosol thermodynamics package	Environ, user's guide, 2000

As noted in Table 2.5, DAQM, RPM, UAM-AERO, UAM-AIM, and SAQM use the lumped SOA yields approach of Pandis et al., (1992). This method makes use of volatile organic compounds (VOCs) specific fractional aerosol coefficients (FACs) of Grosjean and Seinfeld (1989). For CIT, SOA is modeled by the mass transport with absorption mechanism between gas and particulate phases. In the VISHWA model, the lumped SOA yields of Pandis et al., for lumped aromatics and terpenes

have been adjusted downward to match experimental observations. GATOR describes gas-particle partitioning of condensable and soluble organic species.

There are a number of limitations in the atmospheric gas phase chemical mechanisms currently employed in urban and regional scale models to predict SOA formation. These mechanisms do not account for the chemistry of organic precursors that lead to the formation of condensable products in sufficient detail to estimate the SOA generation. In addition, many of the higher molecular weight organics that are not important in ozone production, but are sources of SOA formation, are neglected in most current mechanisms. Finally, gas phase mechanisms such as CBM-IV in CAMx, cannot estimate a production of semi-volatile products from each parent compound, because species are lumped into carbon bond groups based on their chemical structures. For example, decene will be represented by eight paraffinic carbons and two carbons associated with the double bond. Heptene would be represented by five paraffin carbons and two carbons associated with the double bond. So, in a mixture of heptene and decene, the CBM follows only total concentrations of paraffinic and olefinic carbons, not molecular concentrations. Yet heptene and decene have very different SOA yields because of the differences in molecular weights. So, if CBM is used as the chemical mechanism, the SOA formation calculated from simulations will not be specifically from the amount reacted of decene or heptene, but will be from the emissions of decene or heptene. Since there is a large uncertainty for FACs and extent of conversion of hydrocarbons in ambient air, the estimated SOA formation may be inaccurate.

Unlike CBM-IV mechanism, SAPRC mechanism retains the information about molecular weight of hydrocarbons in the reacting mixture, because different parts of molecule are not broken down and treated differently. Compounds in the reacting mixture are lumped as a whole molecule into different groups based on their chemical structures and reactivities. For example, benzene will be lumped in a group of slower aromatic compounds and represented by model species ARO1. Parameters, product yields, and molecular weight of ARO1 are weighted averages from every compound in the group (more details about lumping are described in Chapter 4). Further, the SAPRC model allows the user to modify or update a detailed mechanism including SOA formation for both individual and lumped hydrocarbon precursors. Because of these advantages, SAPRC99 was used in this thesis to quantify the SOA formation for individual and lumped compounds at a variety of initial conditions.

As described earlier, several PM models employ a fixed FAC in evaluating SOA formation for any given compounds. However, by examining the concept of incremental ozone reactivity (Carter, 1994), the hypothesis that FACs are not constant, but can vary depending on the VOC to NOx ratio and the composition of VOCs emerges. This hypothesis was examined in this thesis.

2.3 Summary

This chapter has summarized the current literature on organic particulate matter and PM modeling. The sources and compositions of inorganic aerosol are reasonably well understood, on the other hand, better understanding of sources and compositions of organic particulate matter are needed. Previous investigators have estimated SOA formation using several approaches. The most common approach, which is employed in a variety of PM models, is to use a fixed fractional aerosol coefficient (FAC) for the yields of SOA form any given hydrocarbon (Pandis et al., 1992). The concept of incremental ozone reactivity, however, raises the argument that FAC is not constant, and can vary depending on the initial conditions and other parameters. This research builds on this concept to develop a suitable approach for estimating SOA formation.

Chapter 3 Quantitative models of SOA formation for individual compounds development

3.1 Introduction

Two major topics are addressed in this chapter. The first is the development of quantitative mechanistic models and physical phase partitioning models of secondary organic aerosol (SOA) formation for individual compounds, using data available from smog chamber experiments. The second topic is the use of these models to examine the SOA formation potential for various aromatic hydrocarbons. Since the chemical mechanisms, kinetic models and partitioning models will be incorporated into an existing model of gas phase chemistry (the SAPRC model), the chapter will begin with a discussion of the baseline, gas-phase model. Then the approaches used for modeling the chemistry and phase partitioning of SOA will be described.

3.2 SAPRC model

Aerosol formation is the result of a set of series/parallel reactions of hydrocarbon precursors, and aerosol precursors with OH radicals. The concentration of OH radical is critical in determining the aerosol yields. In atmospheric oxidations, OH radical concentration is highly dependent on concentrations of nitrogen oxides and the concentrations of all hydrocarbons in the reacting mixture, and other parameters. To accurately predict aerosol yields, the mechanism for SOA formation

for a compound, (e.g. trimethylbenzene) must be integrated into a comprehensive gas phase model. The comprehensive model of gas phase chemistry used in this work has been developed by the Statewide Air Pollution Research Center (SAPRC) of the University of California. SAPRC has developed software, SAPRC 99, to model the gas phase chemistry of mixtures of more than 350 common air pollutants. These mechanisms have been evaluated extensively against environmental chamber data for gas phase species (Carter and Lurmann, 1991). The SAPRC model contains a gas phase reaction mechanism for the atmospheric photoreaction of over 350 hydrocarbon precursors, including alkenes, alkanes, aromatics, alcohols, ethers and other compounds representative of the range of reactive organics emitted into atmosphere. Table 3.1 lists all species that are modeled in SAPRC.

Table 3.1: Detailed species that are modeled in SAPRC 99 (Carter, 2000)

Compounds	Model Name	Cs	MWt	kOH (300) (cm^3/molec-sec)
Carbon Monoxide	CO	1	28	2.1e-13
Methane	METHANE	1	16	6.6e-15
Alkanes				
Ethane	ETHANE	2	30	2.6e-13
Propane	PROPANE	3	44	1.1e-12
n-Butane	N-C4	4	58	2.5e-12
n-Pentane	N-C5	5	72	4.0e-12
n-Hexane	N-C6	6	86	5.5e-12
n-Heptane	N-C7	7	100	7.0e-12
n-Octane	N-C8	8	114	8.8e-12
n-Nonane	N-C9	9	128	1.0e-11
n-Decane	N-C10	10	142	1.1e-11
n-Undecane	N-C11	11	156	1.3e-11
n-Dodecane	N-C12	12	170	1.4e-11
n-Tridecane	N-C13	13	184	1.6e-11
n-Tetradecane	N-C14	14	198	1.8e-11
n-Pentadecane	N-C15	15	212	2.1e-11
n-C16	N-C16	16	226	2.3e-11
Isobutane	2-ME-C3	4	58	2.2e-12
Iso-Pentane	2-ME-C4	5	72	3.7e-12
Neopentane	22-DM-C3	5	72	8.6e-13
2,2-Dimethyl Butane	22-DM-C4	6	86	2.4e-12

Compounds	Model Name	Cs	MWt	kOH (300) (cm^3/molec-sec)
2,3-Dimethyl Butane	23-DM-C4	6	86	5.8e-12
2-Methyl Pentane	2-ME-C5	6	86	5.3e-12
3-Methyl Pentane	3-ME-C5	6	86	5.4e-12
2,2,3-Trimethyl Butane	223TM-C4	7	100	4.3e-12
2,2-Dimethyl Pentane	22-DM-C5	7	100	3.4e-12
2,3-Dimethyl Pentane	23-DM-C5	7	100	1.4e-11
2,4-Dimethyl Pentane	24-DM-C5	7	100	5.0e-12
2-Methyl Hexane	2-ME-C6	7	100	1.4e-11
3,3-Dimethyl Pentane	33-DM-C5	7	100	6.0e-12
3-Methyl Hexane	3-ME-C6	7	100	1.4e-11
2,2,3,3-Tetramethyl Butane	2233M-C4	8	114	1.1e-12
2,2,4-Trimethyl Pentane	224TM-C5	8	114	3.6e-12
2,2-Dimethyl Hexane	22-DM-C6	8	114	4.8e-12
2,3,4-Trimethyl Pentane	234TM-C5	8	114	7.1e-12
2,3-Dimethyl Hexane	23-DM-C6	8	114	1.7e-11
2,4-Dimethyl Hexane	24-DM-C6	8	114	1.7e-11
2,5-Dimethyl Hexane	25-DM-C6	8	114	1.7e-11
2-Methyl Heptane	2-ME-C7	8	114	1.7e-11
3-Methyl Heptane	3-ME-C7	8	114	1.7e-11
4-Methyl Heptane	4-ME-C7	8	114	1.7e-11
2,2,5-Trimethyl Hexane	225TM-C6	9	128	1.2e-11
2,3,5-Trimethyl Hexane	235TM-C6	9	128	7.9e-12
2,4-Dimethyl Heptane	24-DM-C7	9	128	2.0e-11
2-Methyl Octane	2-ME-C8	9	128	1.0e-11
3,3-Dimethyl Pentane	33-DE-C5	9	128	4.9e-12
3,5-Dimethyl Heptane	35-DM-C7	9	128	2.1e-11
4-Ethyl Heptane	4-ET-C7	9	128	2.1e-11
4-Methyl Octane	4-ME-C8	9	128	9.7e-12
2,4-Dimethyl Octane	24-DM-C8	10	142	2.3e-11
2,6-Dimethyl Octane	26DM-C8	10	142	1.3e-11
2-Methyl Nonane	2-ME-C9	10	142	1.3w-11
3,4-Diethyl Hexane	34-DE-C6	10	142	7.4e-12
3-Methyl Nonane	3-ME-C9	10	142	2.3e-11
4-Methyl Nonane	4-ME-C9	10	142	2.3e-11
4-Propyl Heptane	4-PR-C7	10	142	2.4e-11
2,6-Dimethyl Nonane	26DM-C9	11	156	2.6e-11
3,5-Diethyl Heptane	35-DE-C7	11	156	2.8e-11
3-Methyl Decane	3-ME-C10	11	156	2.6e-11
4-Methyl Decane	4-ME-C10	11	156	2.6e-11
2,6-Diethyl Octane	36-DE-C8	12	170	3.1e-11
3,6-Dimethyl Decane	36DM-C10	12	170	2.9e-11
3-Methyl Undecane	3-ME-C11	12	170	2.9e-11
5-Methyl Undecane	5-ME-C11	12	170	2.9e-11
3,6-Dimethyl Undecane	36DM-C11	13	184	3.2e-11
3,7-Dietyl Nonane	37-DE-C9	13	184	3.4e-11
3-Methyl Dodecane	D-ME-C12	13	184	3.1e-11
5-Methyl Dodecane	5-ME-C12	13	184	3.1e-11
3,7-Dimethyl Dodecane	37DM-C12	14	198	3.5e-11
3,8-Diethyl Decane	38DE-C10	14	198	3.6e-11
3-Methyl Tridecane	3-ME-C13	14	198	3.4e-11

Compounds	Model Name	Cs	MWt	kOH (300) (cm^3/molec-sec)
6-Methyl Tridecane	6-ME-C13	14	198	3.4e-11
3,7-Dimethyl Tridecane	37DM-C13	15	212	3.8e-11
3,9-Dimethyl Undecane	39DM-C13	15	212	3.9e-11
3-Methyl Tetradecane	3-ME-C14	15	212	3.7e-11
6-Methyl Tetradecane	6-ME-C14	15	212	3.7e-11
3-Methyl Pentadecane	3-ME-C15	16	226	4.0e-11
4,8-Dimethyl Tetradecane	48DM-C14	16	226	4.0e-11
7-Methyl Pentadecane	7-ME-C15	16	226	4.0e-11
Cyclopropane	CYCC3	3	42	8.4e-14
Cyclobutane	CYCC4	5	56	1.5e-12
Cyclopentane	CYCC5	6	70	5.1e-12
Cyclohexane	CYCC6	6	84	7.3e-12
Isoporpyl Cyclopropane	IRP-CC3	6	84	2.7e-12
Methylcyclopentane	ME-CYCC5	7	84	1.1e-11
1,3-Dimethyl Cyclopentane	13DMCYCC5	7	98	1.4e-11
Cycloheptane	CYCC7	7	98	1.3e-11
Ethyl Cyclopentane	ET-CYCC5	7	98	1.5e-11
Methylcyclohexane	ME-CYCC6	7	98	1.0e-11
1,3-Dimethyl Cyclohexane	13DMCYC6	8	112	2.4e-11
Cyclooctane	CYCC8	8	112	1.4e-11
Ethylcyclohexane	ET-CYCC6	8	112	2.4e-11
Propyl Cyclopentane	PR-CYCC5	8	112	1.7e-11
1,1,3-Trimethyl Cyclohexane	113MCYC6	9	126	8.7e-12
1-Eth.-4-Meth. Cyclohexane	1E4MCYC6	9	126	2.7e-11
Propyl Cyclohexane	C3-CYCC6	9	126	2.7e-11
1,3-Diethyl Cyclohexane	13DECYC6	10	140	3.1e-11
1,4-Diethyl Cyclohexane	14DECYC6	10	140	3.1e-11
1-Methyl-3-Isopr, Cyclohex.	1M3IPCY6	10	140	3.0e-11
Butyl Cyclohexane	C4-CYCC6	10	140	3.0e-11
1,3-Diethyl –5-ME. Cyclohex.	13E5MCC6	11	154	3.4e-11
1-Ethyl-2-Propyl Cyclohex.	1E2PCYC6	11	154	3.4e-11
Pentyl Cyclohexane	C5-CYCC6	11	154	3.3e-11
1,3,5-Triethyl Cyclohex.	135ECYC6	12	168	3.8e-11
1-Meth.-4-Pentyl Cyclohex.	1M4C5CYC6	12	168	3.6e-11
Hexyl Cyclohexane	C6-CYCC6	12	168	1.8e-11
1,3-Dieth-5-Pent Cyclohex.	13E5PCC6	13	182	4.1e-11
1-Meth.2-Hexyl-Cyclohex.	1M2C6CC6	13	82	3.9e-11
Heptyl Cyclohexane	C7-CYCC6	13	182	3.8e-11
13-Diprop-5-Eth Cyclohex.	13P5ECC6	14	196	4.4e-11
1-Meth.-4-Heptyl Cyclohex.	1M4C7CC6	14	196	4.2e-11
Octyl Cyclohexane	C8-CYCC6	14	196	4.1e-11
1,3,5-Tripropyl Cyclohex.	135PCYC6	15	210	4.7e-11
1-Methyl-2-Octyl Cyclohex.	1M2C8CC6	15	210	4.4e-1
Nonyl Cyclohexane	C9-CYCC6	15	210	4.4e-11
1,3-Prop,-5-Butyl Cyclohex.	13P5BCC6	16	224	4.9e-11
1-Methyl-4-Nonyl Cyclohex.	1M4C9CY6	16	224	4.7e-11
Decyl Cyclohexane	C10CYCC6	16	224	4.7e-11
Alkenes				
Ethene	ETHENE	2	28	9.2e-12

Compounds	Model Name	Cs	MWt	kOH (300) (cm^3/molec-sec)
Propene	PROPENE	3	42	3.1e-11
1-Butene	1-BUTENE	4	56	3.6e-11
1-Pentene	1-PENTEN	5	70	3.6e-11
3-Methyl –1-Butene	3M-1-BUT	5	70	3.7e-11
1-Hexene	1-HEXENE	6	84	4.2e-11
3,3-Dimethyl-1Butene	33M1-BUT	6	84	3.0e-11
3-Methyl-1-Pentene	3M1-C5E	6	84	6.6e-11
4-Methyl-1-Pentene	4M1-C5E	6	84	6.8e-11
1-Heptene	1-HEPTEN	7	98	4.5e-11
1-Octene	1-PCTENE	8	112	7.0e-11
1-Nonene	1-C9E	9	126	7.2e-11
1-Decene	1-C10E	10	140	6.8e-11
1-Undecene	1-C11E	11	154	7.2e-11
1-Dodecene	1-C12E	12	168	7.2e-11
1-TRIdecene	1-C13E	13	182	7.2e-11
1-Tetradecene	1-C14E	14	196	7.2e-11
1-Pentadecene	1-C15E	15	210	7.2e-11
Isobutene	ISOBUTEN	4	6	5.8e-11
2-Methyl-1-Butene	2M-1-BUT	5	70	7.1e-11
23-Dimethyl-1-Butene	23M1-BUT	6	84	1.2e-10
2-Ethyl-1-Butene	2E1-BUT	6	84	1.2e-10
2-Methyl-1-Pentene	2M1-C5E	6	84	7.2e-11
2,3,3-trimethyl-1-Butene	23M1BUT	7	98	1.2e-10
3-Methyl-2-Isopropyl-1-Butene	3M2I1C4E	8	112	1.2e-10
Cis-2-Butene	C-2-BUTE	4	56	1.1e-10
Trans-2-Butene	T-2-BUTE	4	56	1.5e-10
2-Methyl-2Butene	2M-2-BUT	5	70	3.1e-10
Cis-2-Pentene	C-2-PENT	5	70	1.7e-10
Trans-2-Pentene	T-2-PENT	5	70	1.7e-10
2,3-Dimethyl-2-Butene	23M2-BUT	6	84	8.7e-10
2-Methyl-2 Pentene	2M-2-C5E	6	84	4.8e-10
Cis-2-Hexene	C-2-C6E	6	84	2.3e-10
Cis-3-Hexene	C-3-C6E	6	84	2.0e-10
Cis-3-Methyl-2-Hexene	C3M2-C5E	6	84	4.6e-10
Trans-3-Methyl2-Hexene	T3M2-C5E	6	84	5.1e-10
Trans-4-Methyl-Hexene	T4M2-C5E	6	84	1.6e-10
Trans-2-Hexene	T-2-C6E	6	84	2.3e-10
Trans-3-Hexene	T-3-C6E	6	84	2.1e-10
2,3-Dimethyl-2Hexene	23M2-C5E	7	98	1.2e-9
Cis-3-Heptene	C-3-C7E	7	98	2.3e-10
Trans 4,4-dimethyl-2-Pentene	T44M2C5E	7	98	1.6e-10
Trans-2-Heptene	T-2-C7E	7	98	1.7e-10
Trans-3-Heptene	T-3-C7E	7	98	2.3e-10
Cis-4-Octene	C-4-C8E	8	112	1.7e-10
Trans 2,2-Dimetyl 3-Hexene	T22M3C6E	8	112	1.5e-10
Trans 2,5-Dimethyl 3-Hexene	T25M3C6E	8	112	2.3e-10
Trans-3-Octene	T-3-C8E	8	112	1.3e-10
Trans-4-Octene	T-4-C8E	8	112	3.2e-10
2,4,4-trimethyl-2-Pentene	244M2C5E	8	126	2.3e-10

Compounds	Model Name	Cs	MWt	kOH (300) (cm^3/molec-sec)
Trans-4-Nonene	T-4-C9E	9	128	2.6e-10
3,4-Diethyl-2-Hexene	34E2-C6E	10	140	2.6e-10
Cis-5-Decene	C-5-C10E	10	140	1.8e-10
Trans-4-Decene	T-4-C10E	10	140	2.3e-10
Trans-5-Undecene	T-5-C11E	11	154	2.3e-10
Trans-5-Dodecene	T-5-C12E	12	168	2.3e-10
Trans-5-Tridecene	T-5-C13E	13	182	2.3e-10
Trans-5-Tetradecene	T-5-C14E	14	196	2.3e-10
Trans-5-Pentadecene	T-5-C15E	15	210	2.3e-10
Cyclopentene	CYC-PNTE	5	68	3.1e-10
1-Methyl Cyclopentene	1M-CC5E	5	82	5.6e-10
Cyclohexene	CYC-HEXE	6	82	1.1e-10
1-Methyl Cyclohexene	1M-CC6E	7	96	3.3e-10
4-Methyl Cyclohexene	4M-CC6E	7	96	1.7e-10
1,2-Dimethyl Cyclohexene	12M-CC6E	8	110	8.3e-10
1,3-Butadiene	13-BUTDE	4	54	6.9e-10
Isoprene	ISOPRENE	5	68	1.1e-10
3-Carene	3-CARENE	10	136	1.5e-10
α-Pinene	A-PINENE	10	136	1.2e-10
β-Pinene	B-PINENE	10	136	9.7e-11
d-Limonene	D-LIMONE	10	136	3.1e-10
Sabeiene	SABINENE	10	136	2.0e-10
Styrene	STYRENE	8	104	6.6e-11
Aromatics				
Benzene	BENZENE	6	78	1.2e-12
Toluene	TOLUENE	7	92	5.9e-12
Ethyl Benzene	C2-BENZ	8	106	7.1e-12
Isopropyl Benzene	I-C3-BEN	9	120	6.5e-12
n-Propyl Benzene	N-C3-BEN	9	120	6.0e-12
s-Butyl Benzene	S-C4-BEN	10	134	6.0e-12
m-Xylene	M-XYLENE	8	106	2.4e-11
o-Xylene	O-XYLENE	8	106	1.4e-11
p-Xylene	P-XYLENE	8	106	1.4e-11
1,2,3-Trimethyl Benzene	123-TMB	9	120	3.3e-11
1,2,4-Trimethyl Benzene	124-TMB	9	120	3.3e-11
1,3,5-Trimethyl Benzene	135-TMB	9	120	5.8e-11
Naphthalene	NAPHTHAL	10	128	2.1e-11
Tetralin	TETRALIN	10	132	3.4e-11
Methyl Naphthalene	ME-NAPH	11	142	5.2e-11
2,3-Dimethyl Naphth.	23-DMN	12	156	7.7e-11
Alkynes				
Acetylene	ACETYLEN	2	26	9.2e-13
Methyl Acetylene	ME-ACTYL	3	40	5.9e-12
2-Butyne	2-BUTYNE	4	54	2.7e-11
Ethyl Acetylene	ET-ACTYL	4	54	8.0e-12
Alcohols, Glycols and Eters				
Methanol	MEOH	1	32	9.3e-13
Ethanol	ETOH	2	46	3.3e-12
Isopropyl Alcohol	I-C3-OH	3	60	5.3e-12
n-Propyl Alcohol	N-C3-OH	3	60	5.5e-12

Compounds	Model Name	Cs	MWt	kOH (300) (cm^3/molec-sec)
Isobutyl Alcohol	I-C4-OH	4	74	1.4e-11
n-Butyl Alcohol	N-C4-Oh	4	74	8.6e-12
s-Butyl Alcohol	S-C4-OH	4	74	2.0e-11
t-Butyl Alcohol	T-C4-OH	4	74	1.1e-12
Cyclopentanol	CC5-OH	5	86	1.1e-11
2-Pentanol	2-C5OH	5	88	1.2e-11
3-Pentanol	3-C5OH	5	88	1.2e-11
Pentyl Alcohol	C5OH	5	88	1.1e-11
Cyclohexanol	CC6-OH	6	100	3.5e-11
1-Hexanol	1-C6OH	6	102	1.3e-11
2-Hexanol	2-C6OH	6	102	1.2e-11
1-Heptanl	1-C7OH	7	11	1.4e-11
1-Octanol	1-C8-OH	8	130	2.0e-11
2-Ethyl-1-Hexanol	2-ETC6OH	8	130	2.7e-11
2-Octanol	2-C8-OH	8	130	2.5e-11
3-Octanol	3-C8-OH	8	130	3.1e-11
4-Octanol	4-C8-OH	8	130	2.9e-11
8-Methyl-1-Nonanol	1-C10-OH	10	158	3.1e-11
Ethylene Glycol	ET-GLYCL	2	62	1.5e-11
Propylene Glycol	PR-GLYCL	3	76	2.2e-11
1,2-Butandiol	12-C4OH2	4	90	3.2e-11
Glycetol	GLYCERL	3	92	3.7e-11
1,2-Dihydroxy Hexane	C6-GLYCL	6	118	3.7e-11
2-Methyl-2,4-Pentanediol	2M24C5OH	6	118	1.1e-11
Dimethy Ether	ME-O-ME	2	46	3.0e-12
Trimethylene Oxide	TME-OX	3	58	1.0e-11
Tetrahydrofuran	THF	4	72	1.6e-11
Diethyl Ether	ET-O-ET	4	74	1.3e-11
Dimethoxy methane	METHYLAL	3	76	4.9e-12
Alpha-Methytetrahydrofuran	AM-THF	5	86	2.2e-11
Tetrahydropyran	THP	5	86	1.4e-11
Ethyl Isopropyl Ether	ET-O-IPR	5	88	4.9e-11
Methyl n-Butyl Ether	MNBE	5	88	1.5e-11
Methyl t-Butyl Ether	METBE	5	88	2.9e-12
Di n-Propyl Ether	PR-O-PR	6	102	1.8e-11
Ethyl n-Butyl Ether	ENBE	6	102	2.1e-11
Ethyl t-Butyl Ether	ETBE	6	102	8.8e-12
Methyl t-Amyl Ether	MTAE	6	102	7.9e-12
2-Butyl Tetrahydrofuran	2BU-THF	8	128	5.5e-11
Di-Isobutyl Ether	IBU2-O	8	130	2.6e-11
Di n-Butyl Ether	BU-O-BU	8	130	2.9e-11
Di n-Pentyl Ether	C5-O-C5	10	158	3.5e-11
2-Methoxyethanol	MEO-ETOH	3	76	1.3e-11
1-Methoxy-2-Propanol	MEOC30H	4	90	2.0e-11
2-Ethoxyethanol	ETO-ETOH	4	90	1.9e-11
2-Methoxy-1-Propanol	2MEOC3OH	4	90	5.1e-11
1-Ethoxy-2-Propanol	ETOC3OH	5	104	5.2e-11
2-Propoxyethanol	2PROETOH	5	104	4.9e-11
3-Ethoxy-1-Propanol	3ETOC3OH	5	104	2.2e-11
3-Methoxy-1-Butanol	3MEOC4OH	5	104	2.4e-11

Compounds	Model Name	Cs	MWt	kOH (300) (cm^3/molec-sec)
Diethylene Glycol	DET-GLCL	4	106	5.5e-11
1-Prppoxy-2-Propanol	PROXC3OH	6	118	2.9e-11
2-Butoxyethanol	BUO-ETOH	6	118	2.6e-11
3 methoxy-3-methyl-Butanol	3MOMC4OH	6	118	1.4e-11
2-(2-Methoxyethoxy) Ethanol	MOEOETOH	5	120	6.8e-11
1-tert-Butoxy-2-Propanol	PG-1TB-E	7	132	3.7e-11
2-tert-Butoxy-1-Propanol	PG-3TB-E	7	132	4.9e-11
n-Butoxy-2-Propanol	BUOC3OH	7	132	6.1e-11
2-(2-Ethoxyethoxy) EtOH	CARBITOL	6	134	5.1e-11
Dipropylene Glycol	DPR-GLCL	6	134	7.3e-11
2-Hexyloxyethanol	EGHE	8	146	5.8e-11
2-(2-Propoxyethoxy)ethanol	DGPE	7	148	8.8e-11
Dipropylene Glycol Methyl Ether	DPRGOME	7	148	9.8e-11
2-(2-Buthoxyethoxy)-EtOH	C8-CELSV	8	162	9.0e-11
2-(2-(2-Methoxyethoxy) ethoxy) ethanol	TGME	7	164	1.1e-10
2-(2-Ethylhexyloxy)ethanol	EGEHE	10	174	6.5e-11
2-(2-(2-Ethoxyethoxy) ethoxy) ethanol	TGEE	8	178	1.3e-10
2-(2-Prppoxyethoxy) ethanol	DGHE	10	190	9.6e-11
2-(2-(2-Butoxyethoxy) ethoxyl)ethanol	TGPE	9	192	1.3e-10
2-2-(2-Butoxyethoxy) ethoxyl) ethanol	TGBE	10	206	1.3e-10
Tripropylene Monomethyl ether	TPRGOME	10	206	1.6e-10
2,5,8,11-Tetraoxatridecan-13-ol	TETRAGME	9	208	1.4e-10
3,6,9,12-Tetraoxahexadecan-1-ol	TETRAGBE	12	250	1.7e-10
Methyl Formate	ME-FORM	2	60	2.3e-13
Ethyl Formate	ET-FORM	3	74	1.0e-12
Methyl acetate	ME-ACETE	3	74	3.5e-13
Ethyl Acetate	ET-ACET	4	88	1.6e-12
Methyl Propinate	ME-PRAT	4	88	1.0e-12
n-propyl Formate	C3-FORM	4	88	2.4e-12
Ethyl Propionate	ET-PRAT	5	102	2.1e-12
Isopropyl Acetate	IPR-ACET	5	102	3.4e-12
Methyl Butyrate	ME-BUAT	5	102	3.0e-12
Methyl Isobutyrate	ME-IBUAT	5	102	1.7e-12
n-Butyl Formate	C4-FORM	5	102	3.1e-12
Propyl Acetate	PR-ACET	5	102	3.4e-12
Ethyl Butyrate	ET-BUAT	6	116	4.9e-12
Isobutyl Acetate	IBU-ACET	6	116	9.2e-12
Methyl Pivalate	ME-PVAT	6	116	1.3e-12
n-Butyl Aceetate	BU-ACET	6	116	4.2e-12
n-Propyl Propionate	PR-PRAT	6	116	4.0e-12
s-Butyl Acetate	SBU-ACET	6	116	5.5e-12

Compounds	Model Name	Cs	MWt	kOH (300) (cm^3/molec-sec)
t-Butyl Acetate	TBU-ACET	6	116	4.3e-12
Butyl Propionate	BU-PRAT	7	130	5.1e-12
Amyl Acetate	AM-ACET	7	130	6.1e-12
n-Propyl Butyrate	PR-BUAT	7	130	7.4e-12
2,3-Dimethylbutyl Acetate	23MC4ACT	8	144	1.5e-11
2-Methylbutyl Acetate	2MC5-ACT	8	144	1.5e-11
3-Methylbutyl Acetate	3MC5-ACT	8	144	1.5e-11
4-Methylbutyl Acetate	4MC5-ACT	8	144	1.5e-11
Isobutyl Acetate	IBU-IBTR	8	144	1.1e-11
n-Butyl Butyrate	BU-BUAT	8	144	1.1e-11
n-Hexyl Acetate	NC6-ACET	8	144	1.5e-11
Ethyl 3-Ethoxy Propionate	E3DOC3OH	7	144	3.9e-11
2,4-Dimethylpentyl Acetate	24MC5ACT	9	158	1.8e-11
2-Methylhexyl Acetate	2MC6-ACT	9	158	1.8e-11
3-Ethylpentyl Acetate	3EC5-ACT	9	158	1.9e-11
3-Methylhexyl Acetate	3MC6-ACT	9	158	1.8e-11
4-Methylhexyl Acetate	4MC6-ACT	9	158	1.8e-11
5-Methylhexyl Acetate	5MC6-ACT	9	158	1.8e-11
Isoamyl Isobutyrate	IC5IBUAT	9	158	1.4e-11
n-Heptyl Acetate	NC7-ACET	9	158	1.8e-11
2,4-Dimethylhexyl Acetate	24MC6ACT	10	172	2.2e-11
2-Ethyl-Hexyl Acetate	2ETHXACT	10	172	2.2e-11
3,4-Dimethylhexyl Acetate	34MC6ACT	10	172	2.2e-11
3,5-Dimethylhexyl Acetate	35MC6ACT	10	172	2.1e-11
3-Ethylhexyl Acetate	3EC6-ACT	10	172	2.2e-11
3-Methylheptyl Acetate	3MC7-ACT	10	172	2.1e-11
4,5-Dimethylhexyl Acetate	45MC6ACT	10	172	2.1e-11
4-Methylheptyl Acetate	4MC7-ACT	10	172	2.1e-11
5-Methylheptyl Acetate	5MC7-ACT	10	172	2.1e-11
n-Octyl Acetate	NC8-ACET	10	172	2.1e-11
2,3,5-Trimethylhexyl Acetate	235M6ACT	11	186	2.4e-11
2,3-Dimethylheptyl Acetate	23MC7ACT	11	186	2.5e-11
2,4-Dimethylheptyl Acetate	24MC7ACT	11	186	2.5e-11
2,5-Dimethylheptyl Acetate	25MC7ACT	11	186	2.5e-11
2-Methyloctyl Acetate	2MC8-ACT	11	186	2.4e-11
3,5-Dimethylheptyl Acetate	35MC7ACT	11	186	2.5e-11
3,6-Dimethylheptyl Acetate	36MC7ACT	11	186	2.4e-11
3-Ethylheptyl Acetate	3EC7-ACT	11	186	2.5e-11
4,5-Dimethylheptyl Acetate	45MC7ACT	11	186	2.5e-11
4,6-Dimethylheptyl Acetate	46MC7ACT	11	186	2.4e-11
4-Methyloctyl Acetate	4MC8-ACT	11	186	2.4e-11
5-Methyloctyl Acetate	5MC8-ACT	11	186	2.4e-11
n-Nonyl Acetate	NC9-ACET	11	186	2.3e-11
3,6-Dimethyloctyl Acetate	36MC8ACT	12	200	2.7e-11
3-Isopropylheptyl Acetate	3IPC7ACT	12	200	2.8e-11
4,6-Dimethyloctyl Acetate	46MC8ACT	12	200	2.7e-11
3,5,7-Tirmethyloctyl Acetate	357M8ACT	13	214	3.0e-11
e-Ethyl-6-Methyloctyl Acetate	3E6M8ACT	13	214	3.1e-11
4,7-Dimethylnonyl Acetate	47MC9ACT	13	214	3.0e-11

Compounds	Model Name	Cs	MWt	kOH (300) (cm^3/molec-sec)
2,3,5,7-Tetramethyloctyl Acetate	2357M8AC	14	228	3.4e-11
3,5,7-Tirmethylnonyl Acetate	357M9ACT	14	228	3.4e-11
3,6,8-Trimethylnonyl Acetate	368M9ACT	14	228	3.3e-11
2,4,6,8-Tetramethylnonyl Acetate	2468M8AC	15	242	3.6e-11
3-Ethyl-6,7-Dimethylnonyl Acetate	3E67M9AC	15	242	3.7e-11
4,7,9-Trimethyldecyl Acetate	479MIOAC	15	242	3.6e-11
2,3,5,6,8-Pentaamethylnonyl Acetate	23568M9A	16	256	4.0e-11
3,5,7,9-Tetramethyldecyl Acetate	3579MIOA	16	256	3.9e-11
5-Ethyl 3,6,8-Trimethylnonyl Acetate	5E368M9A	16	256	4.0e-11
Dimethyl Carbonate	DMC	3	99	3.3e-13
Propylene Carbonate	PC	4	102	6.9e-13
2-Methyl Lactate	ME-LACT	4	104	2.8e-12
2-Methoxyehtyl Acetate	MCSVACET	5	118	2.5e-11
Ethyl Lactate	ET-LACT	5	118	3.9e-12
Methyl Isopropyl Carbonate	MIPR-CB	5	118	2.6e-12
1-Methoxy-2-Propyl Acetate	PGME-ACT	6	132	1.4e-11
2-Ethoxyethyl Acetate	CSV-ACET	6	132	3.9e-11
2-Methyoxy-1-propyl Acetate	2PGMEACT	6	132	4.6e-11
Dimethyl Succinate	DBE-4	6	146	1.5e-12
Ethylene Glycol Diacetate	ETGLDACT	6	146	7.6e-12
Diisopropyl Carbonate	DIPR-CB	7	146	1.4e-11
Dimethyl Glutarate	DBE-5	7	160	3.5e-12
2-Butoxyethyl Acetate	2BUETACT	8	160	4.8e-11
Dimethyl Adipate	DBE6	8	174	8.8e-12
2-(2-Ethoxyethoxy) ethyl acetate	DGEEA	8	176	7.7e-11
2-(2-Butoxyethoxy)acetate	DGBEA	10	204	8.6e-11
1-Hydroxy-2,2,4-Trimethylpentyl-3-Isobutyrate	TEXANOL2	12	216	2.6e-11
3-Hydroxy-2,2,4-Trimethylpentyl-3-Isobutyrate	TEXANOL1	12	216	3.2e-11
Oxides				
Ethylene Oxide	ETOX	2	44	7.6e-14
Propylene Oxide	PROX	3	58	5.2e-13
1,2-Epoxybutane	12BUOX	4	72	1.9e-12
Acids				
Formic Acid	FORMACID	1	46	4.5e-13
Acetic Acid	ACETACID	2	60	8.0e-13
Acylic Acid	ACYRACID	3	72	3.7e-11
Propionic Acid	PROPACID	3	74	1.2e-12
Methyl acrylate	ME-ACRYL	4	86	6.6e-11
Vinyl Acetate	VIN-ACET	4	86	7.2e-11

Compounds	Model Name	Cs	MWt	kOH (300) (cm^3/molec-sec)
2-Methyl-2Butene-3-ol	MBUTENOL	4	86	6.6e-11
Ethyl Acrylate	ET-ACRYL	5	100	6.6e-11
Methyl Methacrylate	ME-MACRT	5	100	6.2e-11
Butyl Methacrylate	BU-MACRT	8	142	6.2e-11
Isobutyl Methacrylate	IBUMACRT	8	142	6.2e-11
Formaldehyde	FORMALD	1	30	2.5e-11
Acetaldehyde	ACETALD	2	44	2.1e-11
Propinaldehyde	PROPALD	3	58	2.8e-11
2-Methylpropanal	2MEC3AL	4	72	3.4e-11
Butanol	IC4RCHO	4	72	3.1e-11
2,2-Dimethylpropanal	22DMC3AL	5	86	3.4e-11
3-Methylbutanal	3MC4RCHO	5	86	3.5e-11
Pentanal	IC5RCHO	5	86	3.6e-11
Glutaraldehyde	GLTRALD	5	100	9.1e-11
Hexanal	IC6RCHO	6	100	5.6e-11
Haptanal	IC7RCHO	7	114	5.9e-11
Octanal	IC8RCHO	8	128	6.2e-11
Glyoxal	GLYOXAL	2	58	4.0e-10
Methyl Glyoxal	MEGLYOX	3	72	1.8e-10
Acrolein	ACROLEIN	3	56	9.2e-11
Crotonaldehyde	CROTALD	4	70	1.1e-10
Methacrolein	METHACRO	4	70	1.1e-10
Hydroxy Methacrolein	HOMACR	4	86	1.2e-10
Benzaldehyde	BENZALD	7	106	1.5e-10
Ketones				
Acetone	ACETONE	3	58	2.2e-12
Cyclobutanone	CC4-KET	4	70	2.9e-12
Methyl Ethyl Ketone	MEK	4	72	3.3e-12
Cyclopentanone	CC5-KET	5	84	5.0e-12
2-Pentanone	MPK	5	86	6.6e-12
3-Pentanone	DEK	5	86	4.1e-12
Cyclohexanone	CC6-KET	6	98	8.4e-12
4-Methyl-2-Pentanone	MIBK	6	100	1.6e-11
Methyl n-Butyl Ketone	MNBK	6	100	1.1e-11
Methyl-Butyl Ketone	MTBK	6	100	3.3e-12
2-Heptanone	C7-KET-2	7	114	1.4e-11
2-Methyl-3-Hexanone	2M-3-HXO	7	114	1.6e-11
Di-Isopropyl Ketone	DIPK	7	114	7.4e-12
2-Octanone	C8-KET-2	8	128	1.3e-11
2-Nonanone	C9-KET-2	9	142	1.4e-11
Di-isobutyl ketone	DIBK	9	142	3.0e-11
2-Decanone	C10-K2	10	156	1.5e-11
Biacetyl	BIACETYL	4	86	2.8e-10
Methyl vinyl ketone	MVK	4	70	9.3e-11
Hydroxy acetone	HOACET	3	74	5.1e-12
Methoxy Acetone	MEOACET	4	88	8.8e-12
Diacetone Alcohol	DIACTALC	6	116	5.0e-12
Phenol	PHENNOL	6	94	2.6e-11
o-Cresol	O-CRESOL	7	108	4.2e-11
Nitrobenzene	NO2-BENZ	6	123	1.5e-13

Compounds	Model Name	Cs	MWt	kOH (300) (cm^3/molec-sec)
Nitrogen-Containing Compounds				
Para Toluene Isocyanate	P-TI	7	134	5.9e-12
Toluene Diisocyanate	TDI	9	174	7.4e-12
Ethylene Diphenylene Diisocyanate	MDI	15	250	1.2e-11
Dimethyl Amine	DM-AMINE	2	45	6.6e-11
Ethyl Amine	ET-AMINE	2	45	2.8e-11
Trimethyl Amine	TM-AMINE	3	59	6.1e-11
Ethanolamine	ETOH-NH2	2	1	3.2e-11
Dimethylaminoethanol	DMAE	4	89	9.0e-11
Diethanol Amine	ETOH-HN	4	105	9.4e-11
Triethanolamine	ETOH-N	6	149	1.2e-10
N-Methyl-2-Pyrrolidone	NMP	5	99	2.2e-11
Halogen-Containing Compounds				
Methyl Chloride	CH3-CL	1	50	4.5e-14
Vinyl Chloride	CL-ETHE	2	62	6.9e-12
Ethyl Chloride	C2-CL	2	64	4.2e-13
Dichloromethane	CL2-ME	1	84	1.5e-13
Methyl Bromide	ME-BR	1	95	4.1e-14
1,1-Dichloroethane	11CL2-C2	2	99	2.6e-13
1,2-Dichloroethane	12CL2-C2	2	109	2.5e-13
Ethyl Bromide	C2-BR	2	119	3.1e-13
Chloroform	CHCL3	1	119	1.1e-13
n-Propyl Bromide	C3-BR	3	123	1.2e-12
1,1,1-Trichloroethane	111-TCE	2	133	1.2e-14
1,1,2-Trichloroethane	112CL3C2	2	133	2.0e-13
n-Butyl Bromide	C4-BR	4	137	2.5e-12
1,2-Dibromoethane	11BR2-C2	2	187	2.3e-12
Trans 1,2-Dichloroethene	T-12-DCE	2	97	2.3e-12
2-(Cl-methyl)3-Cl-Propene	CL2IBUTE	4	125	3.2e-11
Trichloroethylene	CL3-ETHE	2	131	2.3e-12
Perchloroethylene	CL4-ETHE	2	165	1.7e-13
Monochlorobenzene	CL-BEN	6	112	7.7e-13
Benzotrifluoride	CF3-BEN	7	146	4.6e-13
p-Dichlorobenzene	CL2-BEN	6	147	5.6e-13
p-Trifluoromethyl-Cl-Benzene	PCBTF	7	180	2.4e-13

The SAPRC mechanism includes the reactions of aromatics, terpenes and alkanes with OH radicals, alkenes with O_3, NO_3, OH radicals and O^3P, and organic radicals with NO_2. Inorganic reactions are also included in SAPRC model.

Hydrocarbons reacting with OH radicals can undergo hydrogen abstraction or OH addition, depending on whether the group has an abstractable hydrogen or a double bond. If the group has an abstractable hydrogen, the reaction is (Carter, 2000)

$$RH + OH^{\cdot} \longrightarrow R^{\cdot} + H_2O$$

Where RH is any H-containing group and $R^{\cdot}$ is the corresponding radical formed when the H atom is removed. If the compound has a double bond, an additional reaction can occur:

$$>C=C< + OH^{\cdot} \longrightarrow >C(OH)-C[^{\cdot}]-$$

For each molecule that reacts with OH, one reaction is generated for each group in the molecule that can react in this way.

Though reactions of VOCs primarily occur by OH radical initiation, under high NOx conditions, reactions of alkenes and aldehydes with NO_3 radical are not negligible. Reactions with NO_3 essentially proceed through the same pathways as reaction with OH radicals. For compounds that have an abstractable hydrogen, the reaction is

$$RH + NO_3 \longrightarrow R^{\cdot} + HNO_3$$

And for molecules with a double bond, the reaction is given by

$$>C=C< + NO_3 \longrightarrow >C(ONO2)-C[^{\cdot}]-$$

Besides reactions with OH radicals and NO_3, reactions of some classes of VOCs (e.g., alkenes) with O_3 are included in SAPRC mechanism. The reactions

involve O_3 addition across the double bond, followed by breaking the bond and the formation of a carbonyl and an excited Crigee biradical. Reactions are given by

$$>C=C< + O_3 \longrightarrow >CO_2[\text{excited}] + >C=O$$

Two reactions are generated for each C=C bond, forming biradical from each of the two groups around the bond.

The final type of reactions is reaction with O^3P radicals. O^3P reactions have found to be non-negligible in some environmental chamber experiments. Reactions of O^3P proceed through the addition of O^3P to C=C bonds, forming an excited adduct that may decompose or undergo collisional stabilization.

The important features of the chemical mechanisms for each compound class included in SAPRC model are described below

Inorganic reactions

Inorganic reactions represented explicitly in SAPRC include the formation and reactions of ground state O^3P oxygen atoms, the oxidation reaction of NO to NO_2, the reactions between HO_2 and NO_3, and the reaction of OH radicals with HO_2. Reaction of O^3P and oxidation of NO are important under relatively high NOx conditions. The reaction of HO_2 with NO_3 cannot be neglected under low NOx conditions and at nighttime. The reaction of OH with HO_2 affects the prediction of H_2O_2 levels, so it is included in base mechanism. In addition to these reactions, the reaction of OH with HONO, which was omitted in the previous SAPRC mechanism is included in SAPRC-99, because of its important as a radical source. A second

photolysis channel for $HONO^{\cdot}$, forming $H^{\cdot} + NO_2$ is also added. This channel estimated to account for approximately 10% of the reaction of HONO under typical atmospheric conditions (Carter, 1990). The removal process of OH radicals by NO_3 is included to account for some nighttime conditions.

Organic reactions

While over 300 organic reactants are represented explicitly in SAPRC, the level of characterization of reaction products is more limited. Nineteen species are employed to represent the reactions of the major organic photooxidation products. The oxygenated products include formaldehyde (HCHO), acetaldehyde (CCHO), propionaldehyde and lumped higher aldehydes (RCHO), acetone (ACET), methyl ethyl ketone and lumped higher ketone (MEK), glyoxal (GLY), methylglyoxal (MGLY), cresols (CRES), peroxyacetyl nitrate (PAN), peroxypropionyl nitrate and higher PAN analogues (PPN), and the PAN analogue formed from glyoxal (GPAN). This mechanism also includes a lumped alkyl nitrate species (RNO3), phenol (PHEN), nitrophenols (NPHE), benzaldehyde (BALD) and its PAN analogue (PBZN). Three species are used to represent uncharacterized aromatic fragmentation products (DCB1, DCB2, and DCB3). The mechanism and rate constants for the reactions for some of these oxygenated products are based on the chamber data by Atkinson (1988,1990). For compounds that do not have sufficient data from chamber experiments, the mechanisms and rate constants are estimated using data from surrogate compounds.

Organic peroxy and acyl peroxy radicals

The photooxidations of most organics involve the formation of intermediate peroxy or acyl peroxy radical species. The major depletion routes for these peroxy radicals are either through the reactions with NO, NO_2, HO_2, or with other peroxy or alkyl peroxy radicals. For example, the removal processes of alkyl peroxy radicals ($RO2^{\cdot}$) proceed through these reactions:

$RO2^{\cdot} + NO$	$\longrightarrow$	$NO_2 + RO.$	**Reaction 1**
$RO2^{\cdot} + NO$	$\longrightarrow$	$RONO_2$	**Reaction 2**
$RO2^{\cdot} + NO_2$	$\longrightarrow$	RO_2NO_2	**Reaction 3**
$RO2^{\cdot} + HO_2$	$\longrightarrow$	$RO_2H + O_2$	**Reaction 4**
$RO2^{\cdot} + RO2^{\cdot}$	$\longrightarrow$	products	**Reaction 5**

Polluted urban atmospheres include a large number of organics that can result in a large number of radical species formed. To reduce the size of mechanism and the number of species, surrogate compounds are used to represent these individual radical species. In addition, the reaction of peroxy + peroxy and peroxy + HO_2 radicals are neglected based on the assumption that under high NOx conditions, these reactions are less important than reaction of peroxy radicals with NO. Finally, organic radicals that either react rapidly or whose reactions do not depend on other reacting species are replaced by the set of products they ultimately form. A few organic radicals are represented explicitly because their reactions are sufficiently different than the reactions of other organics. These compounds include methyl peroxy radicals, acyl peroxy radicals, T-Butoxy radicals, phenoxy radicals, and nitro phenoxy radicals.

In the computational aspects of the model, radicals are categorized into active and steady state species. Active species such as acyl peroxy radicals and PAN analogues are model species whose concentrations need to be calculated by integrating their time rate of change. In contrast, steady state species are model species for which the steady state approximation can be employed. Radicals that react rapidly such as alkyl and alkoxy are classified as steady state species.

Peroxy radical operators

To reduce the potentially large number of peroxy radical mechanisms in the model, the approach of representing organic peroxy radicals with the set of products they would ultimately form, along with a set of chemical "operators" is employed. These operators include RO2R, R2O2, and RO2N.

Operator RO2R

Operator RO2R represents peroxy radical reactions with NO that result in NO to NO_2 conversion and formation of HO_2 radical. For example, the oxidation reaction of 1,3,5-trimethylbenzene with OH radical initiated by H abstraction from the aromatic ring in the presence of O_2 and NO, will result in 3,5-di-methyl-benzaldehyde and formation of HO_2 radical with the conversion of NO to NO_2 (pathway 1 in Section 3.3.2). This full mechanism can be summarized by the use of operator RO2R.

Full mechanism: 135-TMB + HO. + $2O_2$ + NO = NO_2 + HO_2. + 3,5-dimethylbenzaldehyde

Summarized mechanism: 135-TMB + HO. = BALD + 2C + RO2R

Thus the RO2R operator represents an NO to NO_2 conversion, with the creation of an HO_2 radical. The product 3,5-dimethyl-benzaldehyde is represented by the surrogate species benzaldehyde and two carbons are added to the products (2C) to provide a mass balance. Operator RO2R is treated as zero carbon species. The RO2R operator is also used in reactions such as:

$$RO2R + HO_2^{\cdot} \longrightarrow ROOH + O_2 \text{ -3C}$$

This reaction is a sink for RO2R. This reaction consumes 2 free radicals (HO_2 and RO2R, which normally results in the creation of HO_2) makes one less NO to NO_2 conversion possible and produces an organic peroxide (ROOH). When the operator is used, however, the left hand side of the equation has no carbon present, while the right hand side has, on average, 3 carbons (the number of carbons assumed for ROOH). So, to make the reaction balance a carbon adjustment must be included by employing "lost carbon" (C) species in reactions (Carter, 2000). Still other RO2R reactions are used, but will not be described here.

Operator R2O2

Operator R2O2 represents the effect of NO to NO_2 conversion without HO_2 formation. For example, the reaction of acetone with OH radical, O_2, and NO to form HCHO, CCO-O2 and NO_2. The operator R2O2 can be used to represent this full mechanism.

Full mechanism: ACET + HO. + O_2 + NO = HCHO + CCO-O2 + NO_2

Summarized mechanism: ACET + HO. =HCHO + CCO-O2 + R2O2

Unlike other operators, R2O2 does not imply the formation of a radical (such as RO2R implies the formation of $HO_2^{\cdot}$).

Operator RO2N

Operator RO2N represents the reactions of peroxy radicals with consumption of NO and various types of organic nitrate formation. For instance, aerosol precursor (APT1) reacts with OH radical via the addition at the carbon double bond, and the OH adduct then reacts with O_2 and NO to form organonitrate (TPM1) (pathway 4a in Section 3.2.2). This reaction pathway can be summarized by using operator RO2N.

Full mechanism: APT1 + HO. + O_2 + NO = TPM1

Summarized mechanism: APT1 + HO. = TPM1 + RO2N

In contrast to operator RO2R, RO2N conserves carbon. This operator is also used for reactions of peroxy radicals with species other than NO, but these reactions will not be described in detail here.

Alkane reactions

Gas-phase photooxidation reactions of alkanes are initiated primarily by OH radicals. The net effect of these reactions is represented by a single lumped reaction

OH. + alkane $\longrightarrow$ $a_1P_1 + a_2P_2 + \ldots$

Where P_1 and P_2 refer to the set of organic products formed and the various chemical operators, and a_1 and a_2 represent yields of these products or operators. Rate constants and product yields depend on the individual alkanes represented. The OH radical reaction rate constants and the product yields parameters for individual

compounds were derived based on results from chamber experiments by Carter and Atkinson (1985); Atkinson (1987, 1988, 1990).

Alkene reactions

Unlike alkane hydrocarbons, alkenes can react with O_3, NO_3, and OH radicals. SAPRC mechanism contains reactions of alkenes with all these radicals. In addition to primary initiation reactions of alkenes by those radicals, reactions of alkenes with O^3P are not negligible under high NOx conditions such as in plumes. Therefore, they are included in SAPRC mechanism to improve its range of validity.

Aromatic reactions

Mechanisms for aromatic hydrocarbons are based on reactions of OH radicals with aromatics involving hydrogen abstraction or addition of OH radical to the aromatic ring. H abstraction reactions result primarily in aromatic aldehydes, ketones, and small yields of aromatic nitrate. OH-addition to the ring forms phenols or cresols, and various ring fragmentation products.

Aromatic + OH $\xrightarrow{\text{abstraction}}$ Aromatic aldehyde or ketone or aromatic nitrate + operators + HO_2·

Aromatic + OH. $\xrightarrow{\text{addition}}$ Phenol or cresol + α-dicarbonyls and other fragmentation products + operators + HO_2·

Reactive aromatic fragmentation products that do not undergo significant photodecomposition to radicals are represented by DCB1. Reactive aromatic fragmentation products which photolyze with alpha-dicarbonyl-like structures are

denoted by DCB2. DCB3 signifies reactive aromatic fragmentation products which photolyze with acrolein like reactivity. Overall reactions of aromatics are represented as:

$$\text{OH. + aromatic} \longrightarrow y_{RH}\text{HO2.} + Y_{RR}\text{RO2R} + Y_{NR}\text{RO2N} + y_{Q2}\text{RCO-O2} + y_{PH}\text{PHEN} + y_{CR}\text{CRES} + y_{BL}\text{BALD} + y_{KG}\text{PROD2} + y_{GL}\text{GLY} + y_{MG}\text{MGLY} + y_{BA}\text{BACL} + y_{D1}\text{DCB1} + y_{D2}\text{DCB2} + y_{D3}\text{DCB3}$$

Where y_{RH}, y_{RR},….. are stoichiometric parameters. Mechanisms represented in the SAPRC model are assumed to be gas phase. A maximum of four alphanumeric characters are allowed to represent model species . For example, CRES is notation refers to cresol, and BALD is used to represent benzaldehyde.

Rate constants used in SAPRC are based on recommendations derived from Atkinson's atmospheric chamber experiments (1989, 1994, 1997). Unless referred to the falloff expression, these rate constants are given by the expression

$$k = A(T/300)^{B} \exp(-Ea/RT) \qquad \textbf{Equation 6}$$

Where k and A are in units of cm^3/molc-sec , T is the temperature in °K, and R is 0.0019872 kcal/°K-mole. For the fall off expression, the rate constant is both temperature and pressure dependent and is given by

$$k = [(k_0*M)/(1+(k_0*M/k_\infty))]*f^{g} \qquad \textbf{Equation 7}$$

$$g = 1/[1+(\log10[k_0*M/k_\infty]/n)^2] \qquad \textbf{Equation 8}$$

M is the pressure in molecules cm^{-3}, unless indicated otherwise f = 0.6 and n=1. k_0 and k_∞ are the rate constants at the low and high pressure limiting values.

Lumped species in SAPRC-99 model

To reduce the size of the mechanism and the number of species modeled in SAPRC, a group of compounds that have similar chemical and physical properties are lumped together and represented by surrogate compounds. The lumping approaches employed in SAPRC model are the variable lumped parameter and the lumped molecular method. For the first approach, the kinetic and product yield parameters of lumped model species are weighted by reactivity or molar concentration of the mixture of VOCs presented. The details of weighting methods applied in this approach are elaborated in the next chapter. For the second approach, compounds are represented by a model species on a molecule-for molecule basis. More details are addressed in the next chapter. Primary alkane hydrocarbons are lumped and represented by five model species: ALK1, ALK2, ALK3, ALK4, and ALK5, depending on their OH rate constant. Alkenes are separated and represented by two model species: OLE1 and OLE2 based on their OH rate constant. Model species ARO1 and ARO2 represent groups of slow and fast reactivity aromatic hydrocarbons, corresponding to their OH rate constant. Terpenes except isoprene, which is the dominant biogenic, are represented by TRP1. VOCs are lumped into these nine model species using the variable parameter approach. The reactive products of VOCs such as unsaturated aldehydes and ketones are lumped into product structure.

Reactive ketones whose reactions cannot be represented using lumped alkane classes are represented by MEK and PROD2. Emitted species that are represented explicitly include methene, ethene, isoprene, formaldeyde, acetone, methanol, and phenol. Table 3.2 summarizes lumped classes and lumped molecules employed in SAPRC model.

Table 3.2: Summaries of lumped classes and lumped molecule employed in SAPRC-99 model

Model Species	Description
Emitted Compounds Represented Explicitly	
CH4	Methane
ETHENE	Ethene
ISOPRENE	Isoprene
HCHO	Formaldehyde
ACET	Acetone
MEOH	Methanol
PHEN	Phenol
Lumped Molecule Groups	
CCHO	Acetaldehyde and Glycolaldehyde
RCHO	Lumped C3+ Aldehydes
MEK	Ketones that react with OH radicals slower than 5.0E-12 $cm^3/molec^2$-sec
PROD2	Ketones that react with OH radicals faster than 5.0E-12 $cm^3/molec^2$-sec
CRES	Cresols
BALD	Aromatic aldehydes (e.g., benzaldehyde)
METHACRO	Methacrolein and acrolein
ISOPROD	Unsaturated aldehydes other than acrolein and methacrolein
MVK	Unsaturated ketones
Unreactive Compounds	
INERT	Compounds other than CO or methane that do not react, or react only with OH with a rate constant less than approximately half that of ethane, or 2.0E+2 $ppm^{-1}min^{-1}$
Lumped Parameter Groups (Lumped using molar weighting except as indicated)	
ALK1	Alkanes and other non-aromatic compound that are react only with OH, and have an OH rate constant between 2.0E+2 and 5.0E+2 ppm^{-1} min^{-1}
ALK2	Alkanes and other non-aromatic compound that are react only with OH, and have an OH rate constant between 5.0E+2 and 2.5E+3 ppm^{-1} min^{-1}
ALK3	Alkanes and other non-aromatic compound that are react only with OH, and have an OH rate constant between 2.5E+3 and 5.0E+3 ppm^{-1} min^{-1}
ALK4	Alkanes and other non-aromatic compound that are react only with OH, and have an OH rate constant between 5.0E+3 and 1.0E+4 ppm^{-1} min^{-1}
ALK5	Alkanes and other non-aromatic compound that are react only with OH, and have an OH rate constant greater than 1.0E+4 ppm^{-1} min^{-1}
ARO1	Aromatics with kOH less than 2.oE+4 ppm^{-1} min^{-1} (Primarily toluene and other monoalkybenzenes) Benzene and slower reacting aromatics such as halobenzenes are lumped with reactivity weighting based on their OH rate constant relative to that of toluene, all others are lumped using molar
ARO2	Aromatics with kOH greater than 2.oE+4 ppm^{-1} min^{-1} (Primarily xylems and polyalkyl benzenes)

Model Species	Description
OLE1	Alkenes (other than ethane) with kOH less than 7.0E +4 ppm^{-1} min^{-1} (Primarily terminal alkenes)
OLE2	Alkenes with kOH greater than 7.0E+4 ppm^{-1} min^{-1} (Primarily internal or disubstituted alkenes)
TRP1	Biogenic alkenes other than isoprene (primarily terpenes)

Inputs required for SAPRC model

Inputs required to perform SAPRC simulations include four groups of parameters. The first group represents initial conditions, which are the initial composition of reacting mixture, temperature, and relative humidity. The second group describes the geographical data such as locations and date and time the simulations are performed which set solar intensity for photolysis rate calculations. The third group includes emission rates of emitted species. In addition to these three groups, parameters to characterize the loss mechanisms such as chamber wall loss coefficients, and deposition rates are optional inputs. Along with these inputs, the lumped control definitions can be modified and incorporated into the model, in case the lumped model species are assigned differently from the existing definition in SAPRC model.

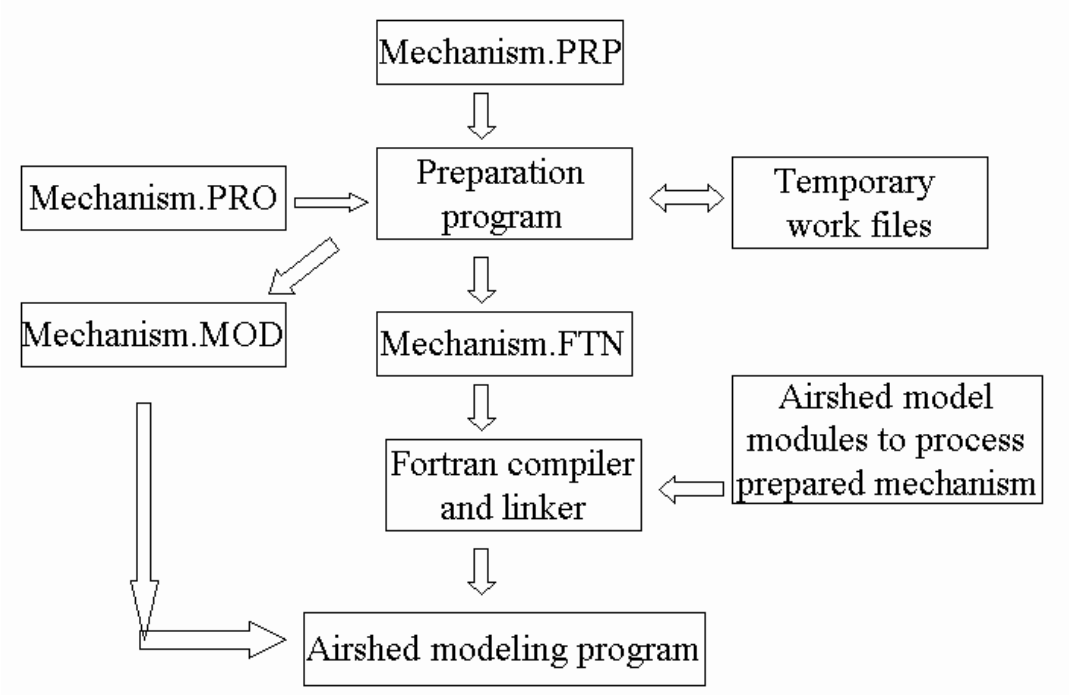

Figure 3.1: Overview of relationships between data files and programs used in the preparation of chemical mechanism for airshed model calculation (Carter, 1988)

Figure 3.1 demonstrates the data preparation process required in modeling simulations by the SAPRC model. All data required to prepare mechanisms and run simulation within SAPRC are provided in file *model.prp*. SAPRC uses these data to generate the file *model.mod* and *model.ftn*, which are required for implementation of the mechanisms in an airshed model. The file *model.pro* is also generated in the preparation process. This file contains the mechanisms generated by SAPRC, which are suitable for use by airshed models, a list of the mechanism species, and kinetic parameters. After all parameters are prepared, the file *model.ftn*, which contains Fortran source code, implements the chemical mechanisms. SAPRC is able to

calculate: 1) rates of all reactions, 2) concentrations of the steady state species, and 3) concentrations and formation and destruction rates of the active species.

3.3 Quantitative models of SOA formation

3.3.1 Previous smog chamber investigations

In order to develop chemical mechanisms for secondary organic aerosol formation it is necessary to identify hydrocarbons that are aerosol precursors and the rates at which they are emitted. Table 2.1 (in Chapter 2) illustrates an emission inventory of reactive organic compounds released into the Southern California air basin, which was organized by Grosjean and Seinfeld (1989). Grosjean and Seinfeld then used expert judgment to estimate aerosol yields from each of these precursors.

The goal of the thesis is to convert the fractional aerosol coefficients developed by Grosjean and Seinfeld based on expert judgment, to a more fundamental mechanistic basis. The analysis is based on a series of smog chamber experiments that were performed by previous investigators (e.g., Eusebi, 1996). These prior investigations examined the products formed in the photooxidation of hydrocarbon precursors, which are important in the formation of SOA. Compounds were selected for the smog chamber experiments based on their relative contribution to secondary loading in Los Angeles and the assumption that similar compounds (e.g., alkenes) would yield similar reaction products (Eusebi, 1996).

The experiments were performed by injecting the selected hydrocarbon precursors along with nitrogen oxides into batch reactors with Teflon walls, illuminated by ambient sunlight. The composition of aerosol produced in the chambers was monitored by collecting aerosol samples using a low pressure impactor and analyzing the collected samples using infrared microscopy. The IR data were used to estimate the relative molar loading of functional groups in the aerosol, and from these data, average product structures were calculated (Appendix A). This information was then used by Eusebi and others to develop qualitative photochemical mechanisms for organic aerosol formation (e.g., Holes et al. 1997, Dekermenjial et al., 1999). A major goal of this work is to convert these qualitative mechanisms into quantitative models of aerosol formation. This is specifically accomplished by developing quantitative mechanistic models of the chemical reactions that convert gas phase hydrocarbons into low volatility particulate matter.

3.3.2 Development of quantitative models of SOA formation

Pandis et al., (1992) found that a majority of secondary organic aerosol is attributed to aromatic precursors. In Los Angeles, aromatics are estimated to contribute 65% of the SOA. The significance of aromatic precursors in SOA formation indicates the importance for further studies into the reaction pathways and products from the atmospheric reactions of these species. For this reason, aromatic hydrocarbon precursors were selected for this study. Aromatic hydrocarbons selected

for this study are species modeled in SAPRC-99. The investigated precursors are listed in Table 3.3.

Table 3.3: VOC Emission Inventory and Secondary Aerosol Yields of Hydrocarbon Precursors Selected for Study

Hydrocarbon Precursor	Amount of VOC emitted (Southern California) (kg / day)	Fractional aerosol coefficient (%)	Fractions of VOC reacted	Amount of aerosol produced (kg / day)	Contribution in the total SOA (%)
Toluene	105,480	5.4	0.12	683.5	13.6
o-Xylene	19,614	5.0	0.26	255.0	5.0
m-Xylene	12,186	4.7	0.4	229.1	4.6
p-Xylene	12,057	1.6	0.28	54.0	1.1
Ethylbenzene	8,481	5.4	0.15	68.7	1.4
1,3,5-Trimethylbenzene	4,667	2.9	0.74	100.1	2.0
1,2,4-Trimethylbenzene	7,029	2.0	0.58	81.5	1.7
1,2,3-Trimethylbenzene	4,133	3.6	0.51	75.9	1.6
n-Propylbenzene	591	1.6	0.12	1.1	0.02
Isopropyl benzene	208	4.0	0.13	1.1	0.02
o-Ethyltoluene	1,282	5.6	0.23	16.5	0.3
m-Ethyltoluene	4,126	6.3	0.31	80.6	1.6
p-Ethyltoluene	1,345	2.5	0.21	7.1	1.4
Sec-butylbenzene	174	2.6	0.19	1.0	0.02

Conversion of gas phase aromatic hydrocarbon species to low volatility particulate matter occurs via a series of oxidation steps. Although ozone and NO_3 can participate, the majority of the oxidation reactions are initiated by hydroxyl radical. As shown below for trimethylbenzene, these reactions can either proceed through abstraction of hydrocarbon or via OH addition.

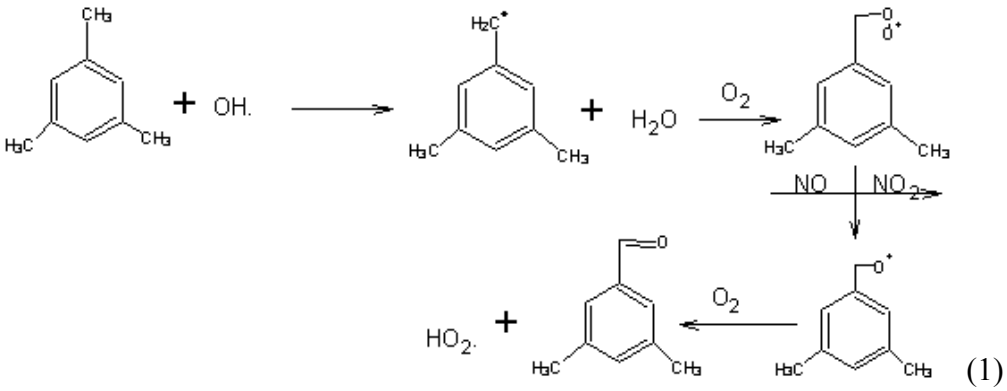

(1)

Figure 3.2: Hydrogen abstraction from 1,3,5-trimethylbenzene by OH radical

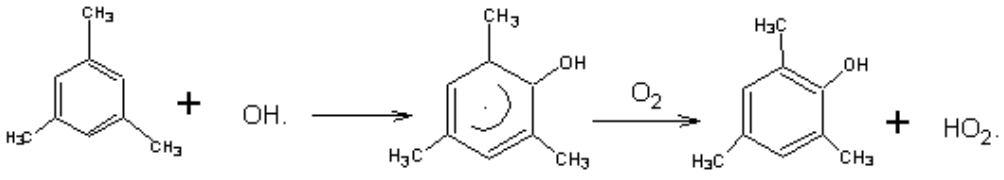

(2)

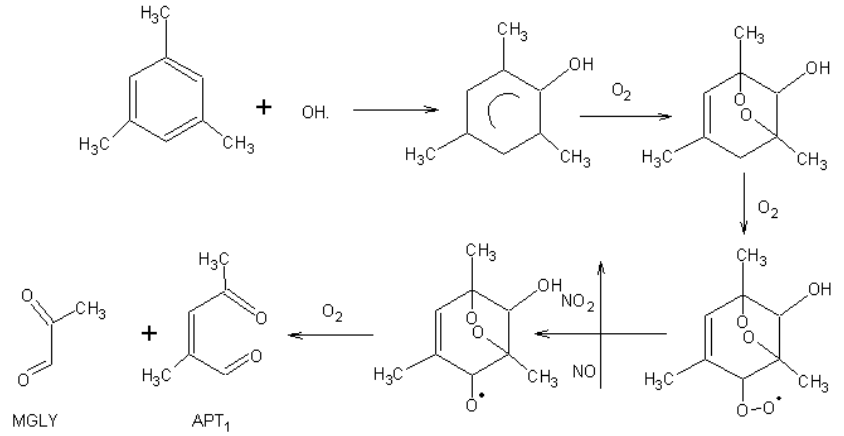

(3)

Figure 3.3: OH addition to 1,3,5-trimethylbenzene reaction pathways

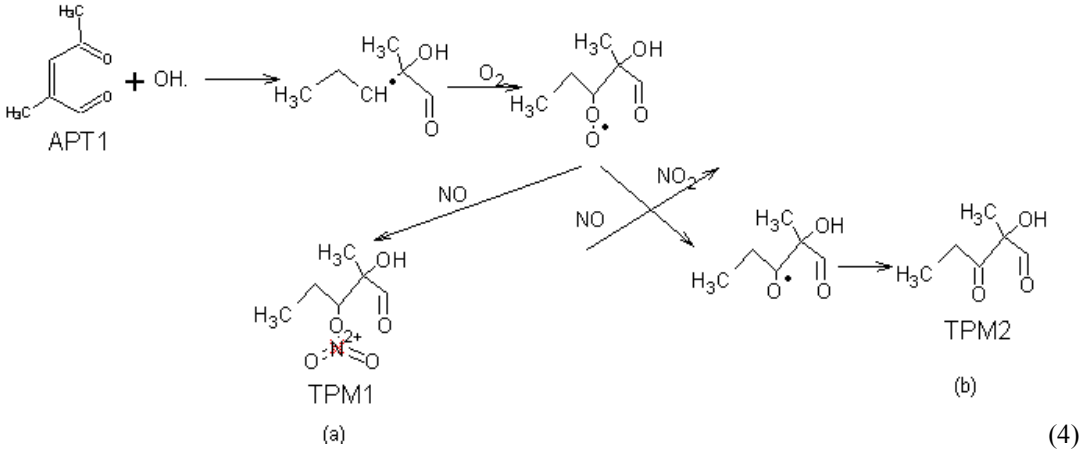

Figure 3.4: Semi-volatile product reaction pathways from aerosol precursors

Pathway 1 in figure 3.2 denotes initiation through H abstraction and pathways 2 and 3 show initiation via OH addition (Atkinson, 1990; 1994). Perry (1977) suggested that only 2.0 to 3.5% of the 1,3,5-trimethybenzene that reacts proceeds through the hydrogen abstraction route. The majority of gas-phase 1,3,5-trimethybenzene photooxidation reaction results in the dicarbonyl ring cleavage product (denoted aerosol precursor from trimethylbenzene, APT1). APT1 further reacts with OH radical to form condensable products TPM1 and TPM2 (trimethylbenzene-derived particulate matter), pathways 4a and 4b. Thus, this overall mechanism is a series/parallel network:

$$A + B \longrightarrow C$$

$$C + B \longrightarrow D$$

Where:

A = 1,3,5-trimethybenzene

B = OH radical

C = APT1 (dicarbonyl)

D = condensable product

In order to convert the current trimethylbenzene reaction in SAPRC, which only accounts for the initial reaction of 1,3,5-trimethylbenzene, into a form that accounts for SOA, a specific format is required.

Gas phase reaction in SAPRC: 135-TMB + $HO^{\cdot}$ = .18$HO2^{\cdot}$ + .804$RO2R^{\cdot}$ + .01RO2N + .621MGLY + .18CRES + .03BALD + .569DCB1 + .097DCB2 + .114DCB3 + 2.273XC

Based on the distribution suggested by Perry, 3% of products resulted from initiation by hydrogen abstraction, and 97% resulted from OH radical addition. In SAPRC notation, the hydrogen abstraction route of 1,3,5-trimethybenzene results in a dimethylbenzaldehydye (represented as benzaldehyde and two extra carbon atoms, BALD + 2C), along with an NO to NO_2 conversion and the production of HO_2 radical. Notation BALD is used to represent benzaldehyde, which has the structure as shown below. Since the product from the hydrogen abstraction of 1,3,5-trimethybenzene has similar structure with benzaldehyde but with two extra carbon atoms (as shown below), and because every single product cannot be included in the SAPRC mechanism, the dimethylbenzaldehyde is represented by BALD + 2XC.

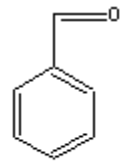

BALD

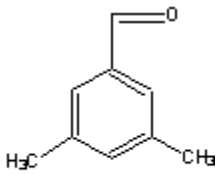

BALD + 2C

3%: 135-TMB + HO. = BALD + 2XC + RO2R **Reaction 6**

This route is assumed to account for 3% of the reacted 1,3,5-trimethybenzene (SAPRC99).

Addition of the OH radical to trimethylbenzene occurs at any of the three unsaturated aromatic carbons. All are equivalent. Initial reaction with OH radical will produce cresol with two extra carbon atoms (CRES +2XC) and HO_2 radical. This pathway accounts for 18.6% of the reacted trimethylbenzene (SAPRC99).

18%: 135-TMB + HO. = CRES + 2XC + HO2. **Reaction 7**

In the original SAPRC mechanism, the remainder of the OH-adduct (79% of total reaction) further reacts with O_2 with conversion of NO to NO_2 to form uncharacterized reactive aromatic ring fragmentation products (DCB1, DCB2, and DCB3), MGLY, and peroxy radical.

79%: 135-TMB + HO. = DCB1 + DCB2 + DCB3 + MGLY + RO2R

In the modified mechanism accounting for aerosol formation, the rest of the OH radical addition products further react with O_2 with conversion of NO to NO_2 to generate methyglyoxal (MGLY), peroxy radical, and unsaturated dicarbonyls (referred to as Aerosol Precursor (APT1)). This pathway accounts for 79% of all reactions (Bandow, 1985).

79%: 135-TMB + HO. = MGLY + APT1 + RO2R **Reaction 8**

Net: 135-TMB + HO. = .03 BALD + .18 CRES + .81 RO2R +
.18 HO2. + .79 MGLY + .79 APT1 + .42 XC **Reaction 9**

The species identified as BALD (pathway 1 in Figure 3.2), CRES (pathway 2 in Figure 3.3), MGLY (pathway 3 in Figure 3.3), TPM1, TPM2 and APT1 (pathway 4 in Figure 3.4) represent actual chemical species. The identifications RO2R, RO2 and RO2N represent operators, which indicate product formation pathways.

Aerosol precursor (APT1) further reacts with OH radicals via addition at the carbon double bond to form two types of condensable products (TPM1 and TPM2). TPM1 is the aerosol product containing organonitrate group (as shown in pathway 4a, Figure 3.4) and TPM2 (pathway 4b in Figure 3.4) is the product without the organonitrate group. TPM1 is produced through OH radical addition to the double bond in APT1. The OH-adduct reacts with O_2 and NO to form organonitrate. Experimental results from Eusebi (1996) suggest that 25% of APT1-OH addition reactions produce TPM1. The remaining APT1-OH-adduct reacts with O_2 and NO to form TPM2, NO_2, and HO_2 radical.

APT1 + HO. = .25 TPM1 + .75 TPM2 + .25 RO2N + .75 RO2R **Reaction 10**

Reactions 13 and 14 describe the condensed mechanisms of SOA formation for 1,3,5-trimethybenzene which proceed through two steps: gas phase reaction of 1,3,5-trimethybenzene with OH radicals to produce aerosol precursor (APT1), and reaction of APT1 with OH radical to form two types of potential aerosol products (TPM1 and TPM2). Stoichiometric coefficients in reactions 10-14 are obtained from the evaluation of atmospheric chamber experiments. Table 3.4 summarizes these coefficients and cites the source of the data.

Table 3.4: Kinetic parameters of 1,3,5-trimethybenzene reactions with OH radicals forming aerosol products and their sources

Notations	Descriptions	Stoichiometric Coefficients (SC)	Sources of SC
CRES	Cresol	0.18	SAPRC-99
BALD	Benzaldehyde	0.03	SAPRC-99
MGLY	Methylglyoxal	0.79	Bandow, 1985
HO2.	Hydroperoxy radicals	0.18	SAPRC-99
RO2R	Operator RO2R	0.82 (reaction 13)	Bandow. 1985, SAPRC-99
		0.75 (reaction 14)	Eusebi, 1996
APT1	Aerosol precursor	0.79	Bandow, 1985
RO2N	Operator RO2N	0.25	Eusebi, 1996
TPM1	Aerosol product species 1	0.25	Eusebi, 1996
TPM2	Aerosol product species 2	0.75	Eusebi, 1996
XC	Extra carbon	0.42	SAPRC-99

Besides 1,3,5-trimethybenzene, 1,2,4-trimethybenzene is a significant source of secondary aerosol formation as well. Odum (1996) performed a set of smog chamber experiments for 1,2,4-trimethybenzene to study the formation of secondary aerosol yield in terms of organic mass concentration. In this research, 1,2,4-trimethybenzene was studied by using information from Odum's experiments, the knowledge of chemical reaction pathways examined by Bandow (1985), and the application of 1,3,5-trimethylbenzene smog chamber results by Eusebi (1996). The reaction pathways for 1,2,4-trimethybenzene are shown in Figures 3.5-3.7.

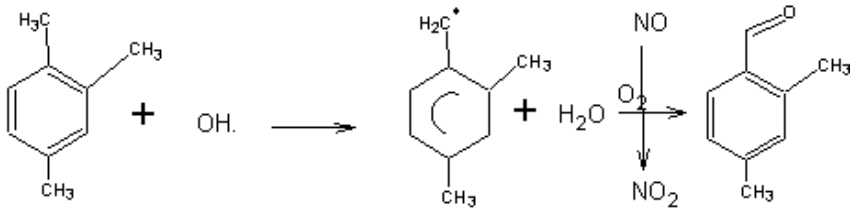

Figure 3.5: The H-abstraction from aromatic ring by the reaction of OH and 1,2,4-TMB

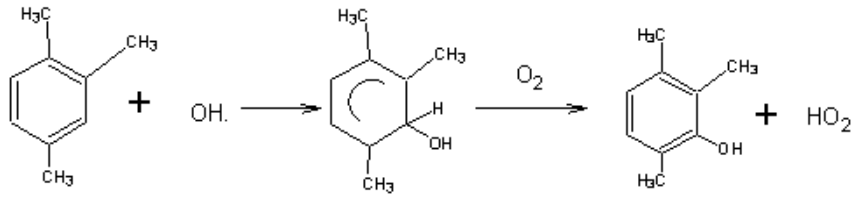

Figure 3.6: The OH-addition from aromatic ring by the reaction of OH and 1,2,4 TMB

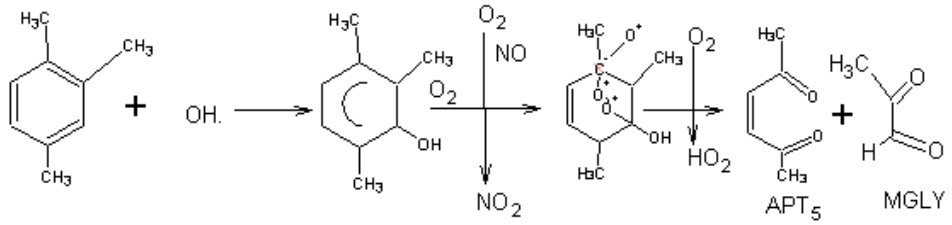

Figure 3.7: The ring fragmentation by the reaction of OH and 1,2,4-TMB

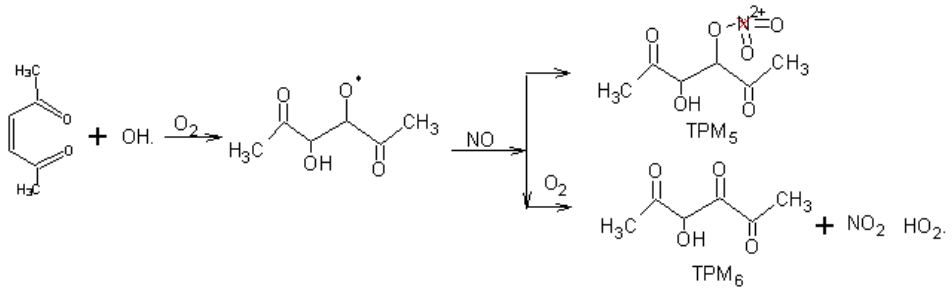

Figure 3.8: Aerosol product formation from oxidation reaction of 1,2,4-TMB

Similar to 1,3,5-trimethybenzene, oxidation of 1,2,4-trimethybenzene either proceeds through OH addition to the aromatic ring, or abstraction of H from the methyl group. It was found that 96% of products resulted from the addition of OH

radical to the aromatic ring, and 4% resulted from initiation by H abstraction (SAPRC99). The H abstraction route occurs primarily from the methyl substituents. In SAPRC notation, hydrogen abstraction reaction route of 1,2,4-trimethybenzene results in benzaldehyde and two extra carbon atoms (BALD + 2XC), with an NO to NO_2 convension and the production of an HO_2 radical (Figure 3.5).

4%: 124-TMB + HO. = BALD + 2XC + RO2R **Reaction 11**

This route is assumed to account for 4% of the 1,2,4-trimethybenzene that reacts. Initial reaction with OH radical can produce cresol with two extra carbon atoms (CRES + 2XC) and HO2 radical (Figure 3.6). This pathway accounts for 18.6% of the reacted 1,2,4-trimethybenzene.

18%: 124-TMB + HO. = CRES + 2XC + HO2. **Reaction 12**

The remaining OH radical addition products further react with O_2 and NO to NO_2 conversion to generate methyglyoxal (MGLY), glyoxal (GLY), biacetyl (BACL), and unsaturated dicarbonyls (refered to as Aerosol Precursors (APT5-9, and AP10). The addition of O_2 to the OH-aromatics adduct occurs at a position which yields conjugated double bonds. The ring cleavage reaction of the O_2-OH aromatics adduct can proceed through six possible positions on the aromatic ring. All of these potential reaction proceed through two similar steps: the abstraction of the O atom by NO, and the abstraction of the H atom by O_2. Figure 3.7 demonstrates the reaction pathway of APT5 production. Although the chemical structures of each speciess are different, the reaction pathway of APT5 production is similar to those for APT6-APT9 and

AP10 production. The cleavage reactions produce 25.4 % of APT5, 8.4 % of APT6, 13.1 % of APT7, 14.6 % of APT8, 4.6 % of APT9, and 10.7% of AP10. In addition to these unsaturated speciess, methyglyoxal (MGLY), glyoxal (GLY), and biacetyl (BACL) are also produced with the yields of 0.469, 0.192, and 0.107, respectively (Bandow, 1985). Formation of APT5-APT9 and AP10 accounts for 78% of all reactions (Bandow, 1985).

79% 124-TMB + HO. = .593MGLY + .243GLY + .135BACL + .321APT5 + .106APT6 + .166APT7 + .184APT8 + .058APT9 + .137AP10 + 1.26RO2R **Reaction 13**

Net: 124-TMB + HO. = .044BALD + .186CRES + .812RO2R + .18HO2. + .469MGLY + .192GLY + .107BACL + .254APT5 + .084APT6 + .131APT7 + .146APT8 + .046APT9 + .107AP10 + .46XC **Reaction 14**

Aerosol precursors (APT5-APT9, and AP10) react with OH radicals via addition at the carbon double bond to form two types of aerosol products, TPM6 and TPM7, which can be classified by the same criteria as for 1,3,5-trimethybenzene products. TPM5 is produced through OH radical addition, similar to TPM1. The OH adduct then reacts with O_2 and NO to form an organonitrate speciess. Results from Eusebi suggest that 25% of APT5-OH addition reaction leading to formation of TPM5 (Eusebi, 1996). The remaining APT5-OH reacts with O_2 and NO to form TPM6, NO_2 and HO_2 radical.

APT5 + HO. = .75TPM6 + .75RO2R + .25TPM5 + .25RO2N **Reaction 15**

Analogous to 1,3,5-trimethylbenzene, reactions 18 and 19 describe the condensed mechanisms of SOA formation for 1,2,4-trimethylbenzene, which proceed through two steps: gas phase reaction of 1,2,4-trimethylbenzene with OH radicals to produce aerosol precursor (APT5-APT9, and AP10), and reaction of aerosol precursors with OH radical to produce two types of condensable products (TPM5 and TPM6). Stoichiometric coefficients in reaction 18-19 are estimated based on smog chamber experiments. Table 3.5 lists these coefficients and cites the source of the data.

Table 3.5: Kinetic parameters of 1,2,4-trimethylbenzene reactions with OH radicals forming aerosol products and their sources

Notations	Descriptions	Stoichiometric coefficients (SC)	Sources of SC
BALD	Benzaldehyde	0.04	SAPRC-99
CRES	Cresol	0.18	SAPRC-99
GLY	Glyoxal	0.192	Bandow, 1985
BACL	Biacetyl	0.107	Bandow, 1985
MGLY	Methylglyoxal	0.469	Bandow, 1985
HO2.	Hydroperoxy radicals	0.18	SAPRC-99
RO2R	Operator RO2R	0.812 (reaction 18)	Bandow, 1985, SAPRC-99
		0.75 (reaction 19)	Estimated from 1,3,5-trimethylbenzene
APT5	Aerosol precursor	0.254	Bandow, 1985
APT6	Aerosol precursor	0.084	Bandow, 1985
APT7	Aerosol precursor	0.131	Bandow, 1985
APT8	Aerosol precursor	0.146	Bandow, 1985
APT9	Aerosol precursor	0.046	Bandow, 1985
AP10	Aerosol precursor	0.107	Bandow, 1985
RO2N	Operator RO2N	0.25	Estimated from 1,3,5-trimethylbenzene
TPM5	Aerosol product species 1	0.25	Estimated from 1,3,5-trimethylbenzene
TPM6	Aerosol product species 2	0.75	Estimated from 1,3,5-trimethylbenzene
XC	Extra carbon	0.46	SAPRC-99

As described above, formation of secondary organic aerosol proceeds through a series/parallel network. To analyze this network quantitatively, all reaction rates must be determined. Many of the reactions are well studied (such as trimethybenzene + OH radical) while for others rate constants must be estimated (e.g., APT1 + OH radical).

The reaction rate constants for the reaction of aerosol precursors, such as APT1 with OH radical, were calculated by using the Atmospheric Oxidation Program. The Atmospheric Oxidation Program for Microsoft Windows 3.1 (AOPWIN) estimates the rate constant for atmospheric gas-phase reactions between photochemically produced hydroxyl radicals and organic chemicals (Meylan, 1998). The estimation methods used by AOP are based on the structure-activity relationship (SAR) method developed by Dr. Roger Atkinson (Atkinson, 1985, 1986, 1987, 1991; Atkinson and Carter, 1984; Biermann et al., 1985; Kwok et al., 1992, Kwok and Atkinson, 1995; Kwok et al., 1996). This method uses the fact that the reactions of gas phase organic compounds with OH radical can proceed by four possible pathways. These pathways are: H-atom abstraction from C-H and O-H group, OH radical addition to >C=C< and -C≡C- bonds, OH radical addition to aromatic rings, and OH radical reaction with N-, S-, and P-atoms.

H-atom abstraction from C-H and O-H bonds

The rate constants for H-atom abstraction from $–CH_3$, $-CH_2$, >CH- groups depend on the identity of the substituents attached to these groups, with

$k(CH3\text{-}X) = k_{prim}F(X)$ **Equation 9**

$k(X\text{-}CH2\text{-}Y) = k_{sec}F(X)F(Y)$ **Equation 10**

$k(X\text{-}CH(Y)(Z)) = k_{tert}F(X)F(Y)F(Z)$ **Equation 11**

Where k_{prim}, k_{sec}, k_{tert} are the group rate constants for H-abstraction from $–CH_3$, $-CH_2-$, and >CH- groups, respectively, and F(X), F(Y), and F(Z) are the substituent factors for the substituent groups X, Y, and Z, respectively. Methyl group is chosen to be the standard substituent group, with $F(-CH_3) = 1.00$. Temperature dependence of the substituent factors F(X) is expressed as (Atkinson, 1995) $F(X) = e^{Ex/T}$. Group rate constants k_{prim}, k_{sec}, and k_{tert} were obtained from available database for the alkanes. The group rate constants at a wide range of temperatures were derived using the correlation $k= CT^2e^{-D/T}$. For compound classes other than alkanes, F(X) were derived from non-linear least square analysis based on the rate constants given by Atkinson (1989, 1994). The comparison between the calculated and experimentally measured rate constants presents an excellent agreement within a factor of 1.37 over the temperature ranges. Only 36 out of total 290 organic compounds (12%) show discrepancies over a factor of 2 between the calculated and experimental values. For example, the calculated and the experimental rate constants for H abstraction for cyclobutanone are 4.5E-12 and 0.87E-12 cm^3/molec-sec, respectively.

OH radical addition to >C=<C and -C≡C- bonds

Rate constants for OH radical addition to carbon-carbon unsaturated bonds depend on the number, identity, and position of substituent groups around these bonds. Conjugated double bond systems are dealt with by considering both double bonds as a single unit. Rate constants for addition to –CH=CH_2-, CH_2=C<, c-and t- -CH=CH-, -CH=C<, and >C=C< groups are based on those for propane, 2-methylpropene, c-and t-2-butene, 2-methyl-2-butene, and 2,3-dimehtyl-2-butene, respectively. If the substituent groups are not alkyl groups, group substituent factors C(X) are utilized. For example, CH_2=CHX

$$k(CH_2=CHX) = k(CH_2=CH)C(X) \qquad \textbf{Equation 12}$$

C(X) were derived by Atkinson from the available database for haloalkens, nitriles, and oxygenated organic compounds containing >C=C< bonds. The calculated and experimental rate constants of reactions involve OH radical addition to carbon-carbon unsaturated bonds are reliable within a factor of 2, and only six of total 98 compounds (6%) are different more than a factor of 2. For instance, the calculated and the experimental rate constants for OH radical addition to >C=C< for CH_2=CCl_2 are 2.67E-12 and 10.9E-12 cm^3/molc-sec, respectively.

OH radical addition to aromatic ring

Rate constants for OH addition to aromatic rings are estimated using the correlation between the OH radical addition rate constant and the sum of the electrophilic substituent constants $\sum\sigma^+$. A least square analysis of monocyclic aromatics and biphenols yield the correlation

$$Log_{10}k_{add} = -11.71-1.34\sum\sigma^{+} \quad \textbf{Equation 13}$$

The electrophilic substituent factors (σ^{+}) were obtained from experimental database by Atkinson (1991). The estimated rate constants from AOP programs for 12 out of 66 for monocyclic aromatics and biphenyls (18%) differ from the experimental values by greater than a factor of 2. For example, the calculated and the experimental rate constants for OH radical addition to o-xylene are 6.51E-12 and 13.7E-12 cm^3/molc-sec, respectively. The upper bound rate constant of ~2.0E-10 $cm^3molc^{-1}sec^{-1}$ is recommended for reactions involving OH addition to aromatic rings. The estimation of rate constants of PAH and alkyl-substituted PAH by AOP is uncertain due to a large number of assumptions such as ionization potential.

OH radical interaction with N-, S-, and P- containing groups

The group rate constants and substituent factors for reactions involving OH radical interaction with N-, S-, and P- containing groups were derived from experimental data by Atkinson, 1989. The calculated rate constants at room temperature for 34 N-, S-, and P- containing organic compounds are consistent with the experimental values to within a factor of 2. These rate constant estimation methods were not used in this work, however, so they will not be described here.

Condensed mechanisms and rate constants for 1,3,5-and 1,2,4-trimethylbenzene, calculated from the AOP program, are reported in the following table.

Table 3.6: Condensed mechanisms and rate constants for 1,3,5-and 1,2,4-trimethylbenzene

Aromatic Precursors	Aerosol Precursors	Condensed Mechanisms	Rate Constants (cm^3/molc-sec)	Source of Rate Constant
1,3,5-Trimethybenzene		135-TMB + HO. = 0.03BALD + 0.18CRES + 0.82RO2R + 0.18HO2. + 0.79MGLY + 0.79APT1+ .42XC	5.79e-11	SAPRC-99
	APT1	APT1 + HO. = 0.25TPM1 + 0.75TPM2 + 0.25RO2N + 0.75RO2R	2.60e-11	AOP Program
1,2,4-Trimethylbenzene		124-TMB + HO. = 0.04BALD + 0.18CRES+ 0.812RO2R + 0.18HO2. +0.469MGLY + 0.192GLY +0.107BACL + 0.254APT5 + 0.084APT6 + 0.131APT7 + 0.146APT8 + 0.046APT9 + 0.107AP10 + 0.46XC	3.35e-11	SAPRC-99
	APT5	APT5 + HO. = 0.25TPM5 + 0.75TPM6 + 0.25RO2N + 0.75RO2R	4.08e-11	AOP program
	APT6	APT6 + HO. = 0.25TPM5 + 0.75TPM6 + 0.25RO2N + 0.75RO2R	2.60e-11	AOP program
	APT7	APT7 + HO. = 0.25TPM5 + 0.75TPM6 + 0.25RO2N + 0.75RO2R	2.60e-11	AOP program
	APT8	APT8 + HO. = 0.25TPM5 + 0.75TPM6 + 0.25RO2N + 0.75RO2R	3.30e-11	AOP program
	APT9	APT9 + HO. = 0.25TPM5 + 0.75TPM6 + 0.25RO2N + 0.75RO2R	1.20e-11	AOP program
	AP10	AP10 + HO. = 0.25TPM5 + 0.75TPM6 + 0.25RO2N + 0.75RO2R	1.00e-11	AOP program

3.4 G/P Partitioning model

3.4.1 Theoretical Background

In addition to understanding the chemical mechanisms leading to secondary organic aerosol formation, it is also necessary to understand the partitioning of semi volatile secondary organic aerosol (SOA) species between gas and particle phases. This partitioning has been described by two conceptual frameworks. The first involves gas/particle partitioning through nucleation and condensation (McMurry and Grosjean, 1985). This principle assumes that once a vapor phase product exceeds its saturation concentration, it begins to condense onto existing seed particles. Aerosol mass then grows as a result of condensation of a condensable species. The second concept involves gas/particle partitioning according to simple thermodynamic principles such as Raoults' law (Pankow, 1994; Odum 1996). In this case, the condensable product will partition to the particulate phase at all gas-phase concentrations. The extent of particle partitioning can be described by the equilibrium between the gas-phase concentration of the condensable products and its concentration in the condensed phase. The basis for work presented in this thesis is the framework described by Odum. Odum et al. (1996) expressed SOA formation using the gas/particle partitioning absorption mechanism of Pankow (1994). In this framework, the amount of condensable product that is in the particulate phase is

related to the total particle mass concentration. A partitioning coefficient for species i (*Kom,i*) can be defined in terms of the organic mass concentration (Odum, 1996).

$$Kom,i = \frac{Fi,om}{Ai * Mo} \qquad \textbf{Equation 14}$$

$$Pi = Ai + Fi,om \qquad \textbf{Equation 15}$$

Where:

Fi,om = concentration of compound i in the absorbing organic material (om) phase ($\mu g/m^3$)

Mo = total organic mass concentration ($\mu g/m^3$)

Ai = gas phase concentration of compound i ($\mu g/m^3$)

Pi = total concentration of product i that is formed ($\mu g/m^3$)

Kom,i = partitioning coefficient of compound i ($m^3/\mu g$)

To examine the dependence of SOA yield on the total organic aerosol mass concentration, Odum assumed that the concentrations of individual products produced from photooxidation of reactive organic gases (ROG) are proportional to the amount of ROG that reacts in which

$$\alpha_i = \frac{P_i}{\Delta ROG} \qquad \textbf{Equation 16}$$

Where:

ΔROG = the amount of reactive organic gas reacts

α_i = proportionality constant relating the amount of ROG reacted to P_i

Combining the above equation with the definition of partitioning coefficient (equation 14) and equation 15 yields the expression for the overall SOA yield as a function of Mo as

$$\sum_i Yi = Mo \sum_i \left(\frac{\alpha_i * Kom,i}{1 + Kom,i * Mo}\right) \qquad \textbf{Equation 17}$$

Odum examined how SOA smog chamber data can be used to identify important sources of SOA in the urban environment using the expressions for secondary aerosol yields (Y_i) (equation 17). The expression was applied to over 30 chamber experiments performed in the summer of 1995. To fit the observed yield to equation (17), oxidation products for each parent hydrocarbon have been represented by two empirical products. Odum fit his experimental data for each compound with 4 adjustable parameters. He assumed four parameters: $Kom,_1$, $Kom,_2$, α_1, and α_2 that would fit the results from model calculations and experiments the best. While this study will use the Odum framework, the 4 adjustable parameters will be condensed to a single adjustable parameter. Alpha values (α_1 and α_2) will be obtained from the chemical mechanism described in the previous section. The partitioning parameters $Kom,_1$ and $Kom,_2$ will be assumed to have the same ratio as the vapor pressure of the aerosol products, i.e., $Kom,_1/Kom,_2$ = *Vapor pressure of other products /Vapor pressure of organonitrate products*. Therefore, compared to Odum study (which used 4 adjustable parameters α_1, α_2, $Kom,_1$, *and* $Kom,_2$) in this work only one parameter ($Kom,_1$) is adjusted to fit the SOA mass changes (ΔM_o).

The goal of this section of thesis is to employ both chemical mechanisms and the absorption partitioning model in determining SOA formation and estimates of SOA yields. This is accomplished by combining results from modified SAPRC mechanisms, as described in the preceding section, with partitioning between gas and particle phases model.

3.4.2 Estimates of Model Parameters

Once the quantitative models of SOA formation were developed and integrated into the SAPRC model, a series of model parameters were required. These parameters can be separated into two groups. The first group includes the kinetic parameters, which were described in the previous section. The second group involves the partitioning parameters, which are based on a single adjustable parameter, *Kom,1*. Table 3.7 lists the partitioning parameters, including their descriptions, and the procedures used to estimate them.

Table 3.7:Partitioning Parameters used in the estimates of SOA formation from reactions of hydrocarbon precursors

Parameters	Descriptions	Calculation Procedures
Kom,i	Partitioning coefficients of compound i	Estimated from chamber data
α_i	Proportionality constant relating the amount of ROG reacted to the total concentration of product i	Estimated from SAPRC rate parameters and branching ratios from chamber data
P_i	Total concentration of product i	SAPRC simulation based on ambient Houston data
ΔROG	Concentration of ROG that reacts	SAPRC simulation based on ambient Houston data
VP_i	Vapor pressure of product i	Antoine method and modified Grain method

A box model has been set up to examine the yields of secondary aerosol from individual hydrocarbon precursors. The box model uses the full SAPRC mechanism, including the additions of pathway to account for aerosol formation. The simulations were conducted under similar conditions to those performed in Odum's studies (1996, 1997). Initial conditions used in Odum's experiments, such as the concentration of parent hydrocarbons, NOx, propene, temperature, and relative humidity, were used in the simulations.

Simulation results include the amount of total product 1 and 2 (P_1 and P_2) produced from the amount of hydrocarbons reacted (ΔROG). For example, for 1,3,5-trimethylbenzene, P1 and P2 represent the total amount of organonitrate product (TPM1) and other product (TPM2) produced, respectively. Chemical structures of TPM1 and TPM2 are shown after Table 3.8. Since $P_1/\Delta ROG$ and $P_2/\Delta ROG$ are known from the SAPRC chemistry, as a function of ΔROG, α_1 and α_2, as a function of conversion, can be calculated. The partitioning coefficients of the two products ($Kom,_1$ and $Kom,_2$) were then estimated by

$$\frac{\alpha_1 * Kom,1}{(1 + Kom,1 * Mo)} + \frac{\alpha_2 * Kom,2}{(1 + Kom2 * Mo)} = \frac{1}{\Delta ROG} \qquad \textbf{Equation 18}$$

$$Kom,2 = \frac{Kom,1 * VP_1}{VP_2} \qquad \textbf{Equation 19}$$

Where:

VP_1 = vapor pressure of product 1 (mm Hg)

VP_2 = vapor pressure of product 2 (mm Hg)

$Kom,_1$ was determined by iteration In this calculation, $Kom,_1$ was the only adjustable parameter, because $Kom,_2$ was expressed as a function of $Kom,_1$, VP_1, and VP_2 as shown in Equation (19).

The vapor pressures of the condensable products from the individual hydrocarbon precursors were estimated by the MPBPWIN program (developed by Syracuse Research Corporation, 1996). MPBPWIN estimates vapor pressure based on three separate methods. The first is the Antoine method, which expressed vapor pressure as:

$$\ln Pvp = A - \frac{B}{T + C} \qquad \textbf{Equation 20}$$

In which T is in Kelvins. The second method is the modified Grain method. This method is applicable to solids, liquids, and gases (Meylan, 1996). The third method employs a correlation suggested by Mackey, in which vapor pressure is given by

$$\ln P = -(4.4 + \ln Tb)[1.803(\frac{Tb}{T} - 1) - 0.803\ln(\frac{Tb}{T})] - 6.8(\frac{Tm}{T} - 1) \qquad \textbf{Equation 21}$$

Where Tb is the normal boiling point (K), T is the VP temperature (K), and Tm is the melting point (K). This expression is derived from aliphatic and aromatic classes and halogenated compounds (also aliphatic and aromatic classes) (Meylan, 1996). MPBPWIN gives all three vapor pressures from the three methods, along with a "suggested" VP. A suggested VP is the average of the Antoine and the modified Grain estimates for liquids and gases. For solids, the modified grain estimate is the

suggested *VP*. The vapor pressure of the target compounds can be predicted by providing the chemical structure into MPBPWIN program.

The estimated partitioning coefficients and vapor pressures of condensable products from the reactions of 1,2,4- and 1,3,5-trimethylbenzene are reported in Table 3.8.

Table 3.8: The Estimated Partitioning Coefficients and Vapor Pressures of Condensable Products from trimethylbenzenes

Parent Hydrocarbon	$K_{om,1}$ ($m^3/\mu g$)	$K_{om,2}$ ($m^3/\mu g$)	VP_1 (mm Hg)	VP_2 (mm Hg)	Temp. (°K)
1,2,4-trimethybenzene	0.00609	0.00046	0.000113	0.0015	297
1,3,5-trimethybenzene	0.00337	0.00029	0.00026	0.0030	302

Condensable products from oxidation of 1,3,5-trimethylbenzene

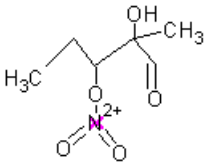

TPM1

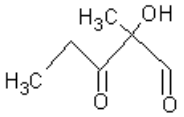

TPM2

Condensable products from oxidation of 1,2,4-trimethylbenzene

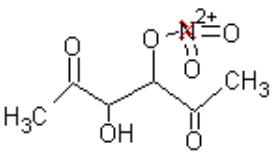

TPM_5

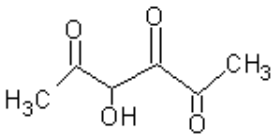

TPM_6

Comparison of SOA yields for 1,2,4-trimethylbenzene

As described in the previous section, chamber data from studies performed by Odum (1996, 1997) and vapor pressure data were used in the estimating of partitioning coefficients ($Kom,_1$ and $Kom,_2$). Six different initial conditions (Odum, 1996) were employed to simulate SOA formation and to estimate partitioning coefficients of low-volatile products for 1,2,4-trimethybenzene. These conditions are shown in Table 3.9. The Estimated partitioning coefficients were reported in Table 3.8.

Table 3.9: A set of simulation conditions for 1,2,4-trimethylbenzene, obtained from Odum's experiments

Date	ROGo (μg/m3)	ΔROG (μg/m3)	Mo (μg/m3)	NOx (ppb)	C_3H_6 (ppb)	ΔHC/NOx (ppb of C/ppb)	Y (%)
10/17B	2391	1996	113	975	300	4.7	5.66
11/02A	3367	2282	155	1178	300	4.3	6.79
11/02B	1607	1198	43	490	300	6.3	3.59
11/07A	1932	1533	78	590	300	6.3	5.09
11/07B	1237	1020	26.5	359	300	7.7	2.60
11/09B	1745	1309	53	528	300	6.2	4.05

SOA yields for 1,2,4-trimethylbenzene from modified SAPRC simulation calculations using a partitioning model were then compared to those from Odum's chamber experiments. Figure 3.9 shows SOA yields against total aerosol mass concentration (M_o).

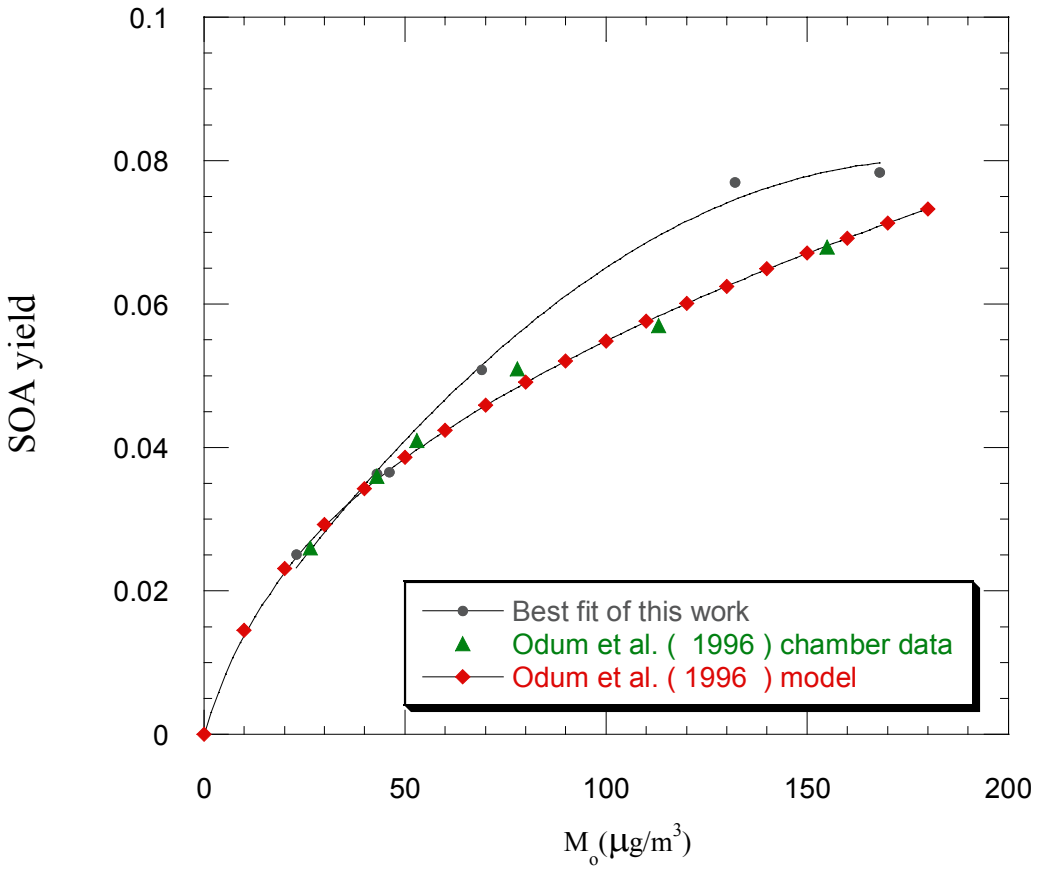

Figure 3.9: SOA yields for 1,2,4-trimethybenzene, NOx = 359-1178 ppb, C_3H_6 = 300 ppb, and ΔHC/NOx = 4.3-7.7 ppbC/ppb

Figure 3.9 illustrates SOA yields from the simulations (labeled best fit of this work), from the observed SOA yields from Odum (labeled as "Odum et al. (1996) chamber data"), and from the prediction of SOA yields from empirical model of Odum (labeled as "Odum et al. (1996) model" in figure). The comparison shows good agreement between two sets of simulations and the observations. This suggests that the quantitative models of SOA formation used in this thesis, relying on only one empirical partitioning parameter are in good agreement with chamber experiments.

3.4.3 Sensitivity Analysis of SOA yields: Case study for 1,3,5-trimethylbenzene

The model developed in this work, based on a chemical reaction mechanism and a single partitioning parameter showed good agreement with Odum's chamber experiments for 1,2,4-trimethylbenzene. The model therefore can be used to investigate the sensitivity of SOA formation to parameters such as VOC/NOx ratio, hydrocarbon composition, and others. These sensitivity analyses of SOA formation were initially performed for 1,3,5-trimethylbenzene (estimates for approximately a dozen compounds will be presented in the next section). 1,3,5-trimethylbenzene was selected for initial examination because of the availability of smog chamber experiments that provided estimates for the branching ratio for organonitrate formation (and hence accurate values of α_1 and α_2) (Holes et al., 1997; Eusebi, 1996). The sensitivity of SOA yields on the ratio of VOCs to NOx, the base

hydrocarbon composition, and other parameters were examined for 1,3,5-trimethybenzene in the presence of a typical urban mix of air pollutants using a box model. The box model used the full SAPRC mechanism. Initial conditions and composition of hydrocarbons used in the simulations are similar to those seen in the Houston area (Carter, 1998). Table 3.10 lists these conditions, while the hydrocarbon composition is displayed in Table B.1 (Appendix B).

Table 3.10: Initial conditions for box simulation for 1,3,5-trimethybenzene in the presence of Houston air pollutants.

Simulation time (hrs)	8
Reporting time (hr)	1
NO (ppm)	0.20806
NO_2 (ppm)	0.01095
CH_4 (ppm)	2.5606
NMOC (ppmC)	6.8367
CO (ppm)	2.1457
Temperature (K)*	312

* Temperature is a function of time; the value reported is at the beginning of the simulation. Temperature is based on ambient condition plus 10 degree to account for heating in chamber.

SOA yield as a function of conversion and VOC/NOx

Shown in Figures 3.10a and 3.10b are the yields of aerosol products as a function of 1,3,5-trimethybenzene conversion and time when VOC/NOx ranges from 4 to 31 (31 is the ratio for base case) ppmC/ppm. While concentration of non-methane organic carbons (NMOC) was fixed, concentrations of NO_2 and NO were changed to vary the VOC/NOx ratio between 4 and 31. In revising to the NOx concentration, the initial ratio of NO to NO_2 was kept constant. Figure 3.10a

suggests that SOA yield (Y), which is the ratio of the amount of condensable products partitioning to particulate phase to the amount reacted of primary hydrocarbon ($\Delta M_o/\Delta ROG$), depends on percent 1,3,5-trimethybenzene conversions. The yield is a parabolic function of conversion. SOA yields at various VOC/NOx ratios presented against percent conversion are essentially collapsed onto a single line. In contrast, figure 3.10b shows that VOC/NOx ratio affects overall VOC reaction rates by effecting OH radical concentration. Therefore, when plotted versus reaction time, the SOA yield depends on VOC/NOx ratio.

$$\Delta M = f(\%\ \text{primary VOCs conversion})$$

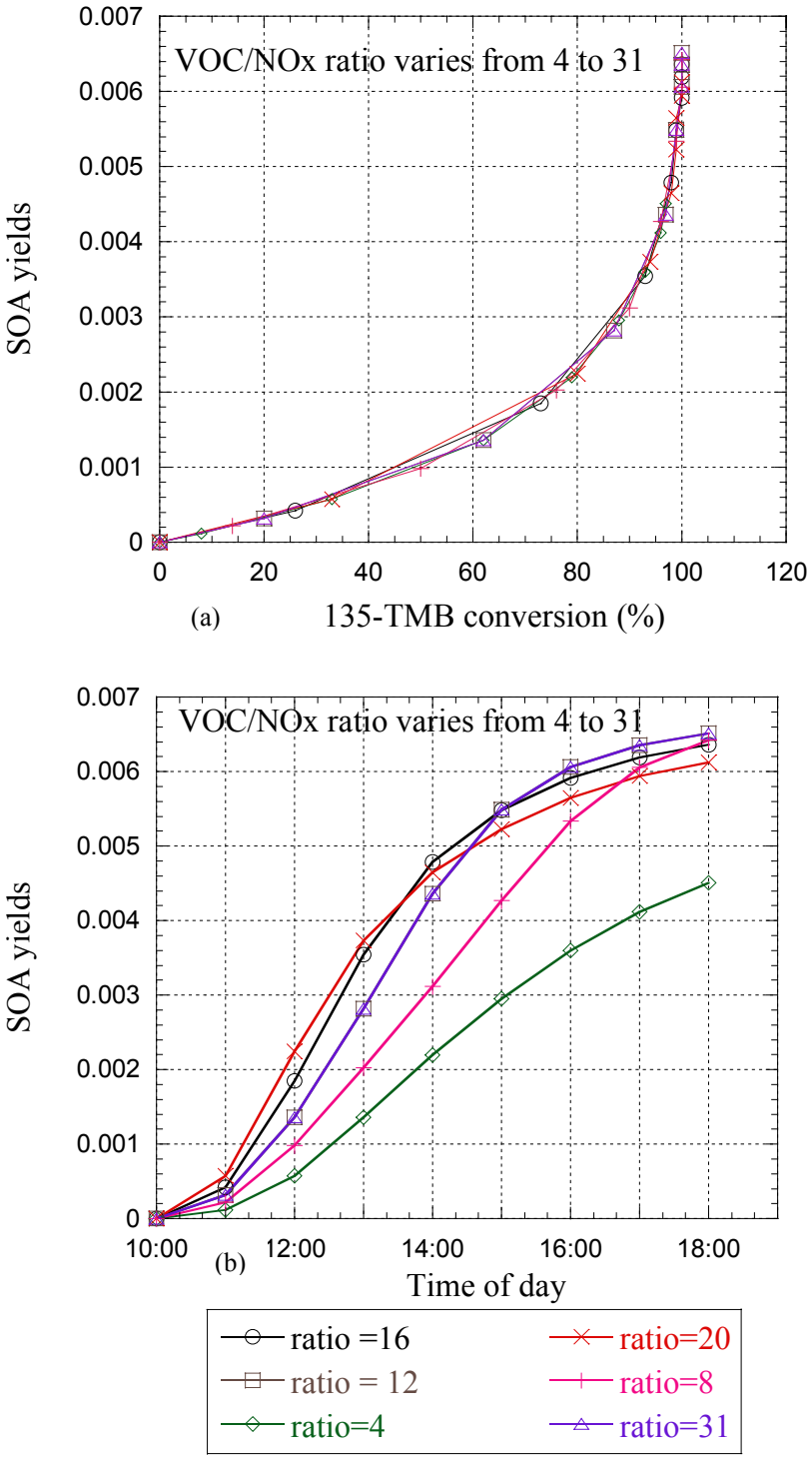

Figure 3.10: SOA yields for 1,3,5-trimethybenzene represented as %conversion and C.D.T, Houston conditions

This has implications in formulating SOA yield parameters for photochemical grid models, as will be described later in this thesis.

SOA yields as a function of hydrocarbon composition

To examine the effect of the base hydrocarbon composition on SOA yield, the composition of alkenes was reduced by 50% from the base case, and the reduced mass was added to alkanes. Then the box model simulation was run again and the SOA yield for 1,3,5-trimethylbenzene was compared to the SOA yield for the organic base hydrocarbon mixture. The calculation was repeated with 50% of the aromatics in the base mixture converted to alkanes. Shown in Figure 3.11 are SOA yields represented as a function of %conversion of 1,3,5-trimethybenzene compared between the organic base case hydrocarbon composition and the modified base hydrocarbons. There is no significant difference among results for all cases in Figure 3.11. These results suggest that SOA yield, expressed as a function of conversion, is independent of base hydrocarbon composition.

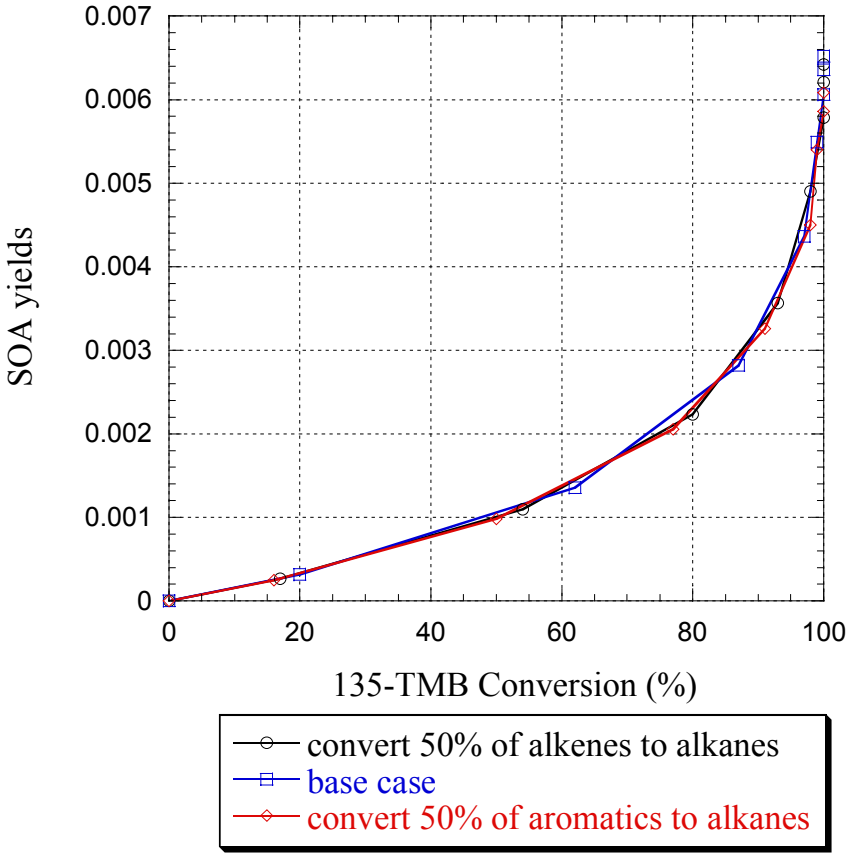

Figure 3.11: SOA yields for 1,3,5-trimethybenzene at different base hydrocarbon composition represented against %conversion and C.D.T., Houston conditions

SOA yields as a function of rate parameters

The sensitivity of SOA yield to the values of rate parameters was examined. The rate constant for the reaction of aerosol precursor for 1,3,5-trimethybenzene (k_{APT1}) was varied from 1.00E-9 to 1.00E-13 cm^3/molc-sec. SOA yields are illustrated against percent 1,3,5-trimethybenzene reacted in Figure 3.12. As is evident from the Figure, SOA yield is rate parameter dependent. Increasing rate

constant of the reaction of aerosol precursor with OH enhances the extent of reaction. However, ultimately SOA yields for the OH rate constant of aerosol precursor converge at the same point for 100% conversion. At k_{APT1} below 1.0E-12 cm^3/molc-sec the production of organic particulate products is barely detectable at most levels of conversion.

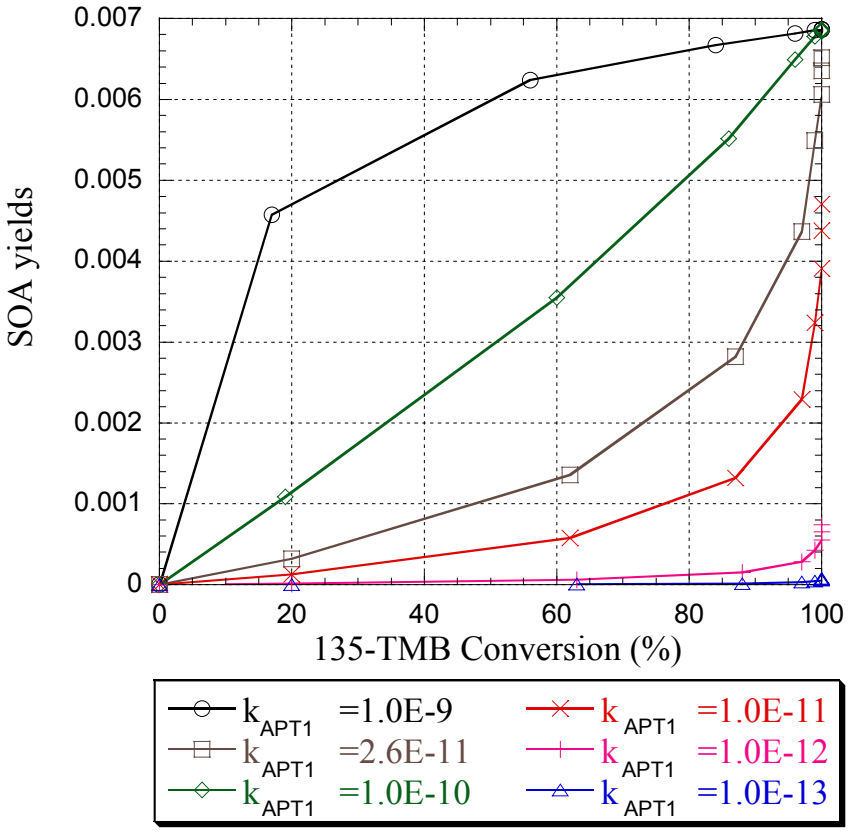

Figure 3.12: SOA yields for 1,3,5-trimethybenzene for rate constant of aerosol precursor varies from 1.0E-9 to 1.0E-13 cm3/molc-sec, Houston conditions

The behavior shown in Figure 3.12 is due to the series nature of the aerosol (TPM) formation chemistry. Hydrocarbon precursor reacts with OH radical to form aerosol

precursor (APT), then APT further reacts with OH radical to form semivolatile product species TPM.

$$\text{TMB} \xrightarrow{k_{TMB}} \text{APT} \xrightarrow{k_{APT}} \text{TPM}$$

As the value of k_{APT} is reduced, APT accumulates as trimethylbenzene reacts, rather than forming aerosol species (TPM).

SOA yields as a function of organic particulate mass

The dependence of gas/particle partitioning on the organic particulate mass was examined for 1,3,5-trimethybenzene. The initial amount of aerosol mass that was used in the box model (M_{int}) was varied from 5 to 15 μg/m^3. SOA yields for both cases were compared as shown in Figure 3.13. The SOA yields for M_{int} equal 5 and 15 μg/m^3 are different by a factor of 2 for the build-up period of aerosol precursor concentrations (up to 40% conversion). Beyond 40% conversion, the differences gradually increase and then reach a constant factor of 3 after 50% conversion. The dependence of aerosol yield on M_{int} can vary depending on the reactivity of parent hydrocarbon and the aerosol precursor compounds. In this thesis, the relationship between the aerosol yield and M_{int} will be assumed to also depend on vapor pressure, which can be expressed by:

$$Y = f(M_{int}, VP)$$

Where VP is vapor pressure of condensable products.

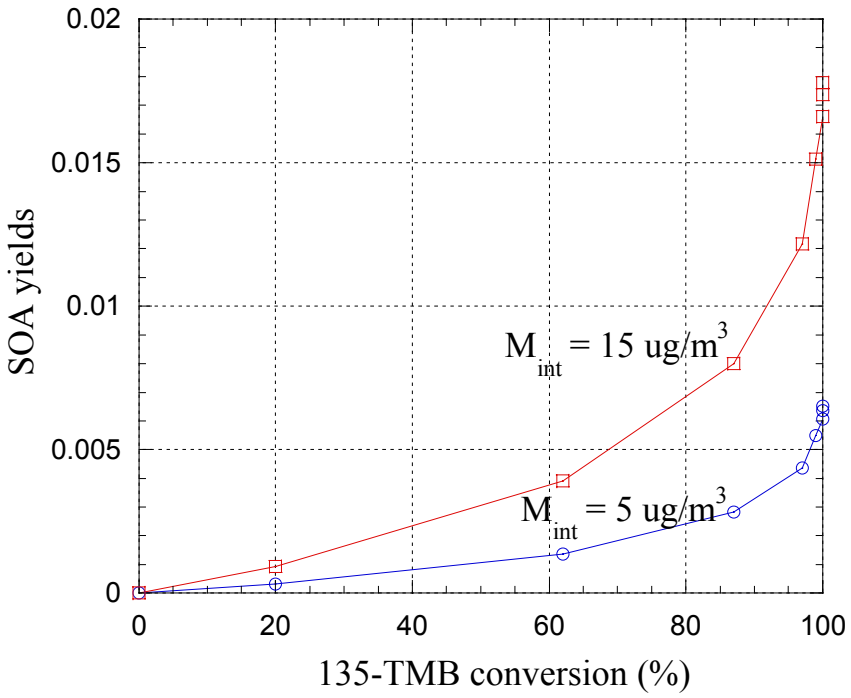

Figure 3.13: SOA yields for 1,3,5-trimethybenzene for organic particulate mass (M_{int}) equals 5 and 15 µg/m^3, Houston conditions

SOA yields as a function of partitioning coefficient (*Kom*)

Partitioning coefficients (*Kom,1* and *Kom,2*) are employed to describe the physical partitioning of semi volatile products onto available organic medium (M_{int}). To examine how SOA yield is sensitive to the values of these parameters, *Kom,1* was varied by factors of 2 and 3 from the original value. Because *Kom,1* and *Kom,2* are related through the vapor pressures of the compounds, changing *Kom,1* will result in proportional changes in *Kom,2*. SOA yields represented as a function of 1,3,5-trimethylbenzene conversion at the base case, double the base case, and triple the base case *Kom* are shown in Figure 3.14. Results reveal that at the early stage of

reaction (up to 40% conversion), the differences of SOA yields for three cases are small. Beyond 40% conversion the differences in SOA yields begin to increase in magnitude. At 60% conversion the yields at triple and double *Kom* are approximately 2.3 and 1.6 times higher than yield at original *Kom*. These results lead to the conclusion that the amount of condensable species partitioning onto the existing organic mass is sensitive to the values of partitioning coefficients (*Kom,1* and *Kom,2*).

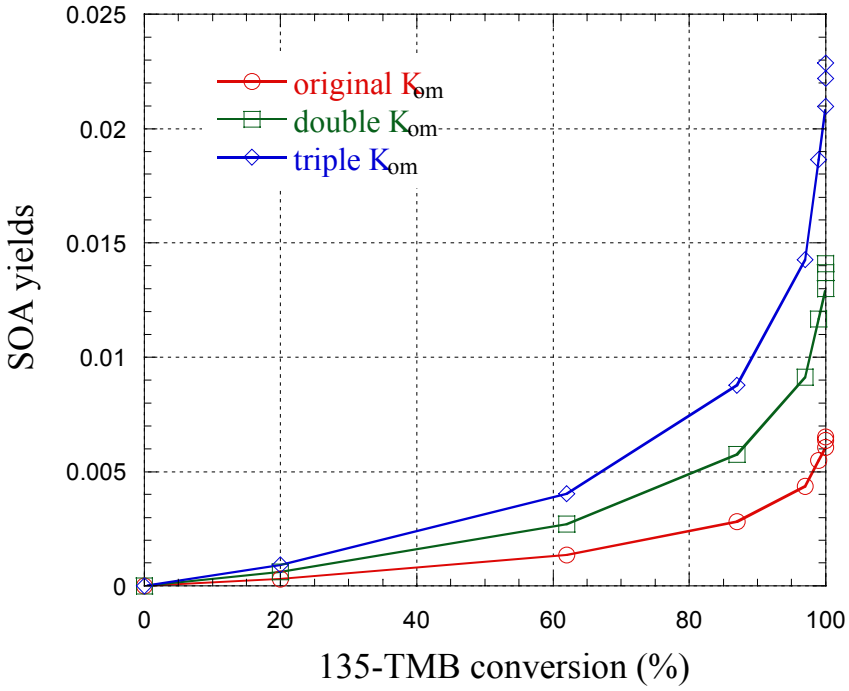

Figure 3.14: SOA yields for 1,3,5-trimethylbenzene for the original, double, and triple values of Kom,1 and Kom,2. Simulation conditions are based on the CARB report (Carter, 1998).

Correlation between SOA yield and chemical and physical parameters

Previous work (Odum et al, 1996; 1997) suggested that secondary organic aerosol formation is best described by a gas/particle partitioning model. This model is described in section 3.4.1. Odum et al. showed that SOA yields for individual hydrocarbon precursors are a function of Mo. Experimental data were fit to a 4 parameter model where the 4 parameters are Kom_1, Kom_2, α_1, and α_2. In Odum's work these parameters were determined empirically and were assumed to be constant. In contrast, the previous sections in this thesis have shown that while SOA yield is a function of Kom_i, the values of these variables have physical and chemical constraints and the α_i's are not constant but depend on extent of conversion. Thus, the Odum approach and the approach described in this work have the following basic differences

- Odum assumes aerosol yield depends only on M_o while this work assumes SOA yield depends on M_o and conversion of the parent hydrocarbon. The conversion dependence in this work is determined by the dependence of α_i on conversion.
- Odum uses four adjustable parameters to described experimental data while this work uses one adjustable parameter with other parameters determined from reaction branching ratios and relative vapor pressure.

Comparison of the results of applying these two approaches was performed for m-xylene and n-propylbenzene. The amount of products partitioning into aerosol

phase (ΔMo) as a function of percent conversions of hydrocarbon were estimated for Odum's model with 4 parameters and for the modified SAPRC model with a single adjustable parameter (this work).

Figure 3.15 illustrates the comparison. Figure 3.15a is the results of simulation using m-xylene as a representative of the low-yield and high reactivity hydrocarbons. It shows that Odum's model (blue) is more linear than compared with the modified SAPRC model (red). The modified SAPRC model does not predict yield of secondary organic aerosol until conversion of parent hydrocarbon proceeds to approximately 70%, and beyond that point, SOA yield dramatically increases. This represents the fact that loss of parent hydrocarbon is not directly related to condensable product formation, but is a consequence of both formation of aerosol precursor and condensable products. As a result Odum's model predicts more SOA yield at lower percentage of conversions and the modified SAPRC model predicts more yield at higher conversion. It also is noted that slope of SAPRC based model is significantly steeper at higher conversion. This might require extra caution in designing experiments to determine SOA yield. Estimates of yield may be affected significantly by the extent of reaction.

Figure 3.15b is the results for n-propylbenzene, which represents species with high PM yield and low reactivity. In this plot, the difference between two models is less distinctive compared to the results for m-xylene.

Results for both m-xylene and n-propylbenzene at M_{int} equal 5 and 15 μg/m^3 show no significant differences. However when available aerosol mass concentration at the initial gets higher (more than 25 μg/m^3), the differences become more evident. This advocates that the condensation of low volatile products relate to initial aerosol mass concentration (M_{int}).

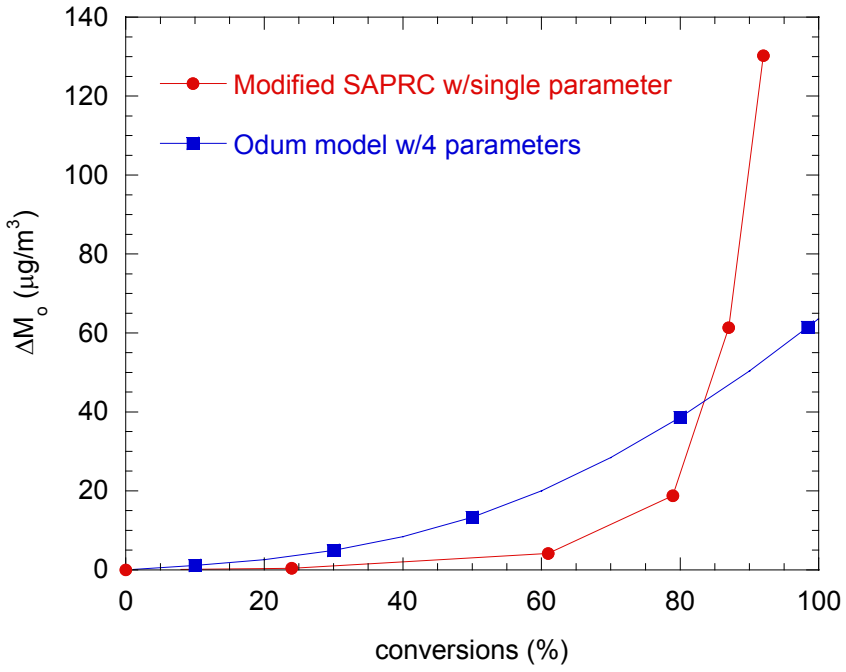

(a)

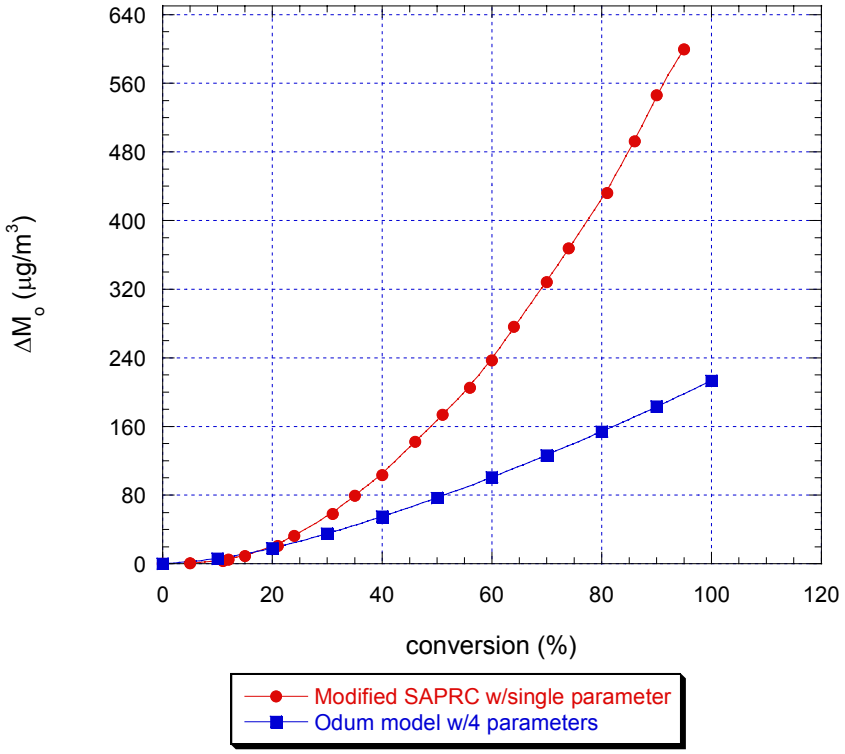

(b)

Figure 3.15: ΔMo versus % conversion of parent hydrocarbons from Odum model with 4 parameters and modified SAPRC model with single parameter

Evidently SOA yields are associated to physical and chemical properties. To develop a quantitative relationship between the amount of condensable species partitioning to aerosol phase and these physical parameters, it is useful to start with a mass balance.

Mass balance in aerosol phase:

$$M_{tot} = M_{\text{int}} + \sum_i massfraction_i * M_{tot} \qquad \textbf{Equation 22}$$

Where

M_{tot} = total amount of organic aerosol mass (μg/m^3)

M_{int} = amount of organic mass served as medium (μg/m^3)

$massfraction_i$ = mass fraction of species i in aerosol phase

Rearranging Equation 22 yields

$$M_{tot} = \frac{M_{\text{int}}}{(1 - \sum_i massfraction_i)} \quad \textbf{Equation 23}$$

Mass Balance for species i in two phases:

$$P_i = A_i + massfraction_i * Mtot \quad \textbf{Equation 24}$$

Where

P_i = total amount of semivolatile particulate matter species i generated from reaction ($\mu g/m^3$)

A_i = mass concentration of semivolatile particulate matter species i in gas phase ($\mu g/m^3$)

At equilibrium:

$$Kom_i = F_{i,om}/A_i * M_o \quad \textbf{Equation 25}$$

$$massfration_i / Kom_i = A_i \quad \textbf{Equation 26}$$

Substituting A_i into Equation 24 gives

$$P_i = massfraction_i / Kom_i + massfraction_i * M_{tot} \quad \textbf{Equation 27}$$

$$massfraction_i = \frac{P_i}{1/Kom_i + M_{tot}} \quad \textbf{Equation 28}$$

Substituting Equation 28 into Equation 23 and rearranging yields:

$$M_{tot} - \sum_i \frac{M_{tot} * P_i}{1/Kom_i + M_{tot}} = M_{\text{int}} \quad \textbf{Equation 29}$$

From Equation 29 M_{tot} can be solved for numerically based on the known parameters ($Kom_{,i}$, and P_i). In this work, equation 29 will be solved numerically using an equation solver in Microsoft excel.

Equation 29 relates a total aerosol mass to an initial aerosol mass through an equilibrium parameter *Kom*, the total mass of semivolatile product P_i, and the volume of the gas phase. Equations 22-28 also hold for a change in P_i, ΔP_i, and a change in aerosol mass ΔM_i. This type of relationship, shown in Equation 30, will be particularly effective for use in 3D Eulerian air quality models. In these grid models, the goal will be to calculate a change in aerosol mass in a grid cell for each time step, based on the amount of semivolatile product produced during that time step. The expression will be of the form:

$$\Delta M_i = (\%DF)_i * (\Delta P_i) \qquad \textbf{Equation 30}$$

Where $\%DF_i$ = distribution factor (expressed as a percentage) of species i in the aerosol phase (and is a function of M_{int} or M_{tot})

Note that this form for ΔM_i differs from the form used in most current grid models, where

$$\Delta Mi = Yi * \Delta ROG \qquad \textbf{Equation 31}$$

In the traditional form, the aerosol yield depends on the amount of hydrocarbon precursor that has reacted. In this formulation, the yield of aerosol (Y) will depend on conversion, partitioning parameters and initial aerosol composition (α_i, $Kom_{,i}$, and

M_o in the model of Odum (1996). In contrast, equation 30 separates the aerosol yield into a conversion dependent component (ΔP_i) and a component dependent on *Kom* and M_{int}. This formulation is useful in a grid model because SOA yield ($\Delta M_i/\Delta ROG$) strongly depends on conversion (see Figure 3.11). In a grid cell, it is impossible to determine whether a given amount of ΔROG (e.g., amounting to 10% conversion) leads to a large amount of semivolatile product (e.g., conversion increasing from 90% to 100%) or to a small amount of product (e.g., conversion increasing from 0% to 10%) and it is very difficult to account for accumulated conversion as material advects between grid cells.

The proposed formulation requires that the concentration of individual aerosol products be followed, but (equation 30) makes the physical partitioning independent of conversion, as demonstrated below.

Demonstrating that $\%DF_i$ depends only M_{int} and is independent of %conversion was done for 1,3,5-trimethylbenzene. M_{int} was changed from 5 to 15 and 25 μg/m^3, and $\%DF_i$ at 25%, 50%, and 75% conversions were then calculated for each M_{int} level. Shown in Figures 14a and b are *%DF* and ΔM for condensable products formed from reaction of 1,3,5-trimethylbenzene with OH radicals against M_{int} at 25%, 50%, and 75% conversions, respectively. Figure 3.16 shows that $\%DF_i$ depends on M_{int}. The values of $\%DF_i$ are independent of % conversion. The polynomial best fit of these results yields the empirical function of $\%DF_i$ and M_{int} for 1,3,5-trimethylbenzene as expressed below.

$$\%DF_i = -0.0005(M_{int})^2 + 0.13(M_{int}) - 0.0375 \quad \textbf{Equation 32}$$

Therefore at any given M_{int}, $\%DF_i$ can be estimated for 1,3,5-trimethylbenzene, and consequently ΔM can be predicted by using Equation 30.

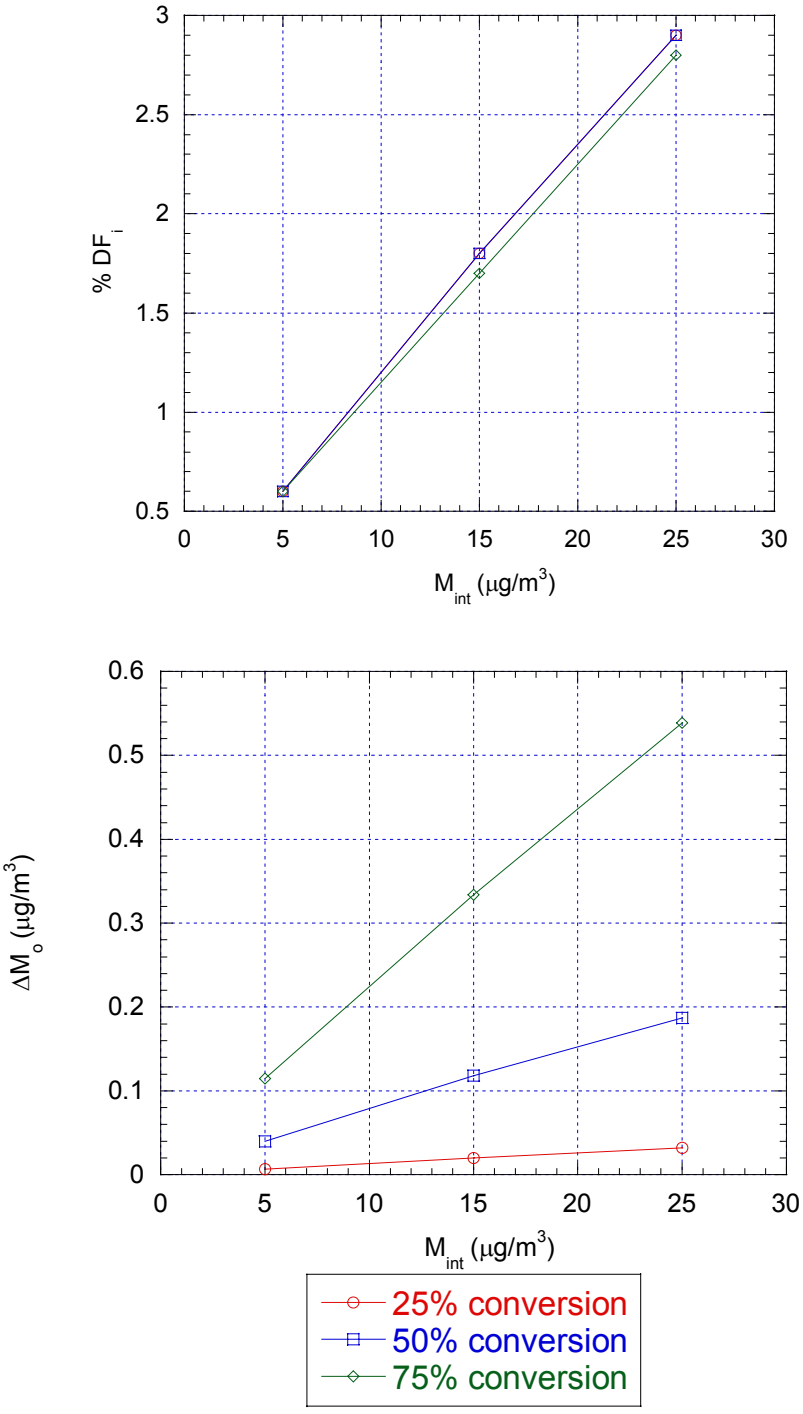

Figure 3.16: *%DF* and *ΔM* as a function of M_{int} at 25%, 50%, and 75% 1,3,5-trimethylbeznene conversions. Simulation conditions were obtained from the CARB report (Carter, 1998)

3.5 Quantitative models of SOA formation for various aromatic hydrocarbons

Section 3.4 described how ΔM_i could be calculated for a single hydrocarbon and showed that a function of the form:

$$\Delta M_i = \%DFi * \Delta P_i$$

could be developed where $\%DF_i$ depended only on *Kom* and M_{int}. However, because $Kom,_i$ is compound specific, the expression for $\%DF_i$ will be compound specific. Section 3.3.2 identified aromatic precursors to SOA formation, and 15 of these aromatic hydrocarbons were selected for examination in this work. This section will give an example of the development of a model for o-xylene. The analogous procedures were reapplied in developing mechanistic models for 1,2,3-trimethylbenzene, m-xylene, p-xylene, m-ethyltoluene, p-ethyltoluene, o-ethyltoluene, ethylbenzene, benzene, n-propylbenzene, iso-propylbenzene, sec-butylbenzene, and toluene. Condensed mechanisms and kinetic parameters for these aromatic hydrocarbons are also presented in this section. SOA yields from simulations were compared against experimental values (Odum, 1997).

3.5.1 Quantitative mechanistic models for aromatic hydrocarbons

Chemistry for o-Xylene

In addition to trimethybenzene, xylene also produces a significant amount of secondary organic aerosol in the urban atmosphere. Reaction pathways of o-xylene with OH radicals are shown in Figures 3.17-3.19.

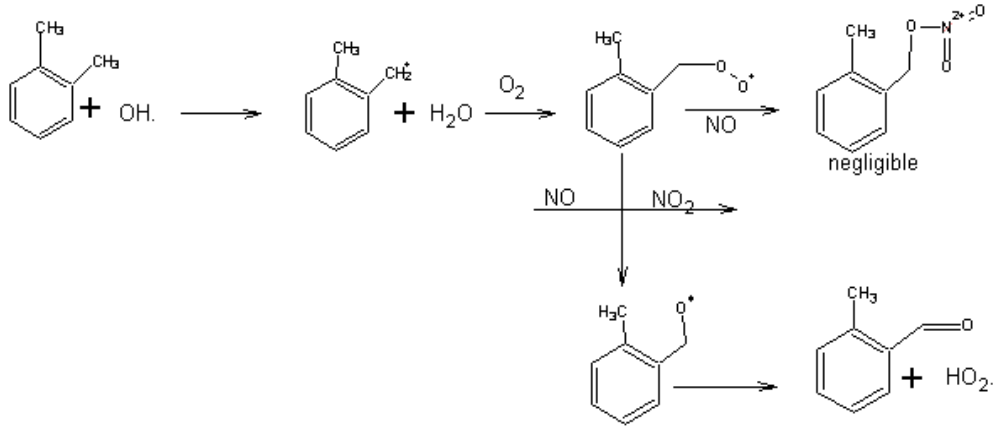

(5)

Figure 3.17: Hydrogen abstraction from o-xylene by OH radical reaction pathway

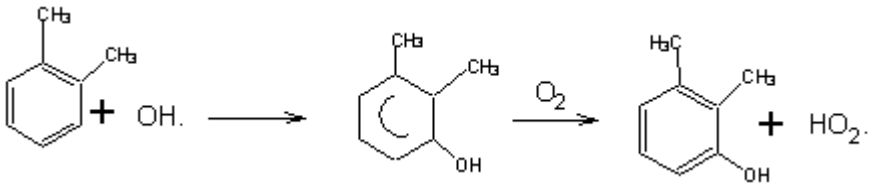

(6)

Figure 3.18: Addition of OH to o-xylene forming methylcresol

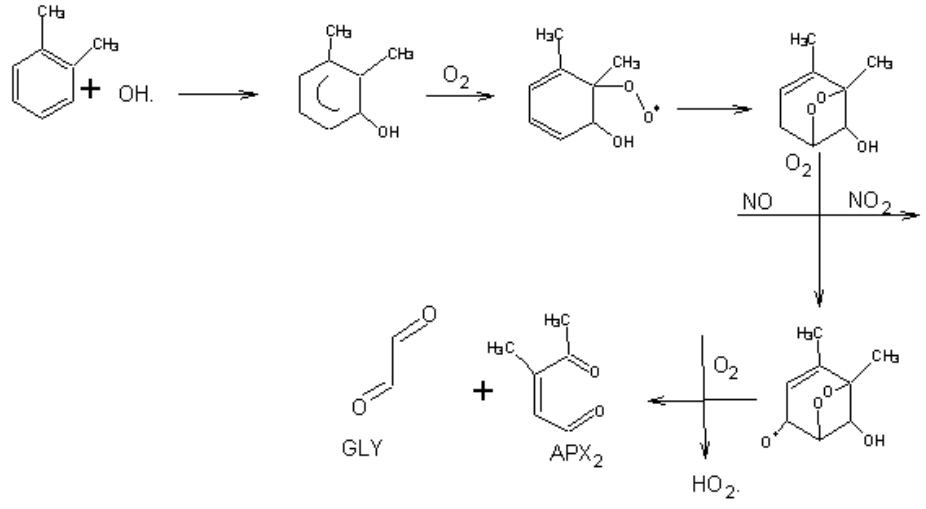

(7)

Figure 3.19: OH addition to o-xylene reaction

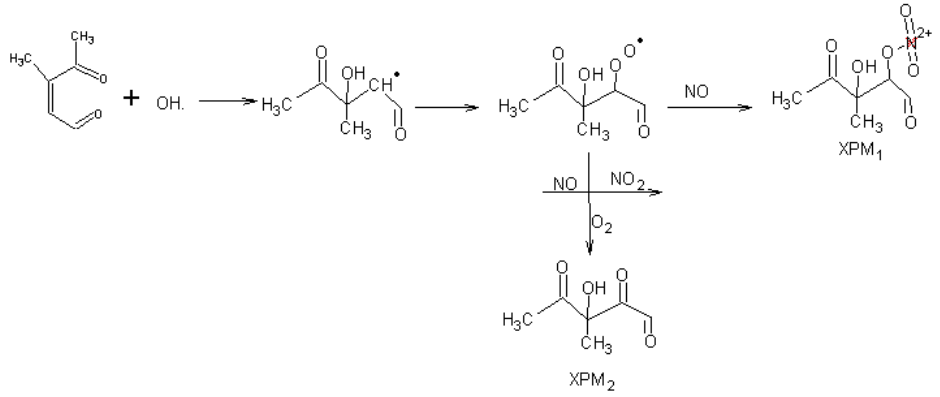

(8)

Figure 3.20: semi-volatile product reaction pathways from aerosol precursors

The major daytime loss process for atmospheric aromatic hydrocarbons is through reaction with OH radicals. As with 1,3,5-trimethybenzene, this reaction can proceed through either the hydrogen abstraction (pathway 5), or addition to the aromatic ring (pathways 6 and 7). For o-xylene, hydrogen abstraction accounts for

4.5% of all reactions (SAPRC99), occurring primarily at the substituent methyl groups. The product of this reaction is benzaldehyde with one extra carbon atom (BALD + 1C), along with an NO to NO_2 conversion and the production of HO_2 radical.

4%: O-XYLENE + HO. = BALD +1C + RO2R **Reaction 16**

Addition of the OH radical will occur at one of the three ring positions, but predominantly adds at the aromatic carbon ortho to one of the carbons attached to the methyl group (Grovenstein, 1970; Atkinson et al., 1980). The initial addition of OH radical to o-xylene results in cresol with one extra carbon atom (CRES + 1C) and HO_2 radical. This pathway accounts for 16.1% of all reactions of o-xylene (SAPRC99).

16%: O-XYLENE + HO. = CRES + 1C + HO2. **Reaction 17**

The remainder of the OH radical addition products from o-xylene will further react with O_2, again with conversion of NO to NO_2. The ring cleavage reaction of the O_2-OH-aromatic-adduct proceeds through four possible positions on the aromatic ring. Figure 3.19 illustrates the reaction pathway leading to formation of aerosol precursor (APX2). Although chemical structures of all aerosol precursors from o-xylene, APX1-APX3 are different, their formation pathways are similar. The cleavage reactions produce 45% of APX1, 14% of APX2, and 20% of APX3 (Bandow, 1985).

In addition to these, MGLY, GLY, and BACL are generated. In total, these pathways account for 79.4% of all reactions of o-xylene with OH radical.

79%: O-XYLENE + HO. = .569 APX1 + .569 MGLY + .17 APX2 + .17 GLY + .253 APX3 + .253 BACL **Reaction 18**

Net: O-XYLENE + HO. = .045 BALD + .161 CRES + .835 RO2R + .161 HO2. + .45 APX1 + .14APX2 + .2 APX3 + .2 BACL + .14 GLY + .45 MGLY + .206 C **Reaction 19**

Aerosol precursors (APX1-APX3) generate two types of aerosol products (XPM1 and XPM2) via the OH-addition at the carbon double bond. Results from previous studies suggested that 25% of APX2-OH addition reaction produce XPM1 (Eusebi, 1996). The remaining APX2-OH reacts with O_2 and NO to form XPM2, NO_2, and HO_2 radicals (Figure 3.20).

APX1-APX3 + HO. = .25 XPM1 + .75 XPM2 +.25 RO2N +.75 RO2R **Reaction 20**

By applying the same procedure used in developing mechanisms for 1,3,5-trimethybenzene and o-xylene, condensed mechanisms for the individual aromatic precursors were developed. Reaction pathways of the photooxidation reactions and detailed mechanisms for each species are given in Appendix C. Condensed mechanisms of SOA formation and rate constants, which were estimated from the AOP program, for these 15 compounds are presented in Table 3.11.

Table 3.11: Condensed mechanisms of SOA formation for 15 aromatic precursors developed in this study

Aromatic Precursors	Aerosol Precursors	Condensed Mechanisms	Rate Constants (cm^3/molc-sec)	Source of rate constants
1,3,5-Trimethybenzene		135-TMB + HO. = 0.03BALD + 0.18CRES + 0.81RO2R + 0.18HO2. + 0.79MGLY + 0.79APT1+ .42XC	5.79e-11	SAPRC-99
	APT1	APT1 + HO. = 0.25TPM1 + 0.75TPM2 + 0.25RO2N + 0.75RO2R	2.60e-11	AOP program
1,2,3-Trimethybenzene		123-TMB + HO. = 0.044BALD + 0.186 CRES + 0.809RO2R + 0.186HO2. + 0.254MGLY + 0.085GLY + 0.431BACL+ 0.431APT2+ 0.254APT3 + 0.085APT4 + 0.46XC	3.27e-11	SAPRC-99
	APT2	APT2 + HO. = 0.25TPM3 + 0.75TPM4 + 0.25RO2N + 0.75RO2R	1.85e-11	AOP program
	APT3	APT3 + HO. = 0.25TPM3 + 0.75TPM4 + 0.25RO2N + 0.75RO2R	2.66e-11	AOP program
	APT4	APT4 + HO. = 0.25TPM3 + 0.75TPM4 + 0.25RO2N + 0.75RO2R	3.36e-11	AOP program
1,2,4-Trimethybenzene		124TMB + HO. = 0.044BALD + 0.186CRES + 0.812RO2R + 0.186HO2. + 0.469MGLY + 0.192GLY + 0.107BACL + 0.254APT5 + 0.084APT6 + 0.131 APT7 + 0.146APT8 + 0.046APT9 + 0.107AP10 + 0.46XC	3.35e-11	SAPRC-99
	APT5	APT5 + HO. = 0.25TPM5 + 0.75TPM6 + 0.25RO2N + 0.75RO2R	4.80e-11	AOP program
	APT6	APT6 + HO. = 0.25TPM5 + 0.75TPM6 + 0.25RO2N + 0.75RO2R	2.60e-11	AOP program
	APT7	APT7 + HO. = 0.25TPM5 + 0.75TPM6 + 0.25RO2N + 0.75RO2R	2.60e-11	AOP program
	APT8	APT8 + HO. = 0.25TPM5 + 0.75TPM6 + 0.25RO2N + 0.75RO2R	3.30e-11	AOP program

Aromatic Precursors	Aerosol Precursors	Condensed Mechanisms	Rate Constants (cm^3/molc-sec)	Source of rate constants
	APT9	APT9 + HO. = 0.25TPM5 + 0.75TPM6 + 0.25RO2N + 0.75RO2R	1.20e-11	AOP program
	AP10	AP10 + HO. = 0.25TPM5 + 0.75TPM6 + 0.25RO2N + 0.75RO2R	1.00e-11	AOP program
o-Xylene		O-XYLENE + HO. = 0.045BALD + 0.161CRES + 0.835RO2R + 0.161HO2. + 0.45MGLY + 0.146GLY + 0.45APX1 + 0.14APX2 + 0.2APX3 + 0.206XC + 0.2BACL	1.37e-11	SAPRC-99
	APX1	APX1 + HO. = 0.25XPM1 + 0.75XPM2 + 0.25RO2N + 0.75RO2R	1.85e-11	AOP program
	APX2	APX2 + HO. = 0.25XPM1 + 0.75XPM2 + 0.25RO2N + 0.75RO2R	2.66e-11	AOP program
	APX3	APX3 + HO. = 0.25XPM1 + 0.75XPM2 + 0.25RO2N + 0.75RO2R	6.96e-12	AOP program
p-Xylene		P-XYLENE + HO. = 0.083BALD +0.188CRES + 0.812RO2R + 0.188HO2. + 0.24MGLY + 0.489GLY + 0.489APX4 + 0.24APX5 + 0.271XC	1.43e-11	SAPRC-99
	APX4	APX4 + HO. = 0.25XPM3 + 0.75XPM4 + 0.25RO2N + 0.75RO2R	4.88e-11	AOP program
	APX5	APX5 + HO. = 0.25XPM3 + 0.75XPM4 + 0.25RO2N + 0.75RO2R	1.00e-11	AOP program
m-Xylene		M-XYLENE + HO. = 0.037BALD + 0.21CRES + 0.789RO2R + 0.21HO2. + 0.564 MGLY +0.188GLY + 0.376APX6 + 0.188APX7 + 0.188APX8 + 0.247XC	1.37e-11	SAPRC-99
	APX6	APX6 + HO. = 0.25XPM5 +0.75XPM7 + 0.25RO2N +0.75RO2R	1.80e-11	AOP program
	APX7	APX7 + HO. = 0.25XPM5 +0.75XPM7 + 0.25RO2N +0.75RO2R	2.60e-11	AOP program

Aromatic Precursors	Aerosol Precursors	Condensed Mechanisms	Rate Constants (cm^3/molc-sec)	Source of rate constants
	APX8	APX8 + HO. = 0.25XPM5 +0.75XPM7 + 0.25RO2N +0.75RO2R	1.05e-11	AOP program
p-ethyltoluene		P-C2-TOL + HO. = 0.49APET1 + 0.2APET2 + 0.04APET3 + 0.24MGLY + 0.49GLY + 0.188HO2. + 0.188CRES + 0.083BALD + 0.856RO2R + 0.702XC + 0.042CO2 + 0.084H2O – 0.042HO.	1.43E-11	SAPRC-99
	APET1	APET1 + HO. = 0.25ETPM1 + 0.75ETPM2 + 0.25RO2N + 0.75RO2R	4.50e-11	AOP program
	APET2	APET2 + HO. = 0.25ETPM1 + 0.75ETPM2 + 0.25RO2N + 0.75RO2R	1.00e-11	AOP program
	APET3	APET3 + HO. = 0.25ETPM1 + 0.75ETPM2 + 0.25RO2N + 0.75RO2R	1.00e-11	AOP program
o-ethyltoluene		O-C2-TOL + HO. = 0.329APET4 + 0.085APET5 + 0.026APET6 + 0.051APET7 + 0.186APET8 + 0.395MGLY + 0.162GLY+0.186BACL + 0.188HO2. + 0.188CRES + 0.054BALD + 0.8404RO2R + 0.7255XC + 0.0659APET9 +0.0325CO2+0.065H2O – 0.0325HO.	1.37e-11	SAPRC-99
	APET4	APET4 + HO. = 0.25ETPM3 + 0.75ETPM4 + 0.25RO2N + 0.75RO2R	1.88e-11	AOP program
	APET5	APET5 + HO. = 0.25ETPM3 + 0.75ETPM4 + 0.25RO2N + 0.75RO2R	1.00e-11	AOP program
	APET6	APET6 + HO. = 0.25ETPM3 + 0.75ETPM4 + 0.25RO2N + 0.75RO2R	2.70e-11	AOP program
	APET7	APET7 + HO. = 0.25ETPM3 + 0.75ETPM4 + 0.25RO2N + 0.75RO2R	2.70e-11	AOP program
	APET8	APET8 + HO. = 0.25ETPM3 + 0.75ETPM4 + 0.25RO2N + 0.75RO2R	6.90e-12	AOP program

Aromatic Precursors	Aerosol Precursors	Condensed Mechanisms	Rate Constants (cm^3/molc-sec)	Source of rate constants
	APET9	APET9 + HO. = 0.25ETPM3 + 0.75ETPM4 + 0.25RO2N + 0.75RO2R	1.80e-11	AOP program
m-ethyltoluene		M-C2-TOL + HO. = 0.054APET10 + 0.134APET11 + 0.08APET12 + 0.106APET13 + 0.226APET14 +0.567MGLY + 0.186GLY + 0.21HO2. + 0.21CRES + 0.037BALD + 0.8085RO2R + 0.6825XC + 0.153APET15+0.0185CO2 + 0.037H2O – 0.0185HO.	1.37e-11	SAPRC-99
	APET10	APET10 + HO. = 0.25ETPM5 + 0.75ETPM6 + 0.25RO2N + 0.75RO2R	1.00e-11	AOP program
	APET11	APET11 + HO. = 0.25ETPM5 + 0.75ETPM6 + 0.25RO2N + 0.75RO2R	1.00e-11	AOP program
	APET12	APET12 + HO. = 0.25ETPM5 + 0.75ETPM6 + 0.25RO2N + 0.75RO2R	2.70e-11	AOP program
	APET13	APET13 + HO. = 0.25ETPM5 + 0.75ETPM6 + 0.25RO2N + 0.75RO2R	2.70e-11	AOP program
	APET14	APET14 + HO. = 0.25ETPM5 + 0.75ETPM6 + 0.25RO2N + 0.75RO2R	1.80e-11	AOP program
	APET15	APET15 + HO. = 0.25ETPM5 + 0.75ETPM6 + 0.25RO2N + 0.75RO2R	1.80e-11	AOP program
Toluene		TOLUENE + HO. = 0.234CRES + 0.515RO2R + 0.234HO2. + 0.167MGLY + 0.238GLY + 0.238APTO1 + 0.167APTO2 + 0.11BALD + 0.25NBEN + 0.25H2O + - 0.25NO2 + 0.25XC	5.95e-12	SAPRC-99
	APTO1	APTO1 + HO. = 0.25TOPM1 +0.75TOPM2 + 0.25RO2N + 0.75RO2R	1.85e-11	AOP program
	APTO2	APTO2 + HO. = 0.25TOPM1 +0.75TOPM2 + 0.25RO2N + 0.75RO2R	6.96e-12	AOP program

Aromatic Precursors	Aerosol Precursors	Condensed Mechanisms	Rate Constants (cm^3/molc-sec)	Source of rate constants
Benzene		BENZENE + HO. = 0.236PHEN + 0.236HO2. + 0.566NBEN + 0.2RO2R + 0.566H2O + -0.566NO2 + 0.2APB1 + 0.2GLY	1.23e-12	SAPRC-99
	APB1	APB1 + HO. = 0.25BPM1 + 0.75BPM2 + 0.25RO2N + 0.75RO2R	6.96e-12	AOP program
Ethyl Benzene		C2-BEN + HO. = 0.19CRES + 0.574RO2R + 0.19HO2. + 0.167MGLY + 0.237GLY + 0.167APEB1 + 0.158APEB2 + 0.079APEB3 + 0.999XC + 0.296NBEN + 0.416H2O + 0.03CO2 + -0.06HO. + -0.296NO2 + 0.11BALD +0.03OCH2	7.10e-12	SAPRC-99
	APEN1	APEB1 + HO. = 0.25EBPM1 + 0.75EBPM2 + 0.25RO2N + 0.75RO2R	6.96e-12	AOP program
	APEB2	APEB2 + HO. = 0.25EBPM1 + 0.75EBPM2 + 0.25RO2N + 0.75RO2R	1.85e-11	AOP program
	APEB3	APEB3 + HO. = 0.25EBPM1 + 0.75EBPM2 + 0.25RO2N + 0.75RO2R	1.00e-11	AOP program
n-Propyl Benzene		N-C3-BENZ + HO. = 0.19CRES + 0.634RO2R + 0.19HO2. + 0.167MGLY + 0.238GLY + 0.296NBEN + 0.167APPB1 + 0.158APPB2 + 0.079APPB3 + 1.702XC + 0.476H2O + 0.12CO2 + -0.12HO. + -0.296NO2 + 0.11BALD + 0.12OCH2	6.00e-12	SAPRC-99
	APPB1	APPB1 + HO. = 0.25PBM1 + 0.75PBM2 + 0.25RO2N +0.75RO2R	6.96e-12	AOP program
	APPB2	APPB2+ HO. = 0.25PBM1 + 0.75PBM2 + 0.25RO2N +0.75RO2R	1.85e-11	AOP program
	APPB3	APPB3 + HO. = 0.25PBM1 + 0.75PBM2 + 0.25RO2N +0.75RO2R	1.85e-11	AOP program

Aromatic Precursors	Aerosol Precursors	Condensed Mechanisms	Rate Constants (cm^3/molc-sec)	Source of rate constants
Isopropyl Benzene		I-C3-BEN + HO. = 0.11BALD + -0.11HO. + 0.19CRES +0.19HO2. + 0.167APB2 + 0.167MGLY + 0.158APB3 + 0.079APB4 + 0.237MGLY + 0.624RO2R +- 0.296NO2 + 0.296NBEN + 0.516 H2O + 1.712XC + 0.11CO2	6.50e-12	SAPRC-99
	APB2	APB2 + HO. = 0.25BPM3 + 0.75BPM4 + 0.25RO2N +0.75RO2R	6.96e-12	AOP program
	APB3	APB3 + HO. = 0.25BPM3 +0.75BPM4 +0.25RO2N +0.75RO2R	1.85e-11	AOP program
	APB4	APB4 + HO. = 0.25BPM3 + 0.75BPM4 + 0.25RO2N +0.75RO2R	1.00e-11	AOP program
s-Butyl Benzene		S-C4-BEN + HO. = 0.11BALD + -0.16HO. + 0.19CRES + 0.19HO2. + 0.167APB5 + 0.167MGLY + 0.119APB6 + 0.119APB7 +0.238GLY + 0.675RO2R + - 0.296NO2 + 0.296NBEN + 0.566H2O + 2.425XC + 0.16CO2	6.00e-12	SAPRC-99
	APB5	APB5 + HO. = 0.25BPM5 +0.75BPM6 +0.25RO2N + 0.75RO2R	6.96e-12	AOP program
	APB6	APB5 + HO. = 0.25BPM5 +0.75BPM6 +0.25RO2N + 0.75RO2R	1.85e-11	AOP program
	APB7	APB5 + HO. = 0.25BPM5 +0.75BPM6 +0.25RO2N + 0.75RO2R	1.00e-11	AOP program

After the chemistry of SOA formation for these aromatic hydrocarbons were implemented into SAPRC-99, results from simulations were used to estimate the partitioning of condensable products. Quantitative mechanistic models of SOA formation were developed for 15 aromatics, but the partitioning coefficients were

estimated for only 11, due to the lack of information from chamber experiments for the remaining 4: benzene, sec-buthylbenzene. Iso-propylbenzene, and 1,2,3-trimethylbenzene. The prediction of SOA formation for these 11 compounds were done by employing partitioning coefficients for individual species (as previously elaborated for example of 1,3,5-trimethylbenzene). Partitioning coefficients for individual compounds listed in Table 3.12 were estimated based on results for SAPRC simulations and Odum's experimental results.

Table 3.12: The Estimated Partitioning Coefficients and Vapor Pressures of Condensable Products from aromatic hydrocarbons

Parent Hydrocarbons	$Kom_{,1}$ (m3/μg)	$Kom_{,2}$ (m3/μg)	VP_1 (mm Hg)	VP_2 (mm Hg)
1,3,5-trimethybenzene	0.00337	0.00029	0.00026	0.0030
1,2,4-trimethybenzene	0.00609	0.00046	0.000113	0.0015
o-xylene	0.00513	0.000412	0.00097	0.0121
p-xylene	0.00451	0.000394	0.00158	0.0181
m-xylene	0.00203	0.000175	0.00066	0.0076
o-ethyltoluene	0.00844	0.000735	0.00049	0.0056
m-ethyltoluene	0.00490	0.000433	0.00038	0.0043
p-ethyltoluene	0.00690	0.000569	0.00045	0.0054
toluene	0.01230	0.001090	0.00066	0.0074
n-propylbenzene	0.07220	0.001980	0.000096	0.0035
ethylbenzene	0.02600	0.002310	0.00039	0.0044

3.5.2 Comparison of SOA yields

In addition to 1,2,4- and 1,3,5-trimethylbenzene, the yields of SOA for 9 aromatic compounds were examined individually. The conditions used in these simulations were identical to those used by Odum, 1997. These conditions are reported in Table D.1, Appendix D. Aromatic precursors were classified into two categories: high-yield aromatics, and low-yield aromatics (Odum, 1997). The high-yield aromatic species are those species containing one or fewer methyl substituent and one or fewer ethyl substituent (i.e., toluene, ethylbenzene, and ethyltoluene). The low-yield aromatics are those species that contain two or more methyl substituents (i.e., xylenes, trimethylbenzenes). Figure 3.21 demonstrates SOA yields of these aromatic species as a function of M_o (or M_{tot}). While there is disagreement between some data points from simulations and observations, the overall trend shows good correspondence in the results of the quantitative models and chamber experiments.

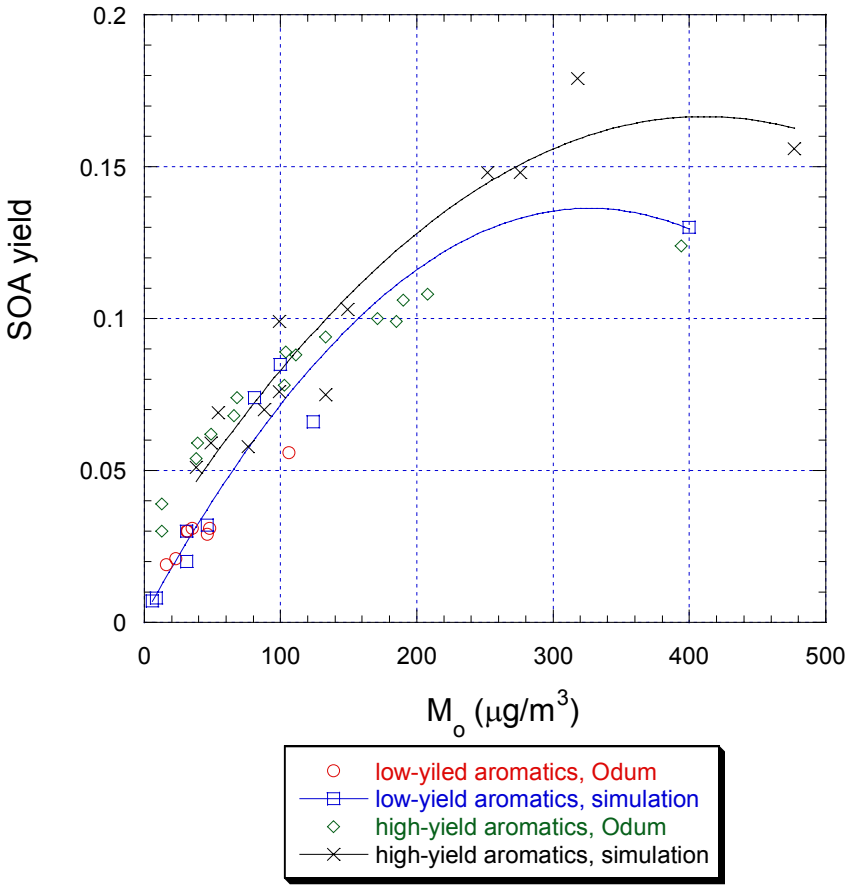

Figure 3.21: SOA yields for high- and low-yield aromatics from simulation calculation compared to chamber experiments

Observed and predicted aerosol yields presented in Figure 3.21 for low- and high-yield aromatics are reported in Table 3.13.

Table 3.13: Aerosol yields for low- and high-yield aromatics: results from simulations and observation

	Chamber experiments by Odum (1997)			SAPRC simulations			
Compounds	ΔROG	ΔM	Y	ΔROG	ΔM	Y	Simulating time (hrs)
135-TMB	1029	31	0.030	1030	31	0.030	2.0
m-xylene	1891	106	0.056	1870	124	0.066	5.0
m-xylene	1571	46	0.029	1450	46	0.032	10.0
m-xylene	1528	48	0.031	1530	31	0.020	10.0
o-xylene	1117	35	0.031	1170	100	0.085	3.0
o-xylene	1082	23	0.021	1170	9	0.008	2.5
p-xylene	823	16	0.019	865	6	0.007	2.5
p-xylene	1063	32	0.030	1090	81	0.074	3.0
Toluene	1413	133	0.094	1440	149	0.103	7.0
Toluene	1268	111	0.088	1300	99	0.076	7.0
Toluene	1710	171	0.100	1700	252	0.148	8.0
toluene	923	68	0.074	960	NA	NA	3.0
o-ethyltoluene	789	49	0.062	833	49	0.059	7.0
p-ethyltoluene	708	38	0.054	751	38	0.051	7.0
m-ethyltoluene	1927	208	0.108	1780	318	0.179	10.0
m-ethyltoluene	971	66	0.068	999	99	0.099	6.0
m-ethyltoluene	334	13	0.039	356	NA	NA	4.0
ethylbenzene	434	13	0.030	465	NA	NA	2.5
ethylbenzene	3176	394	0.124	3060	419	0.136	9.0
ethylbenzene	1872	185	0.099	1870	230	0.122	8.0
ethylbenzene	1169	104	0.089	1260	70	0.055	3.0
n-propylbenzene	1314	103	0.078	1320	76	0.058	6.0
n-propylbenzene	657	39	0.059	781	54	0.069	4.0
n-propylbenzene	1790	190	0.106	1780	133	0.075	6.0

Results in the above table show aerosol mass change and SOA yields from the SAPRC simulation and observations (Odum, 1996). The simulations were conducted under similar conditions as in Odum's chamber experiments, and continue until the amount of ΔROG is relatively equal to ΔROG from experiment was achieved (e.g., 135-TMB requires 2 hours of simulating time to reach the optimal ΔROG similar to Odum's experiment. The total amount of semivolatile products generated from

reaction (P_i), obtained from simulation, and ΔM from Odum results were used in the calculation to estimate partitioning coefficients. The estimated partitioning coefficients were then used to determine the estimated aerosol mass change. The estimated mass changes were compared with those from Odum observation. As seen from Figure 3.21 and Table 3.13, SOA yields from the estimation are comparable within the factor of 0.5 to 2.0 to those from the experimental results, 19% of the results from the simulation are outside the range (i.e., results for o- and p-xylene). The relatively poor agreement for these 4 runs of o- and p-xylene results from the relatively small aerosol mass changes.

3.5.3 Correlation between ΔM and M_{int} for aromatic hydrocarbons

The motivation and procedure for establishing the correlation between ΔM and M_{int} was described in Section 3.4.3 (for 1,3,5-trimethylbezene). With the same purpose and by employing analogous procedures, the correlation between ΔM and M_{int} in terms of $\%DF_i$ for the remaining aromatics was developed. The results are shown below. Figures 3.22a-j demonstrate the relationship between $\%DF_i$ and M_{int} and as a function of hydrocarbon conversion for *1,2,4-trimethylbenzene, ethylbenzene, m-ethyltoluene, o-ethyltoluene, p-ethyltoluene, m-xylene, o-xylene, p-xylene, n-propylbenzene, and toluene*, respectively.

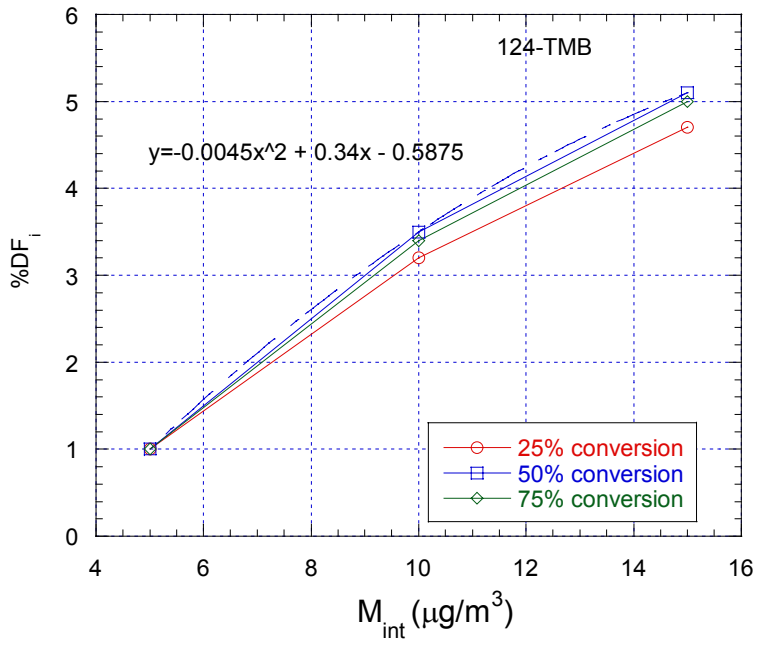
124-TMB
y=-0.0045x^2 + 0.34x - 0.5875
25% conversion
50% conversion
75% conversion
%DF_i
M_int (μg/m^3)
0
1
2
3
4
5
6
4
6
8
10
12
14
16

(a)

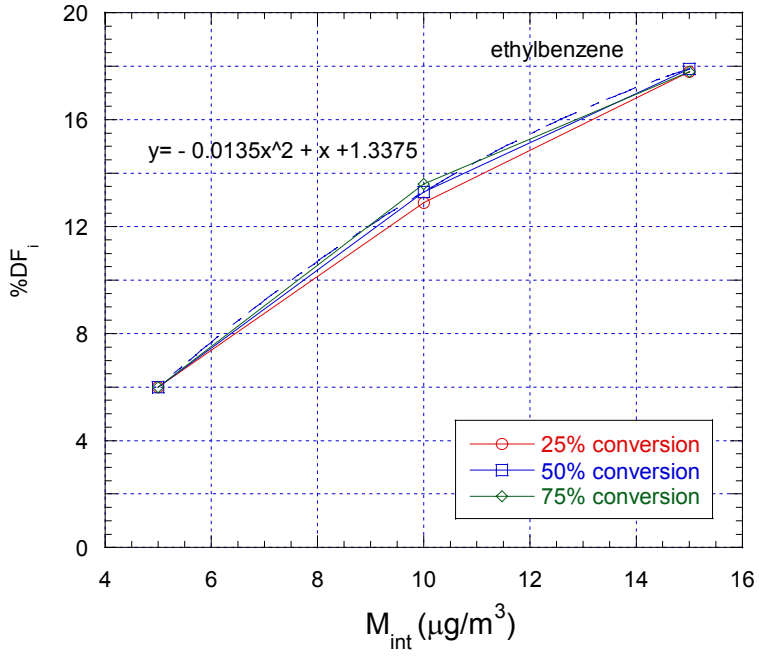
ethylbenzene
y= - 0.0135x^2 + x +1.3375
25% conversion
50% conversion
75% conversion
%DF_i
M_int (μg/m^3)
0
4
8
12
16
20
4
6
8
10
12
14
16

(b)

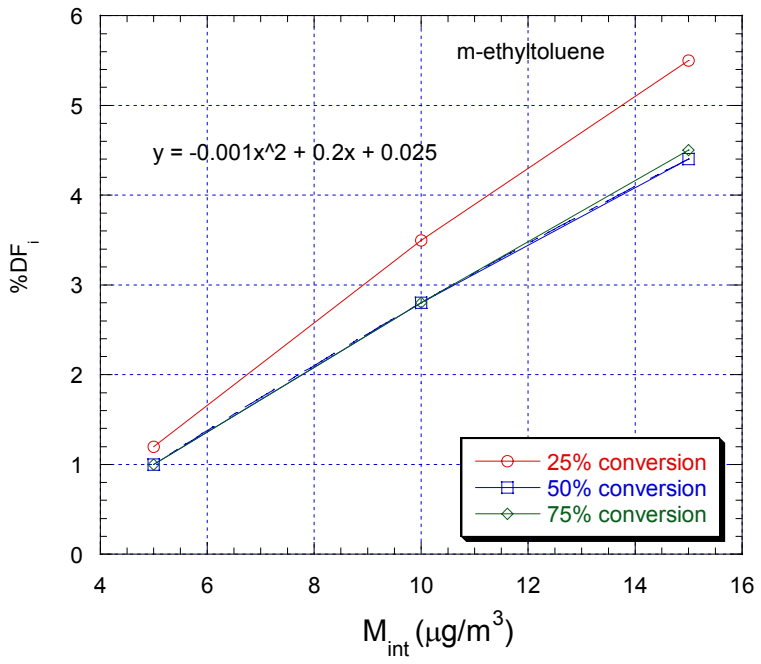
m-ethyltoluene
y = -0.001x^2 + 0.2x + 0.025
25% conversion
50% conversion
75% conversion
%DF_i
M_int (µg/m^3)
0
1
2
3
4
5
6
4
6
8
10
12
14
16

(c)

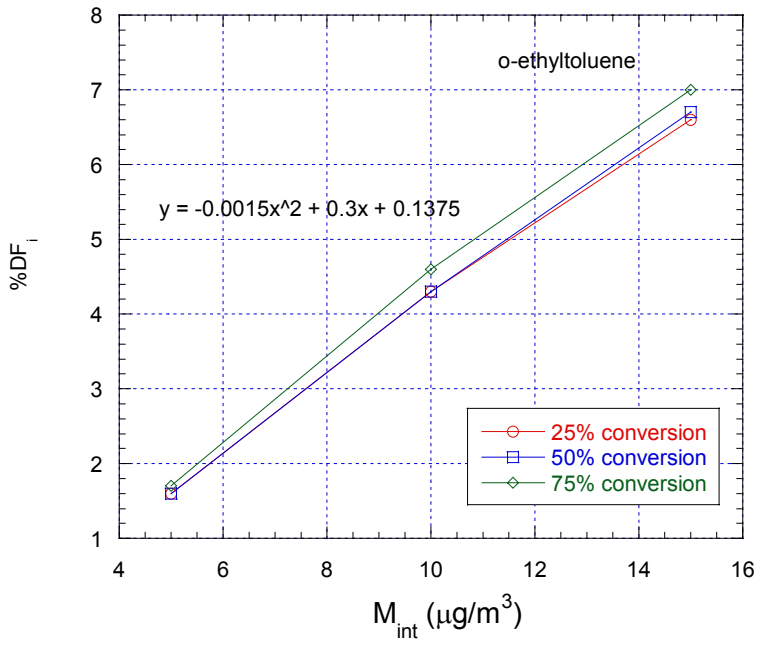
o-ethyltoluene
y = -0.0015x^2 + 0.3x + 0.1375
25% conversion
50% conversion
75% conversion
%DF_i
M_int (µg/m^3)
1
2
3
4
5
6
7
8
4
6
8
10
12
14
16

(d)

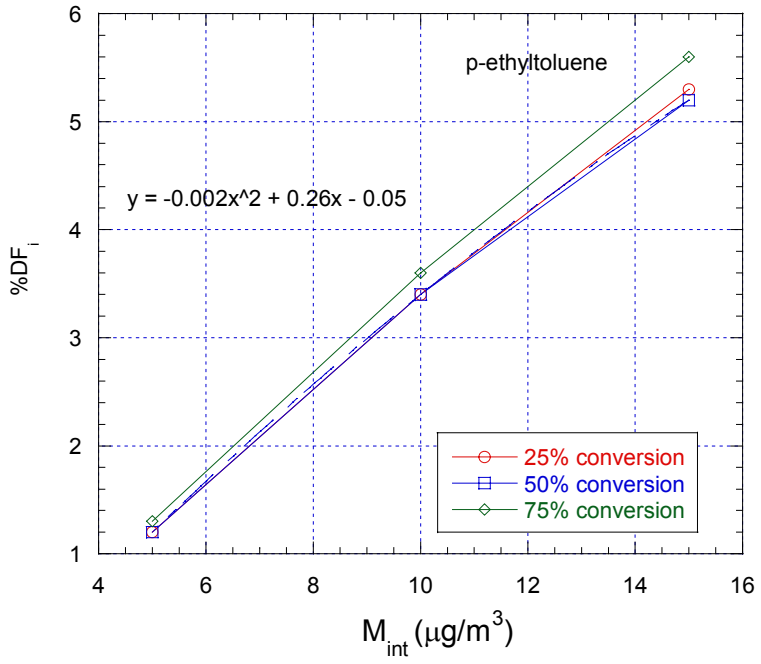
p-ethyltoluene
y = -0.002x^2 + 0.26x - 0.05
%DF_i
M_int (µg/m^3)
25% conversion
50% conversion
75% conversion

(e)

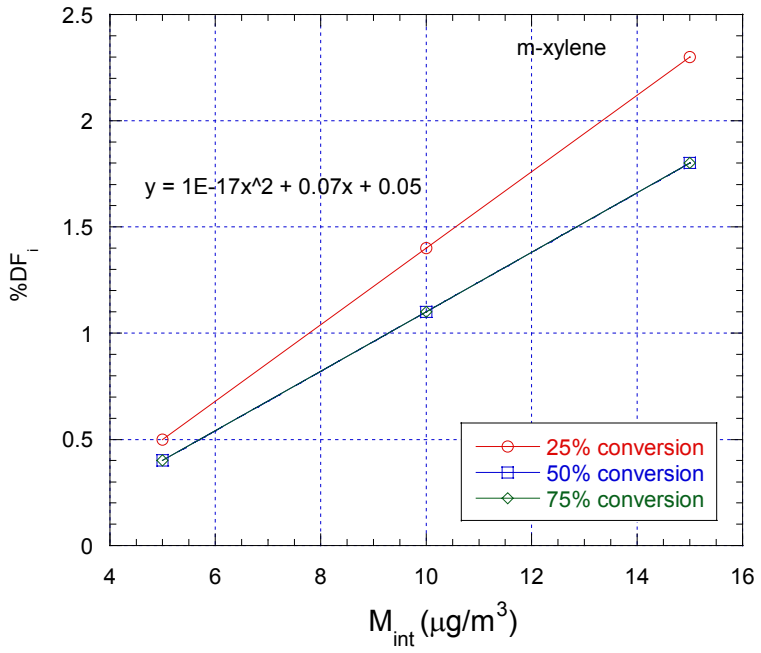
m-xylene
y = 1E-17x^2 + 0.07x + 0.05
%DF_i
M_int (µg/m^3)
25% conversion
50% conversion
75% conversion

(f)

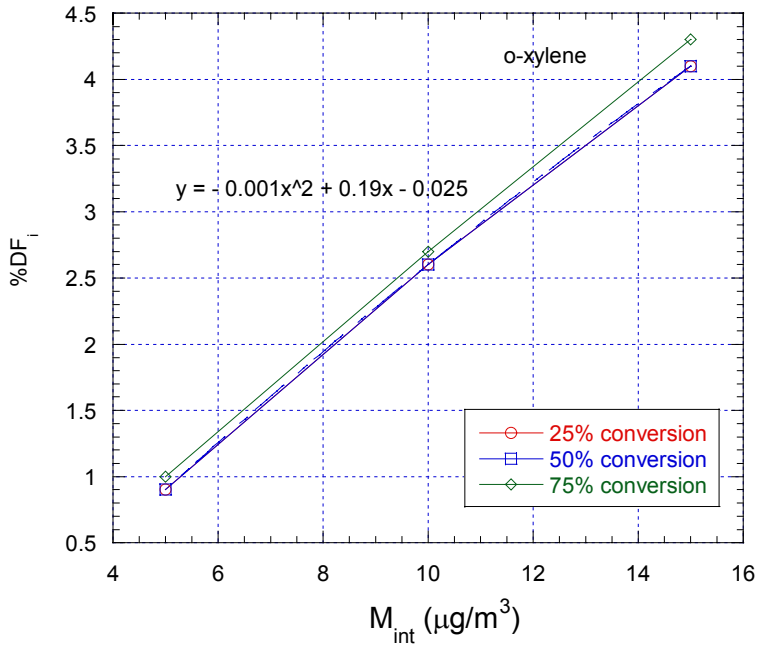
o-xylene
y = - 0.001x^2 + 0.19x - 0.025
%DF_i
M_int (µg/m^3)
25% conversion
50% conversion
75% conversion

(g)

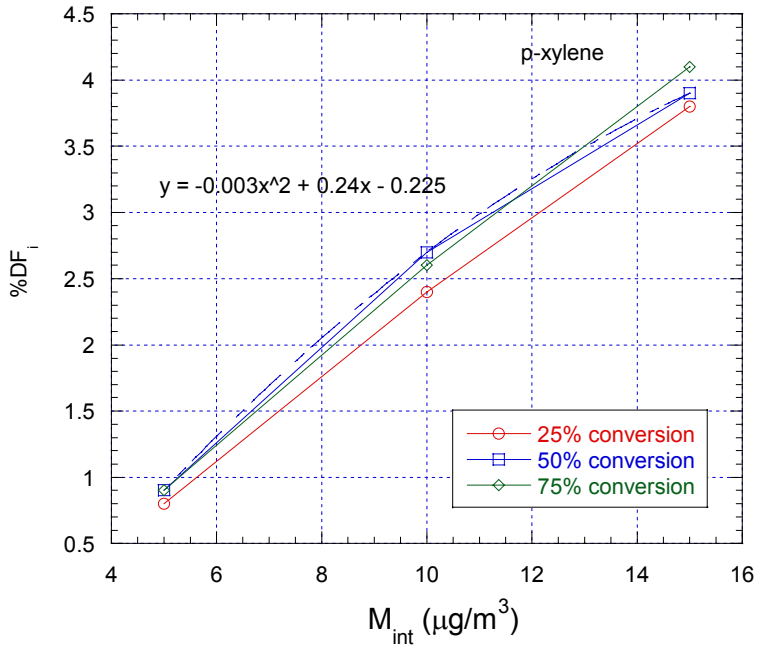
p-xylene
y = -0.003x^2 + 0.24x - 0.225
%DF_i
M_int (µg/m^3)
25% conversion
50% conversion
75% conversion

(h)

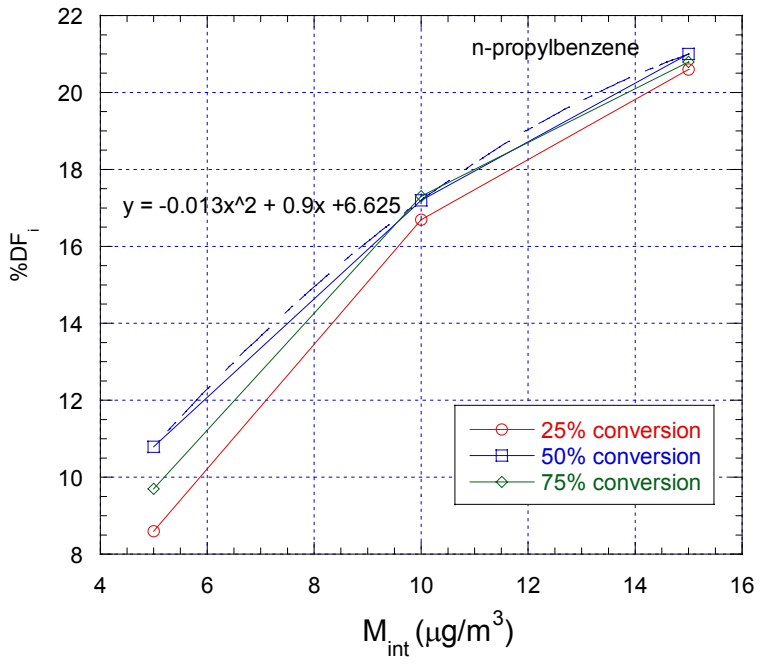

(i)

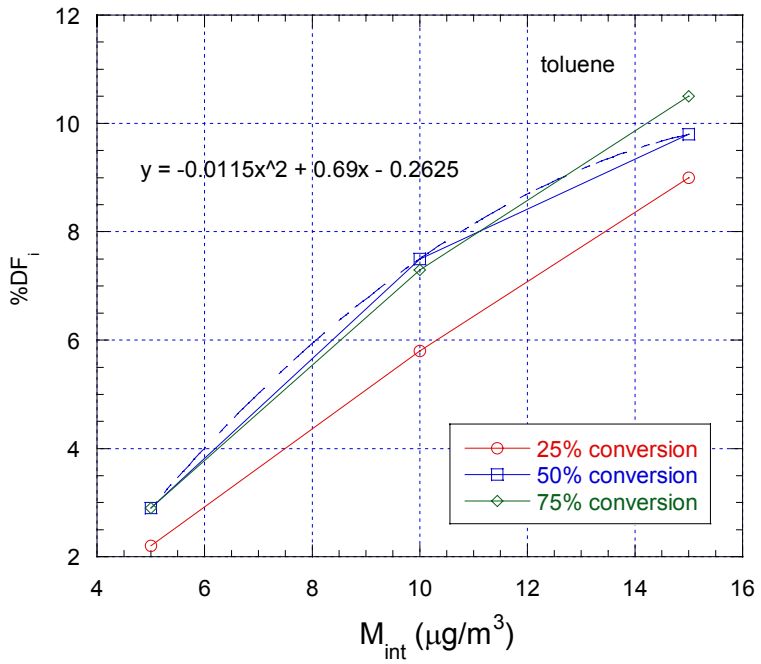

(j)

Figure 3.22: ***%DF$_i$* as a function of *M$_{int}$* at 25, 50, and 75% hydrocarbon conversions for 11 aromatics**

Results for most of species reveal the same behavior as seen for 1,3,5-trimethylbenzene, in which $\%DF_i$ is strongly dependent on M_{int} but not influenced by %conversion (i.e., $\%DF_i = f(M_{int}) \neq f(\%conversion)$). The exceptions are toluene, m-xylene and m-ethyltoluene. For these three compounds, the percentage of product that partitions into the aerosol phase ($\%DF_i$) is similar at 50 and 75% conversions, , but is different for 25% conversion.

The deviation occurs because ΔM_i for these 3 species is comparable to M_{tot}. As the partitioning of condensable species onto M_{int} goes on, total organic mass increases, and this increase can be a substantial fraction of the total aerosol mass, especially at low values of M_{int}. This creates a dependence of $\%DF_i$ on conversion especially when ($\Delta M > 0.6M_{int}$). This is shown in Figure 3.23, ΔM for toluene is plotted against total amount of semivolatile products (P_i) produced from reaction of OH radical with toluene. As seen from the figure, below the upper limit ($\Delta M = 0.6M_{int}$), amount of semivolatile products partitioning to aerosol phase occurs at a relatively constant rate. Above this point, aerosol mass change (ΔM) substantially increases so that its relationship with P_i changes from linear to parabolic function. For relatively low volatility compounds (e.g., products from toluene reaction) at the high level of conversion (such as 75% conversion), the partitioning occurs rapidly so that ΔM is comparable with M_{int}, and the partitioning rate is not constant anymore. Fortunately,

for most aromatics, and in most air quality modeling applications, ΔM is only a small fraction of M_{int}.

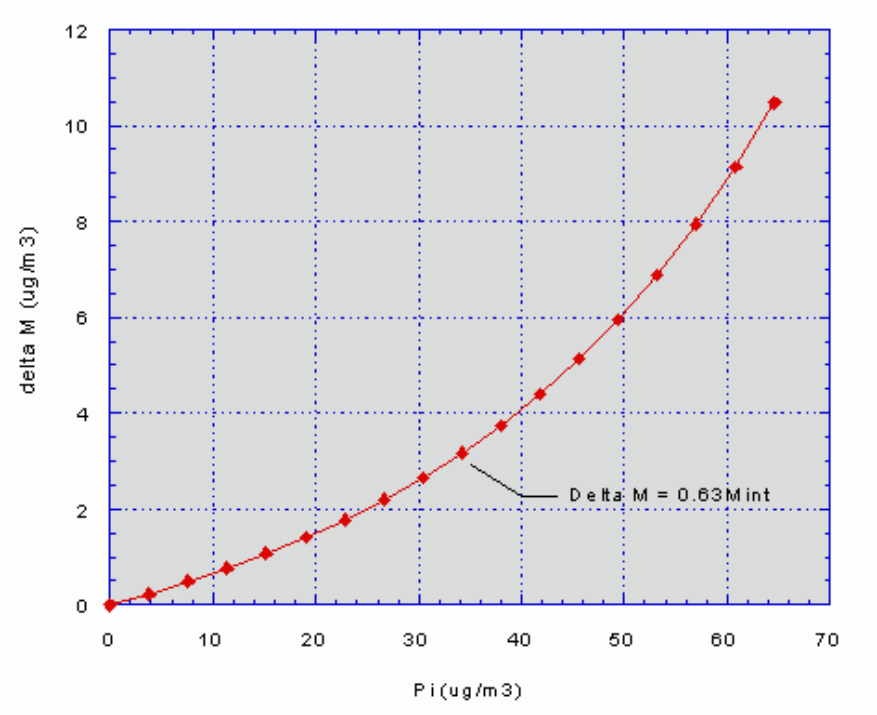

Figure 3.23: ΔM for toluene presented against P_i

Table 3.14 summarizes the results of the evaluation of $\%DF_i$, as a function of M_{int}.

$$\%DF_i = a*M_{int}^2 + b*M_{int} + c \qquad \textbf{Equation 33}$$

$$\Delta M = \%DF_i * P_i \qquad \textbf{Equation 34}$$

Table 3.14: Coefficients *a, b*, and *c* for the correlation equation between $\%DF_i$ and M_{int} for 11 aromatic hydrocarbons

	initial HCs @ 1998 CARB report		
Compounds	a	b	c
1,2,4-trimethylbenzene	-0.005	0.340	-0.588
1,3,5-trimethylbenzene	-0.001	0.130	-0.038
ethylbenzene	-0.014	1.000	1.338
m-ethyltoluene	-0.001	0.200	0.025
m-xylene	0.000	0.070	0.050
n-propylbenzene	-0.013	0.900	6.625
o-ethyltoluene	-0.002	0.300	0.138
o-xylene	-0.001	0.190	-0.025
p-ethyltoluene	-0.002	0.260	-0.050
p-xylene	-0.003	0.240	-0.225
toluene	-0.012	0.690	-0.263

Note: These coefficients were estimated based on the Houston conditions obtained from the CARB Report (Carter, 1998), which represent a typical atmospheric environment.

3.6 Summary

Quantitative models of SOA formation were developed for 15 aromatic hydrocarbons, but the partitioning coefficients were determined individually for only 11 compounds due to the lack of information from chamber experiments for 4 aromatics: iso-propylbenzene, sec-butylbenzene, benzene, and 1,2,3-triemethybenzene. Thus full SOA models were performed for only 11 compounds, though the chemical mechanisms of SOA formation for 15 compounds were implemented into SAPRC. Data available from previous smog chamber experiments were employed in the development. These models were then implemented into a comprehensive gas-phase chemistry which includes reactions of over 350 ambient

species (SAPRC99). A box model was set up to examine SOA yields for individual aromatic hydrocarbon precursors. The gas/particle partitioning absorption mechanism from previous studies was applied with results from the simulations to estimate SOA yields and model parameters. All model parameters estimated in this study are presented in Table 3.15.

Table 3.15: Chemical and physical model parameters for the estimate of secondary aerosol formation

Parameters	Descriptions	Calculation Procedures
Chemistry		
k_{OH}	OH radical rate constant	SAPRC-99, Literature review, and structure activity relationship
a_i	Stoichiometric coefficient of species i	Estimated from chamber data
Physics		
Kom,i	Partitioning coefficients of compound i	Estimated from chamber data
α_i	Proportionality constant relating the amount of ROG reacted to the total concentration of product i	Estimated from SAPRC rate parameters and branching ratios from chamber data
P_i	Total concentration of product i	SAPRC simulation based on ambient Houston data
ΔROG	Concentration of ROG that reacts	SAPRC simulation based on ambient Houston data
VP_i	Vapor pressure of product I	Antoine method and modified Grain method
ΔM	Amount of secondary aerosol produced and portioning into particulate phase	SAPRC simulation calculation
M_{tot}	Total amount of secondary aerosol in particulate phase	SAPRC simulation calculation

SOA yields from the simulation calculations were compared with the observed yields from chamber experiments performed by Odum. The comparison shows a good agreement of SOA formation between the quantitative models and chamber experiments. After testing the reliability of these SOA formation models, the sensitivity analysis was conducted for 1,3,5-trimethylbenzene to investigate which parameters affect the formation and partitioning of SOA. Results from the analysis leading to the correlation between the amount of secondary aerosol produced and partitioning into particulate phase (ΔM) and chemical and physical parameters as expressed below:

$$\Delta M = \%DF_i * \Delta P_i$$

Where

$$\%DF_i = aM_{int}^2 + bM_{int} + c$$

Coefficients a, b, and c are compound specific.

In conclusion, SOA formation depends on three parameters (%conversion, M_{int}, and Kom_i). Parameters affecting the formation and partitioning of condensable products are compound specific.

Chapter 4 Quantitative models of SOA formation for lumped aromatic species development

Chapter 3 presented the development of detailed chemical and physical models for secondary organic aerosol (SOA) formation for individual aromatic species. Use of these models requires a detailed gas phase photochemical model coupled with a compound specific phase partitioning model (SAPRC). Recognizing that in many applications more empirical approaches will be required, this chapter develops two additional modeling approaches: an incremental aerosol reactivity and a lumped photochemical mechanism.

4.1 Analysis of incremental aerosol reactivity

As discussed in Chapter 2, the concept of incremental reactivity has been used in modeling ozone formation to provide an assessment of the relative ozone formation potential for hydrocarbons. The same concept can be applied to particulate matter formation. This section will give the results of the analysis of incremental aerosol reactivity (IAR). A first step in this analysis is to define an IAR. The IAR to be used in this work is defined in Equation 34.

$$IAR = \frac{\Delta(PMproduced)}{\Delta(HCadded)} \qquad \textbf{Equation 35}$$

Units of both nominator and denominator are in $\mu g/m^3$.

In this work, the IAR was calculated by increasing the concentration of a single hydrocarbon, such as 1,3,5-trimethylbenzene, from the base case by an amount equivalent to 5% (based on mole basis) of total hydrocarbon concentration. Carter (1994) found that incremental ozone reactivities depended on the base hydrocarbon mixture, the VOC/NOx ratio, and other parameters. The results presented in Chapter 3 suggest that IAR, as defined in Equation 34, will depend on the base hydrocarbon mixture, the VOC/NOx ratio, and the initial aerosol concentration. If however, a modified definition of IAR is used

$$IAR = \frac{\Delta PMproduced}{\Delta HCadded} \quad \text{(assuming 50\% conversion of HC)} \qquad \textbf{Equation 36}$$

then, as shown in Chapter 3, IAR will depend only on the initial aerosol concentration and conversion of hydrocarbon precursors. Sample sets of IAR (as defined in equation 35) at initial aerosol mass (M_{int}) equals 5 and 15 μg/m^3 and the values of Fractional Aerosol Coefficient (FAC) for 11 aromatic hydrocarbons are given in Table 4.1.

Table 4.1: Incremental aerosol reactivity for 11 aromatic compounds

Compounds	IAR at 25% conv. Mint = 5 μg/m^3	IAR at 50% conv. Mint = 5 μg/m^3	IAR at 75% conv. Mint = 5 μg/m^3	IAR at 25% conv. Mint = 15 μg/m^3	IAR at 50% conv. Mint = 15 μg/m^3	IAR at 75% conv. Mint = 15 μg/m^3	FAC*
1,2,4-trimethylbenzene	0.0006	0.002	0.007	0.0014	0.006	0.0192	0.02
1,3,5-trimethylbenzene	0.00007	0.001	0.001	0.0002	0.002	0.0053	0.029
ethylbenzene	0.00173	0.009	0.041	0.0040	0.02	0.0582	0.054
m-ethyltoluene	0.00043	0.003	0.006	0.0012	0.007	0.0170	0.063
m-xylene	0.00018	0.001	0.002	0.0005	0.002	0.0062	0.047
n-propylbenzene	0.00344	0.019	0.068	0.0061	0.027	0.0705	0.016
o-ethyltoluene	0.00076	0.002	0.013	0.0018	0.009	0.0304	0.056
o-xylene	0.00045	0.002	0.006	0.0012	0.005	0.0165	0.05
p-ethyltoluene	0.00093	0.004	0.013	0.0024	0.011	0.0311	0.025
p-xylene	0.00067	0.003	0.008	0.0007	0.007	0.0209	0.016
toluene	0.00095	0.006	0.019	0.0024	0.012	0.0322	0.054

* FAC = mass of aerosol produced/ mass of hydrocarbon reacted (Grosjean , 1992)

Total of four sets of IAR are calculated at 25 and 75% conversion for M_{int} of 5 μg/m^3, and at 50% conversion for M_{int} of 5and 15 μg/m^3. At 50% conversion, incremental aerosol reactivity ranges from 0.001 (1,3,5-trimethylbenzene) to 0.019 (n-propylbenzene) for M_{int} equal 5 μg/m^3, and from 0.002 (1,3,5-trimethylbenzene) to 0.027 (n-propylbenzene) when M_{int} is 15 μg/m^3. For the same amount of initial aerosol concentration (e.g., 5 μg/m3), IAR increases as the conversion of parent hydrocarbons gets higher. For example, IAR of toluene are 0.00095, 0.006, and 0.019 at 25, 50, and 75%, respectively. These values are somewhat lower than the Fractional Aerosol Coefficients (Grosjean, 1992) reported in Table 4.1. As noted in Chapter 2, these FACs were based on knowledge of the reactions of these compounds and expert judgement. The most probable reason for the FACs values being consistently higher than the models used in this work is due to partitioning. Early models of SOA formation generally assumed all condensable species would reside in the aerosol phase, while current models recognize that a gas phase-condensed phase equilibrium will be established.

IARs of all investigated compounds (shown in Table 21) are positive, which means that adding more hydrocarbon precursors results in higher amounts of aerosol products. This contrasts with incremental reactivities for ozone, which have both positive and negative values (Carter, 1994). IARs for M_{int} equal 15 μg/m^3 are a factor of 2-3 higher than those for M_{int} equal 5 μg/m^3, although the ratio is not consistent for all compounds. These incremental aerosol reactivities may be useful for estimating

aerosol formation potentials from emission ratios. A better approach, as outlined in Chapter 3 would be to estimate aerosol yield based on condensable product formation. If individual reaction products are tracked, then the results of Chapter 3 can be employed. In many cases, however, only lumped reacting species are used. Therefore, the remainder of this chapter will present a lumped mechanism for predicting SOA yield from aromatic precursors.

4.2 SOA formation in Eulerian photochemical models

Airshed model applications include simulations of mixtures of a large number of reacting species. The information and chamber data required for determining the exact kinetic behaviors of individual species are often unavailable. To solve this problem, species with similar reaction rates and mechanisms are commonly grouped together and represented by lumped model species. The lumped model species are treated as a pseudo compound. One of the main benefits of lumping is that the chemistry of a large number of volatile organic compounds (VOCs) can be modeled without complete information for each individual species.

The previous chapter described the development of quantitative models of SOA formation for individual hydrocarbon precursors. This chapter discusses the lumping scheme used for aromatic species and the estimates of model parameters for lumped species, which were developed based on information for groups of individual compounds.

4.3 Quantitative models of SOA formation for lumped species

4.3.1 Theoretical Background

The aggregation system of lumping compounds into groups based on their chemical and physical similarities has been studied by researchers for over three decades. Wei and Kuo (1969) were pioneers in studying aggregation of many monomolecular reacting species. Goliken (1972) investigated the effect of temperature on the reaction rate of group model species. Results revealed that although the activation energies of individual species can be described by the Arrhenius expression, this equation does not adequately describe the activation energies of lumped species. The behavior of the lumped species can differ from that of a single compound. The properties of the grouped species may depend on the compositions and total concentrations of the feed (Golikeri and Luss, 1974). To diminish errors associated with representing individual species by lumped model species, it may be necessary to lump compounds into sub-groups.

There are various types of lumping approaches used in applications of airshed modeling. Carter (2000) recommended several lumping methods. The first method is the lumped molecule approach. In this approach, VOCs are represented by model species in the base mechanisms on a molecule-for-molecule basis (i.e., $C_{lump} = \Sigma C_{i,species}$)(Carter, 2000). For example, in SAPRC the lumped higher aldehyde species, RCHO, are used to represent all aldehydes. This approach is appropriate for compounds with similar chemical characteristics.

The second approach is the variable weighting lumped parameter. In this method, a group of VOCs with similar reactivities are represented by a lumped model species. Kinetic and product yield parameters of the lumped species depend on the concentrations of VOCs in the reacting mixture. Kinetic parameters for the lumped species are weighted averages of emissions of VOCs within the mixture (e.g., $k_{lump} = \Sigma W_i * k_i$, species, where W_i is a weighting factor). This approach is the most accurate lumping method for following reasons. First, compared to the lumped molecule approach (which sum up the concentrations of participating VOCs in the mixture regardless of their reactivities), this approach weights kinetic and product yield parameters depending on reactivities of VOCs in the mixture. Second, model parameters are evaluated based on the characteristics of VOCs in the mixture, while those for the fixed parameter approach (discussed below) are derived using a typical ambient mixture, and used for all applications regardless of the actual concentrations.

There are two weighting methods currently used to estimate the kinetic and product yield parameters of model species in SAPRC. The first method is based on reactivity weighting, and second is based on molar weighting. For reactivity weighting, the contribution of a given VOC is related to the amount of VOC that is estimated to react (Carter, 2000).

$$\text{Amount reacted} = \text{Amount emitted} * \text{Fraction reacted} \quad \textbf{Equation 37}$$

$$\text{Fraction Reacted} = \text{Kinetic reactivity} \approx (1-\exp(-k_{OH}*\text{IntOH})) \quad \textbf{Equation 38}$$

Where k_{OH} is the OH radical rate constant and IntOH is an effective integrated OH radical rate constant. Reactivity weighting is appropriate for slower reacting species (k_{OH} < 2.0E +04 $ppm^{-1}min^{-1}$). For slowly reacting species, 100% conversion is unlikely to happen in a limited simulation time. Therefore, a fraction reacted is utilized to determine the actual amount of each VOC that reacts. In molar weighting, the contribution of a given VOC to the parameters of lumped model species is proportional to the amount of VOC emitted or input. This method is more suitable for faster species (k_{OH} > 2.0E+04 $ppm^{-1}min^{-1}$) (Carter, 2000), since the fast reacting species are more likely to react completely in a shorter period of time.

The third lumping approach is a fixed parameter method. Parameters for the lumped species are estimated from a representative ambient mixture or emission profile. These parameters are then applied in all model simulations irrespective of the actual emissions involved. This approach is accurate if the compositions of VOCs emitted are well represented by the compositions used to derive the mechanisms.

4.3.2 Lumping Scheme

The lumping approach used in SAPRC is the variable weighting lumped parameter method. Aromatic species are lumped into two groups: ARO1 and ARO2 based on their reactivities. ARO1 represents a group of species that react slowly (k_{OH} < 2.0E +04 $ppm^{-1}min^{-1}$ at 300 K). Species that react fast (k_{OH} > 2.0E +04 $ppm^{-1}min^{-1}$) are represented by ARO2. Table 4.2 lists species in ARO1 and ARO2.

Table 4.2: Lists of species represented by model species ARO1 and ARO2

VOC Name	Represented By*	Lumped As
Benzene	BENZENE	0.295ARO1**
Toluene	TOLUENE	ARO1
Ethyl Benzene	C2-BENZ	ARO1
n-Propyl Benzene	N-C3-BEN	ARO1
Isopropyl Benzene (cumene)	I-C3-BEN	ARO1
C9 Monosub. Benzenes	N-C3-BEN	ARO1
s-Butyl Benzene	S-C4-BEN	ARO1
C10 Monosub. Benzenes	N-C3-BEN	ARO1
C11 Monosub. Benzenes	N-C3-BEN	ARO1
C12 Monosub. Benzenes	N-C3-BEN	ARO1
o-Xylene	O-XYLENE	ARO2
p-Xylene	P-XYLENE	ARO2
m-Xylene	M-XYLENE	ARO2
C9-Disub. Benzenes	0.34 M-XYLENE + 0.33 O-XYLENE + 0.33 P-XYLENE	ARO2
C10-Disub. Benzenes	0.34 M-XYLENE + 0.33 O-XYLENE + 0.33 P-XYLENE	ARO2
C11-Disub. Benzenes	0.34 M-XYLENE + 0.33 O-XYLENE + 0.33 P-XYLENE	ARO2
C12-Disub. Benzenes	0.34 M-XYLENE + 0.33 O-XYLENE + 0.33 P-XYLENE	ARO2
1,3,5-Trimethylbenzene	135-TMB	ARO2
1,2,3-Trimethylbenzene	123-TMB	ARO2
1,2,4-Trimethylbenzene	124-TMB	ARO2
C9 Trisub. Benzenes	0.34 135-TMB + 0.33 123-TMB + 0.33 124-TMB	ARO2
C10 Trisub. Benzenes	0.34 135-TMB + 0.33 123-TMB + 0.33 124-TMB	ARO2
C11 Trisub. Benzenes	0.34 135-TMB + 0.33 123-TMB + 0.33 124-TMB	ARO2
C12 Trisub. Benzenes	0.34 135-TMB + 0.33 123-TMB + 0.33 124-TMB	ARO2
C10 Tetrasub. Benzenes	0.34 135-TMB + 0.33 123-TMB + 0.33 124-TMB	ARO2
o-Ethyl Toluene	O-C2-TOL	ARO2
p-Ethyl Toluene	P-C2-TOL	ARO2
m-Ethyl Toluene	M-C2-TOL	ARO2

* represented in SAPRC99

**one mole of benzene is presented by 0.295 moles of ARO1, because kinetic reactivity of benzene is less than 1/3 that of toluene and ARO1 is dominated by toluene and alkylbenzenes

Integrating the quantitative SOA formation into SAPRC requires that aerosol species be lumped as well. Aerosol precursor species (APRs) are separated into four groups: APR1-APR4, based on the reactivities of aromatic reactants and aerosol precursors.

The same criteria used in lumping aromatic reactants are also applied in the second step aggregation (APRs).

- APR1 are aerosol precursors that react slowly that are formed by aromatic precursors that react slowly (ARO1)
- APR2 are aerosol precursors that react slowly that are formed by aromatic precursors that react rapidly (ARO2)
- APR3 are aerosol precursors that react rapidly that are formed by aromatic precursors that react slowly (ARO1)
- APR4 are aerosol precursors that react rapidly that are formed by aromatic precursors that react rapidly (ARO2)

The lists of detailed species of aerosol precursors, along with their rate constants for reactions with OH radicals for each lumped groups are presented in Table 4.3.

Table 4.3: Lists of detailed species and their OH rate constants represented by model species APR1, APR2, APR3, and APR4

Precursors	APRs	kOH (cm^3/molc-sec)	Kom1 ($m^3/\mu g$)	Kom2 ($m^3/\mu g$)	Stoichiometric Coefficients*
APR1 (slow reactivity hydrocarbon precursors and slow reactivity APRs)					
Benzene	APB1 	6.96E-12			0.20
I-C3-Ben	APB2 	6.96E-12			0.167
	APB4 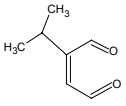	1.00E-11			0.079

Precursors	APRs	kOH (cm^3/molc-sec)	Kom1 (m^3/μg)	Kom2 (m^3/μg)	Stoichiometric Coefficients*
S-C4-Ben	APB5 	6.96E-12			0.167
	APB7 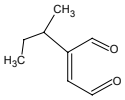	1.00E-11			0.119
Toluene	APTO2 	6.96E-12	0.0123	0.00109	0.167
Ethylbenzene	APEB1 	6.96E-12	0.036	0.00322	0.167
	APEB3 	1.00E-11	0.036	0.00322	0.079
C3-Ben	APPB1 	6.96E-12	0.0722	0.00198	0.167

APR2 (fast reactivity hydrocarbon precursors and slow reactivity APRs)

124-TMB	APT9 	1.27E-11	0.00708	0.000164	0.046
	AP10 	1.00E-11	0.00708	0.000164	0.107
p-xylene	APX4 	1.00E-11	0.0042	0.000367	0.489

Precursors	APRs		kOH (cm^3/molc-sec)	Kom1 (m^3/μg)	Kom2 (m^3/μg)	Stoichiometric Coefficients*
o-xylene	APX3		6.99E-12	0.00459	0.000369	0.20
m-xylene	APX8	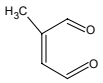	1.00E-11	0.00203	0.000175	0.188
p-C2-Tol	APET2	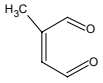	1.00E-11	0.0069	0.000569	0.20
	APET3		1.00E-11	0.0069	0.000569	0.04
o-C2-Tol	APET8		6.99E-12	0.00844	0.000735	0.186
m-C2-Tol	APET10	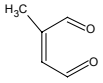	1.00E-11	0.0049	0.000433	0.054
	APET11		1.00E-11	0.0049	0.000433	0.134

APR3 (slow reactivity hydrocarbon precursors and fast reactivityAPRs)

I-C3-Ben	APB3	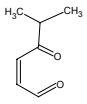	1.85E-11			0.158
S-C4-Ben	APB6	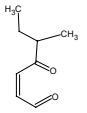	1.88E-11			0.119
Toluene	APTO1	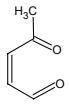	1.85E-11	0.0123	0.00109	0.238

Precursors	APRs		kOH (cm^3/molc-sec)	Kom1 (m^3/μg)	Kom2 (m^3/μg)	Stoichiometric Coefficients*
Ethylbenzene	APEB2		1.85E-11	0.036	0.00322	0.158
C3-Ben	APPB2	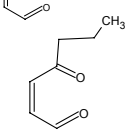	1.85E-11	0.0722	0.00198	0.158
	APPB3	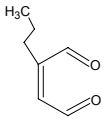	1.85E-11	0.0722	0.00198	0.079

APR4 (fast reactivity hydrocarbon precursors and fast reactivity APRs)

135-TMB	APT1	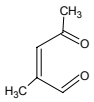	2.66E-11	0.00337	0.000294	0.79
123-TMB	APT2		1.85E-11			0.431
	APT3	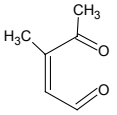	2.66E-11			0.254
	APT4	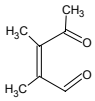	3.66E-11			0.085
124-TMB	APT5	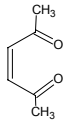	4.88E-11	0.00708	0.000164	0.254
	APT6	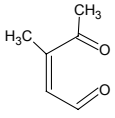	2.66E-11	0.00708	0.000164	0.084
	APT7	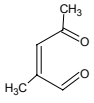	2.66E-11	0.00708	0.000164	0.131

Precursors	APRs		kOH (cm^3/molc-sec)	Kom1 (m^3/μg)	Kom2 (m^3/μg)	Stoichiometric Coefficients*
	APT8	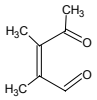	3.36E-11	0.00708	0.000164	0.146
p-xylene	APX5	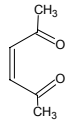	4.88E-11	0.0042	0.000367	0.24
o-xylene	APX1		1.85E-11	0.00459	0.000367	0.45
	APX2		2.66E-11	0.00459	0.000369	0.14
m-xylene	APX6	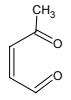	1.85E-11	0.00203	0.000175	0.376
	APX7	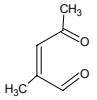	2.66E-11	0.00203	0.000175	0.188
p-C2-Tol	APET1	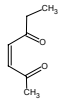	4.57E-11	0.0069	0.000569	0.49
o-C2-Tol	APET4		1.85E-11	0.00844	0.000735	0.329
	APET5	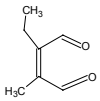	1.00E-11	0.00844	0.000735	0.085
	APET7	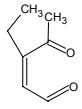	2.70E-11	0.00844	0.000735	0.051
	APET6	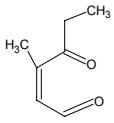	2.70E-11	0.00844	0.000735	0.026
	APET9	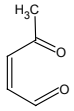	1.85E-11	0.00844	0.000735	0.0659

Precursors	APRs	kOH (cm^3/molc-sec)	Kom1 ($m^3/\mu g$)	Kom2 ($m^3/\mu g$)	Stoichiometric Coefficients*
m-C2-Tol	APET12 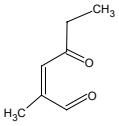	2.70E-11	0.0049	0.000433	0.08
	APET13 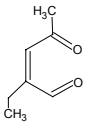	2.70E-11	0.0049	0.000433	0.106
	APET14 	1.85E-11	0.0049	0.000433	0.226
	APET15 	1.85E-11	0.0049	0.000433	0.153

* moles of APRs produced per one mole of precursor reacted

Figure 4.1 depicts lumping scheme of aromatic hydrocarbons and aerosol precursors that is used in the lumped model developed in this thesis. These hydrocarbon and aerosol precursors were lumped using the variable lumped parameter approach.

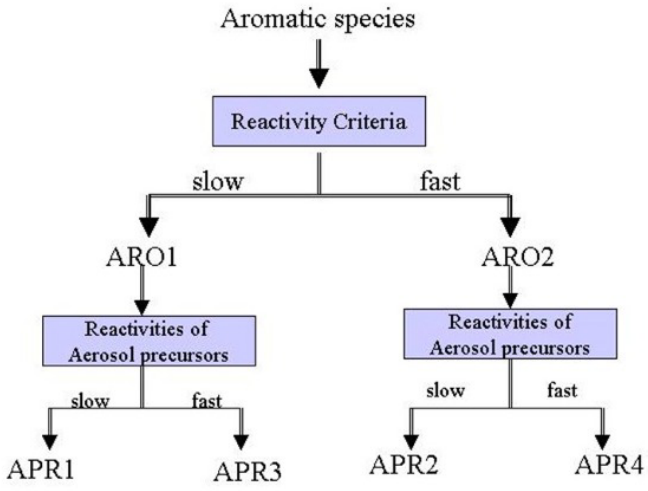

Figure 4.1: Lumping scheme for aromatic species and aerosol precursors modified in SAPRC

As shown in Figure 4.1, the first tier of lumping is for aromatic hydrocarbon precursors. Groups of aromatic species are lumped and represented by two model species: ARO1 and ARO2 based on their reactivities. In the second tier, aerosol precursors are grouped and represented by four lumped model species: APR1-APR4. For example, APR1 represents a group of less reactive aerosol precursors that are produced from slow reactive aromatic reactants. Quantitative models of SOA formations were developed for these six lumped groups.

$$ARO1 + HO. = \text{gas-phase products} + a_1APR1 + a_2APR2 \quad \textbf{Reaction 21}$$

$$ARO2 + HO. = \text{gas-phase products} + a_3APR3 + a_4APR4 \quad \textbf{Reaction 22}$$

$$APR1 + HO. = a_5PM1 + a_6PM2 + a_6RO2R + a_5RO2N \quad \textbf{Reaction 23}$$

$$APR2 + HO. = a_7PM3 + a_8PM4 + a_8RO2R + a_7RO2N \quad \textbf{Reaction 24}$$

$$APR3 + HO. = a_9PM5 + a_{10}PM6 + a_{10}RO2R + a_9RO2N \quad \textbf{Reaction 25}$$

$$APR4 + HO. = a_{11}PM7 + a_{12}PM8 + a_{12}RO2R + a_{11}RO2N \quad \textbf{Reaction 26}$$

Where a_1-a_{11} are stoichiometric coefficients. Coefficients a1-a4 were estimated using either the reactivity or molar weighting method from SAPRC. Coefficients a5-a11 were derived using the reactivity weighting method and simulations. These estimates will be described in the next section. PM1 through PM8 are low-volatility products produced from reactions of aerosol precursors with OH radicals.

4.3.3 Estimates of Model Parameters

After the models of SOA formation for lumped aromatic species were developed and incorporated into SAPRC, the model parameters for each lumped species listed in Table 4.4 were estimated. Analogous to model parameters for individual compounds, model parameters for lumped species can be classified into two categories. The first group of parameters is used to describe the reactions. This group contains rate constants, stoichiometric coefficients, and molecular weights of the lumped species. The second group of parameters is used to estimate the phase partitioning of semivolatile products. This group contains partitioning coefficients.

Table 4.4: Model Parameters Used to Simulate SOA Formation from Lumped Aromatic Species

Parameters	Descriptions	Calculation Procedures
Chemical model		
k_i	Rate constant of compound i	Fitting method, weighting method
a_i	Stoichiometric coefficient of compound i	Fitting method, weighting method
MWi	Molecular weight of compound i	Weighting method
Physical model		
Kom,i	Partitioning coefficient of compound, i	Fitting method, weighting method
SOA production		
A_i	Gas phase concentration of product i	Simulation Calculation
Fi,om	Concentration of product i in the absorbing om phase	
ΔMo	Organic aerosol mass concentration produced for a given amount of ROG reacted	Simulation calculation
Y_i	Fractional aerosol yields for product i	Simulation calculation

There are two methods used in this study to estimate model parameters: the weighting method and the simulations. As described in the preceding section, the weighting methods can further be categorized into two groups: reactivity weighting and molar weighting. Model parameters for ARO1, which is the model species that represents a group of slower aromatic compounds, were estimated using reactivity weighting (based on data in SAPRC). Parameters for ARO2, which represents a group of faster aromatic compounds, were determined using molar weighting (based on data in SAPRC). Model parameters for APR1-APR4 were estimated based on reactivity weighting. Although the molar weighting can be used for fast reacting species (APR2 and APR4), it is more appropriate to use the reactivity weighting for the following reasons. First, these model species represent groups of aerosol precursors with widely varying kinetic reactivities. Second, the reactivity weighting is reduced to the molar weighting for fast reacting species. Finally reactivities of some of aerosol precursors are relatively close to the reactivity used to separate molar and reactivity weighting in SAPRC (2.0E+4 $ppm^{-1}min^{-1}$). Thus, employing the reactivity weighting to estimate model parameters for APR1-APR4 covers the entire range of slow and fast reacting species. To describe the expressions used to estimate the model parameters, the consecutive reactions resulting in the condensable products must be considered.

$$A + OH. \xrightarrow[k_2]{k_1} a_1B$$

$$B + OH. \xrightarrow{} a_2C$$

Where A is aromatic reactant, B is aerosol precursor, and C is condensable product. The concentration at any given time is expressed by the following equations.

$$C_A(t) = C_{A0}e^{-k_1 IntOH} \quad \textbf{Equation 39}$$

$$C_B(t) = a_1 C_{A0} k_1/(k_2-k_1)[e^{-k_1 IntOH} - e^{-k_2 IntOH}] \quad \textbf{Equation 40}$$

$$C_C(t) = C_{A0}-C_A-C_B = a_2 k_2 a_1 k_1 C_{A0}/(k_2-k_1)[(e^{-k_2 IntOH})/k_2 - (e^{-k_1 IntOH})/k_1 - (1/k_2-1/k_1)] \quad \textbf{Equation 41}$$

Where: $C_A(t)$ = concentration of hydrocarbon precursor at time t (ppm)

$C_B(t)$ = concentration of aerosol precursor at time t (ppm)

$C_C(t)$ = concentration of semivolatile product at time t (ppm)

k_1 = OH rate constant of hydrocarbon precursor ($ppm^{-1}min^{-1}$)

k_2 = OH rate constant of aerosol precursor ($ppm^{-1}min^{-1}$)

a_1 = stoichiometric coefficient of aerosol precursor produced from oxidation reaction of hydrocarbon precursor

a_2 = stoichiometric coefficient of semivolatile product produced from aerosol precursor reaction

C_{A0} = initial concentration of hydrocarbon precursor (ppm)

IntOH = an effective integrated OH radical rate constant, which is the concentration of OH integrated during the specific time. For the purpose of lumping, OH concentration is assumed to be constant. (*IntOH* =1.0E-4 ppm-min for regional model applications, Carter, 2000)

The weighting factor (*WF*) is based on the amount for hydrocarbon and aerosol precursors that react. Weighting factor of A and B at time t are given by

$$WF_A = C_A(t)^R = C_{A0} - C_A(t) = C_{A0}(1-e^{-k_1 * IntOH}) \quad \textbf{Equation 42}$$

$$WF_B = 1/a_2 * C_C(t) = C_B(t)^R = C_B^{generated}(t) - C_B(t) = k_2 a_1 k_1 C_{A0}/(k_2-k_1)[(e^{-k_2 IntOH})/k_2 - (e^{-k_1 IntOH})/k_1 - (1/k_2-1/k_1)] \quad \textbf{Equation 43}$$

Where: $C_A(t)^R$ = amount of hydrocarbon precursor that reacts (ppm)

$C_B(t)^R$ = amount of aerosol precursor that reacts (ppm)

$C_A^{generated}(t)$ = amount of hydrocarbon precursor generated (ppm)

$C_B^{generated}(t)$ = amount of aerosol precursor generated (ppm)

The weighting factor used to estimate model parameters for ARO1 was determined using equation 42. The weighting factor for ARO2 (fast reacting group) was simply the emitted amount of VOCs in the group (i.e., $WF_{ARO2} = C_{ARO20}$, where C_{ARO20} is the initial concentration of model species ARO2 (ppm)). Equation 43 is applied to evaluate weighting factors for aerosol precursors (APR1-APR4).

Besides using weighting factors, empirical fitting was also employed in the parameter estimates for lumped model compounds (APR1-APR4). The concentrations of the lumped model species were compared to the summed concentrations of individual species in that group. Parameters such as OH rate constant of lumped aerosol precursors (k_{lump}) were adjusted to improve the fit. For example, OH rate constant of model species APR1 was estimated by comparing the

concentration of APR1 with the summed concentrations of individual species it represents (i.e., fitting $C_{APR1} = \Sigma C_{i,\,species}$ by adjusting $k_{OH,lump}$ of APR1).

Estimates of Rate Constants of lumped aerosol precursors (APR1-APR4) with OH Radical

The rate constants of lumped species (APR1-APR4) representing aerosol precursors can be determined using weighting method as expressed below:

$$k_{OH,lumped} = \frac{\sum_i k_{OH,i} * WFi}{\sum_i WFi} \qquad \textbf{Equation 44}$$

Where WF_i is expressed as equation 43 and $k_{OH,i}$ is rate constant of aerosol precursor species *i* represented by lumped species.

In addition to weighting method, k_{OH} of the lumped species (APR1-APR4) can be estimated by fitting the rate constant to the results from simulations using single compound. The concept of this method is to fit the concentration of a lumped aerosol precursor to the summed concentrations of individual aerosol precursor (equation 45). The summation of concentrations of individual species is denoted as:

$$\sum C_{APR,i} = \sum_i a_{1,i} C_{A0,i} k_{1,i} / (k_{2,i} - k_{1,i})[e^{-k_{1,i}IntOH} - e^{-k_{2,i}IntOH}] \qquad \textbf{Equation 45}$$

Where: C_{APRi} = concentration of aerosol precursor species i (ppm)

$C_{A0,i}$ = initial concentration of hydrocarbon precursor responsible in producing aerosol precursor species i (ppm)

$k_{1,i}$ = OH rate constant of hydrocarbon precursor responsible in producing aerosol precursor species i ($ppm^{-1}min^{-1}$)

$k_{2,i}$ = OH rate constant of aerosol precursor species i (ppm-1min-1)

$a_{1,i}$ = stoichiometric coefficient of aerosol precursor species I produced from reaction of hydrocarbon precursor

The concentration of lumped aerosol compounds is given by

$$C_{\text{lumped APR}} = a_{1,\text{lumped}} * C_{A0,\text{lumped}} * k_{1,\text{lumped}} / (k_{2,\text{lumped}} - k_{1,\text{lumped}}) [e^{-k1,\text{lumped}*\text{IntOH}} - e^{-k2,\text{lumped}*\text{IntOH}}] \quad \textbf{Equation 46}$$

Where: $C_{\text{lumped APR}}$ = concentration of lumped aerosol precursor (APR1-APR4) (ppm)

$C_{AO,\text{lumped}}$ = initial concentration of lumped hydrocarbon precursor (ARO1 or ARO2) responsible in producing lumped species APR1-APR4 (ppm)

$k_{1,\text{lumped}}$ = OH rate constant of lumped hydrocarbon precursor (ARO1 or ARO2) ($ppm^{-1}min^{-1}$)

$k_{2,\text{lumped}}$ = OH rate constant of lumped aerosol precursor (APR1-APR4) ($ppm^{-1}min^{-1}$)

$a_{1,\text{lumped}}$ = stoichiometric coefficient of lumped aerosol precursor (APR1-APR4) produced from reaction of lumped hydrocarbon precursor (ARO1 or ARO2)

Figure 4.2 shows the results of applying fitting and weighting methods to calculate k_{OH} for lumped aerosol precursors as well as the summation of concentrations of individual aerosol precursors. Results for APR1, APR2, and APR4

show a good fit among the three sets of data points. These results indicate that the estimated rate constants of lumped APR species are a good representative for those of individual species in the groups. The concentration of lumped APR2 estimated from the weighting method differs from the summation of concentrations of individual aerosol precursors ($\sum C_{APRi}$) by approximately 5-30%. This reveals that the reactivity of lumped APR2 estimated using the weighting factor is overestimated. However, OH rate constant of lumped APR2 obtained from the fitting method agrees better with the summation of concentrations of individual species (ΣC_{APRi}), therefore this OH rate constant can be used for APR2. The estimated rate constants for lumped APR1 thorough APR4 are reported in Table 4.5. The disadvantage of using the rate parameter derived from the fitting method is that these results depend on the specific composition of the base mixtures in ways that are not precisely defined. The gas hydrocarbon composition used in the work is defined in appendix and is based on data for Houston, Texas.

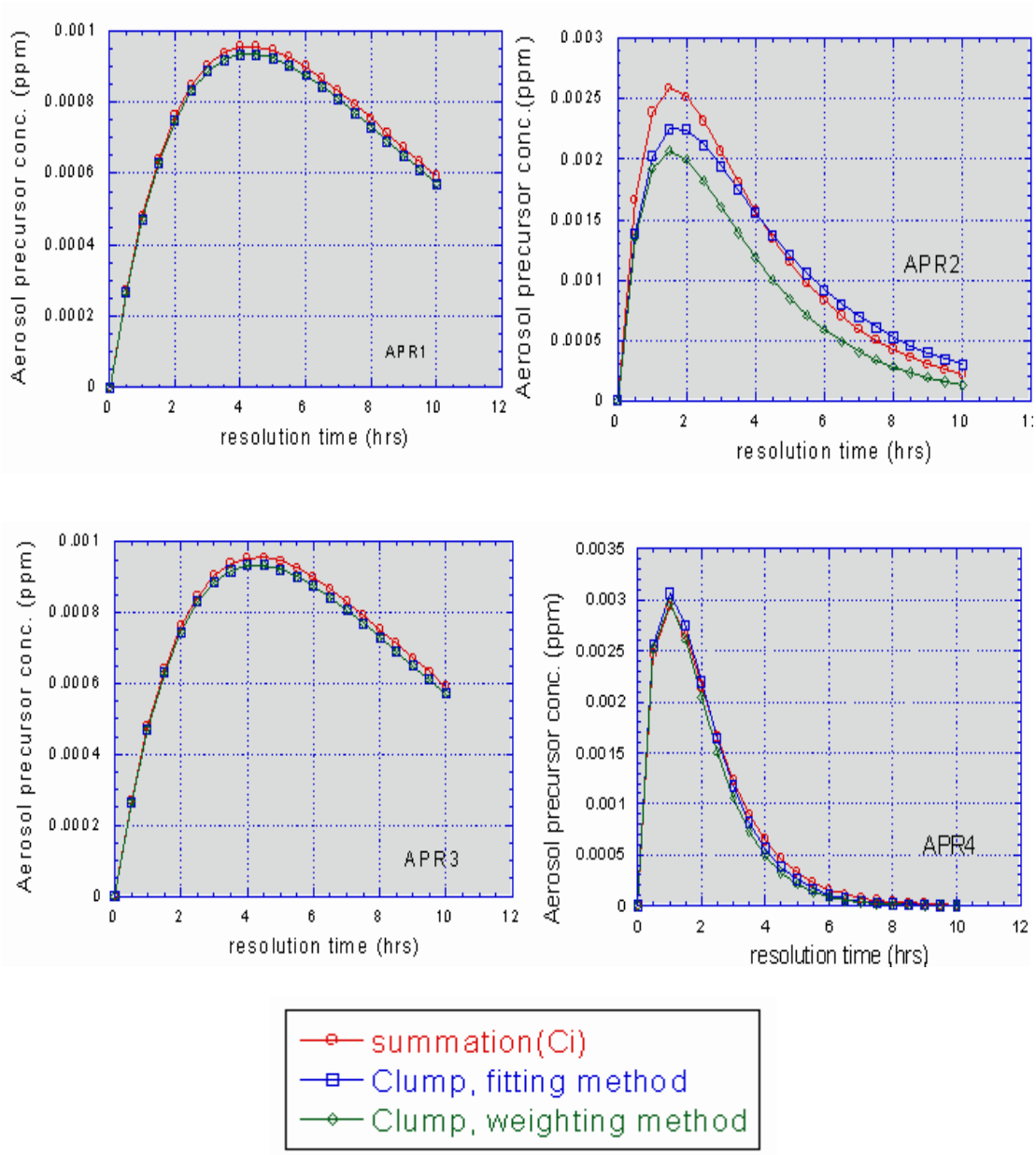

Figure 4.2: Concentrations of aerosol precursors as a function of time, three sets of data: (1) summation of concentrations of individual species in the group, (2) obtained by using fitting method (Clump, fitting method), and (3) estimated using weighting factor (Clump, weighting method)

Estimates of Stoichiometric Coefficients

Semivolatile products produced from lumped APR1-APR4 are denoted as PM1-PM8. Semivolatile products with organonitrate groups were classified as PM1, while products without organonitrate groups were denoted as PM2. PM1 and PM2 are formed from the reaction of APR1, and so on for PM3-PM8. Stoichiometric coefficients of PM1-PM8 can be estimated using either the weighting or fitting method. By using the weighting method, stoichiometric coefficients for lumped condensable species (PM1-PM8) are determined by

$$a_{lumpedPM} = \frac{\sum_i a_{2,i} * WFi}{\sum_i WFi} \qquad \textbf{Equation 47}$$

Where: $a_{2,i}$ = stoichiometric coefficient of semivolatile product species *i* being represented by lumped model species

$a_{lumpedPM}$ = stoichiometric coefficient of lumped semivolatile product (PM1-PM8)

WFi = weighting factor for species i as expressed by Equation 43.

For empirical fitting, the concentration of lumped semivolatile product ($C_{PM1} - C_{PM8}$), expressed by equation 48, was fitted to the summed concentration of detailed products in the groups (equation 49) by adjusting the stoichiometric coefficient for the lumped species (parameter "$a_{2,lumped}$ in equation 48).

$$C_{lumped\ PM} = a_{2,lumped} * k_{2,lumped} * a_{1,lumped} * k_{1,lumped} * C_{A0lumped} / (k_{2,lumped} - k_{1,lumped}) *$$
$$[(e^{-k2,lumped*IntOH})/k_{2,lumped} - (e^{-k1,lumped*IntOH})/k_{1,lumped} - (1/k_{2,lumped} - 1/k_{1,lumped})]$$

Equation 48

$$\sum C_{PM,i} = \sum_{i} a_{2,i} k_{2,i} a_{1,i} k_{1,i} C_{A0,i} / (k_{2,i} - k_{1,i})[(e^{-k_{2,i}IntOH})/k_{2,i} - (e^{-k_{1,i}IntOH})/k_{1,i} - (1/k_{2,i} - 1/k_{1,i})]$$

Equation 49

Where: $C_{lumped\ PM}$ = concentration of lumped semivolatile product (ppm)

$a_{2,lumped}$ = stoichiometric coefficient of lumped semivolatile product

$a_{2,i}$ = stoichiometric coefficient of semivolatile product species i

Seen in Figure 4.3 are the estimates of the concentration of lumped semivolatile products for APR1 (PM1 and PM2) using the weighting and fitting method, and the summation of concentrations of semivolatile products for individual aerosol precursors. Results of all products from four lumped aerosol species are displayed in Appendix E. As shown in Figure 4.3, concentrations of PM1 and PM2 fit extremely well among the three sets of data points. Stoichiometric coefficients of condensable products generated from the individual species in each group are well represented by those of products produced from lumped aerosol precursors. The estimated stoichiometric coefficients of semivolatile products for the four lumped aerosol precursors (APR1-APR4) are reported in Table 4.5.

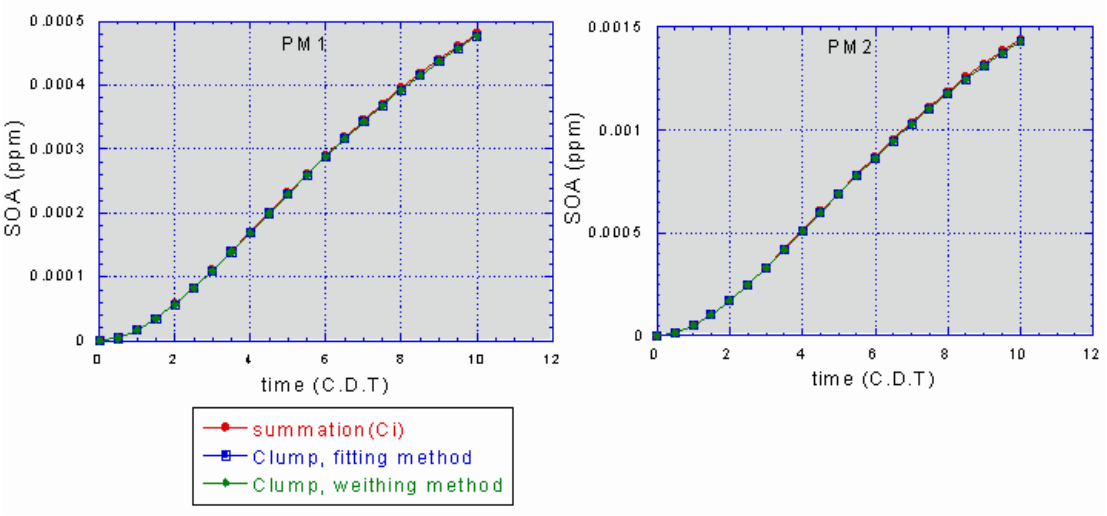

Figure 4.3: Concentrations of condensable products, three sets results: summation of concentrations from individual species, concentration of lumped species obtained by using the fitting method, and by using weighting factor

Estimates of Partitioning Coefficients

A gas/particle partitioning absorption mechanism developed by Pankow (1996) was employed in this study to estimate the amount of semivolatile products partitioning to the aerosol phase. The partitioning coefficient for compound i (*Kom,i*) is expressed in terms of total aerosol mass concentrations as:

$$Kom,i = F_{i,om}/A_i * Mo \qquad \textbf{Equation 50}$$

And

$$A_i = P_i - F_{i,om} \qquad \textbf{Equation 51}$$

Where:

A_i = gas phase concentration of product species i ($\mu g/m^3$)

$F_{i,om}$ = concentration of semivolatile product species i in the absorbing om phase ($\mu g/m^3$)

P_i = total concentration of semivolatile product species i ($\mu g/m^3$)

Mo = total aerosol mass concentration ($\mu g/m^3$)

The estimated *Kom,i* for lumped species obtained using the weighting method is given by

$$Kom,lumped = \frac{\sum_i Kom,i * WFi}{\sum_i WFi} \qquad \textbf{Equation 52}$$

Where *Kom,lumped* is partitioning coefficient of lumped semivolatile product ($m^3/\mu g$), and WFi is given by Equation 43.

The estimated partitioning coefficients are then applied in equation (53) and (54) to determine SOA mass changes (ΔM) for lumped products. In addition to using the weighting method, *Kom* for lumped products can also be calculated using the empirical fitting. *Kom* for lumped species (parameters "*Kom,lumped*" in equation (54)) was adjusted until the difference between ΔM of lumped species and the summed aerosol mass change from individual products in the group ($\sum \Delta Mi$) is minimized. $\sum \Delta Mi$ and ΔM_{lumped} are given by the following equations:

$$\sum \Delta M_i = \sum_i \frac{K_{om,1i} * Mo * P_{1i}}{1 - Mo * K_{om,1i}} + \frac{K_{om,2i} * Mo * P_{2i}}{1 - Mo * K_{om,2i}} \qquad \textbf{Equation 53}$$

$$\Delta M_{lumped} = \frac{K_{om,lumped1} * Mo * P_{1lumped}}{1 - Mo * K_{om,lumped1}} + \frac{K_{om,lumped2} * Mo * P_{2lumped}}{1 - Mo * K_{om,lumped2}} \qquad \textbf{Equation 54}$$

Where: $Kom_{1,i}$ = partitioning coefficient of product type 1 produced from aerosol precursor species i ($m^3/\mu g$)

$Kom_{2,i}$ = partitioning coefficient of product type 2 produced from aerosol precursor species i ($m^3/\mu g$)

$P_{1,i}$ = total semivolatile product type 1 produced from aerosol precursor species i ($\mu g/m^3$)

$P_{2,i}$ = total semivolatile product type 2 produced from aerosol precursor species i ($\mu g/m^3$)

ΔM_i = aerosol mass changes for aerosol precursor species i ($\mu g/m^3$)

ΔM_{lumped} = aerosol mass changes for lumped aerosol precursor ($\mu g/m^3$)

$Kom_{lumped,1}$ = partitioning coefficient of lumped product type 1 (e.g., Kom for PM1) produced from lumped aerosol precursor ($m^3/\mu g$)

$Kom_{lumped,2}$ = partitioning coefficient of lumped product type 2 (e.g., Kom for PM2) produced from lumped aerosol precursor ($m^3/\mu g$)

$P_{1,lumped}$ = total semivolatile lumped product type 1 (e.g., PM1)produced from lumped aerosol precursor ($\mu g/m^3$)

$P_{2,lumped}$ = total semivolatile lumped product type 2 (e.g., PM2) produced from lumped aerosol precursor ($\mu g/m^3$)

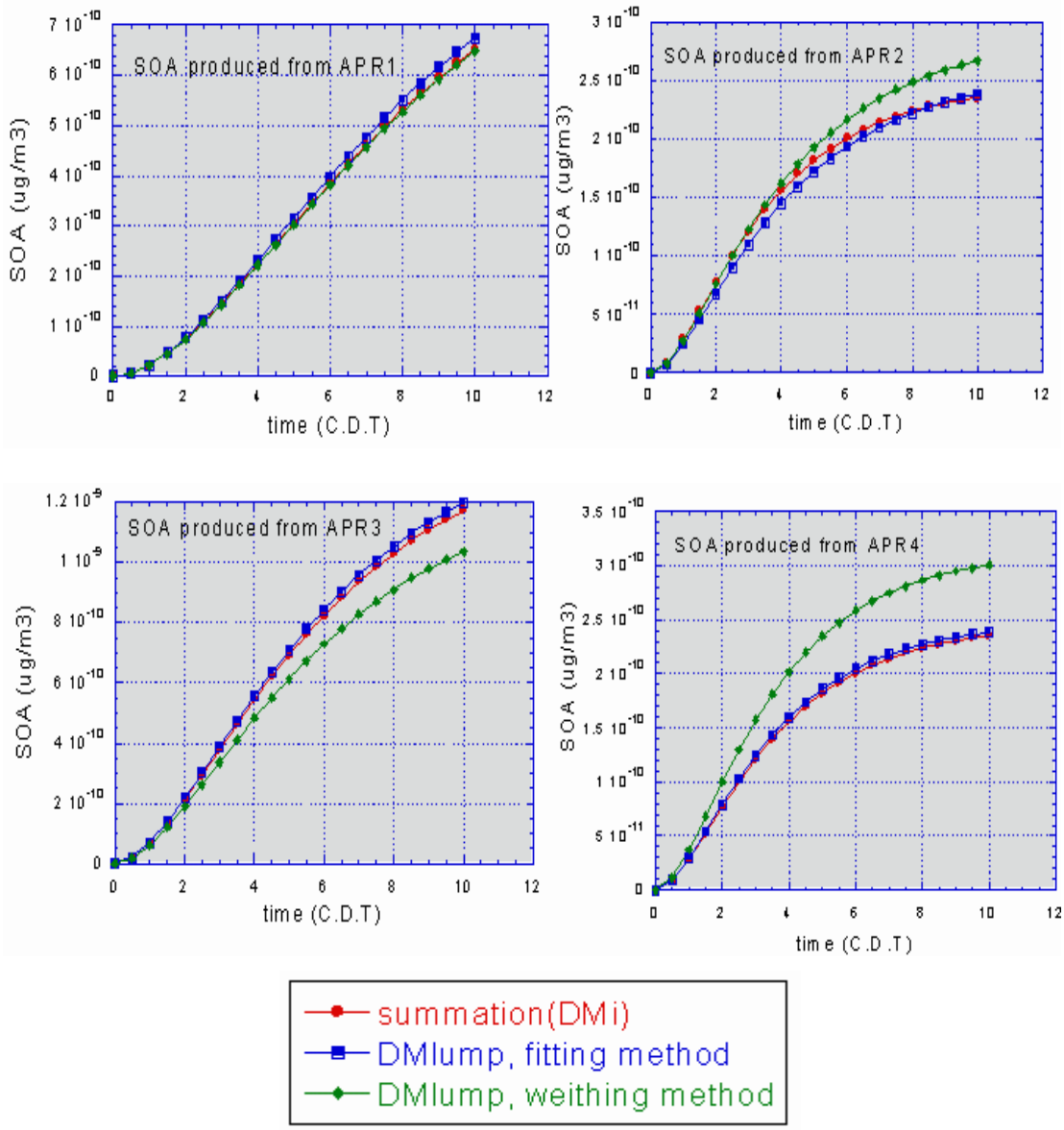

Figure 4.4: SOA mass changes from four lumped aerosol species: three sets of data point: ∑ΔMi from individual species in the groups, ΔM for lumped products obtained from fitting and weighting methods

Results of comparison among *ΔM* for the lumped products using the fitting methods, and the summation of *ΔM* of individual products indicate good

correspondence between them for the four lumped aerosol precursors. The calculated SOA mass changes determined using the weighting method differ from $\sum \Delta Mi$ in the ranges of 5-17%. It can be implied from these results that the partitioning coefficients determined for the lumped products are good representatives for those of individual products. The estimated partitioning coefficients are presented in Table 4.5.

Estimates of Molecular Weights of Lumped Species

Molecular weights of the lumped species were obtained by using the weighting method. This method averages number of hydrogen and carbon atoms in the product species for each lumped group. Aerosol precursors from the individual parent hydrocarbon in the same groups share the same base structure, but can differ in the total numbers of carbon and hydrogen atoms. For example, if APT2 and APX8 will be lumped together in the same group, and their structures are

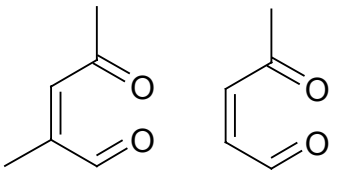

APT1 APX8

Therefore, APT1 and APX8 share base structure, which is $C_5H_6O_2$. APT1 has one carbon and two hydrogen atoms more than base structure. In turn, the molecular weights of lumped species are the combination of the molecular weight of base

structure and the weighted averages of the molecule weight of the excess carbon and hydrogen atoms from the individual aerosol precursors in these groups. The molecular weights of the lumped species are given by

$$MW_{lumped} = MW_{base\ structure} + XC2*12 + XH2 \quad \textbf{Equation 55}$$

Where XC2 and XH2 are the weighted averages of the extra carbon and hydrogen atoms from the individual aerosol precursors in the groups. The weighting of these parameters is based on the reactivities of the aerosol precursors and parent hydrocarbons, and the emissions of hydrocarbons. Tables 4.5 and 4.6 enumerate the estimated parameters for the lumped species obtained from both the fitting and weighting methods. Ambient conditions for Houston, TX (Carter, 1998) were used in the estimates of model parameters reported in Table 4.5. While the estimated molecular weights of lumped species, as listed in Table 4.6, were determined for the ambient mixtures at the Clinton site observed on the First and Second of September 2000.

Table 4.5: The estimated parameters for lumped species from fitting method (FT) and weighting method (WF)

	APR1		APR2		APR3		APR4	
	FT	**WF**	**FT**	**WF**	**FT**	**WF**	**FT**	**WF**
k_{APR} (cm^3/molc-sec)	7.17E-12	7.19E-12	7.83E-12	1.05E-11	1.82E-11	1.85E-11	2.8E-11	3.0E-11
Stoichiometric coefficients	-	0.179	-	0.260	-	0.209	-	0.499
Stoichiometric coefficients of semivolatile product type 1 produced from	0.25	0.25	0.30	0.25	0.25	0.25	0.24	0.25
Stoichiometric coefficients of semivolatile product type 2 produced from	0.75	0.75	0.70	0.75	0.75	0.75	0.76	0.75
Partitioning coefficients of semivolatile product type 1 produced from	0.016	0.023	0.003	0.00359	0.0224	0.0214	0.0027	0.0039
Partitioning of coefficient of semivolatile product type 2 produced from	0.00144	0.00156	0.00026	0.00032	0.00264	0.00137	0.000233	0.000328

Table 4.6: The estimated molecular weights of lumped species from weighting method

Date	**MW**					
Sep-01	**ARO1**	**ARO2**	**APR1**	**APR2**	**APR3**	**APR4**
	89.9	106.0	84.0	98.0	98.0	109.7
	PM1	**PM2**	**PM3**	**PM4**	**PM5**	**PM6**
	163.0	117.0	177.0	131.0	177.0	131.0
Sep-02	**ARO1**	**ARO2**	**APR1**	**APR2**	**APR3**	**APR4**
	87.8	114.8	85.2	99.0	100.0	110.0
	PM1	**PM2**	**PM3**	**PM4**	**PM5**	**PM6**
	178.0	132.0	179.0	133.0	190.0	178.0

As discussed in Chapter 3, Odum fit adjustable 4 parameters, $Kom,_1$, $Kom,_2$, α_1, and α_2, that provided the best fit of SOA yields from his model to observations made in environmental chamber. These values are 0.038, 0.042, 0.167, and 0.0014 for α_1, $Kom,_1$, α_2, and $Kom,_2$, respectively for high-yield aromatics. Odum found α_1, $Kom,_1$, α_2, and $Kom,_2$ for low-yield aromatics are 0.071, 0.053, 0.138, 0.0019, respectively. In this study, high-and low-yield aromatics are represented by model species ARO1 and ARO2. ARO1 produces aerosol precursors represented by lumped model species APR1 and APR3. Model species APR2 and APR4 represent aerosol precursors generated from ARO2. Thus $Kom,_i$ for semivolatile products produced from APR1 and APR3 (PM1,PM2,PM5,and PM6) are compared with Kom,i for high-yield aromatics of Odum, and Kom,i for products formed from APR2 and APR4 (PM3, PM4, PM7, and PM8) are compared with those for low-yield aromatics. Table 4.7 recaps model parameters for lumped species estimated from this work and from Odum's study.

Table 4.7: Summaries of model parameters for lumped species

	Low-yield aromatics		High-yield aromatics	
Parameters	Estimates*	Odum's study	Estimates*	Odum's study
K_{om1}	0.0033	0.042	0.0207	0.053
K_{om2}	0.000286	0.0014	0.0018	0.0019

*Values were estimated from this work

4.3.4 Correlation between SOA yields and chemical and physical parameters

Chapter 3 presented empirical correlations for SOA yield for individual aromatic compounds. This section will present correlations for lumped aromatic compounds. The following expressions, developed for individual compounds, were also applied for lumped aromatics:

$$\Delta Mi = (\%DF_i) * (\Delta P_i) \quad \textbf{Equation 56}$$

$$\%DF_i = a*M_{int}^2 + b*M_{int} + c \quad \textbf{Equation 57}$$

In these expressions, $\%DF_i$ is distribution factor of lumped semivolatile product species i in the aerosol phase.

In Chapter 3 it was shown that $\%DF_i$ depends only on M_{int} and is independent of % conversion (for about a dozen aromatic compounds). This is expected be observed for lumped compounds as well. To assess this hypothesis, M_{int} was changed from 5 to 15 and 25 μg/m^3, and $\%DF_i$ at 25, 50, and 75% conversions were then calculated for each M_{int} level.

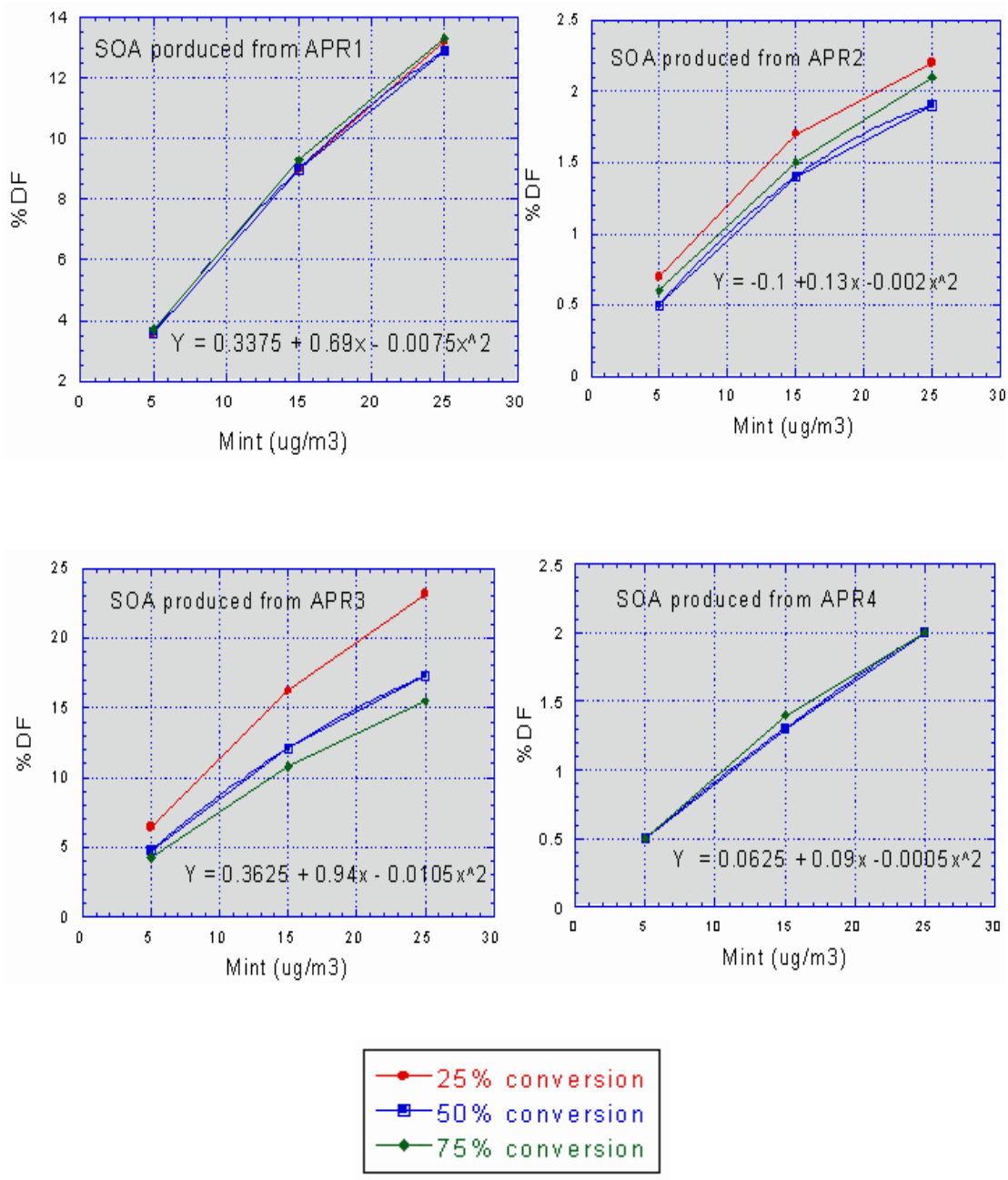

Figure 4.5: *%DFi* as a function of M_{int} at 25, 50 and 75% conversions for lumped species APR1-APR4

Seen in Figure 4.5 are $\%DF_i$ as a function of M_{int} at 25, 50, and 75% conversions for lumped aerosol precursors APR1- APR4. Results for these lumped species show the dependency of $\%DF_i$ on M_{int} but little dependence on % conversion. The exceptions are APR2 and APR3. For APR2 and APR3, the percentage of product that partitions into the aerosol phase ($\%DF_i$) is similar at 50 and 75% conversions, but is different for 25% conversion. The biggest deviations between $\%DF_i$ at 25 and 50% conversion for APR2 and APR4 are 13 and 33%, respectively. Similar reason causing the digression for individual compounds, which is the amount of ΔM_i is comparable to M_{tot}. The polynomial fitting was performed for $\%DF_i$ at 50% conversion for these lumped species. Table 4.8 lists the results of the evaluation of $\%DF_i$, as a function of M_{int} (as expressed in Equation 56).

Table 4.8: Coefficients a, b, and c for the correlation equation between $\%DF_i$ and M_{int} for lumped species APR1-APR4

Lumped species	a*	b*	c*
APR1	-0.0075	0.69	0.3375
APR2	-0.002	0.13	-0.1
APR3	-0.0105	0.94	0.3625
APR4	-0.005	0.09	0.625

* These coefficients were evaluated based on the base hydrocarbon composition and concentrations as seen in Houston, TX on September 2, 2000

4.4 Summary

The variable parameter lumping approach was used to lump aromatic hydrocarbon precursors into two groups. The aerosol precursors produced from the two lumped aromatic species (ARO1 and ARO2) were further separated into four groups (APR1-APR4) based on how rapidly these aerosol precursors react with OH

radical. Quantitative models of SOA formation for six lumped model species were developed and integrated into SAPRC99. Rate constants, stoichiometric coefficients, partitioning coefficients, and molecular weight of the lumped species were estimated from information on the individual species in the groups. Table4.5 summarizes the source of data for the parameters used in the model. The approaches used in these calculations were the fitting and weighting methods. These parameters were estimated based on emissions of the parent hydrocarbon in the reacting mixtures and the reactivities of the hydrocarbon and aerosol precursors. An ambient hydrocarbon mixture for Houston,TX area from 1998 data (Carter, 1998) was used in the estimates of the fixed model parameters, with the exception of the estimates of molecular weights of lumped species. Molecular weights were determined for the Houston conditions observed on the First and Second of September 2000. Overall results indicate that when an appropriate group of hydrocarbons is aggregated together, the accuracy of representing individual compounds by the lumped model species is enhanced. The SOA formation model developed in this study gives researchers an effective procedure to predict ambient SOA formation independent of complete information and understanding of individual ambient species. The models and reaction parameters developed in this chapter are applied to characterize SOA formation in Houston, TX in Chapter 5.

Chapter 5 Characterization of ambient SOA formation in Houston area

5.1 Introduction

Regional air quality models currently in use often neglect the formation of SOA in the aerosol module. This is due to the lack of complete understanding of secondary organic aerosol and its sources. With the implementation of proposed daily and annual PM-2.5 standards (NAAQS), many areas such as Houston, TX would likely to be declared non-attainment areas. Since SOA is a major contributor to ambient PM-2.5, meeting the proposed standards requires the reduction of emissions of hydrocarbons leading to SOA formation. In order to develop an effective strategy to reduce PM-2.5 concentrations, the sources and mechanisms describing SOA formation must be integrated into current air quality models.

Quantitative models of SOA formation for lumped aromatic hydrocarbons, developed in this study, were employed to characterize ambient SOA formation in the Houston, TX region. This chapter reports on the sensitivity of SOA formation in Houston to changes in concentrations of NOx, as well as the effect of SOA formation on ozone formation chemistry.

5.2 Case Study Scenario

PM_2.5 in Texas

Figure 5.1 reveals the average constituent concentration ($\mu g/m^3$) found in PM_2.5 in several cities in Texas. High levels of organic compounds have been found in PM_2.5, range from 4-5.6 $\mu g/m^3$ in, Houston, Mauriceville, and Dallas.

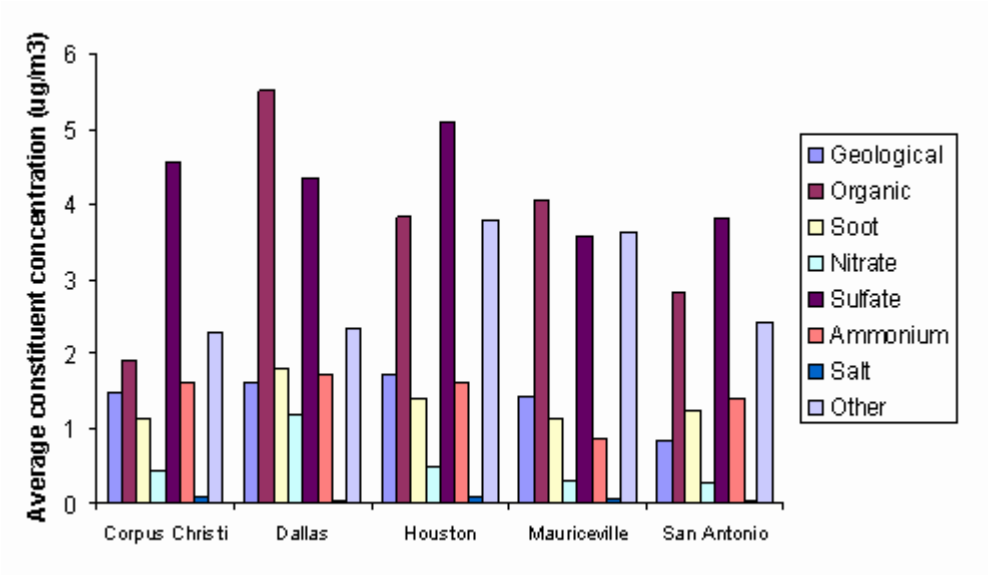

Figure 5.1: Average concentrations of constituents found in $PM_{2.5}$ collected between 3/97 and 3/98 (Tropp et. al., 1998) for various Texas cities.

The Houston area was selected for investigation due to the potential for high daily average concentrations of PM_2.5. Figure 5.2 shows the annual average organic carbon (OC), elemental carbon (EC), and OC/EC ratios in the Houston area in 1998. These data was taken from the Desert Research Institute $PM_{2.5}$ study of 1997/1998 (Tropp, et al., 1998). Monitoring sites are denoted in green. EC ranges

from 0.2-1.5, region that has the relatively highest EC in the map is downtown Houston. OC map shows that OC ranges about 3.0-3.9 spatially, except in the south east of downtown Houston. During 1997/1998, the OC/EC ratio for this region ranges from 0.7 to 4.0. The higher ratios are observed outside of the urban or industrial area. Fractions of secondary organic carbons cannot be estimated, because the primary OC/EC ratios are not known. However, if it is assumed that the OC/EC ratio from primary emissions is relatively constant spatially, then the results in figure would suggest that there is more OC relative to EC outside the urban area and that in these areas SOA formation is significant. Thus these data indicate that SOA formation cannot be ignored in air quality simulations in the Houston area.

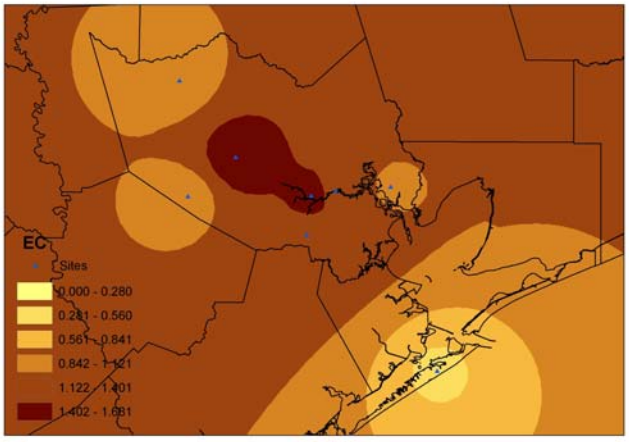
EC
Sites
0.000 - 0.280
0.281 - 0.560
0.561 - 0.841
0.842 - 1.121
1.122 - 1.401
1.402 - 1.681

EC

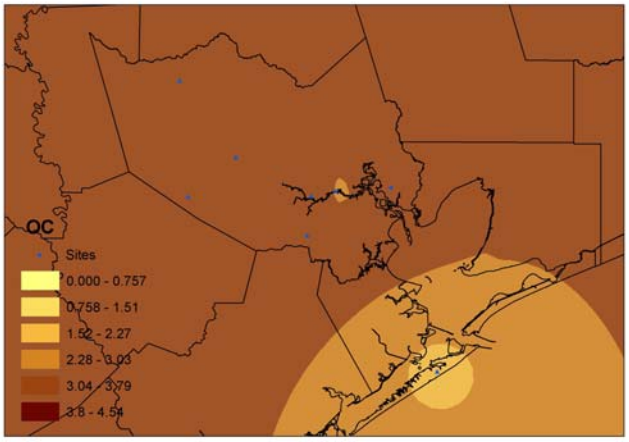
OC
Sites
0.000 - 0.757
0.758 - 1.51
1.52 - 2.27
2.28 - 3.03
3.04 - 3.79
3.8 - 4.54

OC

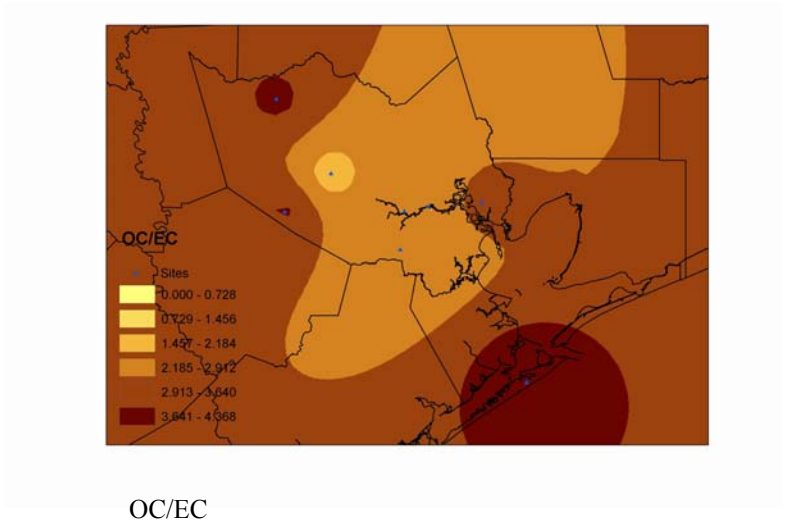

OC/EC

Figure 5.2: The annual average OC, EC, and OC/EC ratio at Houston areas on February 4, 1998, data was extracted from the Desert Research Institute PM2.5 study of 1997/1998

Sensitivity of SOA formation with respect to changes in concentration of NOx and primary hydrocarbons were performed under three case study scenarios. The first case or base case characterizes ambient SOA formation at the Clinton site, Houston, TX on the first and the second of September 2000, assuming that it a closed system. This case is denoted as case A. The second case, case B, analyzes the sensitivity of SOA formation to changes of emission rates of NOx. The third case, comprising of two sub-cases (case C1 and C2), examines the effects of NOx emission rates on SOA formation when the system is dominated by NOx emissions (i.e., VOC limiting), and by VOC emissions (i.e., NOx limiting), respectively. Table 5.1 summarizes these case studies.

Table 5.1: Case studies for characterization and sensitivity analysis of SOA formation

Case	Summarized description	Objectives to examine	NOx emission	VOC emission	NO: NO2
A	Closed system: ambient pollutants at the Clinton site, Houston, TX on the First and the Second of September 2000 at 4:00 pm	Characterize and compare formation of ambient SOA	-	-	
B	Case A with the emission of NOx	Investigate the effect of emission rate and composition of NOx on SOA formation	*1050 tons/day/155km^2	-	0.85:0.15 0.90:0.10 0.95:0.05
C1	Case A with the emission of NOx and VOC: VOC limiting	Examine the sensitivity of SOA formation to changes of NOx emission with the presence of VOC emission for higher emission of NOx than VOC	*1050 tons/day/155 km^2	**275 tons/day/155 km^2	0.85:0.15
C2	Case A with the emission of NOx and VOC: NOx limiting	Analyze the effect of emission rate of NOx on SOA formation with the presence of VOC emission for higher emission of VOC than NOx	**150 tons/day/ 155km^2	**145 tons/day/155 km^2	0.85:0.15

*Data obtained from 1998 inventory in Houston Ship Channel area
**Data obtained from 1996 inventory in Houston Ship Channel area

5.2.1 September 2000 Episode

Data observed during September 1-2, 2000 (during the Texas Air Quality Study (TEXAQS) period) at the Clinton site were chosen to define the base case. This episode was selected due to high concentrations of m-and p-xylene at the site on September 1, 2000. This event occurs suddenly between 3:00- 4:00 pm is believed to be due to a large release of m-and p-xylene directly into the atmosphere. Data on

September 1, 2000 represents non-routine release of VOCs. Data on September 2, 2000, on the other hand, represents typical conditions. Bar graphs in Figure 5.3 illustrate the concentrations of three compound classes: aromatics, alkenes, alkanes, and NOx during the September episode at the Clinton site between 3:00- 4:00 pm. Total emission on the first of September is approximately 17 times higher than that on the second. Concentration at the site on September 1, 2000 are dominated by aromatic hydrocarbons. Figure 5.4 shows a speciated distribution of aromatic hydrocarbon concentrations during the September episode. Data indicate that the combination of p-and m-xylene is a major component of the emissions on September 1, 2000. Quantitative models were used to characterize formation of SOA on this episode.

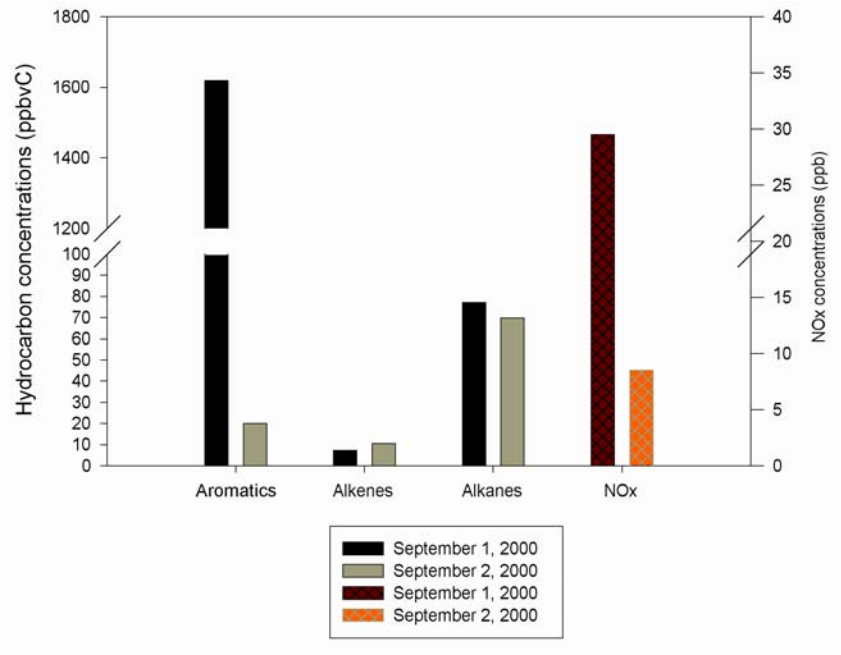

Figure 5.3: Hydrocarbon concentrations observed from TexAQS at the Clinton site on September 1 and 2, 2000 at 4:00 pm

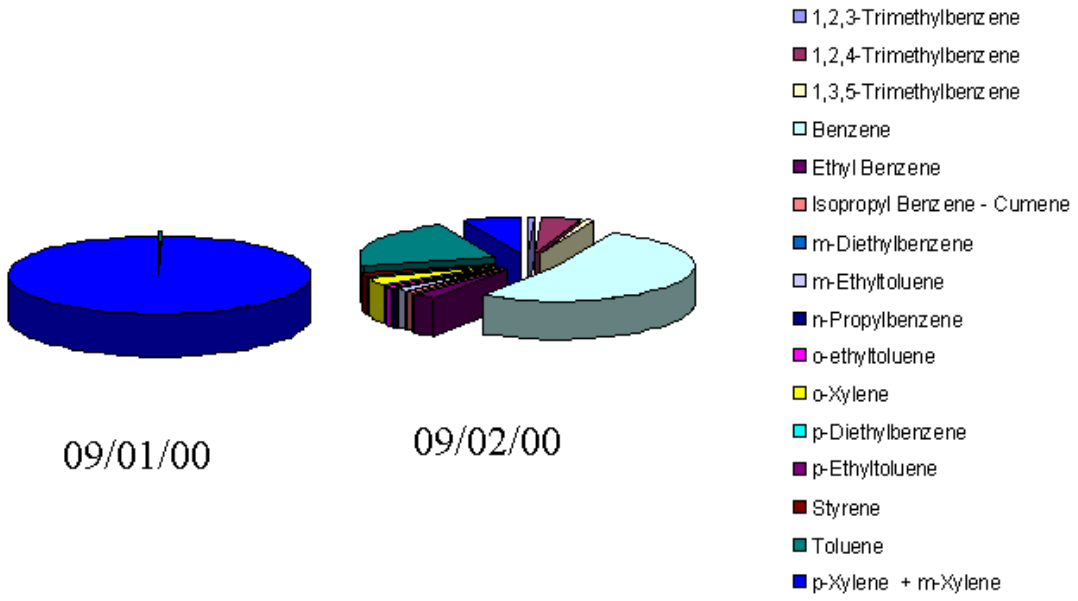

Figure 5.4: Monitoring speciated concentrations of aromatic hydrocarbons on September 1 and 2, 2000 at the Clinton site at 4:00 pm

5.2.2 Case Study Description

Case A: Closed system

Box model simulations were performed to characterize SOA formation at the Clinton site for the September 1-2, 2000 episode. Monitoring data collected during this episode were used as the initial conditions for the box model simulations, and are reported in Table 5.2. The goal of the case study is to characterize SOA formation under typical and non-routine hydrocarbon releases into atmosphere. Simulations started at 4:00 pm and ended at 10:00 pm. Results were reported every half hour.

The estimated SOA mass changes, yields, and ozone concentrations on each day are compared. These results are presented in the next section.

Table 5.2: Initial conditions used in box model simulations for the September episode

Date	TOT.HCs (ppbvC)	NO (ppb)	NO_2 (ppb)	T (F)	% RH
Sep 1	1705	4.5	25.2	102.5	48.1
Sep 2	106	0.1	8.4	102.3	46.7

Case B: Box model with NOx emissions

Case study B investigated the effects of NOx emission rates on SOA formation. The concentrations within a plume of air traveling form the Clinton site along the Ship Channel area were investigated. Case B used initial conditions from the first of September, 2000, with the addition of NOx emission at a constant rate. Figure 5.5 shows point sources of NOx in the Houston Ship Channel area. NOx emission data were extracted from the TNRCC point source database for 1997 or 1998. The emissions are reported as NO_2. The NOx emission for the entire 155 km2 Houston Ship Channel area is 1050 tons/day. Assuming that mixing height is 500 meters, NOx emission rate is 1.37E-8 tons/m^3/day.

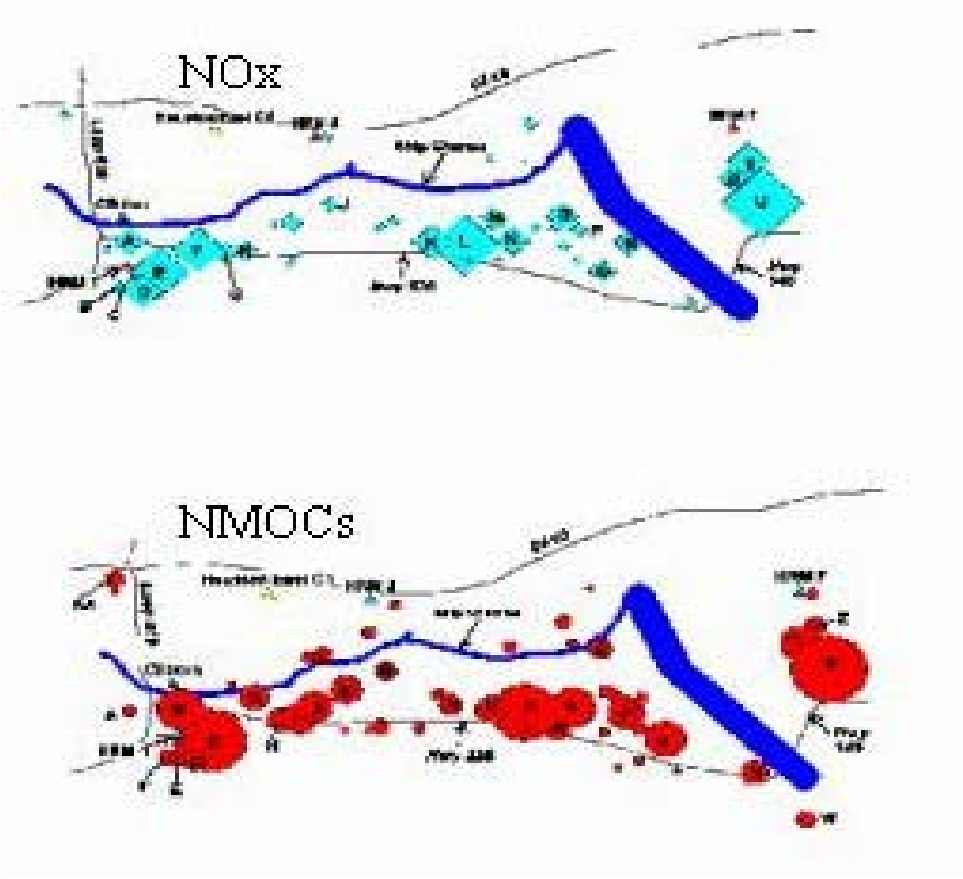

Figure 5.5: NOx and VOC point sources in Houston Ship Channel area (TNRCC, 1998)

A sensitivity analysis of SOA formation to changes in emissions of NOx was examined. Rates of NOx emissions were reduced from the base case by 10-100%, and also increased by 10-70%. The fraction of NO was also varied from 0.85-0.95 simultaneously with the changes of NOx emission to investigate the effect of NOx composition on SOA formation. Emission rates of NOx estimated for NO: NO2 equal to 0.85:0.15 are listed in Table 5.3.

Table 5.3: Emission rates of NOx at Houston Ship Channel area, fraction of NO is equal 85%

Changes from base case (%)	Emission rates of NO ($mmol/m^3/min$)	Emission rates of NO_2 ($mmol/m^3/min$)
Base case	1.75E-04	2.79E-05
-100 (no NOx emission)	0.00E-00	0.00E-00
-95	8.77E-06	1.55E-06
-90	1.75E-05	3.10E-06
-80	3.51E-05	6.19E-06
-70	5.26E-05	9.29E-06
-50	8.77E-05	1.55E-05
-30	1.23E-04	2.17E-05
-10	1.58E-04	2.79E-05
+10	1.93E-04	3.41E-05
+30	2.28E-04	4.02E-05
+50	2.63E-04	4.64E-05
+70	2.98E-04	5.26E-05

Case C: Box model with VOC and NOx emissions

Case C1: VOC limiting

Case C1 examines the sensitivity of SOA formation to changes in NOx emission in the presence of VOC emissions under VOC limiting conditions (i.e., higher emission of NOx than emission of VOC). Initial conditions and NOx emission rates as described in Case B were used in this case with the addition of VOC emissions along Houston Ship Channel area. VOC point sources are illustrated in Figure 5.6. The estimated emission rate of VOC over the entire area is 257 tons/day. The emissions are reported on a carbon and hydrogen basis. Using the C/H mass ratio of 12/14, the mass basis emission was converted to mole basis, which is 1.66E-04 $mmolC/m^3/min$. The ratio between VOC and NOx emissions for this case is 0.80 mmolC/mmol, which is generally regarded as VOC limited. The composition of the hydrocarbon emissions was assumed to be the same as reported by Carter (1998). For

the sensitivity analyses, NOx was reduced by 10-100%, and increased by 10-70% from the base case. Emissions of VOCs were kept constant.

Case C2: NOx limiting

Case study C2 investigates the effect of emission rate of NOx on SOA formation for the NOx limiting system (i.e., VOC emission is higher than NOx emission). In this scenario, NOx and VOC point sources at Houston Ship Channel area from the 1996 inventory were employed. VOC point sources are illustrated in Figure 5.6. The emission rate of VOC is approximately 145 tons/day, and using C/H ratio of 12/14, this rate can be converted to 9.37E-05 mmolC/m^3/min. The rate of NOx emission, which is reported as NO_2, is 155 tons/day. Assuming that the fraction of NO is 0.85, emission rates of NO and NO_2 are 2.78E-5 and 4.90E-6 mmol/m3/min, respectively. The ratio between VOC and NOx emission is 2.86 mmolC/mmol. To examine the sensitivity analysis of SOA formation, base case emission of NOx was changed to ± 10-100 %. The composition of hydrocarbons for emission is identical to that of case C1.

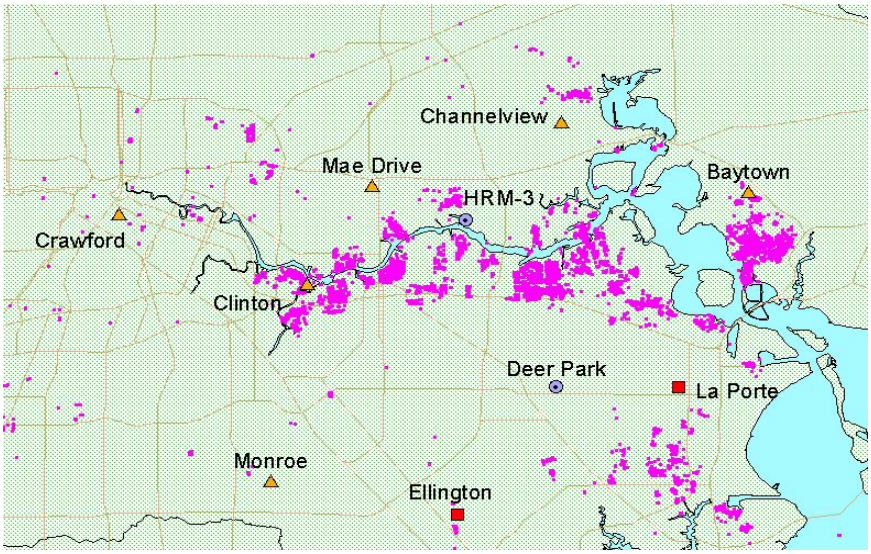

Figure 5.6: VOC point sources in Ship Channel area from 1996 inventory

5.3 Case Study Results

Quantitative models of SOA formation, developed in this study, were employed to characterize SOA production during the September episode. The goal is to investigate SOA formation when high concentrations of reactive parent hydrocarbon are present. The analysis will help identifying an important role of sources and physical and chemical processes of SOA formation. Results for each case study are displayed in the following sections.

5.3.1 Case A: Box model

Box model simulations were conducted under initial conditions as described previously. The comparison of SOA mass changes (ΔM_o) on September 1 and 2, 2000 are shown in Figure 5.7. ΔM_o were estimated for M_{int} equals 15 μg/m^3. As

seen in the Figure, ΔM_o on the first date are 13-16 times higher than those on the second date. The high production of ΔM_o on the first date results from a massive release of reactive hydrocarbon (m-and p-xylene) into ambient air.

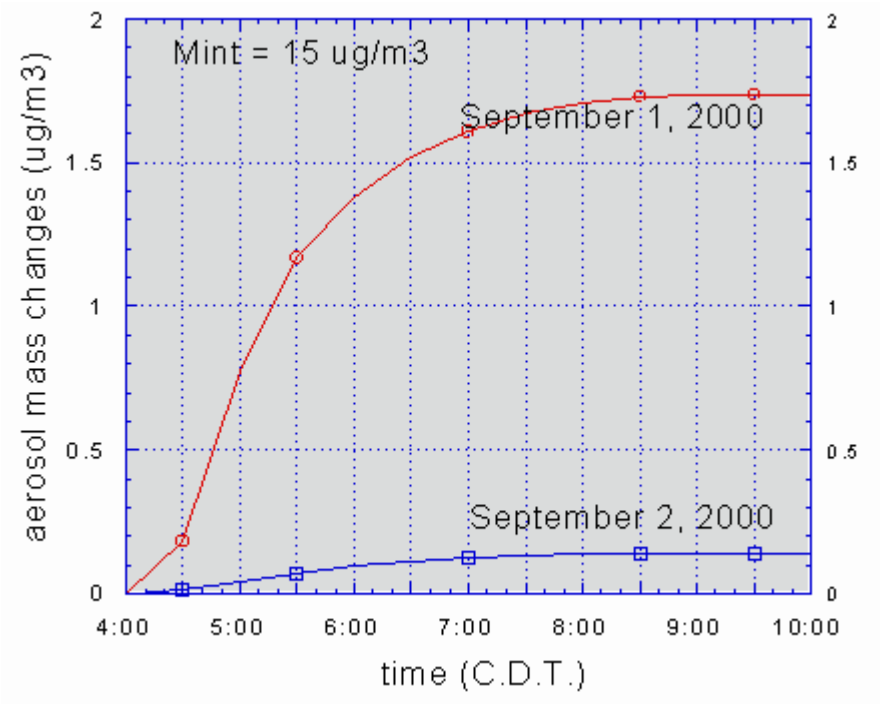

Figure 5.7: SOA mass changes (ΔM_o) at the Clinton site at 4:00 pm on the September episode, aerosol seed varies from 5-15 μg/m^3.

Each lumped model aerosol species will produce two types of condensable products that will partition into aerosol phase. The first type is compound with organonitrate groups, and the second is compounds with carboxylic acid groups. Products from the four lumped aerosol precursors (APR1-APR4) are referred to as: PM1, PM2, PM3. PM4, PM5, PM6, PM7, and PM8. Partitioning of individual products depend on their vapor pressures and molecular weights (i.e., lower vapor

products can relatively partition more into aerosol phase). Mass concentrations of these semivolatile products in particulate phase (PM1-PM8) during the September episode are illustrated in Figure 5.8.

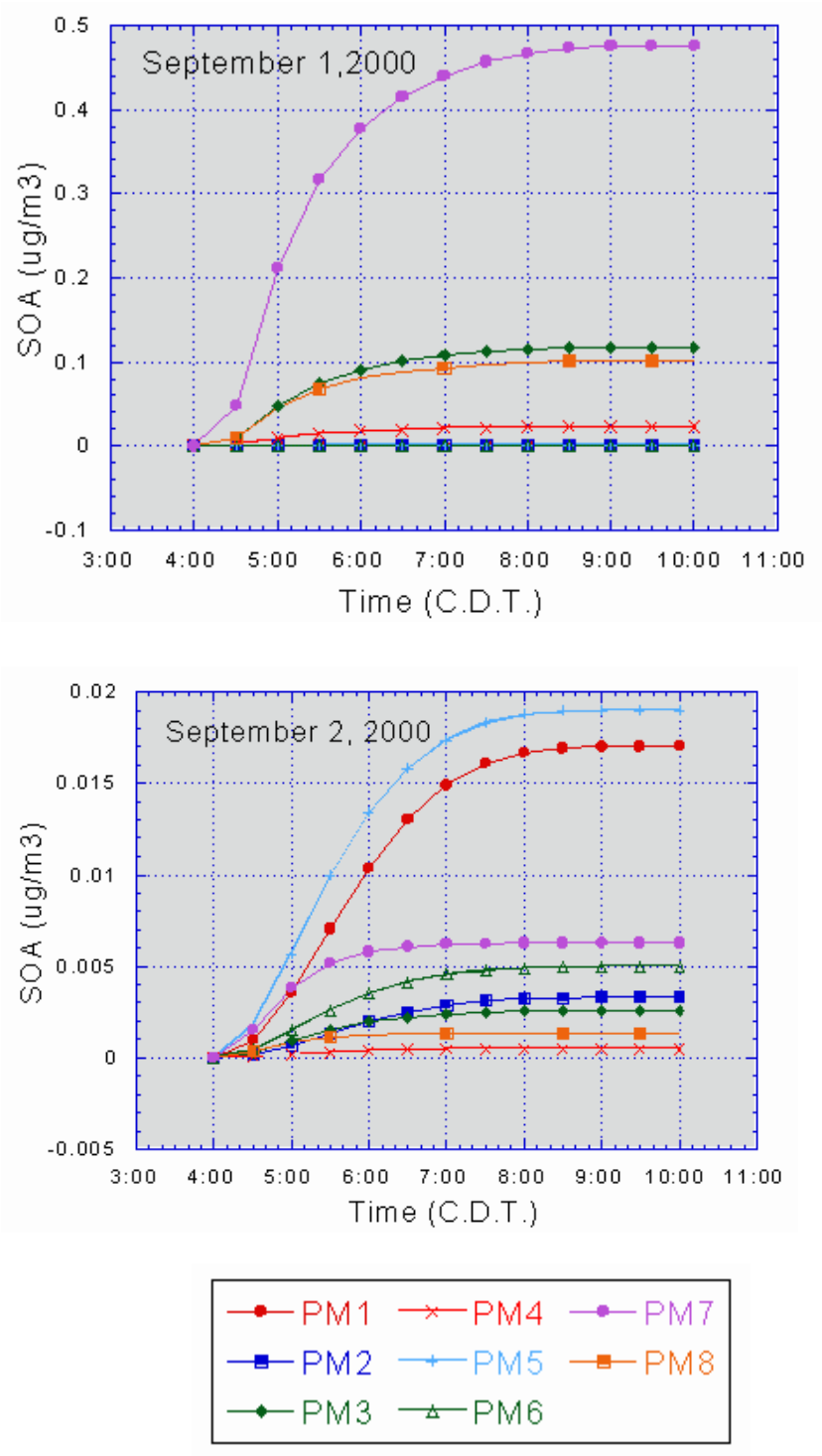

Figure 5.8: Speciated aerosol mass changes of eight aerosol products (PM1-PM8) during the September episode, M_{int} = 5μg/m^3

For September 1, 2000, there was non-routine release of m-and p-xylene, which was represented by lumped species ARO2 in SAPRC-99. ARO2 produces aerosol precursors represented by lumped species APR2 and APR4. From the figure, aerosol mass change (ΔM) of PM7 dominates the total mass changes in aerosol phase. This can be explained by following reasons. First, the reactivities of both ARO2 and APR4 are faster than the other lumped species. Thus, rate of production of semivolatile product species PM7 and PM8 from lumped species APR4 are higher than that of the others. Secondly, the partitioning coefficient of product PM7 is higher than that of product PM8, therefore PM 7 partitions more into particulate phase. However, results from September 1, 2000 are not typical ambient conditions. When there are no unusual emissions of individual compounds (e.g., September 2, 2000), the major components of total aerosol mass are products PM1 and PM5, because partitioning coefficients of PM1 and PM5 are higher than those of the others. Generally, the simulations suggest that fractions of products with organonitrate group are higher than those of products with carboxylic acid group.

Mass changes of individual aerosol products (ΔM_o of PM1-PM8) are normalized by the reacted amount of hydrocarbons responsible for their production (i.e., Yields). Table 5.4 lists the yields of each product, and the ratios of yield for each product to the minimum yield among these 8 products (Y_i/Y_{min}). The ratios indicate that PM5 has the highest yield among all products independent of the initial ambient conditions.

Table 5.4: SOA yields of each aerosol products on the September episode

Date	Products	PM1	PM2	PM3	PM4	PM5	PM6	PM7	PM8
9-1-2000	Yields	9.9E-04	1.9E-04	3.0E-04	5.8E-05	3.0E-03	7.8E-04	1.2E-03	2.6E-04
	Y_i/Y_{min}	17.0	3.3	5.1	1.0	51.2	13.4	20.8	4.4
9-2-2000	Yields	5.1E-03	9.8E-04	1.3E-03	2.5E-04	5.7E-03	1.5E-03	3.2E-03	6.8E-04
	Y_i/Y_{min}	20.4	4.0	5.2	1.0	22.8	6.0	12.8	2.7

Besides secondary aerosol formation, ozone formation is another important issue to be examined in this study. Box model simulations with only gas phase chemistry (SAPRC 99) were performed under conditions from the September episode. The ozone concentrations from gas phase chemistry and from case study, which includes SOA formation chemistry, are illustrated in Figure 5.9. The comparison shows that ozone concentrations from gas phase chemistry are higher than those from aerosol case study. The difference is approximately 21% on September 1, 2000 and 7% on September 2, 2000. Causes of these differences include as: introducing chemistry of SOA formation into a gas phase mechanism consume reactive hydrocarbons (APR) that might otherwise contribute to ozone formation by photolysis reaction.

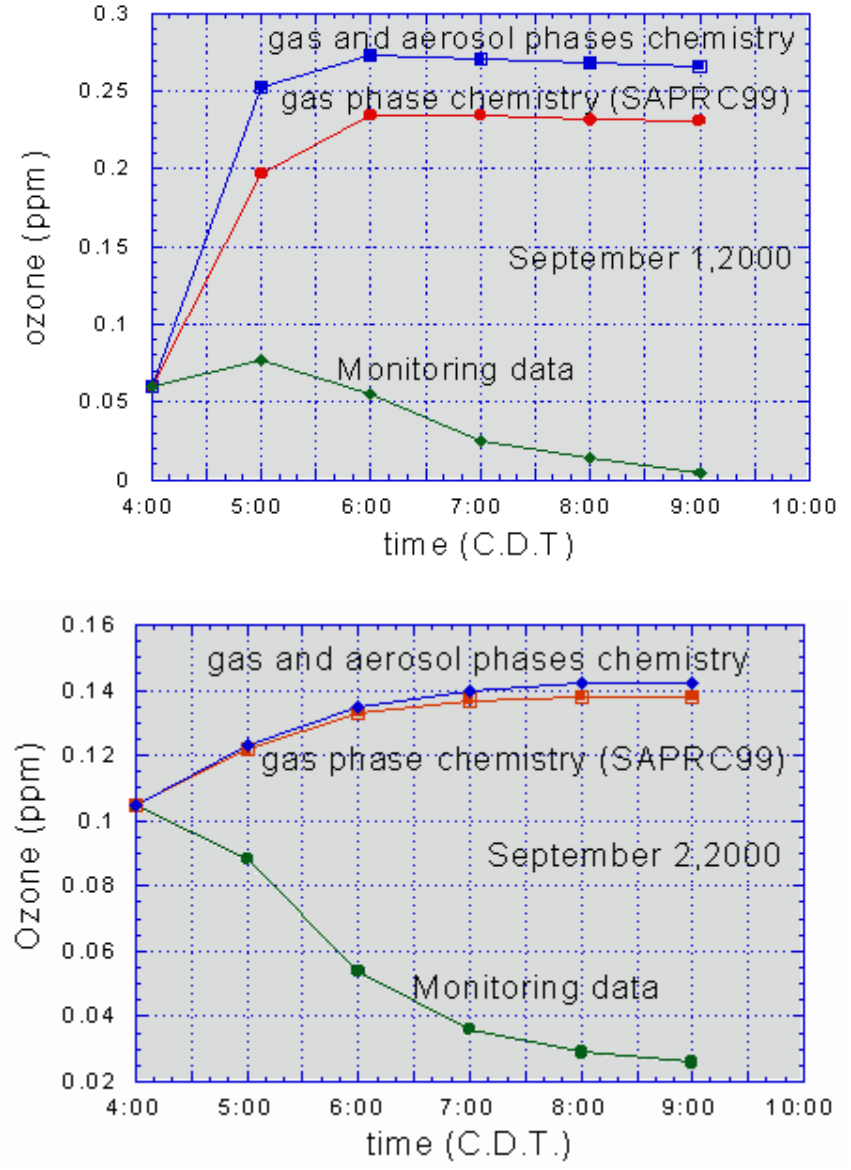

Figure 5.9: Ozone concentrations at the Clinton site on the September episode from 4:00 pm, data points are from case study simulation, gas-phase chemistry simulation, and monitors

The ground monitoring ozone concentrations at the Clinton site from 4:00 pm are also presented in Figure 5.9. Results from simulations are not comparable with monitoring data, because simulations were performed for box model (closed system).

The parcel containing the high concentrations of air was not followed. Further, the loss mechanisms, such as the depositions, are not handled in SAPRC simulation. It is evident from aircraft monitoring data (Twin Otto, afternoon flight on September 1, 2000) that there are plumes of high ozone concentrations (120-165 ppb) in Houston area from 3:45-4:21 pm (Figure 5.10). This elevated ozone concentrations may due to the enormous release of reactive hydrocarbons at the Clinton site between 3:00 and 4:00 pm. These high concentrations could not be observed from the ground monitors. Therefore, this explains the discrepancy between simulation and ground monitoring data.

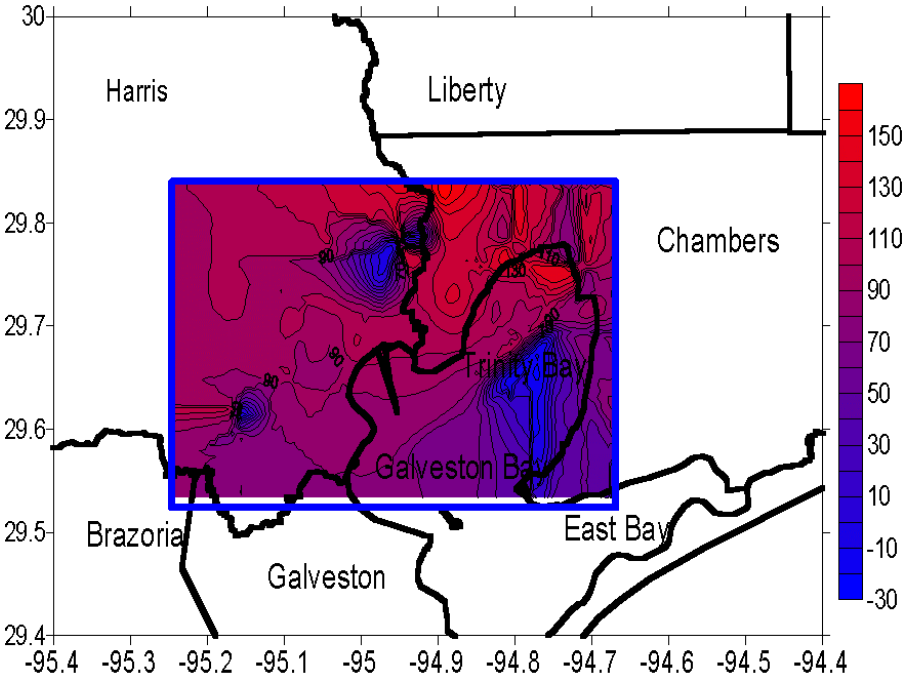

Figure 5.10: Ozone concentrations on September 1, 2000 around 3:30 to 4:30 pm, at the Ship Channel area, Houston TX

5.3.2 Case B: Box model with NOx emission

NOx emissions were added into the box model to investigate the sensitivity of SOA yields to changes in the concentrations of NOx. M_{int} is equal 5 μg/m^3, and the fraction of NO is equal 85% in case study B, C1 and C2. The simulations were conducted under conditions as described in the case study scenario section. Results from simulations are depicted in Figures 5.11 and 5.12. The estimated SOA mass changes decrease 5-60% from base case when NOx emissions are increased 10-70%. Yields (Y) and ΔM_o increase when NOx emissions are reduced up to 80%. Beyond 80%, aerosol masses and yields begin to decline. To understand this phenomenon, it is useful to consider these following reactions:

$$NO_2 \xrightarrow{hv} NO + O^* \qquad \textbf{Reaction 27}$$

$$ROO^* + NO \longrightarrow NO_2 + RO^* \qquad \textbf{Reaction 28}$$

$$NO2 \longrightarrow O + NO \qquad \textbf{Reaction 29}$$

$$O + O2 \longrightarrow O3 \qquad \textbf{Reaction 30}$$

$$O_3 + NO \longrightarrow NO_2 + O_2 \qquad \textbf{Reaction 31}$$

$$O_3 + H_2O \longrightarrow 2OH^{\cdot} + O_2 \qquad \textbf{Reaction 32}$$

Where ROO* is hydrocarbon radical. NO plays the role of an ozone sinks, while NO_2 is ozone source. In the case study, NOx emissions are dominated by NO (85%). Therefore, increasing NOx emissions will enhance the ozone depletion by NO, which consequently decreases the formation of OH radicals and SOA. On the other hand, when NOx emissions decrease up to 80% from base case, the ozone titration by NO

decreases. Therefore, ozone concentration and SOA formation is getting higher as the reduction of NOx emissions increases. However, when the reduction of NOx emission goes beyond 80% from base case, the depletion of ozone by NO does not play an important role in ozone production and destruction. Therefore, SOA formation and ozone concentration decline at the high reductions of NOx emissions (i.e., > 80%).

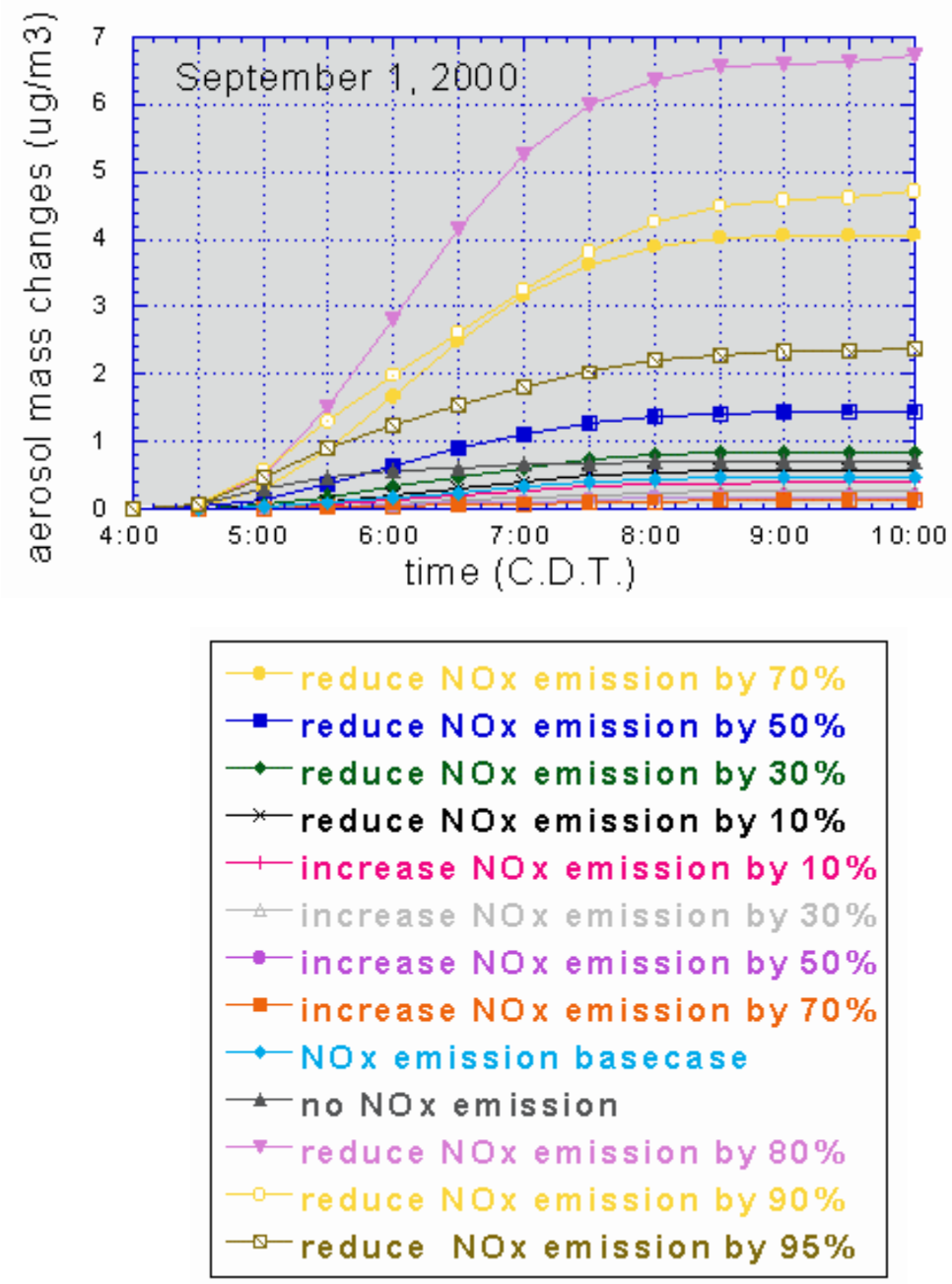

Figure 5.11: SOA mass changes at the Clinton site from 4:00 on September 1,2000: results from varying NOx emissions by ±10-100% from base case, M_{int} = 5 μg/m^3, fraction of NO = 0.85

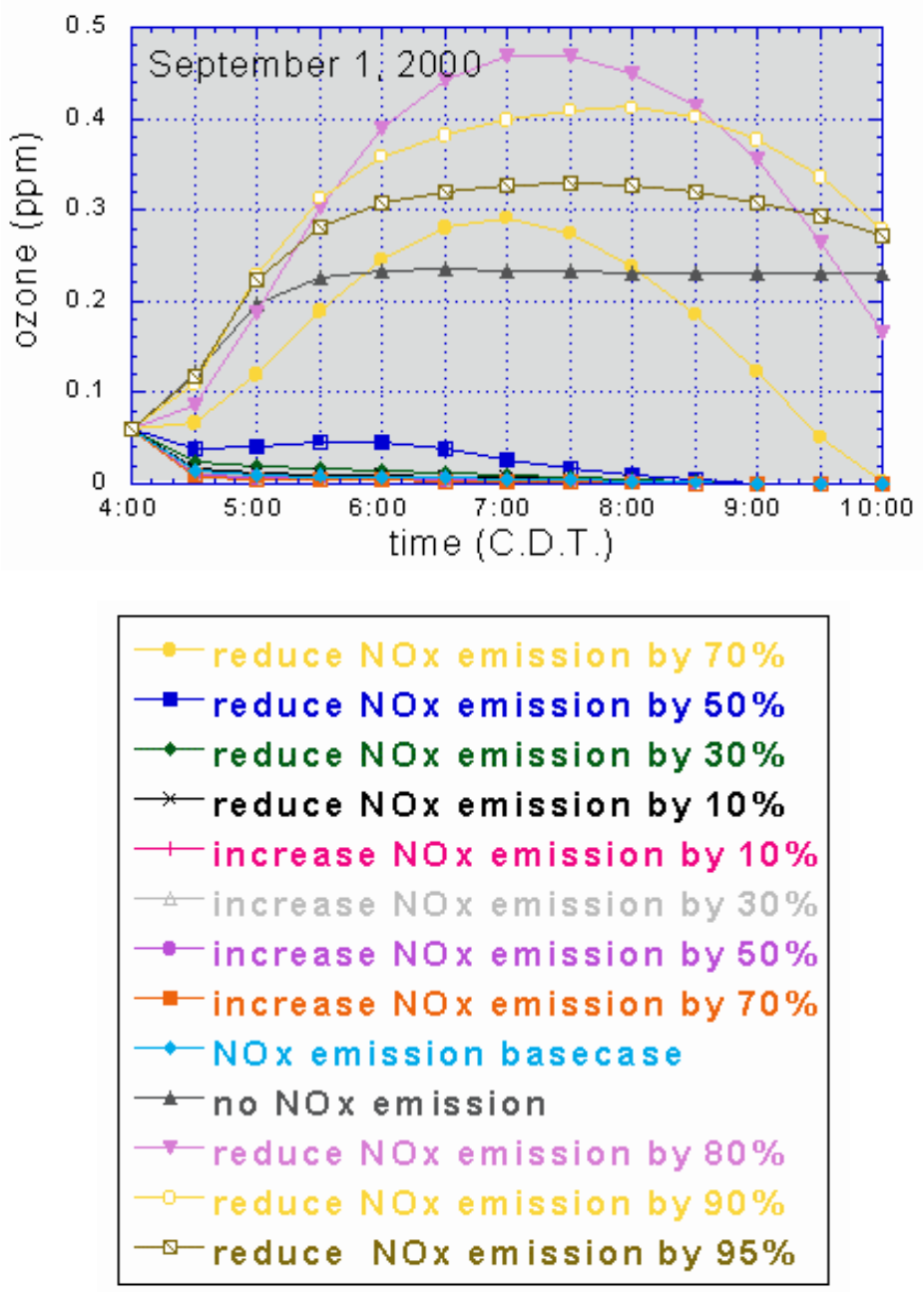

Figure 5.12: Ozone concentrations at the Clinton site from 4:00 on September 1,2000: results from varying NOx emissions by ±10-100% from base case, M_{int} = 5 μg/m^3, fraction of NO = 0.85

Impact of composition of NOx on SOA formation was also examined. The fraction of NO was varied from 85-95%. SOA mass changes for ± 50% NOx emissions from base case at all levels of fraction of NO are shown in Figure 5.13. Results indicate that varying composition of NOx does not influence formation of SOA significantly.

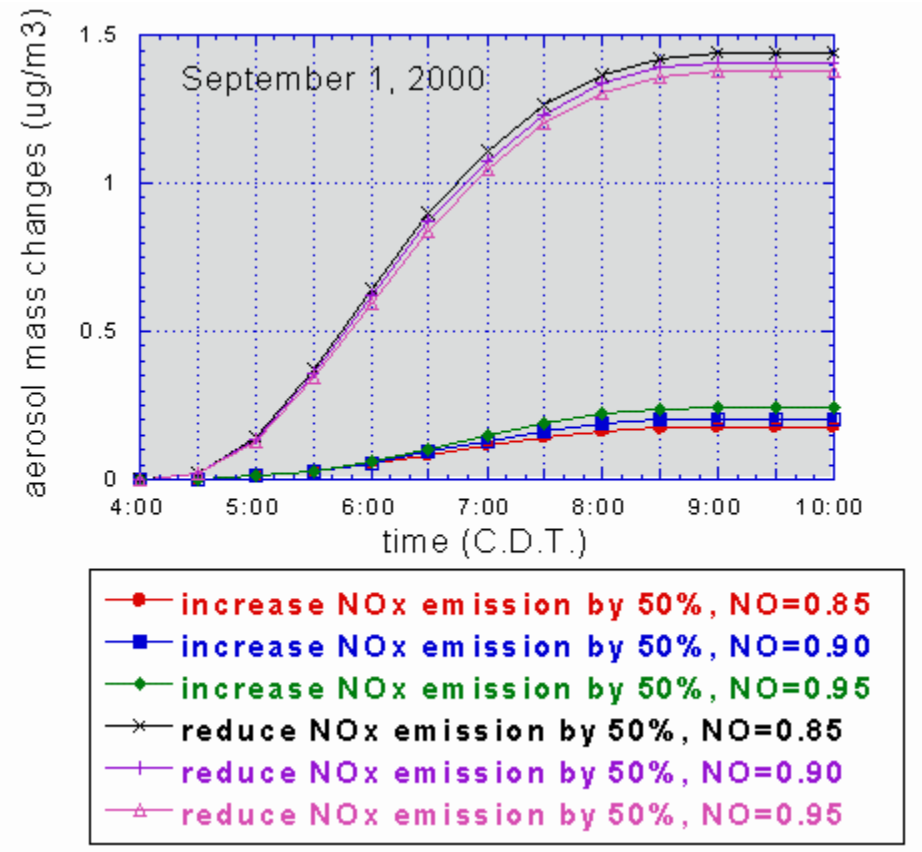

Figure 5.13: SOA yields at the Clinton site on September 1, 2000 from 4:00 pm, results from changing NOx emissions ±50% from base case, and varying fraction of NO from 0.85-0.95, M_{int} = 5 μg/m^3

5.3.3 Case C: Box model with NOx and VOC emissions

There are two sub-cases for this scenario: VOC limiting and NOx limiting. Simulations were conducted under conditions as described in the preceding section for cases C1 and C2. For these cases, the amount of hydrocarbon that reacts is estimated by

$$\int_0^t R dt = \frac{E}{V}\int_0^t dt - \int_{C_0}^{C_t} dC \qquad \textbf{Equation 58}$$

Where:

R = the amount of hydrocarbon that reacts ($\mu g/m^3/min$)

E = emission of hydrocarbon ($\mu g/min$)

V = Volume of system (m^3)

C_0 = Initial concentration of hydrocarbon ($\mu g/m^3$)

Results of these two cases are illustrated in Figures 5.14 - 5.17. For case C1 (VOC limiting), results are similar to Case B, in which increasing NOx emissions results in declining SOA formation and ozone concentration. Decreasing NOx emissions 70-80% from the base case enhances SOA formation and ozone concentration. The causes of this behavior are similar to case B.

Case C2 (NOx limiting) shows behavior opposite to case C1. As seen in Figure 5.16 and 5.17, when NOx emissions are raised by 10-70% from base case, formation of SOA and ozone increases. In this case the formation of SOA and ozone are strongly influenced by the concentration of NOx in the system.

The sensitivity analyses from case C1 and C2 reveal that the strategy to control SOA formation depends strongly on the base case scenarios (i.e., NOx or VOC limiting).

Case C2: NOx limiting

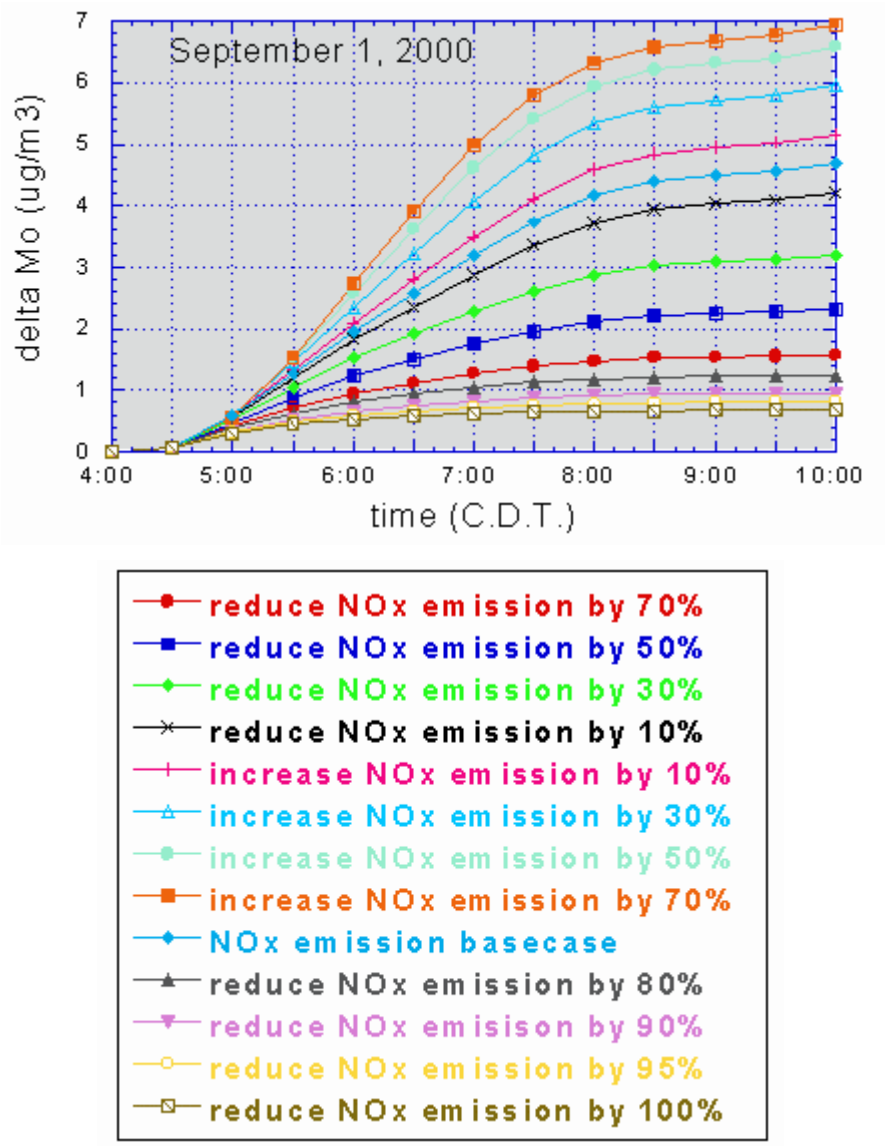

Figure 5.14: Aerosol mass changes (μg/m^3) as the puff of air from the Clinton site moves along the Houston Ship Channel area for case C2, results from varying NOx emissions by ±10-95% from base case, SOA seed = 5μg/m^3, and fraction of NO = 0.85

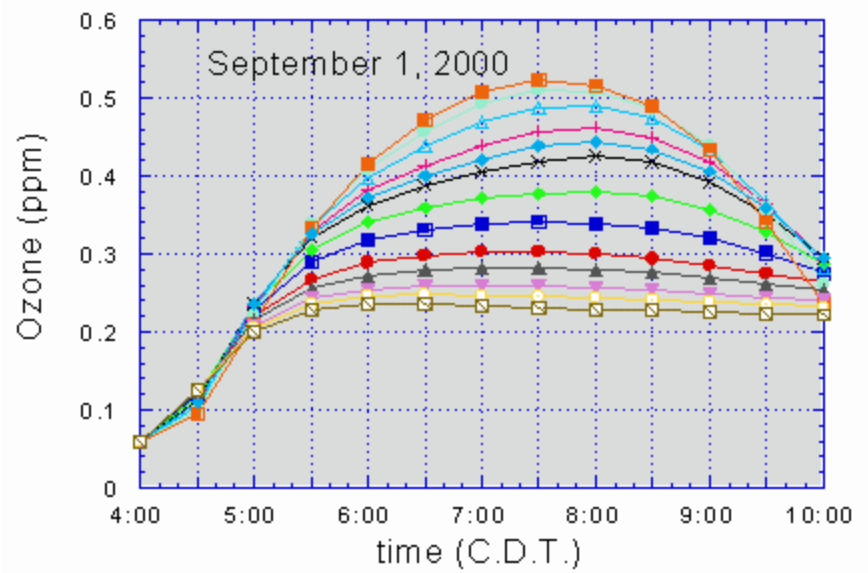

Figure 5.15: Ozone concentrations as the puff of air from the Clinton site moves along the Houston Ship Channel area for case C2, results from varying NOx emissions by ±10-95% from base case, SOA seed = 5μg/m^3, and fraction of NO = 0.85

Case C1: VOC limiting

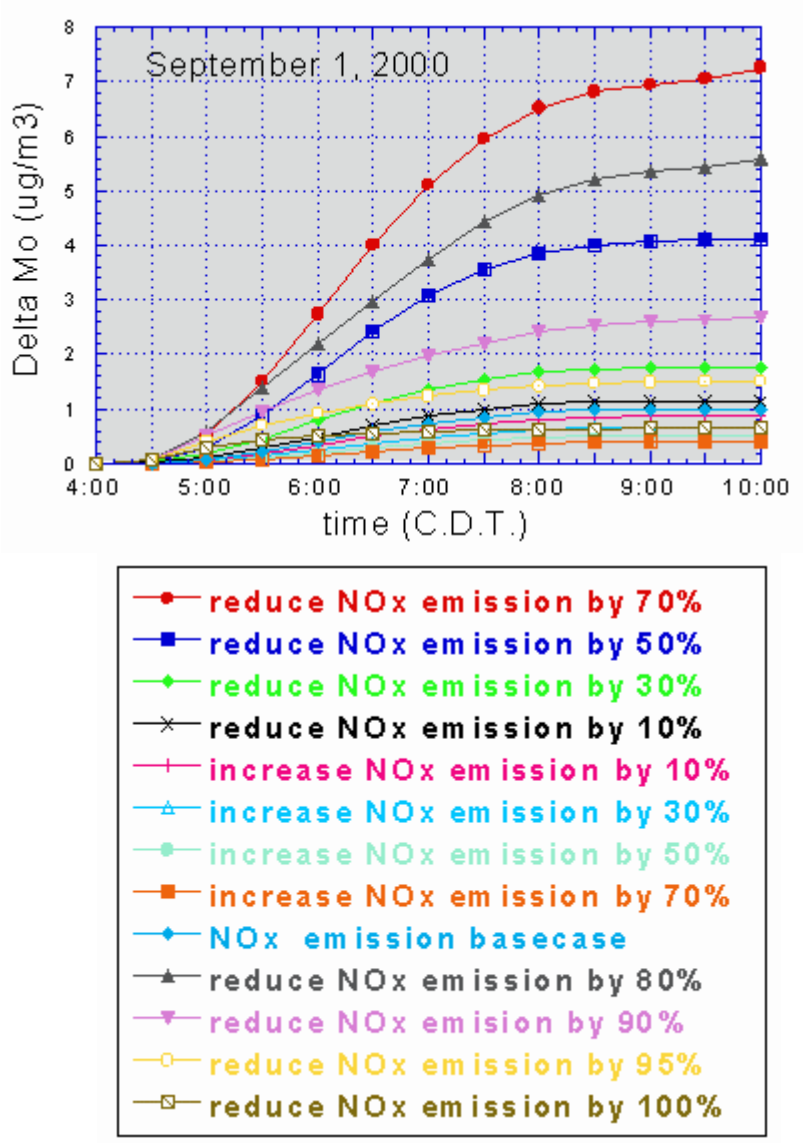

Figure 5.16: Aerosol mass changes (μg/m^3) as the puff of air from the Clinton site moves along the Houston Ship Channel area for case C1, results from varying NOx emissions by ±10-95% from base case, SOA seed = 5μg/m^3, and fraction of NO = 0.85

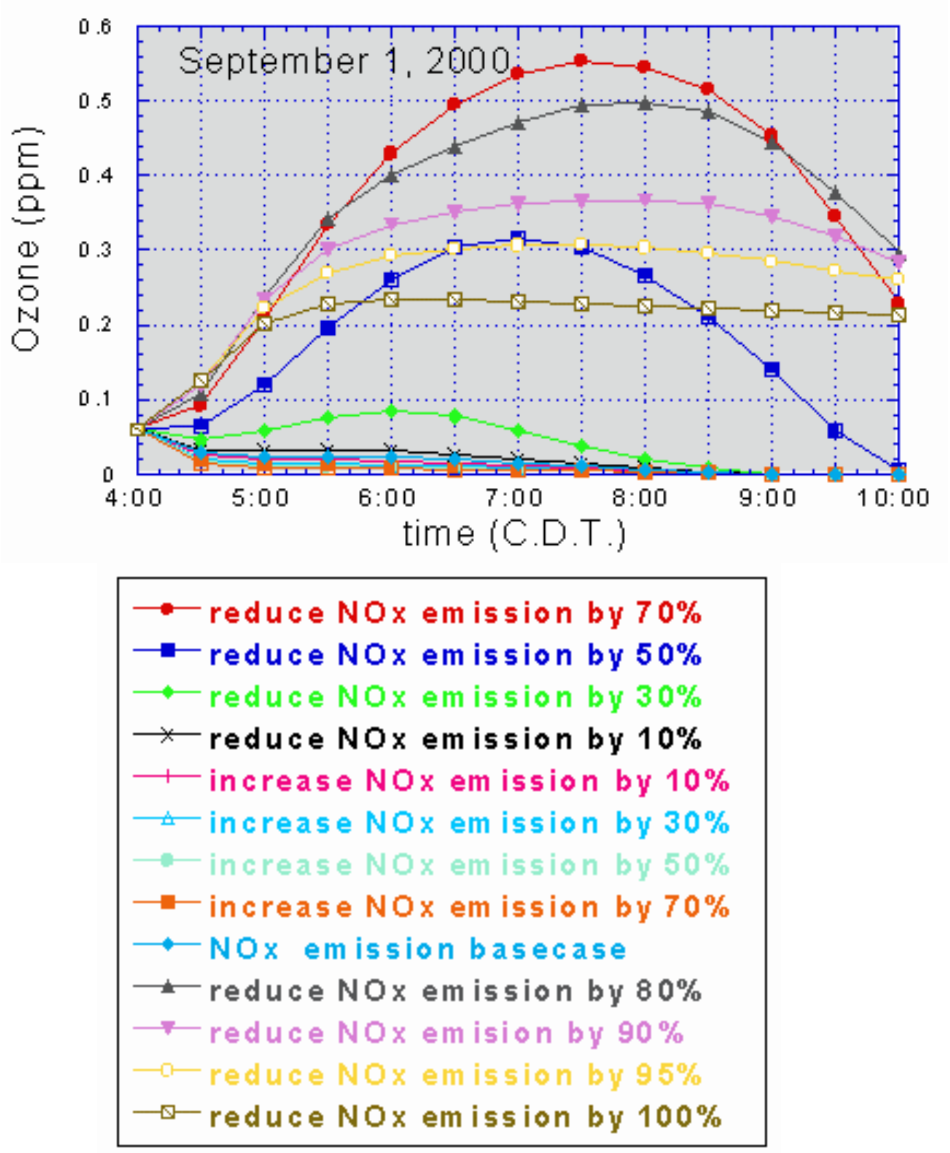

Figure 5.17: Ozone concentrations as the puff of air from the Clinton site moves along the Houston Ship Channel area for case C1, results from varying NOx emissions by ±10-95% from base case, SOA seed = 5μg/m^3, and fraction of NO = 0.85

Results from sensitivity for cases C1 and C2 indicate that the impact of changing NOx emissions on aerosol formation is similar to that on ozone production. Figure 5.18 shows a correlation between changes in ozone concentration and changes

in SOA concentrations for the scenarios shown in Figures 5.14 – 5.17. Changes of 0.1 ppm in ozone concentration lead to changes in SOA concentrations of approximately 2.5 μg/m^3.

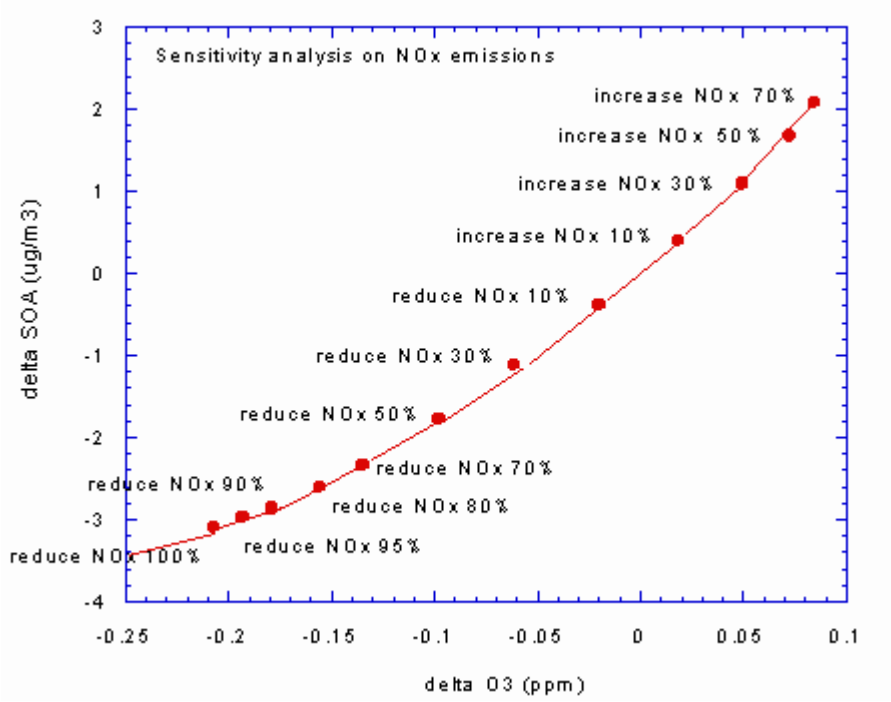

Figure 5.18: ΔO_3 versus ΔSOA compared to base case NOx emissions when NOx emissions were decreased to 100%, and increased to 70% from the base case

5.4 Summary

Quantitative models of SOA formation for lumped aromatic hydrocarbons were applied to characterize the formation of SOA in the Houston area. A number of case studies were performed to examine the key parameters controlling SOA formation. Monitoring data for a September 2000 episode were employed as initial conditions for all case studies. Results indicate that the incorporation of SOA

formation chemistry into gas phase chemistry (SAPRC99) strongly influences ozone formation chemistry

The concentration of NOx is another essential aspect in SOA formation, because it influences the generation of OH radical. Therefore, the concentration of NOx is believed to be the one of the limiting factors in SOA formation. For VOC limited scenario, decreasing NOx emissions will enhance the formation of SOA and ozone, while raising NOx emissions will deplete ozone and SOA formation. For NOx limited case, formation of ozone and SOA is proportional to the concentration of NOx in the system.

The development of quantitative models of SOA formation by this study provides an effective tool in characterizing SOA production more accurately and directly from its sources, as well as in identifying the key features in controlling SOA formation.

Chapter 6 Summaries and Future Work

6.1 Summaries

Quantitative models of secondary organic aerosol (SOA) formation for 15 individual aromatic hydrocarbons and two lumped aromatic species were developed based on data available from smog chamber experiments. These models were used to characterize the SOA formation in Houston areas, and to examine the key components in controlling SOA formation. The finds are summarized below.

Key Conclusions

- Improving the modeling of secondary organic aerosol needs to account for the fact that SOA is produced from the second generation products of hydrocarbons with OH radical (HCs $\xrightarrow{OH}$ Aerosol precursor $\xrightarrow{OH}$ SOA).
- Fractional Aerosol Coefficients (FACs) are not constant for each VOC, but can vary depending on several factors especially the extent of conversion and the amount of seed aerosol.
- The concentration of NOx is a determining factor in SOA formation. Sensitivity analyses indicate that changing the concentration of NOx can have significant positive and negative effects on SOA formation. The effect of NOx is represented by a direct correlation of ozone and SOA formation.
- Aerosol yields of organonitrate products are higher than those of carbonyl products. Because the organonitrate aerosol products have lower vapor

pressure than the carbonyl products but lower reaction yields. The vapor pressure effect is stronger.

- SOA formation chemistry strongly influences ozone formation chemistry. Production of SOA competes the consumption of hydrocarbon precursors leading to ozone formation.

6.2 Future Work

Further studies that are recommended are:

- Apply models with more extensive chamber data.
- Extend the development of SOA module to other hydrocarbon classes: alkenes, alkanes, and terpenes.
- Incorporate SOA mechanisms into regional air quality models (e.g., CAMx) so the module can be employed to estimate the formation of SOA in regional and urban ambient conditions
- Integrate SOA mechanism with chlorine chemistry. There is evidence that chlorine chemistry promotes ozone formation (Tanaka, 2000), and the reactivity of alkanes with chlorine radical is much higher than that with OH radical. This may enhance the production of OH radicals in urban environments, and consequently increase production of SOA.

Nomenclatures

*Listed as presented chronically in the dissertation

NAAQS	National Ambient Air Quality Standards
EPA	Environmental Protection Agency
SOA	Secondary Organic Aerosol
FACs	Fractional Aerosol Coefficients
SAPRC	Statewide Air Pollution Research Center
PM	Particulate Matter
OC	Organic Carbon (Volatile carbon)
EC	Elemental Carbon (non-volatile carbon)
VOCs	Volatile Organic Carbons
MIR	Maximum Incremental Reactivity
MOIR	Maximum Ozone Incremental Reactivity
EBIR	Equal Benefit Incremental Reactivity
RO2R	Operator represents peroxy radical reactions with NO that result in NO to NO_2 conversion and formation of HO_2 radical
R2O2	Operator represents the effect of NO to NO_2 conversion without HO_2 formation
RO2N	Operator represents the reactions of peroxy radicals with consumption of NO and various types of organic nitrate formation
135-TMB	1,3,5-trimethylbenzene

APT1	Aerosol precursor from 1,3,5-trimethylbenzene
BALD	Benzaldehyde
CRES	Cresol
MGLY	Methylglyoxal
TPM1	Aerosol product with organonitrate groups from 1,3,5-trimethylbenzene
TPM2	Aerosol product with carbonyl groups from 1,3,5-trimethylbenzene
124-TMB	1,2,4-trimethylbenzene
GLY	Glyoxal
BACL	Biacetyl
APT5	Aerosol precursor from 1,2,4-trimethylbenzene
APT6	Aerosol precursor from 1,2,4-trimethylbenzene
APT7	Aerosol precursor from 1,2,4-trimethylbenzene
APT8	Aerosol precursor from 1,2,4-trimethylbenzene
APT9	Aerosol precursor from 1,2,4-trimethylbenzene
AP10	Aerosol precursor from 1,2,4-trimethylbenzene
TPM5	Aerosol product with organonitrate groups from 1,2,4-trimethylbenzene
TPM6	Aerosol product with carbonyl groups from 1,2,4-trimethylbenzene
$K_{om,i}$	G/P Partitioning Coefficient of species I

$F_{i,om}$	Concentration of compound i in the absorbing om phase
A_i	Gas phase concentration of compound i
P_i	Total concentration of condensable product i that is formed
M_o or M_{tot}	Total organic aerosol mass concentration
ΔROG	Amount of reactive organic gas reacts
α_i	Proportionality constant relating the amount of ROG reacted to form P_i
Y_i	Aerosol yield
ΔM_o or ΔM_i	Aerosol mass formed from photolysis reaction and partitioning into aerosol phase
M_{int}	Initial amount of aerosol mass
$\%DF_i$	Distribution factor of species i in the aerosol phase (expressed as a percentage)
IAR	Incremental Aerosol Reactivity
HC	Hydrocarbon
ARO1	Lumped species represents a group of aromatics that react slowly
ARO2	Lumped species represents a group of aromatics that react rapidly
APR1	Lumped species represents a group of slow reactive aerosol precursors produced from slow reactive aromatic precursors

APR2	Lumped species represents a group of fast reactive aerosol precursors produced from slow reactive aromatic precursors
APR3	Lumped species represents a group of slow reactive aerosol precursors produced from fast reactive aromatic precursors
APR4	Lumped species represents a group of fast reactive aerosol precursors produced from fast reactive aromatic precursors
PM1	Aerosol product species 1 produced from APR1
PM2	Aerosol product species 2produced from APR1
PM3	Aerosol product species 1 produced from APR2
PM4	Aerosol product species 2 produced from APR2
PM5	Aerosol product species 1 produced from APR3
PM6	Aerosol product species 2 produced from APR3
PM7	Aerosol product species 1 produced from APR4
PM8	Aerosol product species 2 produced from APR4

Appendix A : Data from smog chamber experiment

Table A.1: Relative Molar Loading (Eusebi, 1996)

Hydrocarbon Precursors	Aliphatic C-H bonds	Aromatic C-H bonds	Ketone + Aldehyde	Alcohol	Organic Acid	Alkyl Nitrate	Nitro Aromatics	% of Initial Hydrocarbon
1-Decane	0.79	-	0.07	0.13	0.00	0.01	-	0.62
1-Dodecane	0.96	-	0.01	0.03	0.00	0.01	-	2.7
o-Xylene	0.63	ND	0.19	0.12	0.04	0.03	ND	0.38
1,3,5-Trimethybenzene	0.58	0.006	0.22	0.12	0.05	0.02	0.01	0.27
α-Pinene	0.80	-	0.06	0.09	0.04	0.005	-	13
R(+)-Limonene	0.65	-	0.23	0.09	0.02	ND	-	1.8
β-Caryophyllene	0.85	-	0.10	0.04	0.006	ND	-	1.7

Table A.1 lists the relative molar loadings of the observed functional groups for each of the smog chamber experiments by Eusebi (1996), and the total carbon mass of the secondary aerosol. Eusebi suggested some patterns for the aerosol generated by different hydrocarbon precursors. Photooxidation of the aromatic hydrocarbons leads to products that have strong carbonyl and organonitrate bands. They also shows moderate C-H absorbances. The aerosol produced from oxidation reaction of olefins exhibit strong C-H stretch absorbances and organonitrate bands. The carbonyl absorbance is relatively weak in these spectra.

Table A.2: Predicted composition of SOA from the photooxidation of hydrocarbon precursors (Eusebi, 1996)

Hydrocarbon Precursors	Number of Carbons	Aliphatic C-H bonds	Aromatic C-H bonds	Ketone + Aldehyde	Alcohol	Organic Acid	Alkyl Nitrate	Nitro Aromatics
1-Decane	10	16.24	-	1.44	2.67	0.00	0.21	-
1-Dodecane	12	24.47	-	0.25	0.76	0.00	0.25	-
o-Xylene	5	5.91	ND	1.78	1.13	0.38	0.28	ND
1,3,5-Trimethybenzene	6	6.21	-	3.21	0.89	0.07	0.27	-
	9	5.27	0.055	2.73	0.76	0.06	0.23	0.06
α-Pinene	10	14.10	-	1.06	1.59	0.7	0.09	-
R(+)-Limonene	9	10.32	-	3.65	1.43	0.32	0.00	-
β-Caryophyllene	14	21.37	-	2.51	1.01	0.20	0.00	-

The method developed by Eusebi (1996) for calculating the predicted functional group distributions per average secondary aerosol molecule aonsists of five simple computational steps. The first step is to predict the number of carbons per average product structure based on dominant gas-phase products and oxidation mechanisms of original hydrocarbon precursors. For exaple, 1,3,5-trimethylbenzene has nine carbons in average product. The second step is to calculate the number of potential bonding positions accessible to functional group bonding on the carbon chain, 1,3,5-trimethylbenzene has 12 potential bonding positions. Then the next step is to determine the number of bonding position required by each non-aliphatic C-H functional group per molecule, per mole of aliphatic C-H. This is done by multiplying the relative molar loadings reported in Table A.1 by the number of bonding position required by each functional group, and dividing by the relative molar loading of aliphatic C-H. The fourth step is to calculate the number of aliphatic bonds on the carbon chain by deviding the toal number of potential bonding positions by the total number of bond required per alophatic C-H bond. The final step is to back calculate the functional gorup distribution based on the relative molar loading by multiplying the ratios of the relative molar loading by the number of alophatic C-H bons per average molecule (calculated in step 4).

Appendix B : Houston atmospheric hydrocarbon composition, obtained from the CARB Report (Cater, 1998)

Table B1: Houston atmospheric hydrocarbon composition used in the case study for sensitivity analysis

Compounds	ppb/ppbC
ETHANE	1.69E-02
PROPANE	1.41E-02
N-C4	1.81E-02
N-C5	6.13E-03
N-C6	1.32E-03
N-C7	1.20E-03
N-C8	7.45E-04
N-C9	7.45E-04
N-C10	1.84E-03
N-C11	1.62E-04
N-C12	3.24E-04
N-C13	1.91E-05
2-ME-C3	7.89E-03
2-ME-C4	1.52E-02
2-ME-C5	3.56E-03
3-ME-C5	2.53E-03
22-DM-C4	4.58E-04
23-DM-C4	9.56E-04
23-DM-C5	6.03E-04
24-DM-C5	1.27E-03
3-ME-C6	1.12E-03
CYCC5	7.07E-04
ME-CYCC5	1.60E-03
CYCC6	6.88E-04
ME-CYCC6	6.78E-04
ET-CYCC6	1.82E-04
BR-C6	2.39E-04
BR-C7	2.09E-03
BR-C8	4.04E-03
BR-C9	1.71E-03
BR-C10	1.56E-03
BR-C11	1.62E-04
BR-C12	3.24E-04
BR-C13	1.91E-05
CYC-C7	1.24E-04

Compounds	ppb/ppbC
ETHENE	1.35E-02
PROPENE	3.18E-03
1-BUTENE	1.15E-03
C4-OLE1	1.43E-04
3M-1-BUT	3.24E-04
1-PENTEN	8.03E-04
1-HEXENE	3.35E-04
ISOBUTEN	1.15E-03
2M-1-BUT	9.16E-04
T-2-BUTE	1.15E-03
C-2-BUTE	9.08E-04
2M-2-BUT	5.17E-04
13-BUTDE	6.21E-04
ISOPRENE	1.30E-03
CYC-HEXE	1.72E-04
A-PINENE	5.06E-04
3-CARENE	1.91E-04
C5-OLE1	4.39E-04
C6-OLE1	2.22E-03
C7-OLE1	1.18E-03
C8-OLE1	2.39E-04
C9-OLE1	5.17E-04
C10-OLE1	9.56E-05
C11-OLE1	1.91E-04
C4-OLE2	1.43E-04
C5-OLE2	3.18E-03
C6-OLE2	1.00E-03
C7-OLE2	4.39E-04
C8-OLE2	2.20E-04
C9-OLE2	2.49E-04
C10-OLE2	9.56E-05
C11-OLE2	1.91E-04
C7-OL2D	1.91E-04
BENZENE	3.31E-03
TOLUENE	9.25E-03
C2-BENZ	1.28E-03
N-C3-BEN	3.64E-04
I-C3-BEN	1.91E-04
C9-BEN1	1.62E-04
S-C4-BEN	2.30E-04
C10-BEN1	1.82E-04
C11-BEN1	6.51E-04

Compounds	ppb/ppbC
C12-BEN1	2.87E-05
O-XYLENE	1.82E-03
P-XYLENE	2.20E-03
M-XYLENE	2.20E-03
C9-BEN2	2.47E-03
C10-BEN2	1.54E-03
C11-BEN2	9.56E-05
C12-BEN2	8.60E-05
135-TMB	7.26E-04
123-TMB	7.55E-04
C9-BEN3	2.36E-03
C10-BEN3	1.60E-03
C11-BEN3	9.56E-05
C12-BEN3	8.60E-05
C10-BEN4	4.21E-04
C9-STYR	4.77E-04
C10-STYR	3.64E-04
ACETYLEN	9.75E-03
FORMALD	7.93E-03
ACETALD	4.77E-03
PROPALD	6.97E-04
C4-RCHO	3.16E-04
C5-RCHO	1.07E-03
C6-RCHO	7.37E-04
BENZALD	1.62E-04
ACETONE	3.10E-03
MEK	1.10E-03

Appendix C : Reaction pathways and mechanistic models of SOA formation of aromatic hydrocarbons modeled in SAPRC-99

1,2,3-trimethylbenzene

Oxidation of 1,2,3-trimethybenzene proceeds either through the abstraction of hydrogen, or by addition of the OH radicals to the aromatic ring. Most of reactions proceed through the addition of OH radicals to the aromatic ring (pathway 1). Hydrogen abstraction which accounts for only 4.4 % of all reactions with the OH radicals (SAPRC 99) results in a products represented in SAPRC 99 as benzaldehyde plus two carbon atoms (BALD + 2XC) with an NO to NO_2 conversion and the production of HO_2 radical (pathway 1).

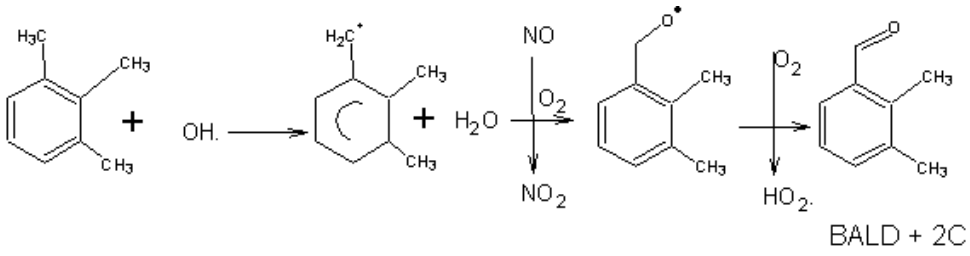

(1)

4.4%: 123-TMB + HO. = BALD + 2XC +RO2R **Reaction 1**

When OH is added to the ring, the OH radicals add primarily to the ortho position of each side chain. Initial reaction with OH radical addition can produce cresol plus two

carbon atoms (CRES + 2XC) as a gas phase product, which accounts for 18.6 % of all reactions (SAPRC 99).

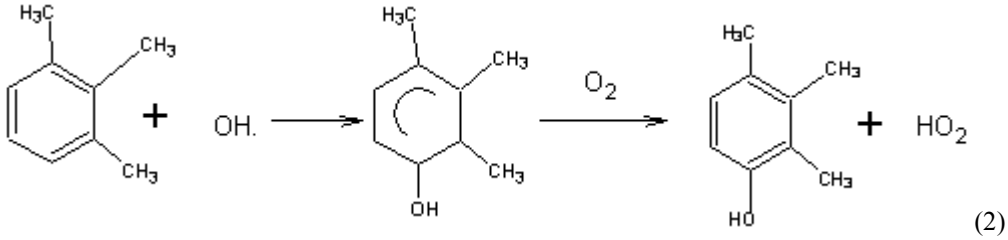

(2)

18.6%: 123-TMB + HO. = CRES + 2XC + HO2. **Reaction 2**

Another reaction pathway that can occur following the formation of the OH-aromatic adduct is bridging of O_2 across the ring as shown in pathway 3. Another O_2 addition occurs to the OH-aromatic-O_2 adduct, then with the abstraction of O atom by NO, the alkoxyl-type radicals are formed. The alkoxyl-type radicals undergoes hydrogen abstraction by O_2, and unsaturated dicarbonyls or aerosol precursors are produced. Experimental results from Bandow (1985) indicates that 43 % of the addition of O_2 to the OH-aromatics adduct results in biacetyl (BACL) and unsaturated dicarbonyl compound, denoted as APT2, 25 % results in methygyloxal (MGLY) and APT3 and approximately 8.5 % results in glyoxal (GLY) and APT4. Pathways 3-5 show the reaction pathways leading to the formation of APT2-APT4.

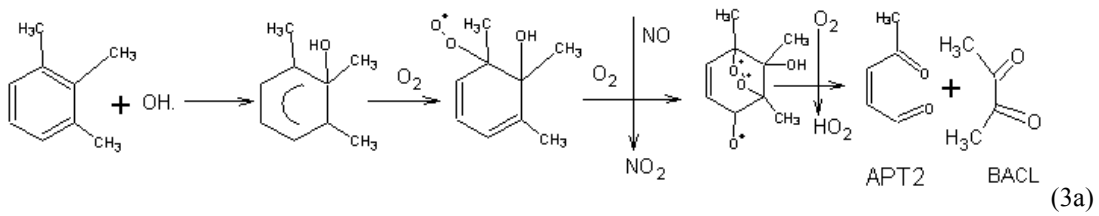

(3a)

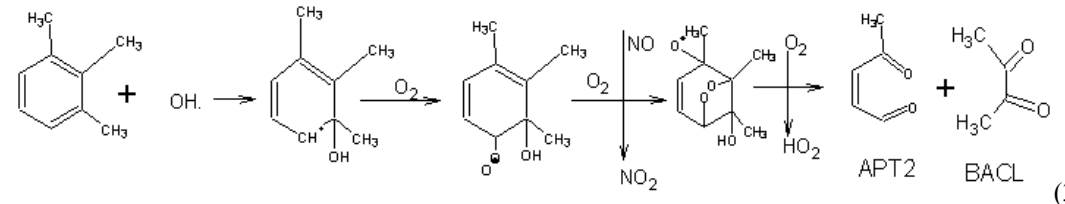

(3b)

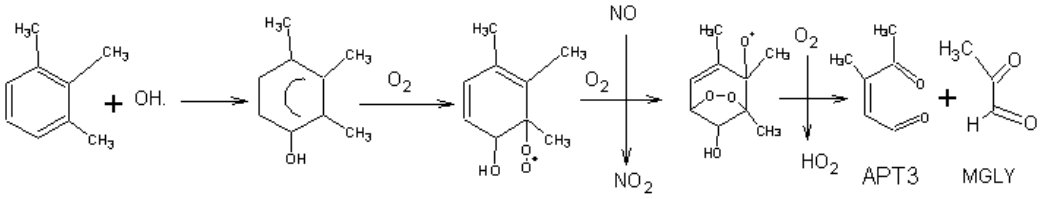

(4a)

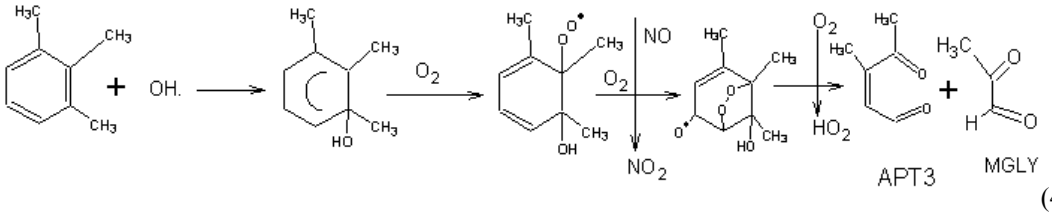

(4b)

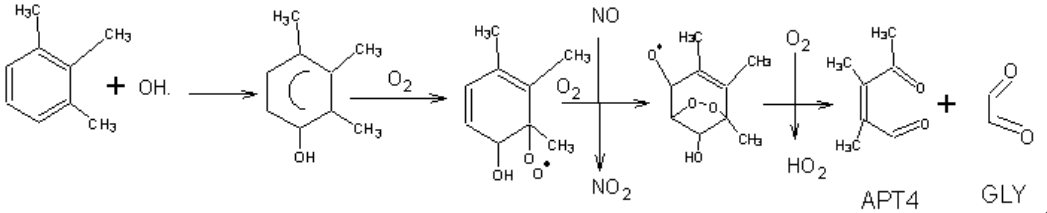

(5)

123-TMB + HO. = 0.431APT2 + 0.254APT3 + 0.085APT4 + 0.431BACL + 0.254MGLY + 0.085GLY + 0.77RO2R **Reaction 3**

Net: 123-TMB + HO. = 0.044BALD + 0.186CRES + 0.809 RO2R + 0.186 HO2. +0.254MGLY + 0.085GLY + 0.431BACL + 0.431APT2 + 0.254APT3 + 0.085APT4 + 0.46XC **Reaction 4**

Aerosol precursors (APT2-APT4) react further with OH radicals via addition at the carbon bond to form two types of aerosol products, TPM3 and TPM4, TPM3 is the aerosol product with organonitrate group (pathways 6a-8a), and TPM4 is the product with hydroxy carbonyl group (pathways 6b-8b). Relative yields of TPM3 and TPM4 were based on data for products for 1,3,5-trimethylbenzene (Eusebi, 1996).

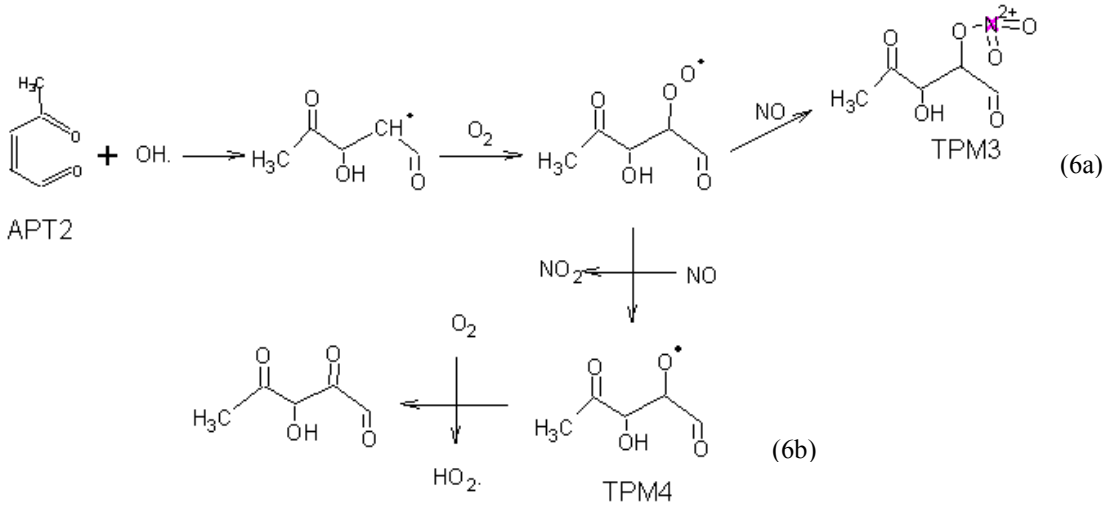

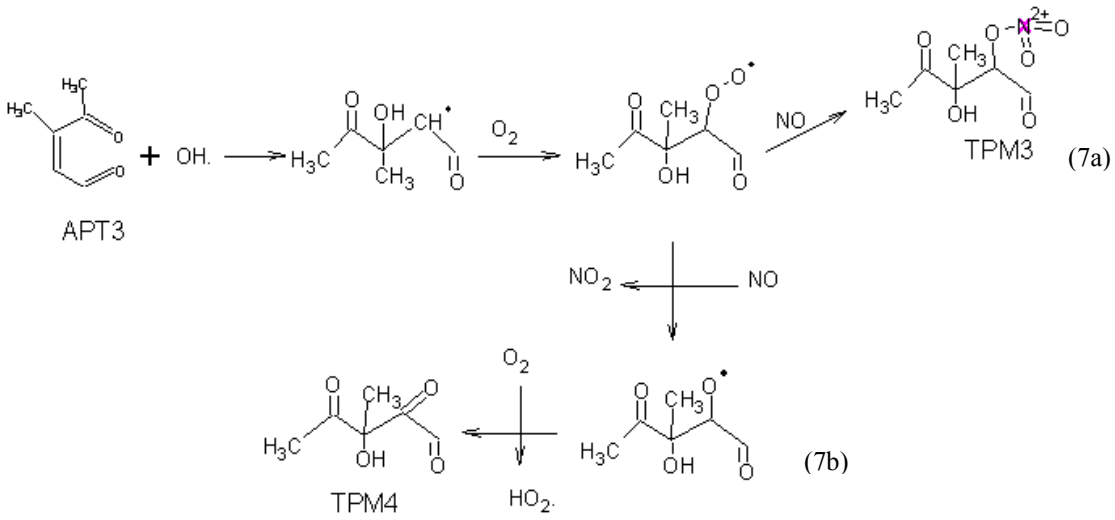

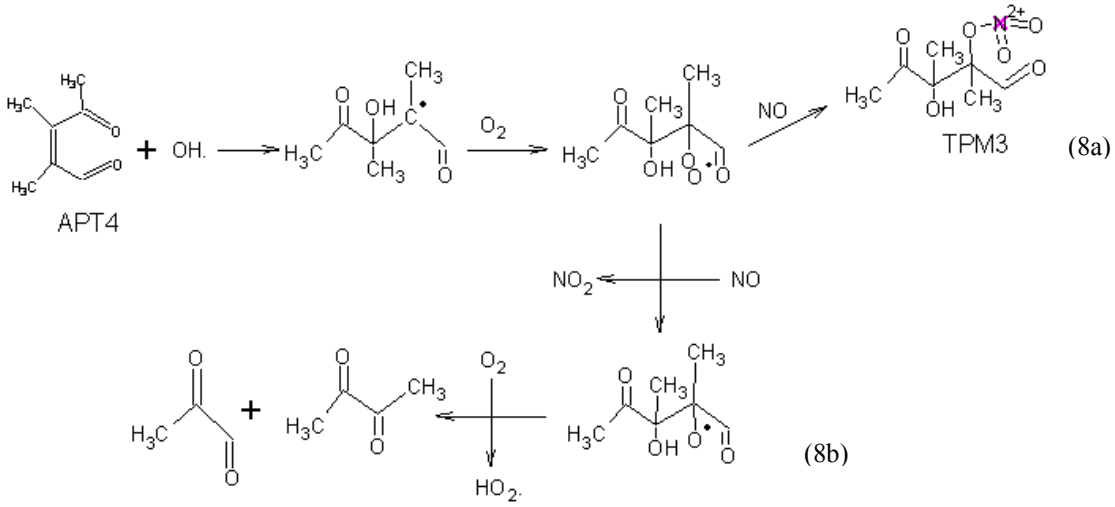

APT2 + HO. = 0.25TPM3 + 0.75TPM4+ 0.25RO2N + 0.75RO2R **Reaction 5**

APT3 + HO. = 0.25TPM3 + 0.75TPM4 + 0.25RO3N + 0.75RO2R **Reaction 6**

APT4 + HO. = 0.25TPM3 + 0.75MGLY + 0.75BACL + 0.25RO2N +0.75RO2R **Reaction 7**

Reactions 4-7 describe the condensed mechanisms of SOA formation for 1,2,3-trimethylbenzene which proceed through two steps: gas phase reaction of 1,2,3-trimethylbenzene with OH radicals to produce aerosol precursors (APT2-APT4), and reactions of APT2-4 with OH radical to form two types of semivolatile products (TPM3 and TPM4). Stoichiometric coefficients in reactions 1-7 are obtained from the evaluation of atmospheric chamber experiments. Table C1 summarizes these coefficients and cites the source of the data.

Table C.1: Kinetic parameters of 1,2,3-trimethylbenzene reactions with OH radical forming aerosol products and their source

Notations	Descriptions	Stoichiometric Coefficients (SC)	Source of SC
CRES	Cresol	0.186	SAPRC-99
BALD	Benzaldehyde	0.044	SAPRC-99
MGLY	Methylglyoxal	0.254	Bandow, 1985
GLY	Glyoxal	0.085	Bandow, 1985
HO2.	Hydroperoxy radical	0.186	SAPRC-99
BACL	Biacetyl	0.431	Bandow, 1985
RO2R	Operator RO2R	0.809 (reaction 4) 0.75 (reaction 5-7)	Bandow, 1985 Estimated from 1,3,5-trimethylbenzene
APT2	Aerosol precursor APT2	0.431	Bandow, 1985
APT3	Aerosol precursor APT3	0.254	Bandow, 1985
APT4	Aerosol precursor APT4	0.085	Bandow, 1985
TPM3	Aerosol product species 1	0.25	Estimated from products from 1,3,5-trimethylbenzene
TPM4	Aerosol product species 2	0.75	Estimated from products from 1,3,5-trimethylbenzene
RO2N	Operator RO2N	0.25	Estimated from products from 1,3,5-trimethylbenzene
XC	Balance extra carbon	0.46	SAPRC-99, Bandow, 1985

1,2,4-trimethylbenzene

Oxidation of 1,2,4-trimethybenzene either proceeds through the OH addition to the aromatic ring, or the abstraction of H from the methyl group. Most of the reactions, 77%, proceed through the addition of OH radical to the aromatic ring (SAPRC 99). Hydrogen abstraction occurs primarily from the methyl substituents. The hydrogen abstraction reaction results in benzaldehyde plus two carbon atoms (BALD + 2XC), pathway 9. This accounts for 4.4 % of all reactions of 124-trimethybenzene with OH radical (SAPRC 99).

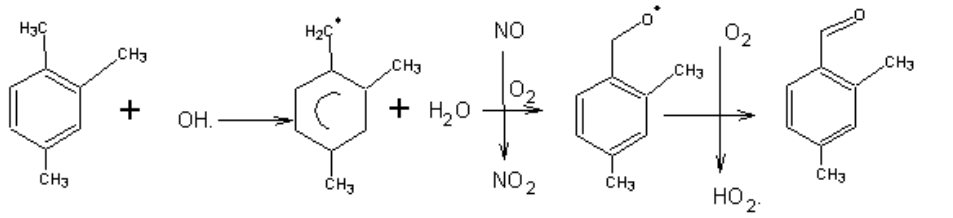

(9)

4.4%: 124-TMB + HO. = BALD +2XC + RO2R **Reaction 8**

When OH adds to the ring, the OH radicals add primarily to the ortho position of each side chain. 18.6 % (SAPRC 99) of initial reactions with OH radicals result in cresol plus two carbon atoms (CRES + 2XC), pathway 10.

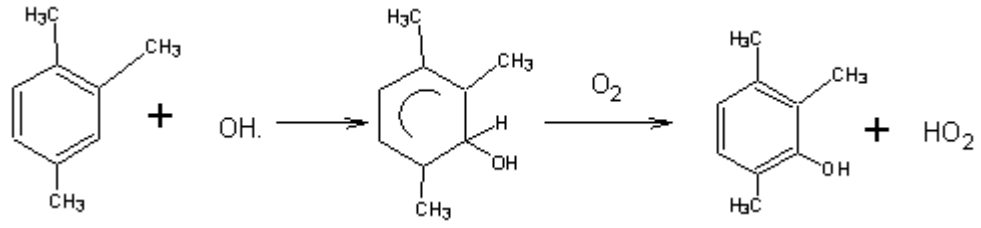

(10)

18.6%: 124-TMB + HO. = CRES +2XC + HO2. **Reaction 9**

Another reaction pathway that can occur following the formation of the OH-aromatic adduct is bridging of O_2 across the ring as shown in pathway 11, which leads to the ring clevage reactions. The ring cleavage reaction of the O_2-OH aromatics adduct can proceed through ten possible pathways (pathways 11-16). All of these ten reaction pathways proceed through two similar steps, the abstraction of O atom by NO, and the abstraction of H atom by O_2. The cleavage reactions produce 25.4 % unsaturated dicarbonyl species or aerosol precursor APT5, 8.4 % of APT6, 13.1 % of APT7, 14.6 % APT8, 4.6 % APT9, and 10.7% AP10 (Bandow, 1985). Along with those unsaturated species, methyglyoxal (MGLY), glyoxal (GLY), and biacetyl (BACL) are also produced with the yields of 0.515, 0.146, and 0.107, respectively (Bandow, 1985).

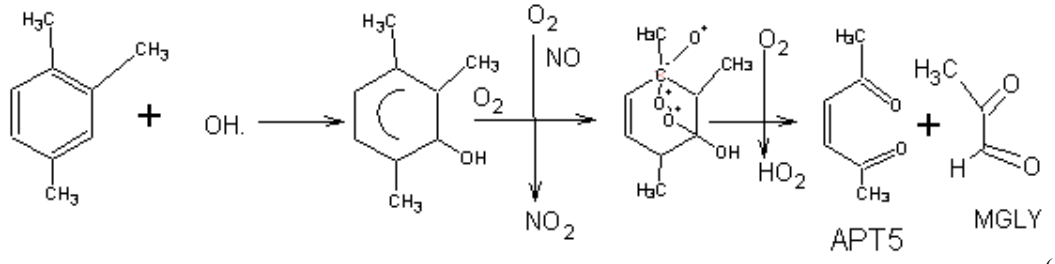

(11a)

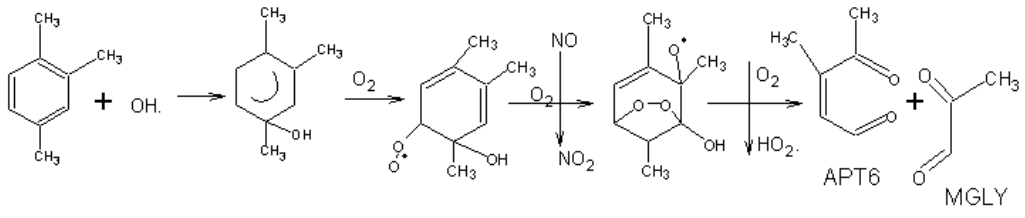

(12a)

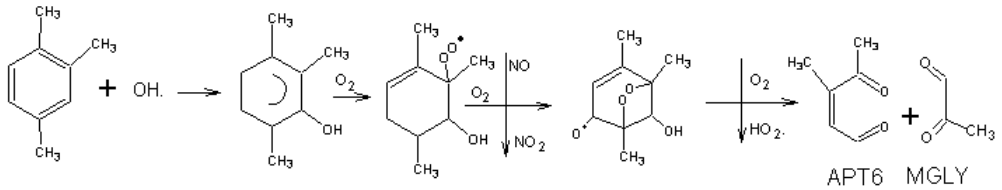

(12b)

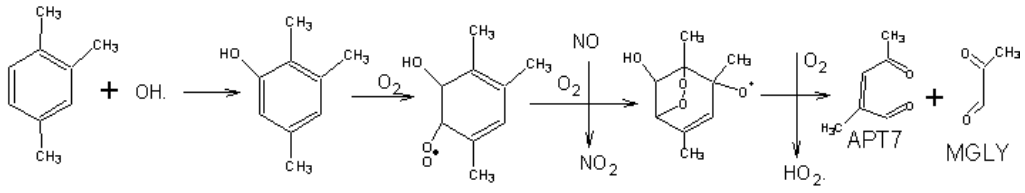

(13a)

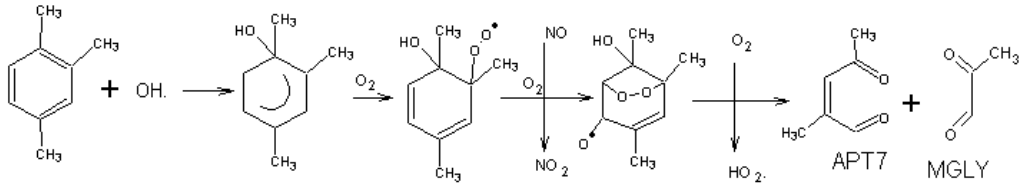

(13b)

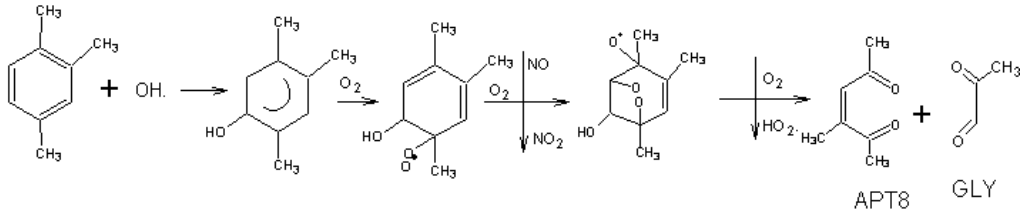

(14a)

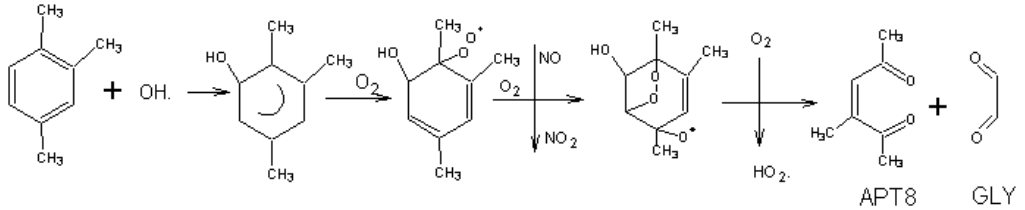

(14b)

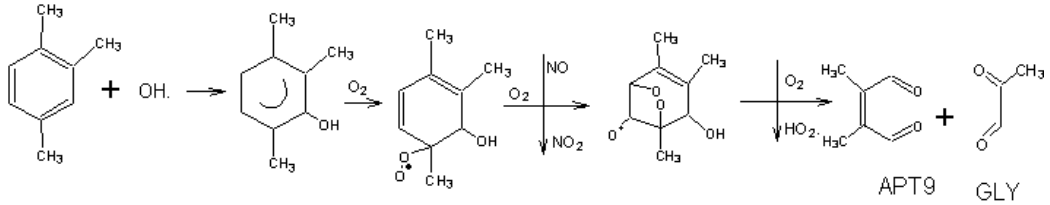

(15)

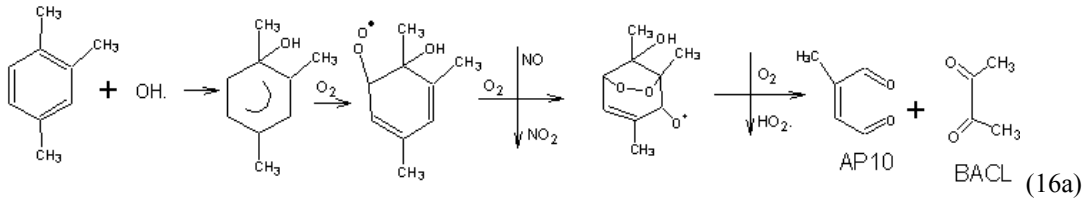

(16a)

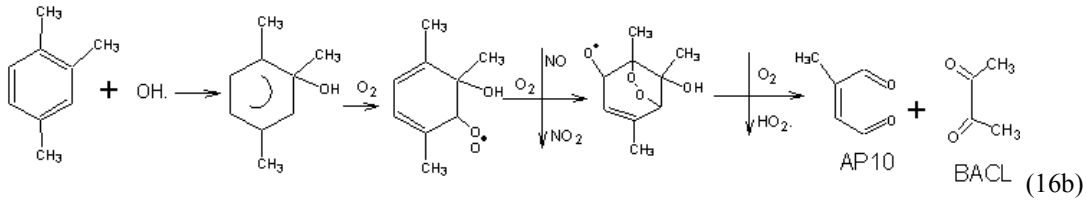

(16b)

80.4%: 124-TMB + HO. = 0.254APT5 + 0.084APT6 + 0.131APT7 + 0.146APT8 + 0.046APT9 + 0.107AP10 + 0.469MGLY + 0.192GLY + 0.107BACL + 0.804RO2R **Reaction 10**

Net: 124-TMB + HO. = 0.044BALD + 0.186CRES + 0.8122RO2R + 0.186HO2. + 0.469MGLY + 0.192GLY + 0.107BACL + 0.254APT5 + 0.084APT6 + 0.131 APT7 + 0.146APT8 + 0.046APT9 + 0.107AP10 + 0.46XC **Reaction 11**

Aerosol precursors (APT5-APT9, and AP10) can further oxidize to form two types of aerosol products, TPM5 and TPM6. TPM5 is the aerosol product with organonitrate group and TPM6 is a hydroxylic carbonyl. The formation of TPM5 proceeds through the addition of O_2 and NO to the OH-dicarbonyl adduct (pathways 17a-22a) , while the production of TPM6 undergoes the addition of O_2, and the abstraction of O atom by NO (pathways 17b-22b). Yields of TPM5 (25%) and TPM6 (75%) were estimated from experimental results by Eusebi (1996) for 1,3,5-trimethylbenzene.

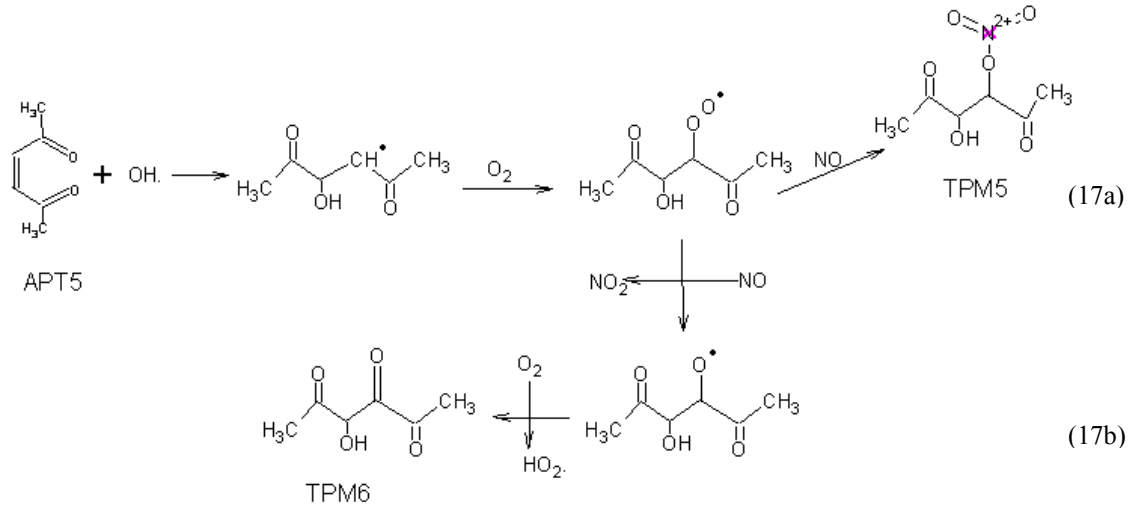

(17a)

(17b)

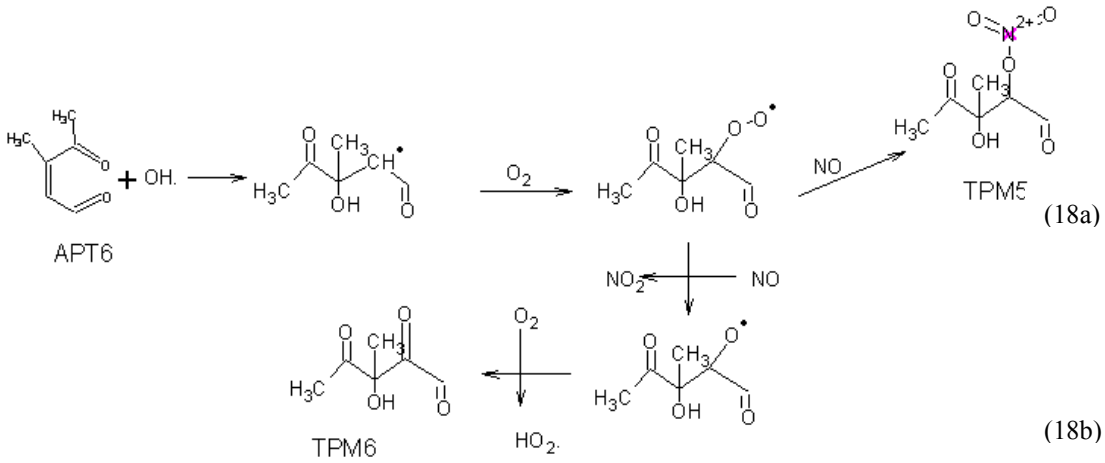

(18a)

(18b)

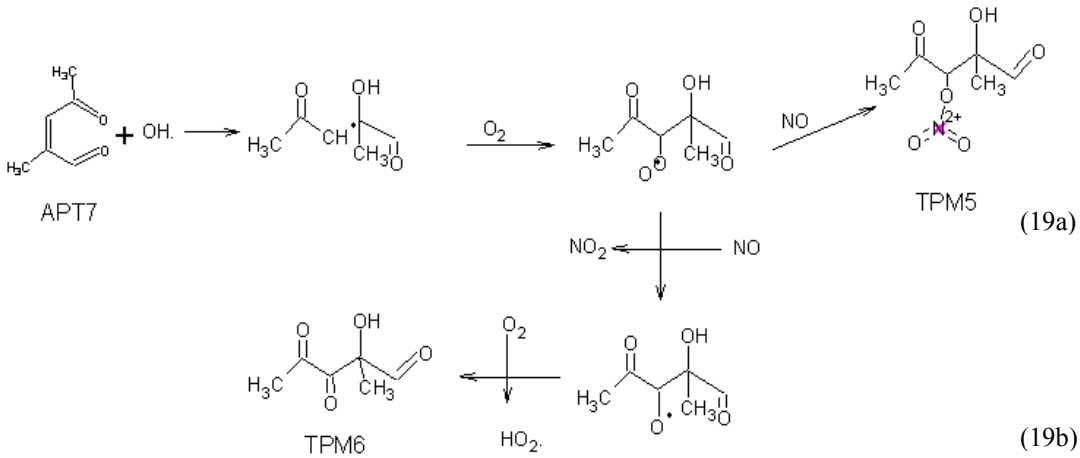

(19a)

(19b)

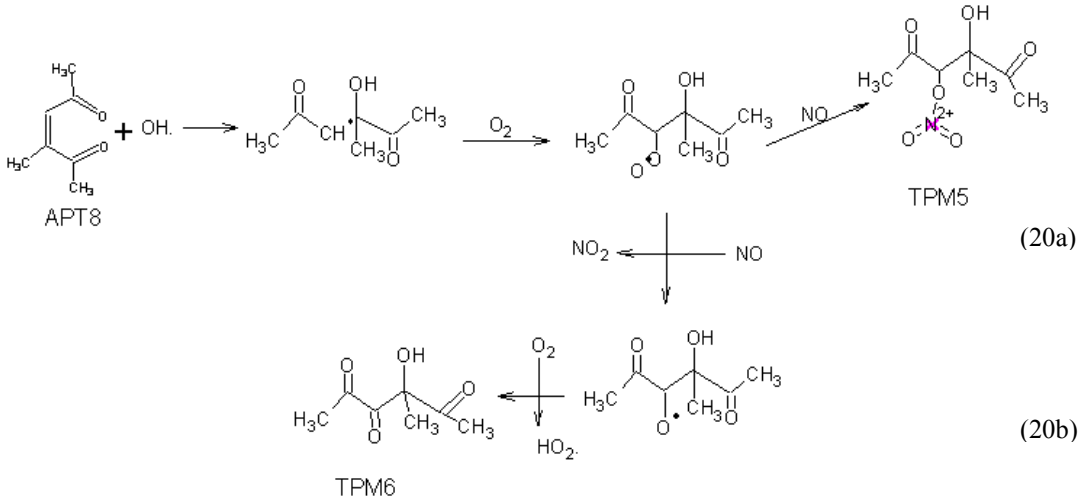

(20a)

(20b)

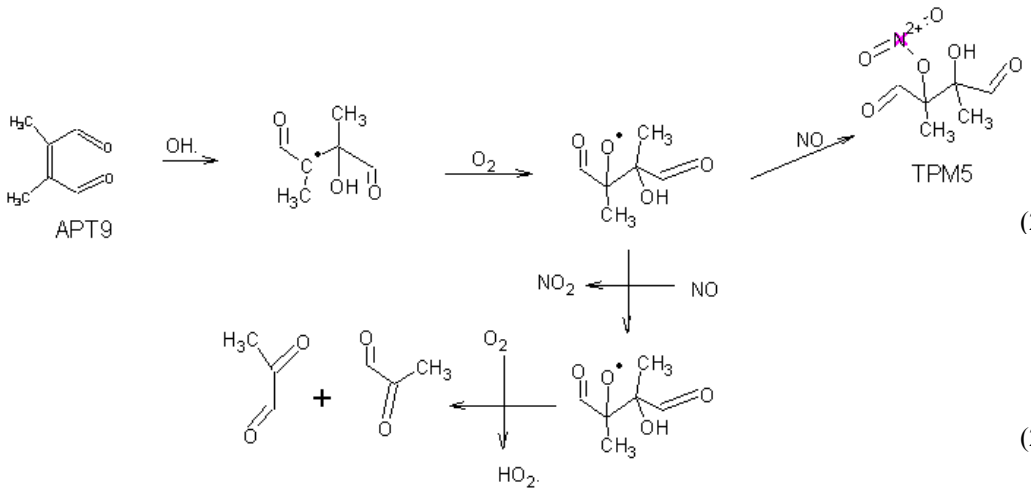

(21a)

(21b)

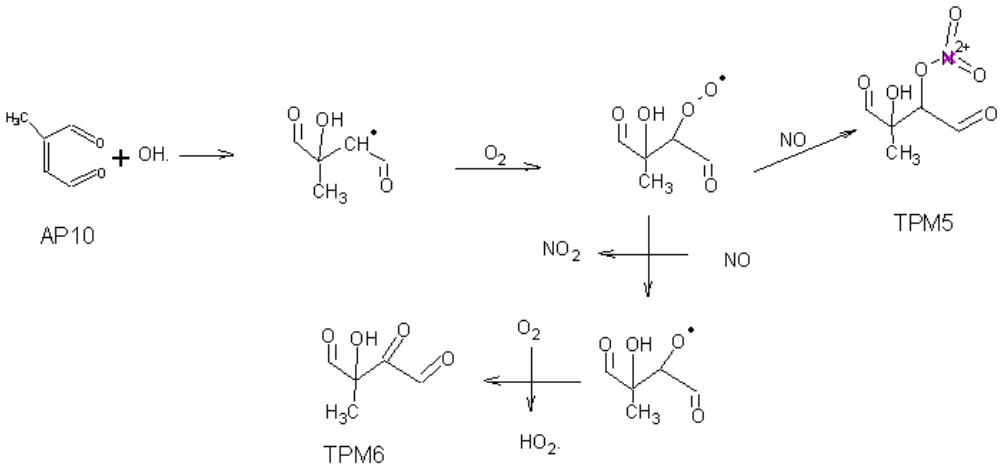

(22a)

(22b)

APT5 + HO. = 0.25TPM5 + 0.75TPM6 + 0.25RO2N + 0.75RO2R **Reaction 12**

APT6 + HO. = 0.25TPM5 + 0.75TPM6 + 0.25RO2N + 0.75RO2R **Reaction 13**

APT7 + HO. = 0.25TPM5 + 0.75TPM6 + 0.25RO2N + 0.75RO2R **Reaction 14**

APT8 + HO. = 0.25TPM5 + 0.75TPM6 + 0.25RO2N + 0.75RO2R **Reaction 15**

APT9 + HO. = 0.25TPM5 + 0.75(2MGLY) + 0.25RO2N + 0.75RO2R **Reaction 16**

AP10 + HO. = 0.25TPM5 + 0.75TPM6 + 0.25RO2N + 0.75RO2R **Reaction 17**

Formation of semivolatile products for 1,2,4-trimethylbenzene proceed through steps similar to those for 1,2,3-trimethylbenzene. Stoichiometric coefficients and sources of the data are summarized in Table C2.

Table C.2: Kinetic parameters of 1,2,4-trimethylbenzene reactions with OH radical forming aerosol products and their source

Notations	Descriptions	Stoichiometric Coefficients (SC)	Source of SC
CRES	Cresol	0.186	SAPRC-99
BALD	Benzaldehyde	0.044	SAPRC-99
MGLY	Methylglyoxal	0.469	Bandow, 1985
GLY	Glyoxal	0.192	Bandow, 1985
HO2.	Hydroperoxy radical	0.186	SAPRC-99
BACL	Biacetyl	0.107	Bandow, 1985
RO2R	Operator RO2R	0.8122 (reaction 11)	Bandow, 1985

		0.75 (reaction 12-17)	Estimated from 1,3,5-trimethylbenzene
APT5	Aerosol precursor APT5	0.254	Bandow, 1985
APT6	Aerosol precursor APT6	0.084	Bandow, 1985
APT7	Aerosol precursor APT7	0.131	Bandow, 1985
APT8	Aerosol precursor APT8	0.146	Bandow, 1985
APT9	Aerosol precursor APT9	0.046	Bandow, 1985
AP10	Aerosol precursor AP10	0.107	Bandow, 1985
TPM3	Aerosol product species 1	0.25	Estimated from 1,3,5-trimethylbenzene
TPM4	Aerosol product species 2	0.75	Estimated from 1,3,5-trimethylbenzene
RO2N	Operator RO2N	0.25	Estimated from 1,3,5-trimethylbenzene
XC	Balance extra carbon	0.46	SAPRC-99, Bandow, 1985

o-xylene

In addition to trimethylbenzene, xylene also produces a significant amount of secondary organic aerosol in the urban atmosphere. The major daytime loss process for atmospheric aromatic hydrocarbons is through reaction with hydroxyl radical. As with 1,3,5-trimethybenzene, this reaction can proceed through either hydrogen abstraction, or addition to the aromatic ring. For o-xylene, hydrogen abstraction accounts for 6.5% of all reactions (SAPRC99), occurring primarily at the substituent methyl groups. The product of this reaction is benzaldehyde with one extra carbon atom (BALD + 1XC), along with an NO to NO_2 conversion and the production of HO_2 radical (pathway 23).

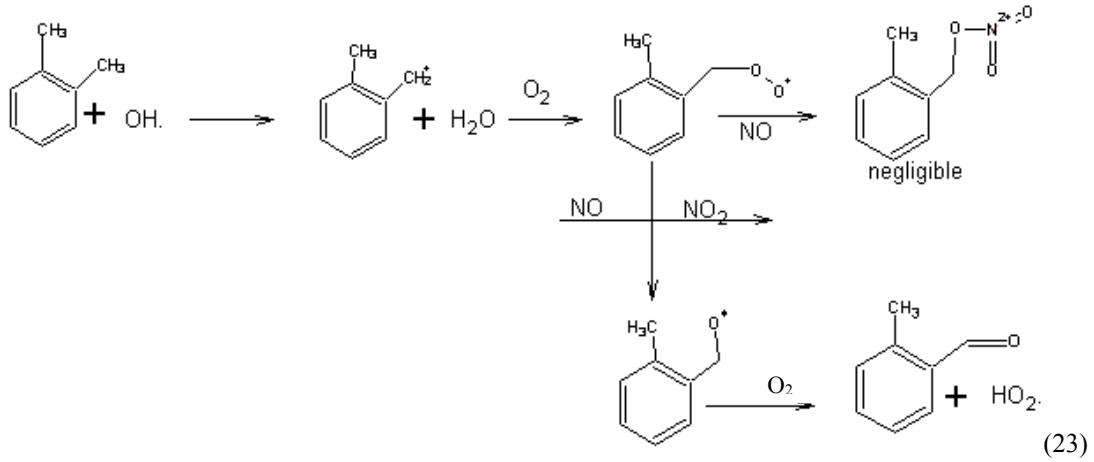

(23)

4.5%: O-XYLENE + HO. = BALD +1XC + RO2R **reaction 18**

Addition of the OH radical will occur at one of the three ring positions, but predominantly adds at the aromatic carbon ortho to one of the carbons attached to the methyl group (Grovenstein, 1970; Atkinson et al., 1980). The initial addition of OH radical to o-xylene results in cresol with one extra carbon atom (CRES + 1XC) and HO_2 radical (pathway 24). This pathway accounts for 18% of all reactions of o-xylene (SAPRC99).

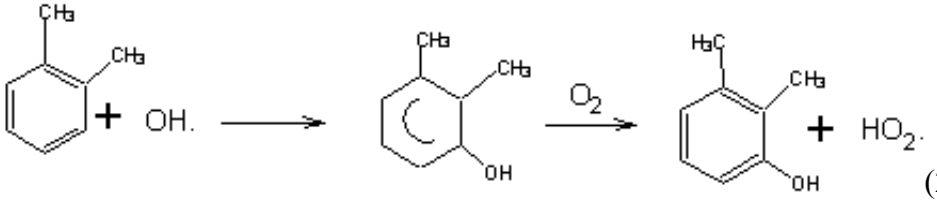

(24)

16.1%: O-XYLENE + HO. = CRES + 1XC + HO2. **Reaction 19**

The remainder of the OH radical addition products from o-xylene will further proceed through the addition of O_2, forming the bridge of O_2 across the ring. This structure then reacts further with O_2, with conversion of NO to NO_2 and formation of HO_2 radical as shown in pathway 25 to produce the ring cleavage products. The ring cleavage reaction of the O_2-OH-aromatic-adduct proceeds through four possible positions on the aromatic ring (pathways 25-27). Although chemical structures of all aerosol precursors from o-xylene, APX1-APX3 are different, their formation pathways are similar. The cleavage reactions produce 45% of APX1, 14% of APX2, and 20% of APX3 (Bandow, 1985). In addition to these, MGLY, GLY, and BACL are generated. In total, these pathways account for 74% of all reactions of o-xylene with OH radical.

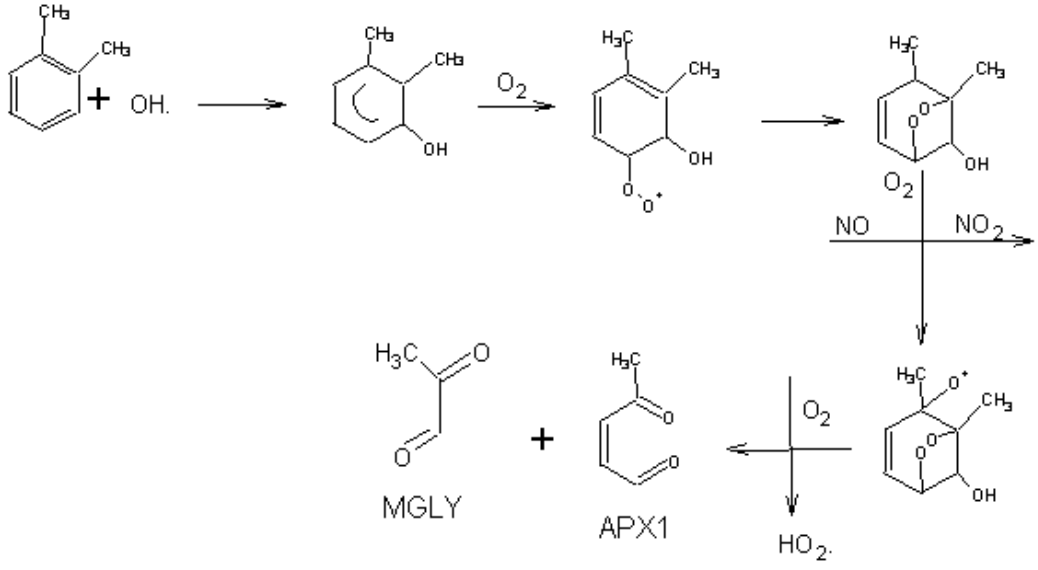

(25a)

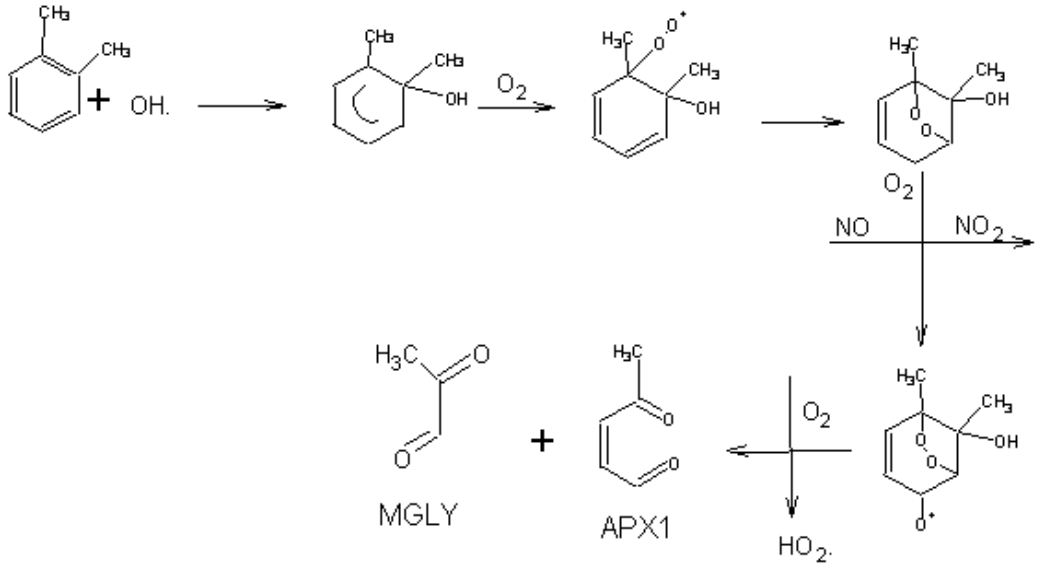

(25b)

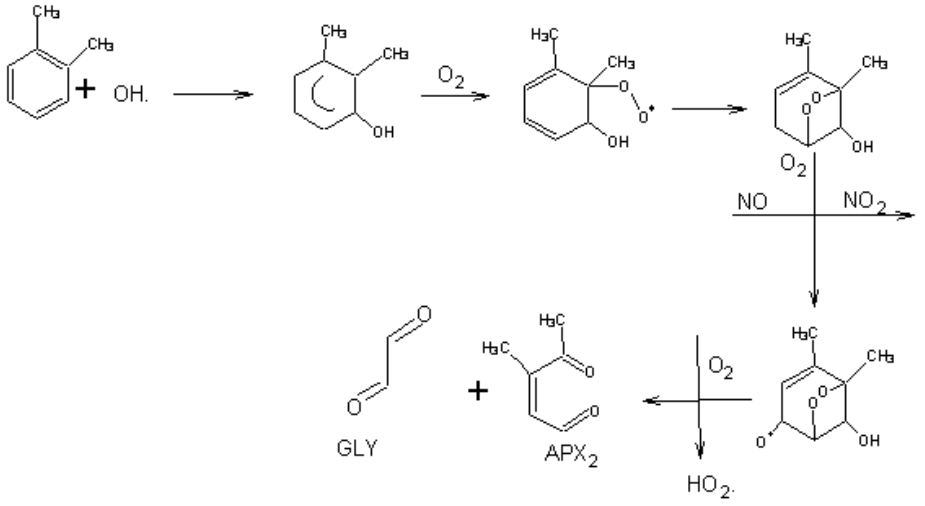

(26)

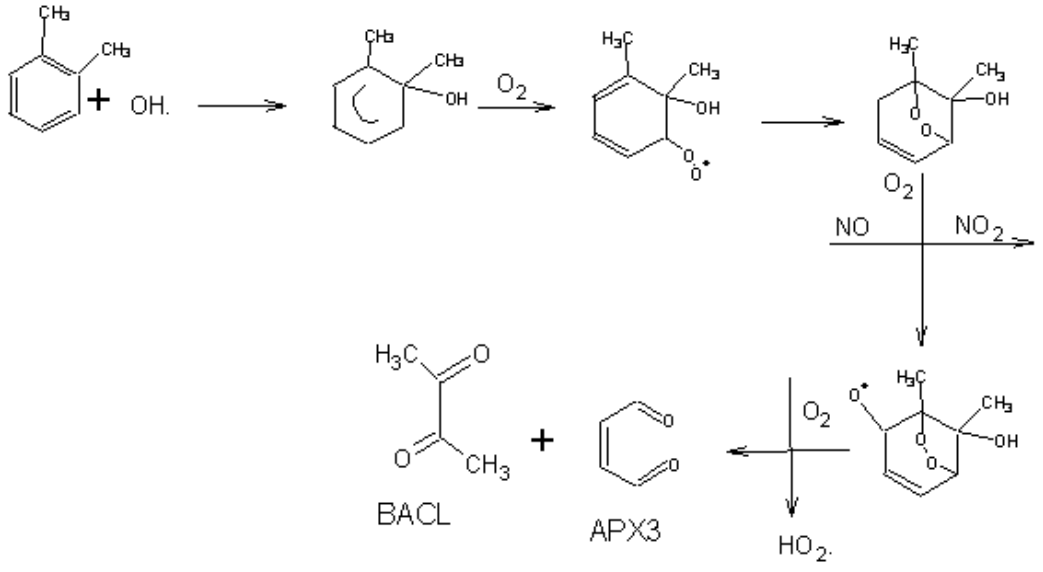

(27)

79 % O-XYLENE + HO. = .45 APX1 + .45 MGLY + .14 APX2 + .14 GLY + .20 APX3 + .20 BACL + 0.79RO2R **Reaction 20**

Net: O-XYLENE + HO. = .045 BALD + .161 CRES + .835 RO2R + .161 HO2. + .45 APX1 + .14APX2 + .2 APX3 + .2 BACL + .14 GLY +.45 MGLY + .206 XC **Reaction 21**

Aerosol precursors (APX1-APX3) further react to generate two types of aerosol products (XPM1 and XPM2) via the OH-addition at the carbon double bond. Results from previous studies suggested that 25% of APX2-OH addition reaction produce XPM1 (pathways 28a -30a) (Eusebi, 1996). The remaining APX2-OH reacts with O_2 and NO to form XPM2, NO_2, and HO_2 radicals (pathways 28b-30b).

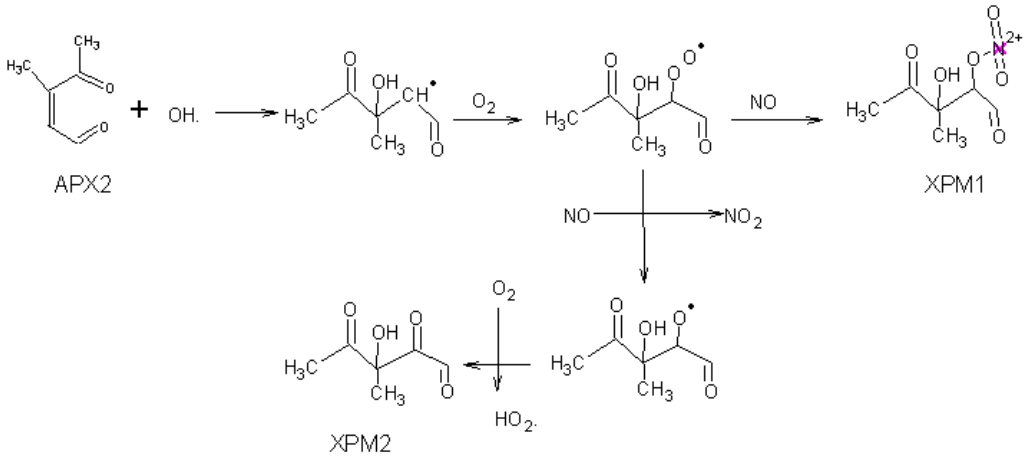

(28a)

(28b)

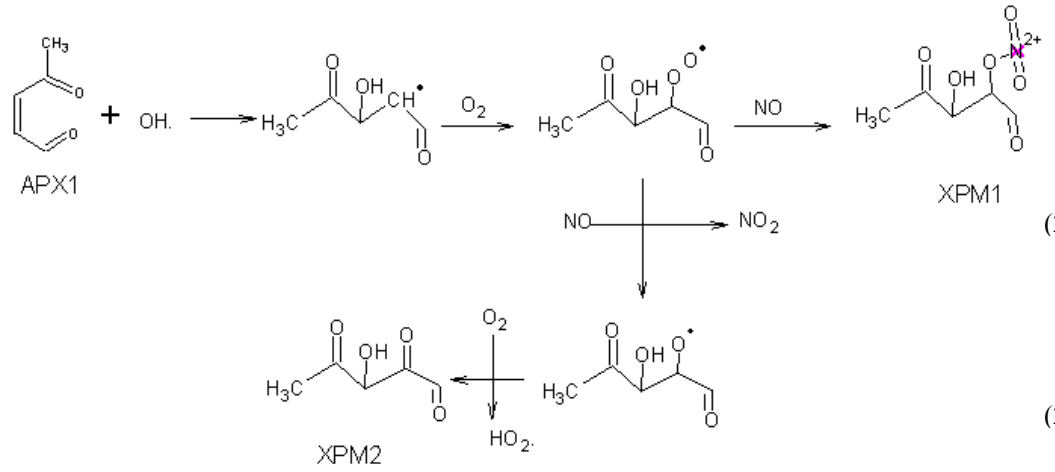

(29a)

(29b)

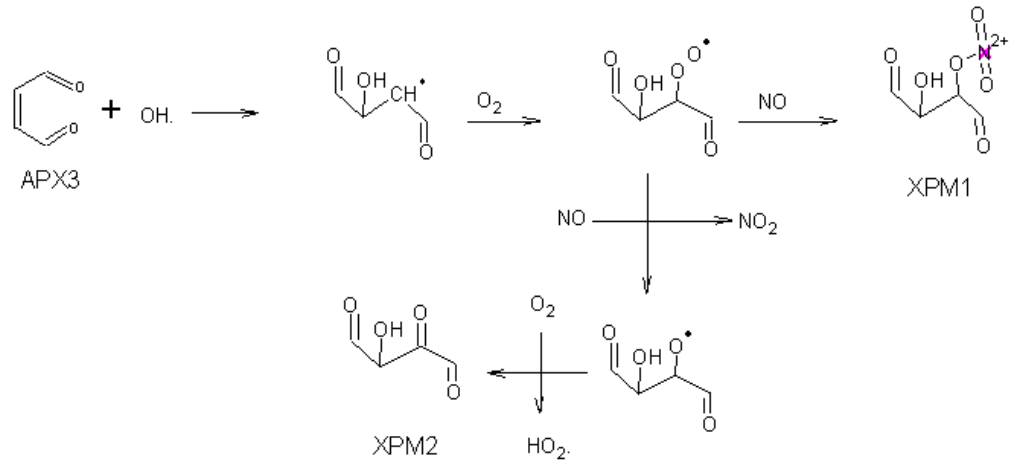

(30a)

(30b)

APX1 + HO. = .25 XPM1 + .75 XPM2 + .25 RO2N + .75 RO2R **Reaction 22**

APX1 + HO. = .25 XPM1 + .75 XPM2 + .25 RO2N + .75 RO2R **Reaction 23**

APX1 + HO. = .25 XPM1 + .75 XPM2 + .25 RO2N + .75 RO2R **Reaction 24**

Reactions 21-24 describe the condensed mechanisms of SOA formation for o-xylene, which proceed through steps similar to 1,3,5-trimethylbenzene. Table C3 summarizes stoichiometric coefficients in reaction 21-24 and cites sources of the data.

Table C.3: Kinetic parameters of o-xylene reactions with OH radical forming aerosol products and their source

Notations	Descriptions	Stoichiometric Coefficients (SC)	Source of SC
CRES	Cresol	0.161	SAPRC-99
BALD	Benzaldehyde	0.045	SAPRC-99
MGLY	Methylglyoxal	0.450	Bandow, 1985
GLY	Glyoxal	0.146	Bandow, 1985
HO2.	Hydroperoxy radical	0.188	SAPRC-99
BACL	Biacetyl	0.200	Bandow, 1985
RO2R	Operator RO2R	0.835 (reaction 21) 0.75 (reaction 22-24)	Bandow, 1985 Eusebi, 1996
APX1	Aerosol precursor APX1	0.450	Bandow, 1985
APX2	Aerosol precursor APX2	0.140	Bandow, 1985
APX3	Aerosol precursor APX3	0.200	Bandow, 1985
XPM1	Aerosol product species 1	0.25	Eusebi, 1996
XPM2	Aerosol product species 2	0.75	Eusebi, 1996
RO2N	Operator RO2N	0.25	Eusebi, 1996
XC	Balance extra carbon	0.24	SAPRC-99, Bandow, 1985

p-xylene

Reaction of p-xylene with OH radical can proceed through either the hydrogen abstraction, or addition to the aromatic ring. The hydrogen abstraction, accounting for 8.3 % of the reactions (SAPRC 99), occurs primarily at the substituent

methyl groups. The product of this reaction is benzaldehyde plus one carbon atom (BALD + 1XC), pathway 31.

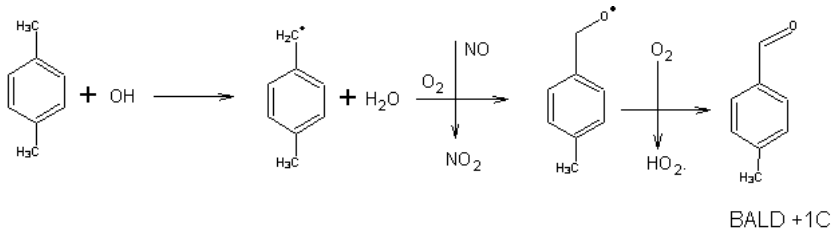

(31)

8.3%: P-XYLENE + OH. = BALD + 1XC + RO2R **Reaction 25**

Addition of OH radical can occur at one of the three ring positions, but predominantly attaches at the aromatic carbon ortho to one of the carbons attached to the methyl group (Grovenstein, 1970; Atkinson. et al., 1980). The initial addition of OH radical to the aromatic can result in the gas phase product, cresol plus one carbon atom (CRES + 1XC), which accounts for 18.8 % of all reactions of o-xylene with OH radical (SAPRC 99).

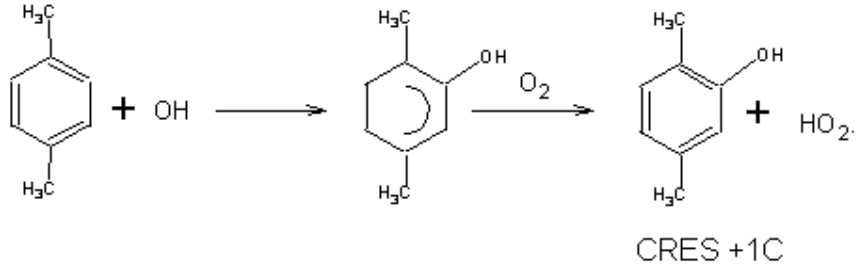

(32)

18.8%: P-XYLENE + OH. = CRES + HO2. + 1XC **Reaction 26**

Another reaction pathway that can occur following the formation of the OH-aromatic adduct is bridging of O_2 across the ring. Another O_2 addition occurs to the OH-

aromatic-O_2 adduct, then with the abstraction of O atom by NO, the alkoxyl-type radicals are formed. The alkoxyl-type radical undergoes hydrogen abstraction by O_2, leading to the production of ring-cleavage products. The xylene-ring cleavage reactions generate individually 48.9% of APX4 and GLY, and 24% of APX5 and MGLY (pathways 33-34).

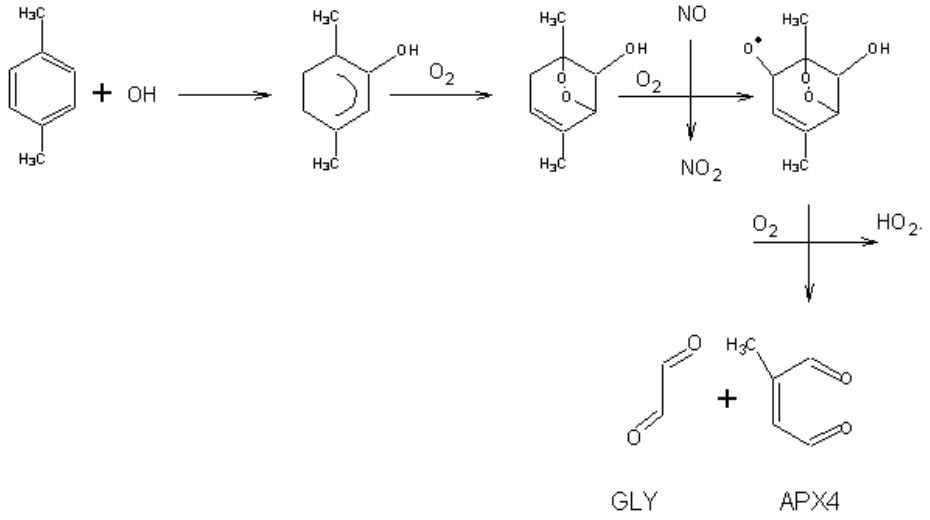

(34)

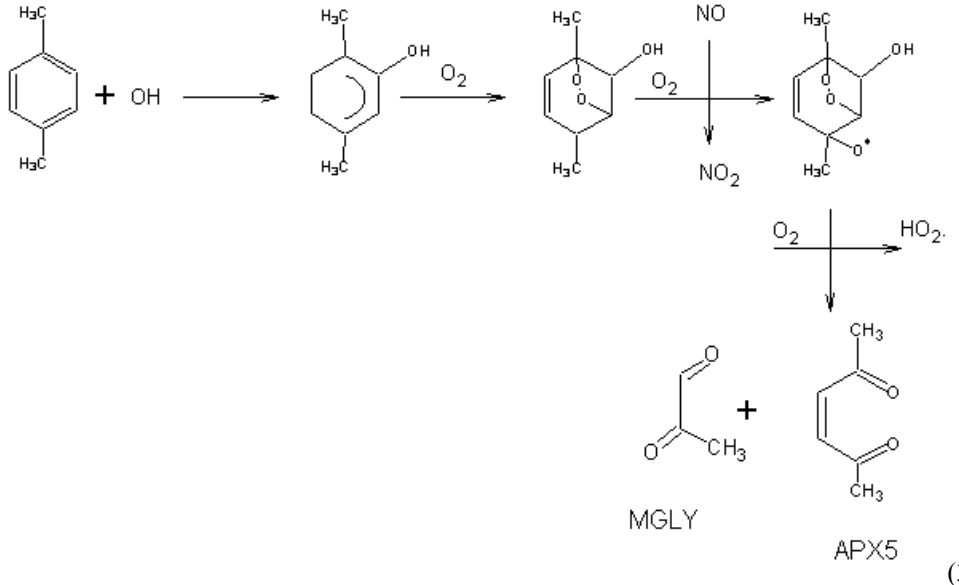

(35)

72.9 % P-XYLENE + OH. = 0.489APX4 + 0.240APX5 + 0.489GLY + 0.240MGLY + 0.729RO2R **Reaction 27**

Net: P-XYLENE + OH. = 0.489APX4 +0.240APX5 + 0.489GLY + 0.240MGLY + 0.188HO2. + 0.188CRES + 0.083BALD + 0.812RO2R + 0.271XC **Reaction 28**

Aerosol precursors (APX4-APX5) react further with OH radicals through addition at the carbon double bond to produce two types of semivolatile products (XPM3 and XPM4), where XPM3 are the products with organonitrate groups, and XPM4 is a product with a carbonyl. Pathways 35a-36a and 35b-36b demonstrate the formation of XPM3 and XPM4, respectively. Yields of XPM3 (25%) and XPM4 (75%) were estimated from experimental results for o-xylene from Eusebi (1996).

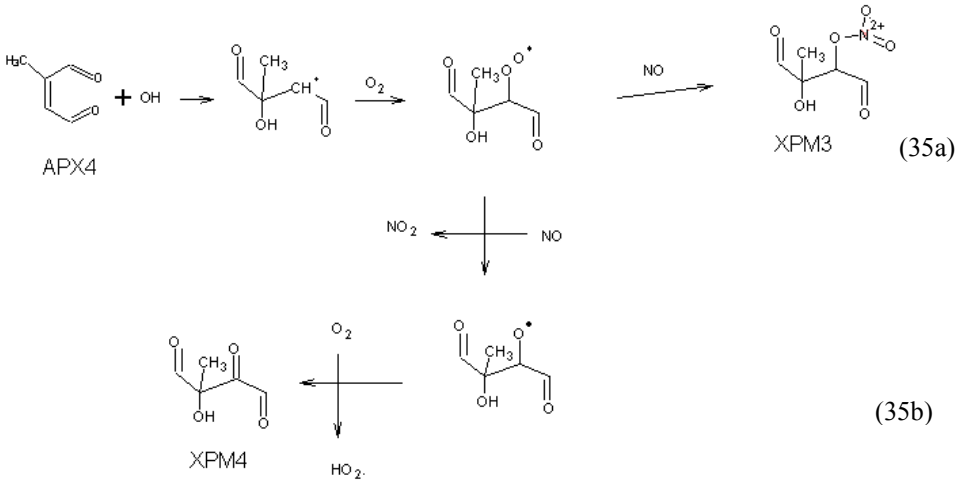

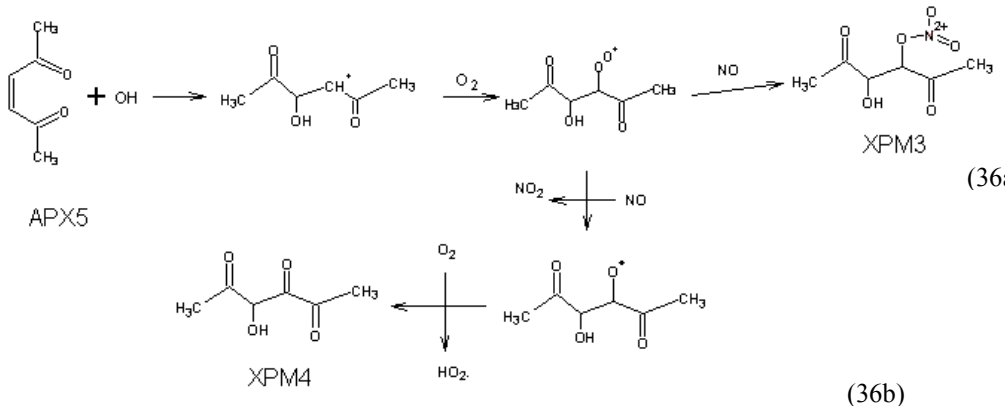

(36a)

(36b)

APX4 + OH. = 0.25XPM3 + 0.75XPM4 + 0.25RO2N + 0.75RO2R **Reaction 29**

APX5 + OH. = 0.25XPM3 + 0.75XPM4 + 0.25RO2N + 0.75RO2R **Reaction 30**

Analogous to 1,3,5-trimethylbenzene, reactions 28-30 describe the formation of two types of semivolatile products formed from the oxidation reaction of p-xylene through two steps. The first step is the reaction of p-xylene with OH radical to form aerosol precursors, and the second step is the reaction of aerosol precursors with OH radical to produce semivolatile products. Table 4 summarizes stoichiometric coefficients in reactions 28-30, and cites sources of the data.

Table C.4: Kinetic parameters of p-xylene reactions with OH radical forming aerosol products and their source

Notations	Descriptions	Stoichiometric Coefficients (SC)	Source of SC
CRES	Cresol	0.188	SAPRC-99
BALD	Benzaldehyde	0.083	SAPRC-99
MGLY	Methylglyoxal	0.240	Bandow, 1985
GLY	Glyoxal	0.489	Bandow, 1985
HO2.	Hydroperoxy radical	0.188	SAPRC-99
RO2R	Operator RO2R	0.812(reaction 28)	Bandow, 1985
		0.75 (reaction 29-30)	Estimated from o-xylene
APX4	Aerosol precursor APX4	0.489	Bandow, 1985
APX5	Aerosol precursor APX5	0.240	Bandow, 1985

XPM3	Aerosol product species 1	0.25	Estimated from products from o-xylene, Eusebi, 1991
XPM4	Aerosol product species 2	0.75	Estimated from products from o-xylene, Eusebi, 1991
RO2N	Operator RO2N	0.25	Estimated from products from o-xylene, Eusebi, 1991
XC	Balance extra carbon	0.271	SAPRC-99, Bandow, 1985

m-xylene

Reaction of m-xylene proceeds through either hydrogen abstraction, or addition of OH radical to the aromatic ring. Hydrogen abstraction accounts for 3.7 % (SAPRC 99) of the reaction, and occurs primarily at the substituent methyl groups. The main product of this reaction is benzaldehyde plus one carbon atom (BALD + 1XC), pathway 37.

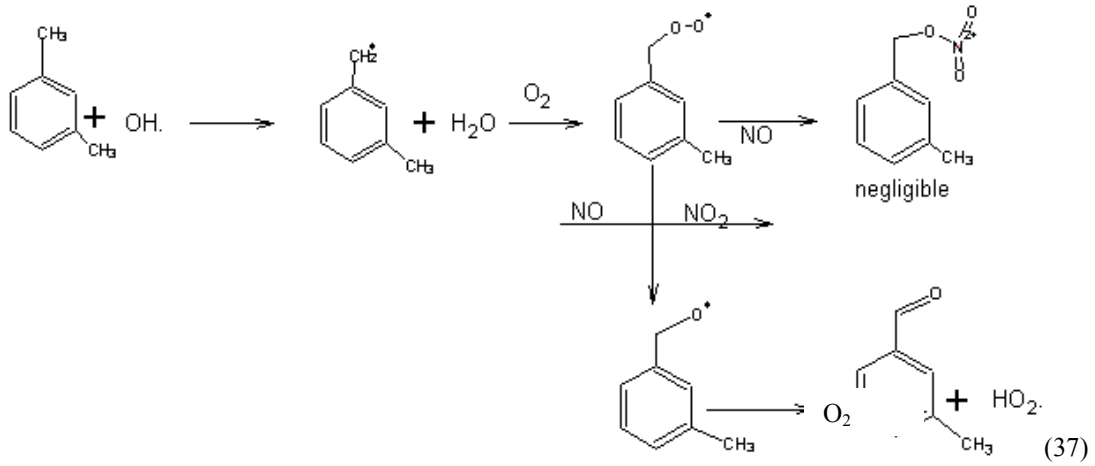

(37)

3.7%: M-XYLENE + OH. = BALD + 1XC + RO2R **Reaction 31**

When OH is added to the ring, the OH radicals add primarily to the ortho position of each side chain. Initial addition of OH radical to the aromatic can result in the gas phase product, cresol plus one carbon atom (CRES + 1XC), which accounts for 21 % of all reactions of o-xylene with OH radical (SAPRC 99).

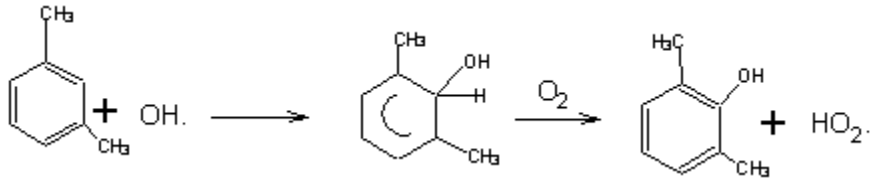

(38)

21%: M-XYLENE + OH. = CRES + HO2. + 1XC **Reaction 32**

Another reaction pathway that can occur following the formation of the OH-aromatic adduct is bridging of O_2 across the ring. The OH-O2- aromatic adduct further reacts with O_2 with conversion of NO to NO_2 and formation of HO_2 radical to generate ring cleavage products. The xylene-ring cleavage reactions produce 37.6% APX6, 18.8% APX7, and 18.8% APX8 (pathways 39-41), Bandow, 1985. Along with those aerosol precursors MGLY and GLY are also formed with yields of 56.4% and 18.8%, respectively (Bandow, 1985).

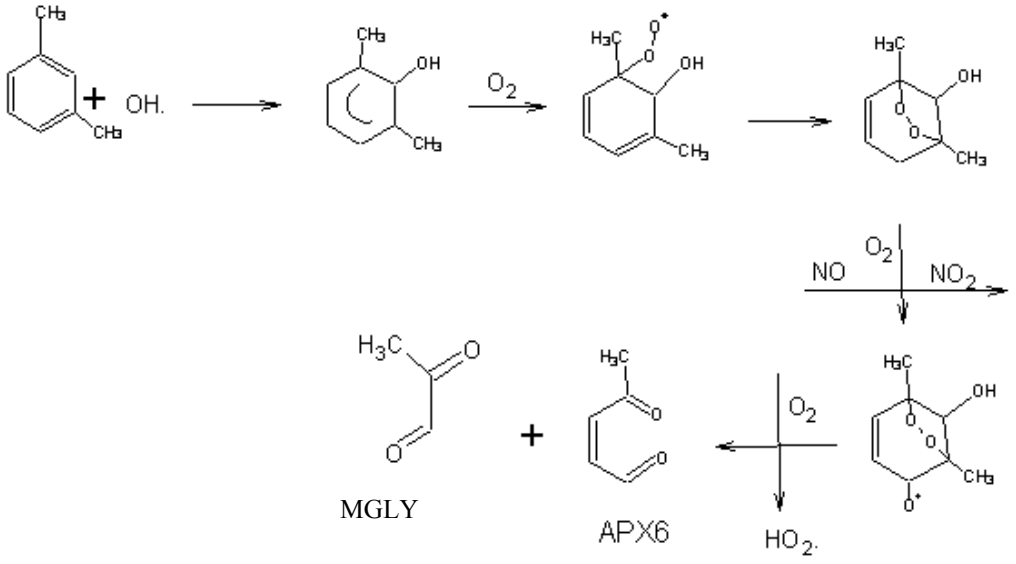

(39)

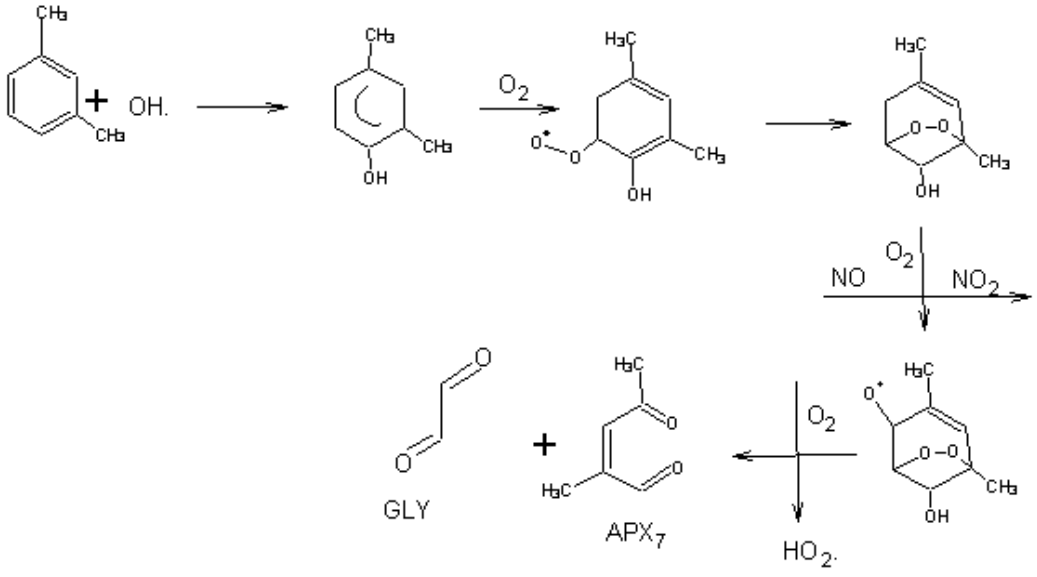

(40)

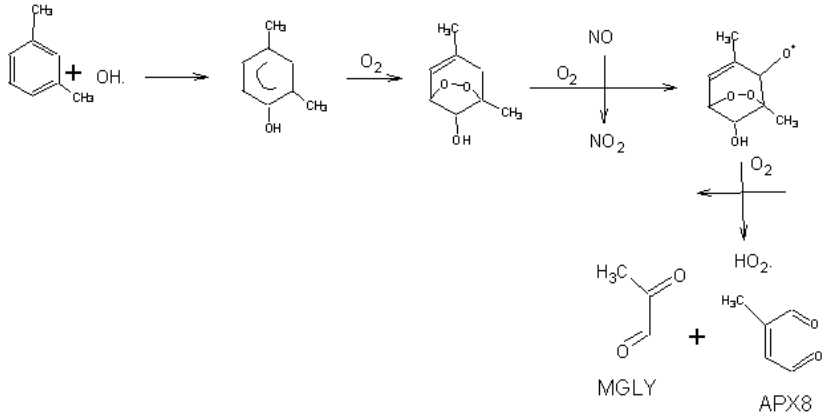

(41)

75.2 % M-XYLENE + OH. = 0.376APX6 +0.188APX7 + 0.188APX8 + 0.564MGLY + 0.188GLY + 0.752RO2R **Reaction 33**

Net: M-XYLENE + OH. = 0.21HO2. + 0.21CRES + 0.037BALD + 0.376APX6 +0.188APX7 + 0.188APX8 + 0.564MGLY + 0.188GLY + 0.789RO2R + 0.247XC **Reaction 34**

Aerosol precursors (APX6-APX8) react further with OH radicals through addition at the carbon double bond to produce two types of semivolatile products (XPM5 and XPM6), where XPM5 is a product with organonitrate group, and XPM6 is a product with carbonyl groups. Pathways 42a-44a and 42b-44b demonstrate the formation of XPM5 and XPM6, respectively. Yields of XPM5 (25%) and XPM6 (75%) were estimated from experimental results for o-xylene from Eusebi (1996).

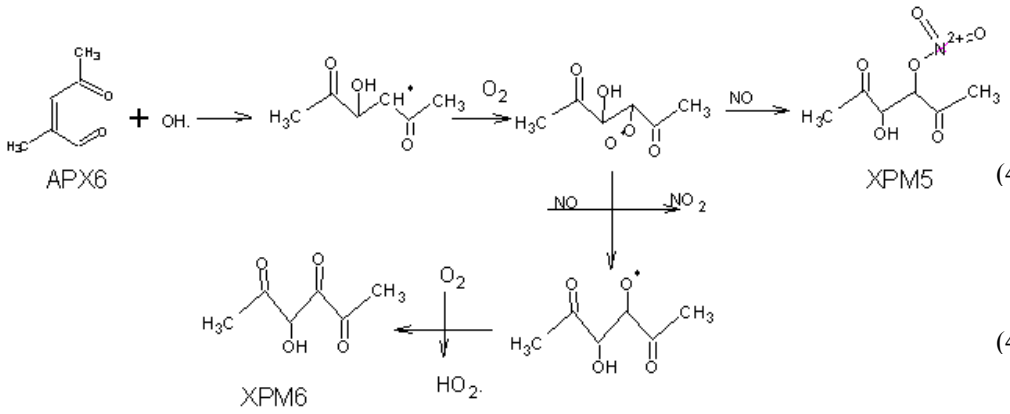

(42a)

(42b)

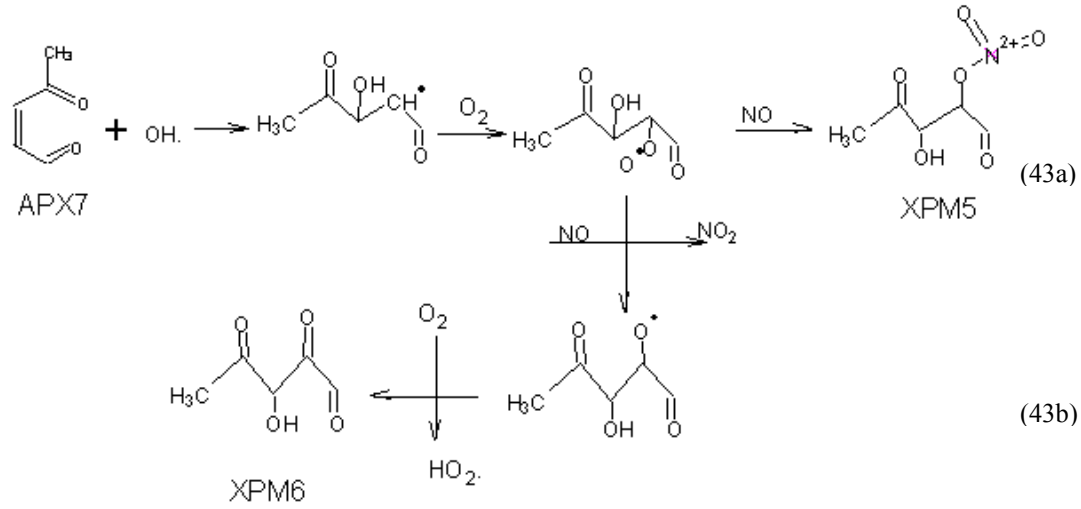

(43a)

(43b)

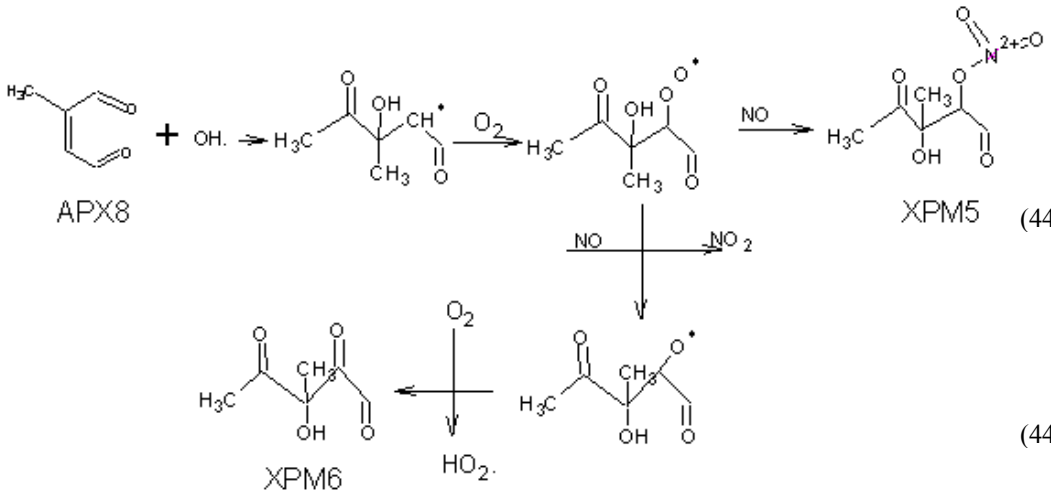

(44a)

(44b)

APX6 + OH. = 0.25XPM5 + 0.75XPM6 + 0.25RO2N + 0.75RO2R **Reaction 35**

APX7 + OH. = 0.25XPM5 + 0.75XPM6 + 0.25RO2N + 0.75RO2R **Reaction 36**

APX8 + OH. = 0.25XPM5 + 0.75XPM6 + 0.25RO2N + 0.75RO2R **Reaction 37**

Reactions 34-37 describe the formation of two types of semivolatile products from the oxidation reaction of p-xylene through two steps. The first step is the reaction of p-xylene with OH radical to form aerosol precursors, and the second step is the reaction of aerosol precursors with OH radical to produce semivolatile products. Table C5 summarizes stoichiometric coefficients in reactions 34-37, and cites sources of the data.

Table C.5: Kinetic parameters of m-xylene reactions with OH radical forming aerosol products and their source

Notations	Descriptions	Stoichiometric Coefficients (SC)	Source of SC
CRES	Cresol	0.21	SAPRC-99
BALD	Benzaldehyde	0.037	SAPRC-99
MGLY	Methylglyoxal	0.564	Bandow, 1985
GLY	Glyoxal	0.188	Bandow, 1985
HO2.	Hydroperoxy radical	0.21	SAPRC-99
RO2R	Operator RO2R	0.789(reaction 34) 0.75 (reaction 35-37)	Bandow, 1985 Estimated from o-xylene
APX6	Aerosol precursor APX6	0.376	Bandow, 1985
APX7	Aerosol precursor APX7	0.188	Bandow, 1985
APX8	Aerosol precursor APX8	0.188	Bandow, 1985
XPM5	Aerosol product species 1	0.25	Estimated from products from o-xylene, Eusebi, 1996
XPM6	Aerosol product species 2	0.75	Estimated from products from o-xylene, Eusebi, 1996
RO2N	Operator RO2N	0.25	Estimated from products from o-xylene, Eusebi, 1996
XC	Balance extra carbon	0.247	SAPRC-99, Bandow, 1985

Toluene

Similar to other aromatic precursors, the oxidation reaction of toluene primarily occurs via addition and abstraction by OH radical. The hydrogen abstraction accounts for approximately 11% of all reactions (Bandow, 1985). The reaction proceeds through the abstraction of hydrogen atom by OH radical to form H_2O , then the radical reacts further with O_2 and with conversion of NO to NO_2 and formation of HO_2 radical to produce benzaldehyde (BALD).

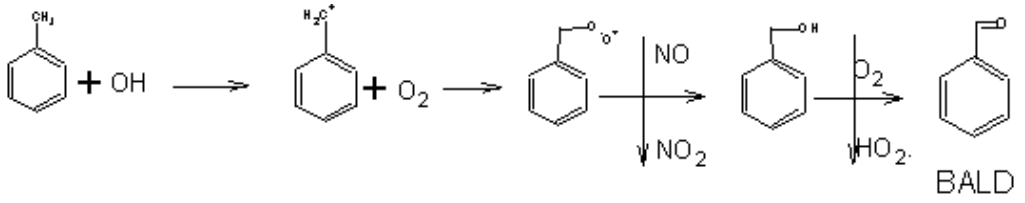

(45)

11%: TOLUENE + OH. = BALD + RO2R **Reaction 38**

When OH adds to the ring, the OH radicals add primarily to the ortho position. The addition of OH radical to toluene produces either cresol or nitrotoluene (NTOL), which accounts for 23.4 (SAPRC-99) and 25% (Bandow, 1985) of all reactions, respectively. While cresol is formed through the reaction of OH addition to toluene in the presence of O_2 to form HO_2 radical (pathway 46), nitrotoluene is generated via the addition of NO_2 to OH-aromatic adduct and the formation of H_2O (pathway 47).

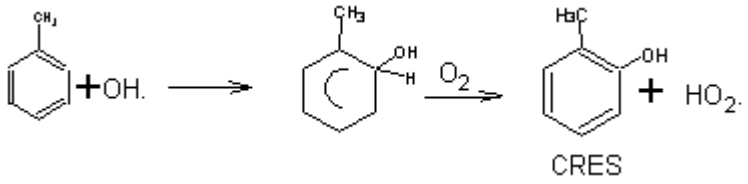

(46)

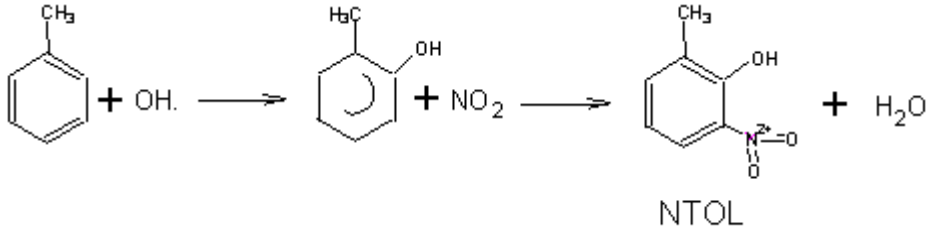

(47)

23.4%: TOLUENE + OH. = CRES + HO_2. **Reaction 39**

25.0%: TOLUENE + OH. = NBEN + H_2O – NO_2 + XC **Reaction 40**

The remainder of OH-aromatic ring adduct leads to the formation of ring-cleavage products. The OH-aromatic adduct reacts with O_2 to from bicyclo compounds, then with the abstraction of O atom by NO, alkoxyl-type radicals are formed. The alkoxyl-type radicals undergo hydrogen abstraction by O_2 with the formation of HO_2 radical, and the ring-cleavage product (denoted as aerosol precursors) are generated. Experimental results from Smith (1998) indicates that 23.8% of the addition of O_2 to the OH-aromatic adduct resuts in glyoxal and unsaturated dicrabonyl compound, denoted as APTO1 in this work, and 16.7% results in methylglyoxal and APTO2 (pathways 48 and 49).

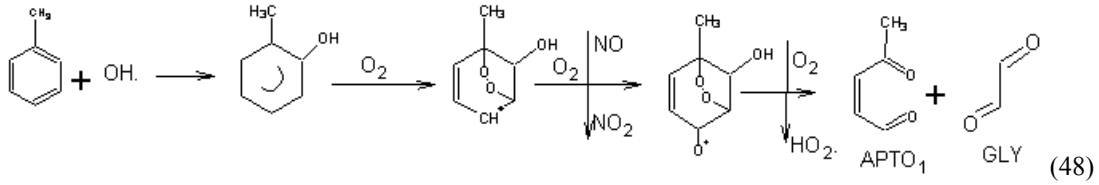

(48)

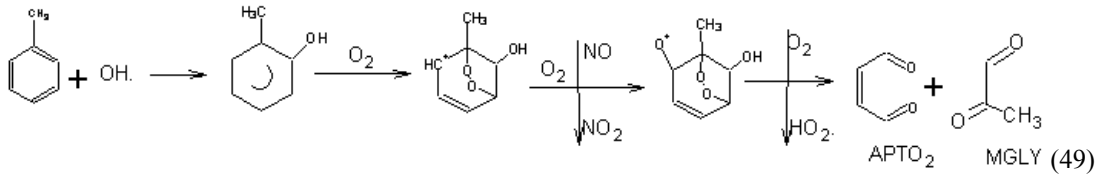

(49)

23.8%: TOLUENE + OH. = APTO1 + RO2R + GLY **Reaction 41**

16.7%: TOLUENE + OH. = APTO2 + MGLY + RO2R **Reaction 42**

Net: TOLUENE + OH. = 0.234CRES + 0.234HO_2. + 0.11BALD + 0.238APTO1 + 0.167APTO2 + 0.238GLY + 0.167MGLY + 0.515RO2R + 0.25H_2O + 0.25NBEN – 0.25NO_2 + 0.25XC **Reaction 43**

Aerosol precursors (APTO1 and APTO2) undergo on oxidation reaction with OH radical to form two types of semivolatile products (TOPM1 and TOPM2). Yields of TOPM1 (25%) and TOPM2 (75%) were estimated relatively from products for 1,3,5-trimethylbenzene from chamber experiements by Eusebi (1996). Reactions leading to formation of TOPM1 and TOPM2 are deplicted by reaction pathways 50a and 51a, and 50b and 51b, respectively.

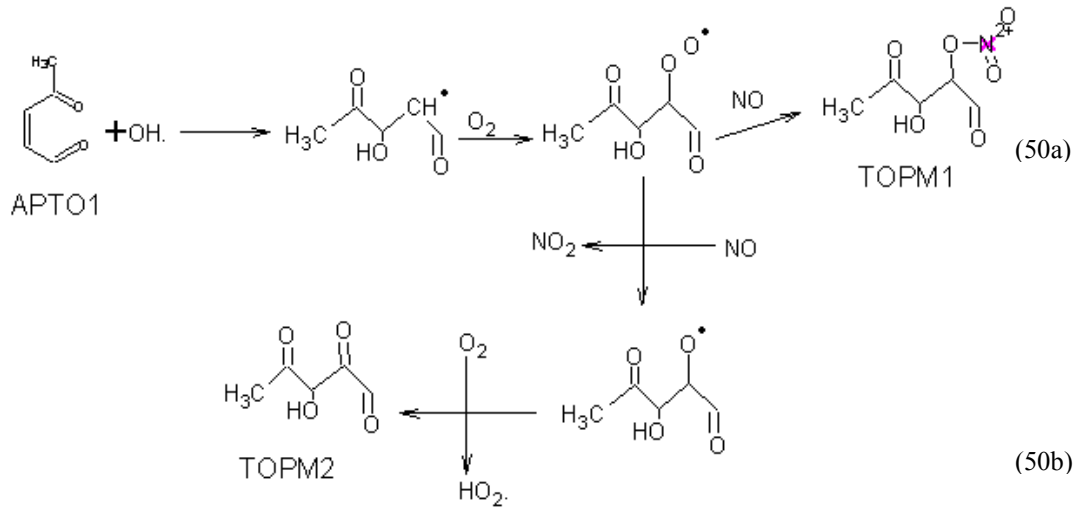

(50a)

(50b)

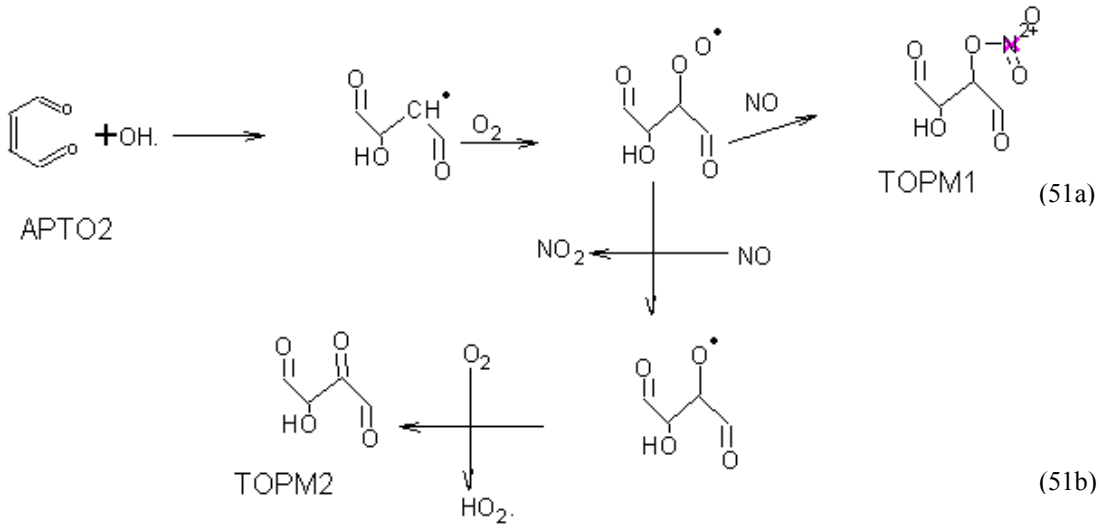

(51a)

(51b)

APTO1 + OH. = 0.25TOPM1 + 0.75TOPM2 +0.25RO2N + 0.75RO2R **Reaction 44**

APTO2 + OH. = 0.25TOPM1 + 0.75TOPM2 +0.25RO2N + 0.75RO2R **Reaction 45**

Reactions 43-45 show the formation of semivolatile products for toluene which undergo two oxidation steps with OH radical. The stoichiometric coefficients and sources of the data are summarized in Table C6.

Table C.6: Kinetic parameters of toluene reactions with OH radical forming aerosol products and their source

Notations	Descriptions	Stoichiometric Coefficients (SC)	Source of SC
CRES	Cresol	0.234	SAPRC-99
BALD	Benzaldehyde	0.11	Bandow, 1985
MGLY	Methylglyoxal	0.167	Bandow, 1985
GLY	Glyoxal	0.238	Bandow, 1985
HO2.	Hydroperoxy radical	0.234	SAPRC-99
H2O	Water	0.25	Bandow, 1985
NBEN	Nitrobenzene	0.25	Bandow, 1985
RO2R	Operator RO2R	0.515(reaction 43) 0.75 (reaction 44-45)	Bandow, 1985 Estimated from 1,3,5-trimethylbenzene
APTO1	Aerosol precursor APTO1	0.238	Smith, 1998
APTO2	Aerosol precursor APTO2	0.167	Smith, 1998
TOPM1	Aerosol product species 1	0.25	Estimated from 1,3,5-trimethylbenzene
TOPM2	Aerosol product species 2	0.75	Estimated from 1,3,5-trimethylbenzene
RO2N	Operator RO2N	0.25	Estimated from 1,3,5-trimethylbenzene
XC	Extra carbon	0.25	Bandow, 1985

Benzene

The photooxidation reaction of benzene predominantly occurs via the addition of OH radical. Experimental resutls from Bandow (1985) suggest that approximaetly 56.6% of all reactions result in nitrobenzene, 23.6% form phenol, and the remainder produce ring-cleavage products. The addition of NO_2 to the OH-aromatic adduct, followed by the abstraction of hydrogen by O_2 to form H_2O lead to the formation of nitrobenzene (pathway 52). Phenol is produced via the abstraction of hydrogen by molecular oxygen from the OH-aromatic adduct (pathway 53).

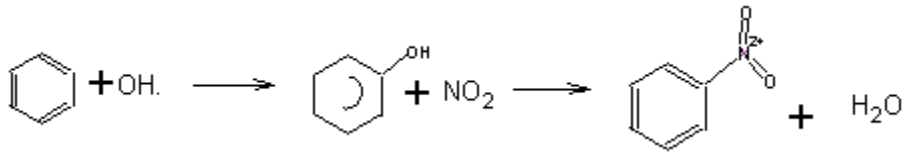

(52)

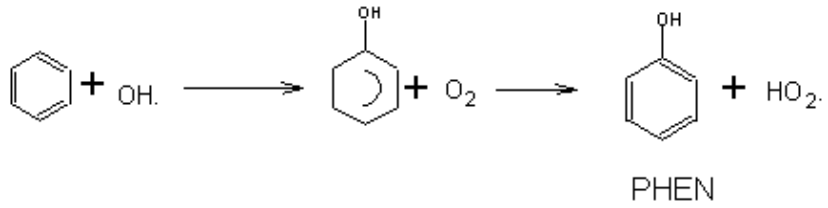

(53)

56.6%: Benzene + OH. = NBEN + H2O – NO2 **Reaction 46**

23.6%: Benzene + OH. = PHEN + HO2. **Reaction 47**

The remainder of OH-aromatic adduct reacts with O_2 to form on OH-O_2-aromatic adduct. As for toluene, the OH-O_2-aromatic adduct of benzene undergoes the cyclization reaction, with the conversion of NO to NO_2 and formation of HO_2 radical to produce a ring-cleavage product, denoted as APB1 (pathway 54). This pathway accounts for 20% of all reaction of benzene with OH radicals (Bandow, 1985

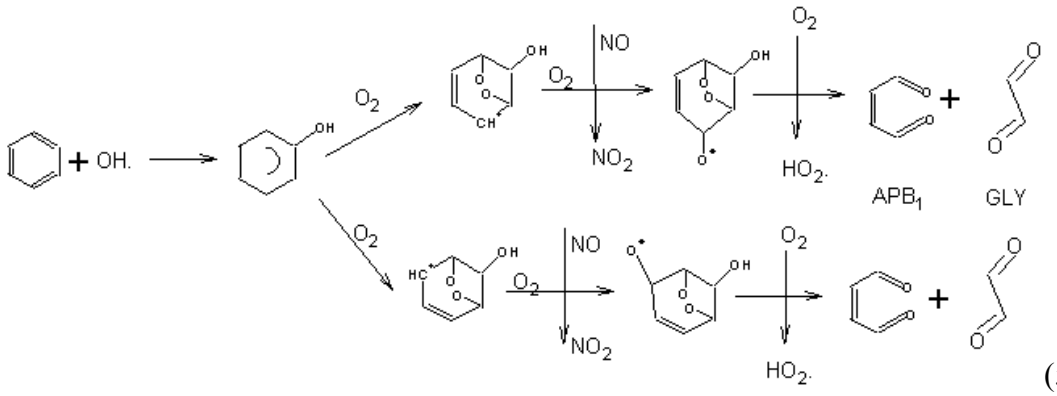

(54)

20%: BENZENE + OH. = APB1 + RO2R + GLY **Reaction 48**

Net: BENZENE + OH. = 0.236PHEN + 0.236HO2. +0.566NBEN + 0.566H2O – 0.566NO2 + 0.2APB1 +0.2GLY + 0.2RO2R **Reaction 49**

Aerosol precursor (APB1) further reacts with OH radical to produce two types of condensable products (BPM1 and BPM2). The product with an organonitrate functional group is presented by BPM1, while the product with hydroxy carbonyl functional groups is represented by BPM2. BPM1 is formed through the addition of NO to OH-O_2 aromatic adduct (pathway 55a). BPM2 is produced via the conversion of NO to NO_2 and the abstraction of hydrogen atom by O_2 from the OH-O-aromatic adduct (pathway 55b). Yields of BPM1 (25%) and BPM2 (75%) were relatively estimated from the products for 1,3,5-trimethylbenzene, which were obtained from chamber experiments (Eusebi, 1996).

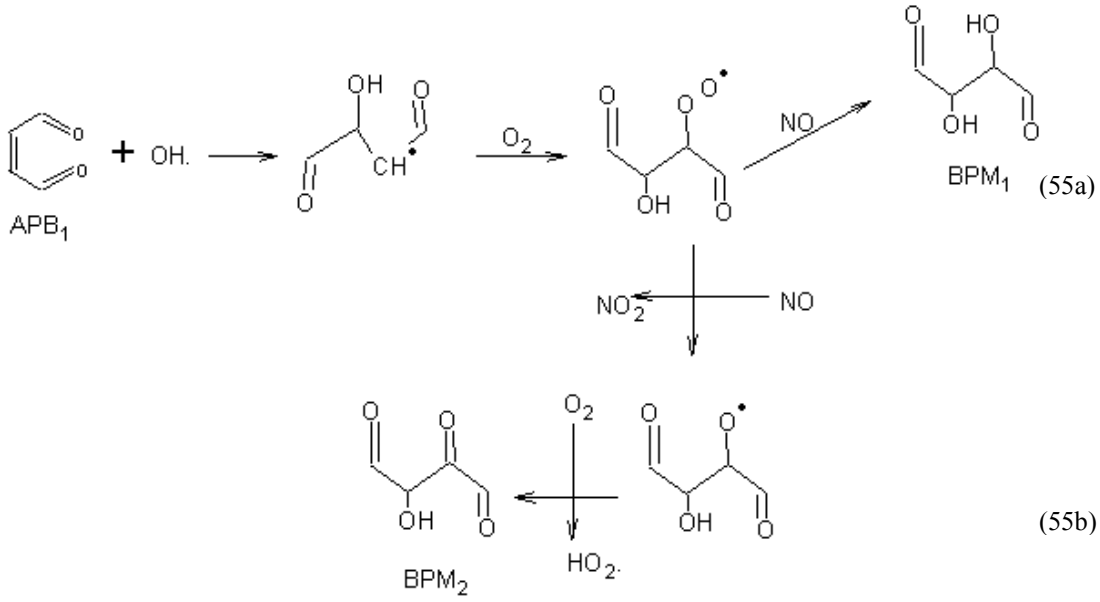

APB1 + OH. = 0.25BPM1 + 0.75BPM2 +0.25RO2R +0.75RO2N **Reaction 50**

The condensed mechainsims of formation of semivolatile products (BPM1 and BPM2) for benzene is expressed by reactions 49 and 50. Table C7 summarizes the stoichiometric coefficients and cites sources of the data in those reactions.

Table C.7: Kinetic parameters of benzene reactions with OH radical forming aerosol products and their source

Notations	Descriptions	Stoichiometric Coefficients (SC)	Source of SC
PHEN	Phenol	0.236	SAPRC-99
GLY	Glyoxal	0.20	Bandow, 1985
HO2.	Hydroperoxy radical	0.236	SAPRC-99
H2O	Water	0.566	Bandow, 1985
NBEN	Nitrobenzene	0.566	Bandow, 1985
RO2R	Operator RO2R	0.20(reaction 49) 0.75 (reaction 50)	Bandow, 1985 Estimated from 1,3,5-trimethylbenzene
APB1	Aerosol precursor APB1	0.20	Bandow, 1985
BPM1	Aerosol product species 1	0.25	Estimated from product for 1,3,5-trimethylbenzene, Eusebi, 1996

			1996
BPM2	Aerosol product species 2	0.75	Estimated from product for 1,3,5-trimethylbenzene,Eusebi, 1996
RO2N	Operator RO2N	0.25	Estimated from 1,3,5-trimethylbenzene, Eusebi, 1996

Ethylbenzene

Similar to toluene, the oxidation reactions of ethylbenzene primarily occur via the addition and abstraction by OH radical. The hydrogen abstraction accounts for approximately 11% of all reactions estimated from the yield of BALD for toluene, Bandow, 1985. The reaction proceeds through two possible pathways. The first pathway, hydrogen atom is abstracted by OH radical forming secondary radical and H_2O, then the secondary radical reacts further with O_2 and with coversion of NO to NO_2 and formation of HO_2 radical to produce benzaldehyde plus one carbon atom (BALD + 1XC) as shown in pathway 56. This pathway accounts for 5% of all reaction (estimated from toluene (Smith, 1998)).

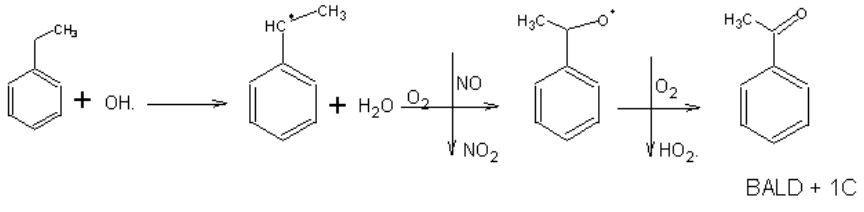

(56)

5%: C2-BENZ + OH. = BALD + 1XC + RO2R **Reaction 51**

The second possible pathway occurs through the abstaction of hydrogen atom to form a primary radical. The primary radical further oxidizes, along with conversion of NO to NO_2 and HO_2 radical formation to produce $C_6H_5C_2H_3O$. H atom from $C_6H_5C_2H_3O$ is then abstracted by OH radical to form $C_6H_5C_2H_2O^{\cdot}$ and H_2O. $C_6H_5C_2H_2O^{\cdot}$ undergoes decomposition to form $C_6H_5CH_2^{\cdot}$ by either two possible pathways as shown in the following figure. $C_6H_5CH_2^{\cdot}$ undergoes oxidization with the presence of NO to generate NO_2, HO_2 radical , and benzaldehyde (BALD). These reactions account for 6% of all reactions (estimated from toluene (Smith, 1998)), and are expressed by pathway 57.

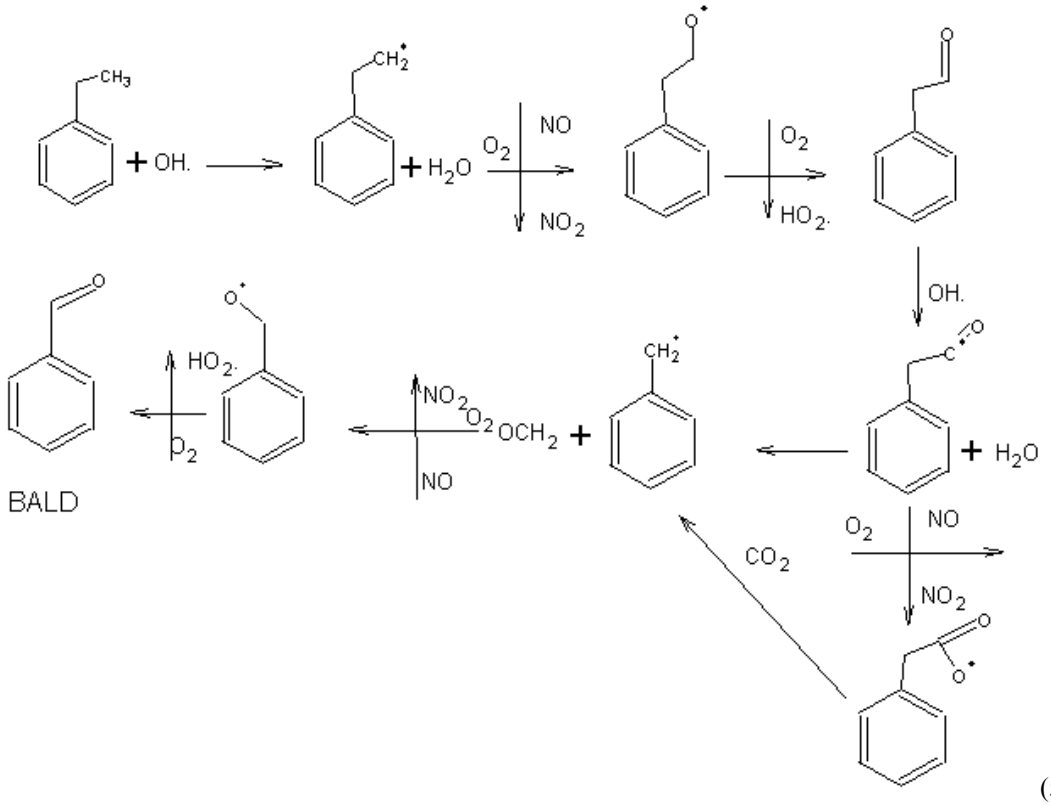

(57)

6%: C2-BENZ + 2OH. = BALD + 2RO2R + 0.5CO_2 + 0.5HCHO + 2H2O **Reaction 52**

When OH is added to the ring, the OH radicals add primarily to the ortho position. Initial reaction with OH radical addition can produce cresol plus one extra carbon atom (CRES + 1XC) or nitrobenzene plus two extra carbon atoms (NBEN + 2XC) which account for 19% (SAPRC-99) and 29.6% (estimated from toluene (Smith, 1998)), respectively.

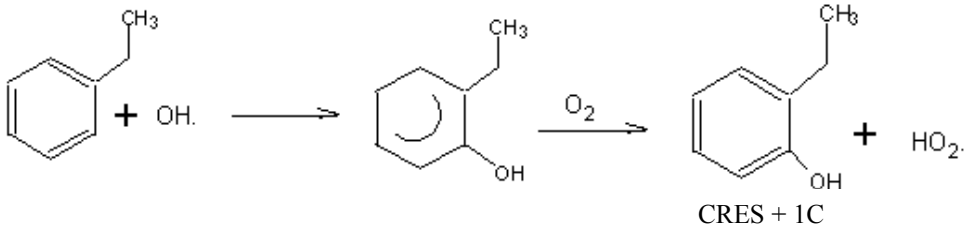

(58)

CRES + 1C

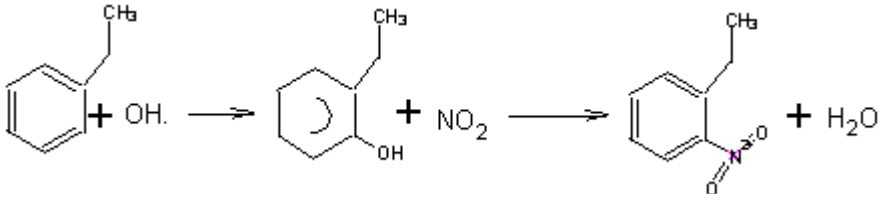

(59)

NBEN + 2C

19%: C2-BENZ + OH. = CRES +1XC + HO2· **Reaction 53**

29.6%: C2-BENZ + OH. = NBEN +2XC + H2O – NO2 **Reaction 54**

The remainder of the OH reactions further oxidizes produce ring-cleavage products. Ring-cleavage products are produced through four possible pathways (pathways 60-62). All of these four possible pathway proceed through similar steps, the abstraction of O atom by NO forming NO_2, and the abstraction of H atom by O_2. The cleavage

reactions produce 16.7% APEB1 and MGLY +1C, 15.8% APEB2, 7.9% of APEB3, and 23.7% GLY (estimated from toluene (Smith, 1998)).

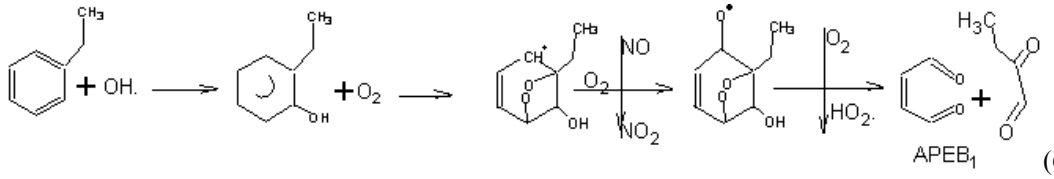

(60)

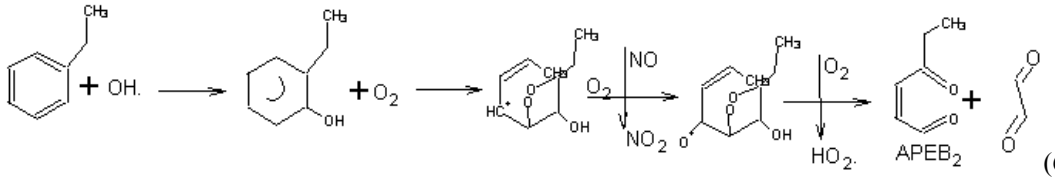

(61a)

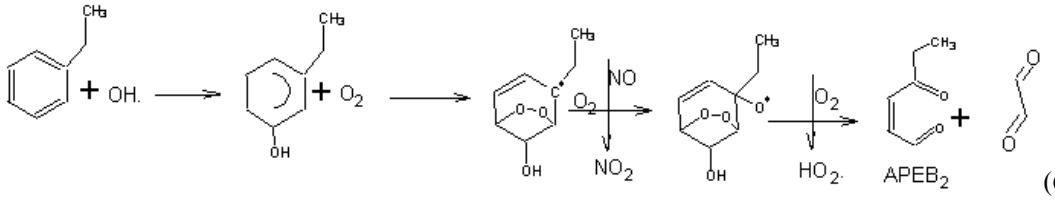

(61b)

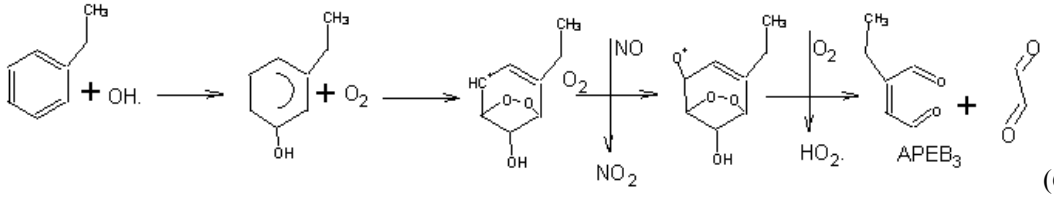

(62)

40.4 % C2-BENZ + OH. = 0.167APEB1 + 0.158APEB2 + 0.079APEB3 + 0.167MGLY + 0.167C + 0.237GLY + 0.404RO2R **Reaction 55**

Net: C2-BENZ + OH. = 0.11BALD + 0.03CO2 –0.06OH. + 0.03HCHO +0.19CRES + 0.296NBEN + 0.416H2O – 0.296NO2 + 0.19HO2· + 0.167APEB1 + 0.167MGLY + 0.158APEB2 + 0.079APEB3 + 0.237GLY +0.574RO2R + 0.999XC **Reaction 56**

Aerosol precursors (APEB1-APEB3) react further to generate two types of condensable products (EBPM1 and EBPM2). The addition of OH radical occurs at carbon double bonds to form dicarbonyl radicals. Dicarbonyl radicals either react with NO forming EBPM1 (pathway 63a-65a), or further oxidizes in the presence of NO to generate NO_2, HO_2 radical, and EBPM2 (pathway 63b-65b). Yields of EBPM1 (25%) and EBPM2 (75%) were estimated from semivolatile products for 1,3,5-trimethylbenzene.

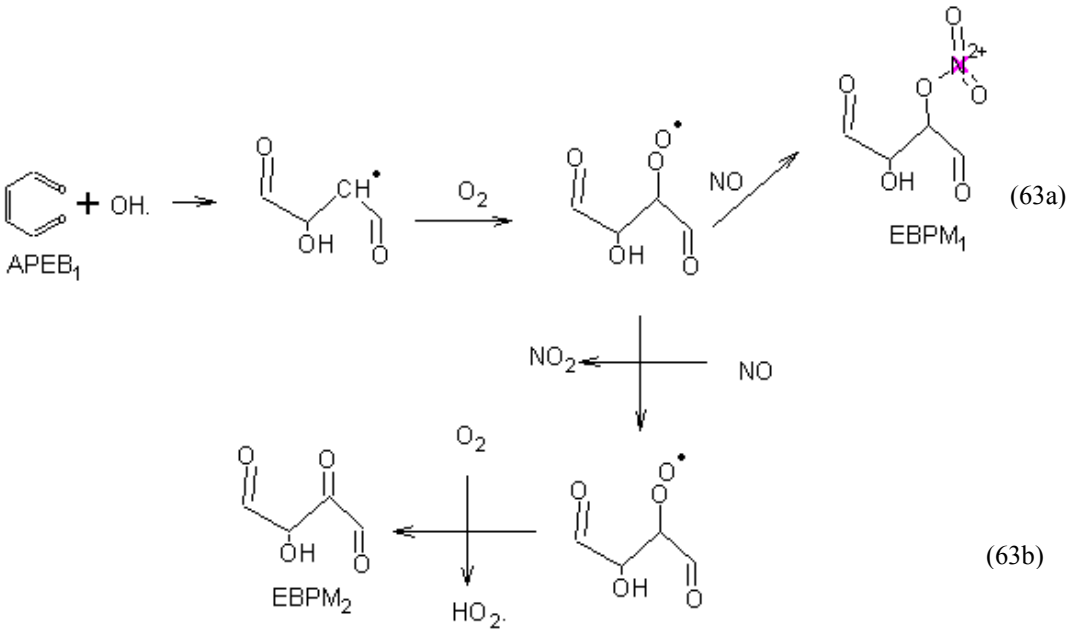

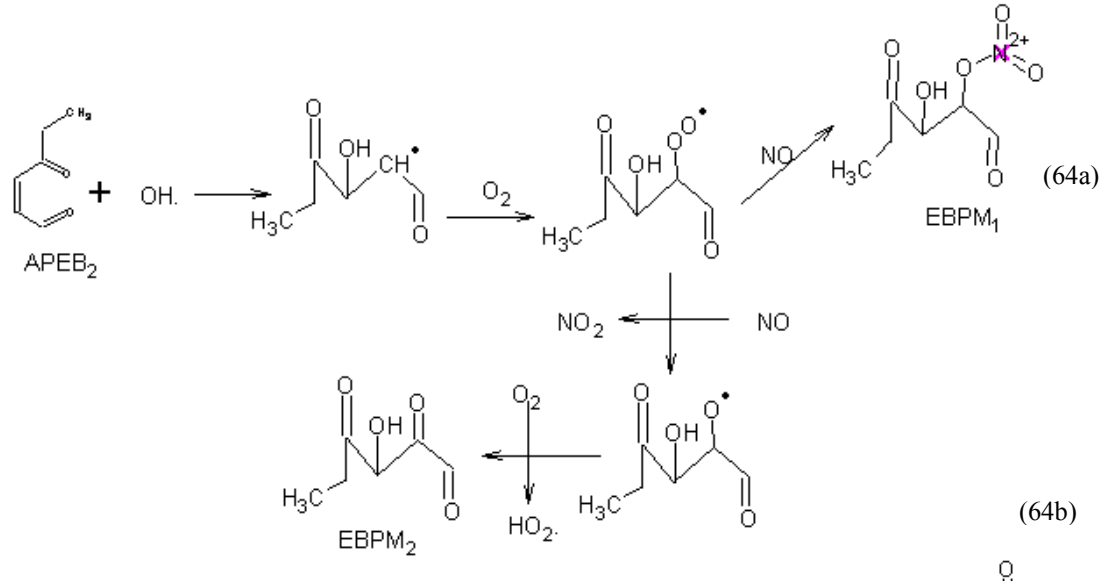

(64a)

(64b)

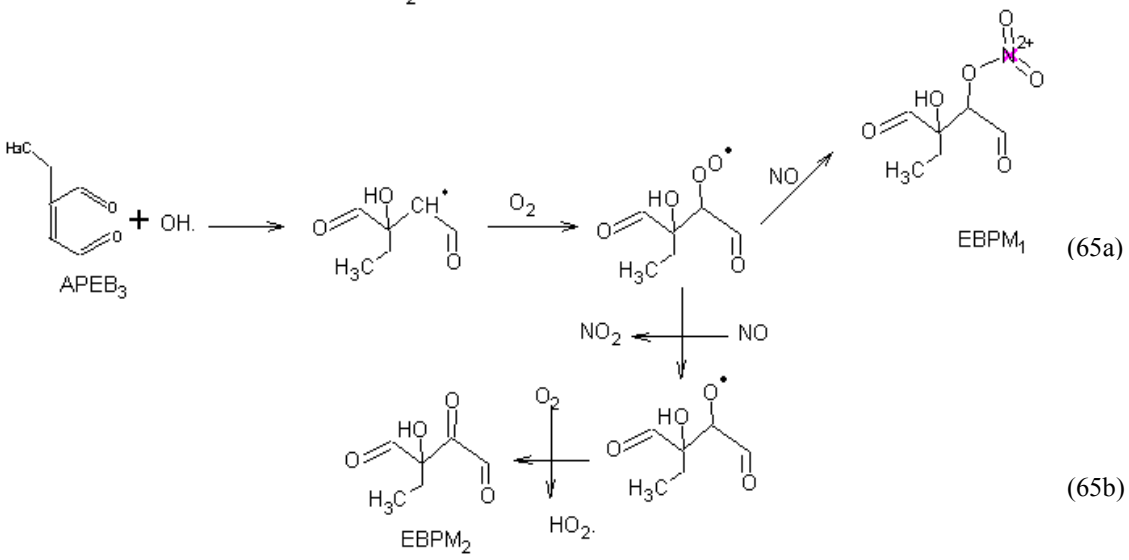

(65a)

(65b)

APEB1 + OH. = 0.25EBPM1 +0.75EBPM2 +0.25RO2N + 0.75RO2R **Reaction 57**

APEB2 + OH. = 0.25EBPM1 +0.75EBPM2 +0.25RO2N + 0.75RO2R **Reaction 58**

APEB3 + OH. = 0.25EBPM1 +0.75EBPM2 +0.25RO2N + 0.75RO2R **Reaction 59**

The stoichiometric coefficients in reactions 56-59 for ethyl benzene are summarized in Table 8.

Table C.8: Kinetic parameters of ethylbenzene reactions with OH radical forming aerosol products and their source

Notations	Descriptions	Stoichiometric Coefficients (SC)	Source of SC
CRES	Cresol	0.19	SAPRC-99
BALD	Benzaldehyde	0.11	Estimated from toluene, Bandow, 1985
MGLY	Methylglyoxal	0.167	Estimated from product for toluene, Smith 1998
GLY	Glyoxal	0.237	Estimated from product for toluene, Smith 1998
HO2.	Hydroperoxy radical	0.19	SAPRC-99
H2O	Water	0.416	Estimated from product for toluene, Smith 1998
NBEN	Nitrobenzene	0.296	Estimated from product for toluene, Smith 1998
CO2	Carbon dioxide	0.03	Estimated from product for toluene, Smith 1998
HCHO	Formaldehyde	0.03	Estimated from product for toluene, Smith 1998
RO2R	Operator RO2R	0.574(reaction 56)	Estimated from product for toluene, Smith 1998
		0.75 (reaction 57-59)	Estimated from 1,3,5-trimethylbenzene (Eusebi, 1996)
APEB1	Aerosol precursor APEB1	0.167	Estimated from product for toluene, Smith 1998
APEB2	Aerosol precursor APEB2	0.158	Estimated from product for toluene, Smith 1998
APEB3	Aerosol precursor APEB3	0.079	Estimated from product for toluene, Smith 1998
EBPM1	Aerosol product species 1	0.25	Estimated from product for 1,3,5-trimethylbenzene (Eusebi, 1996)
EBPM2	Aerosol product species 2	0.75	Estimated from product for 1,3,5-trimethylbenzene (Eusebi, 1996)
RO2N	Operator RO2N	0.25	Estimated from 1,3,5-trimethylbenzene (Eusebi, 1996)
XC	Balance carbon atom	0.999	SAPRC-99

n-propylbenzene

The oxidation reactions of n-propylbenzene are primarily initiated by OH radical. Reaction can either proceed through the addition of OH to the aromatic ring or the abstraction of an H atom by OH radical. As for the reactions for ethylbenzene, the abstraction of H atom by OH radical for n-propylbenzene can occur via two possible pathways. In the first pathway, the abstraction can occur at the carbon adjacent to the aromatic ring, then oxidation occurs in the presence of NO to form benzaldehyde plus two extra carbon atoms (BALD + 2XC) (pathway 66). Yiled of this pathway (5%) was estimated from that for toluene (Smith, 1998).

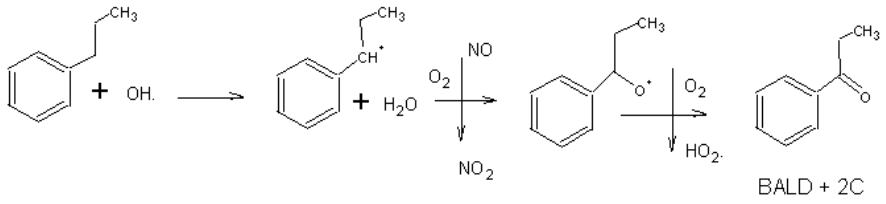

(66)

5%: N-C3-BEN + OH. = BALD + 2XC + RO2R **Reaction 60**

The second pathway for the abstraction proceeds similary to that for ethylbenzene. H atom at the methyl substituent group is abstracted by OH radical. The oxidization then occurs in the presence of NO to form NO_2, HO_2 radical, and $C_6H_5C_3H_5O$. The abstraction of H atom from carboxylic acid group by OH radical occurs, followed by the decomposition to form either CO_2 or OCH_2 with polysubstituent-aromatic radical. The polysubstituent-aromatic radical undergoes oxidization in the presence of NO to form NO_2, HO_2 radical, and $C_6H_5C_2H_3O^{\cdot}$ The consecutive reactions of H atom

abstraction, decomposition, and the oxidization then occur again to finally form benzaldehyde. Pathway 67 elaborates the steps of reactions. Yield of this pathway (6%) was estimated from that for toluene (Smith, 1998).

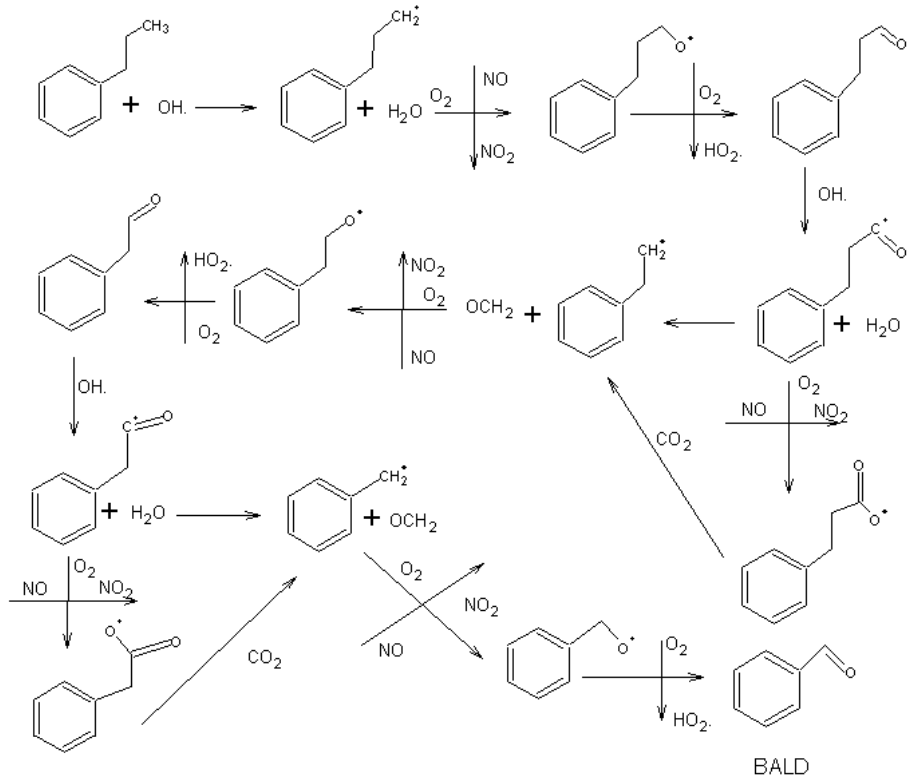

(67)

6%: N-C3-BEN + OH. = BALD + 3RO2R + CO2 + HCHO - 2OH.+ 3H2O

Reaction 61

When OH adds to the ring, the OH radicals add primarily to the ortho position. Initial reaction with OH radical addition can produce cresol plus two extra carbon atoms (CRES + 2XC) or nitrobenzene plus three extra carbon atoms (NBEN + 3XC) which account for 19% (SAPRC-99) and 29.6% (estimated from toluene (Smith, 1998)), respectively.

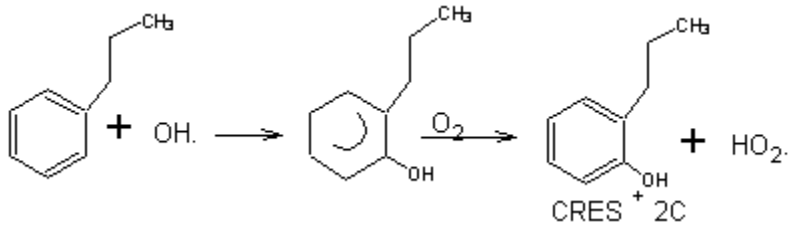

(68)

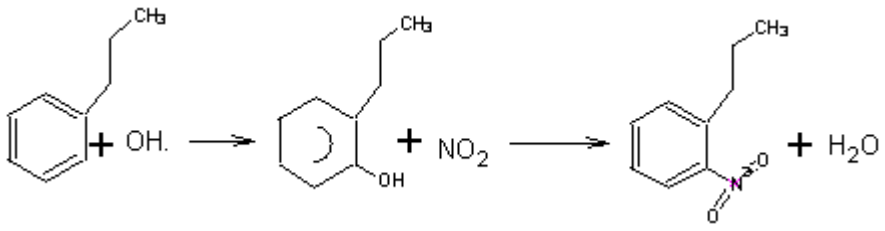

(69)

19%: N-C3-BEN + OH. = CRES + 2XC + HO2. **Reaction 62**

29.6%: N-C3-BEN + OH. = NBEN + 3XC + H2O – NO2 **Reaction 63**

The remainder of the OH additional reaction further oxidizes producing ring-cleavage products. Ring-cleavage products are produced through four possible pathways (pathways 70-72). All of these four possible pathway proceed through two similar steps, the abstraction of O atom by NO forming NO_2, and the abstraction of H atom by O_2. The cleavage reactions produce each 16.7% of APPB1 and MGLY + 2XC, 15.8% of APPB2, 7.9% of APPB3, and 23.7% GLY (relatively estimated from toluene (Smith, 1998)).

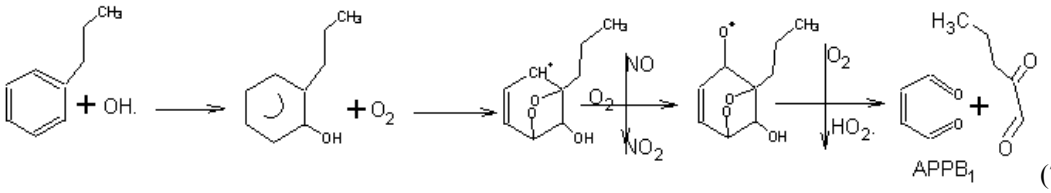

(70)

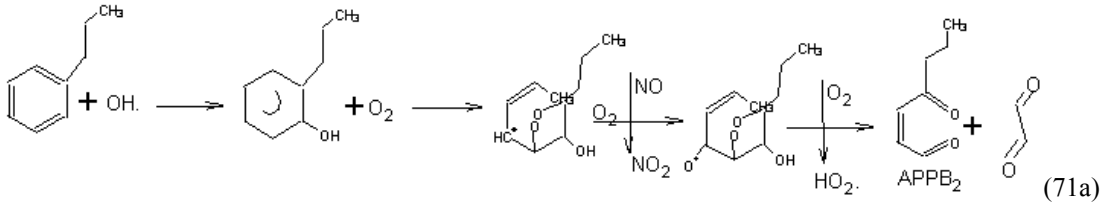

(71a)

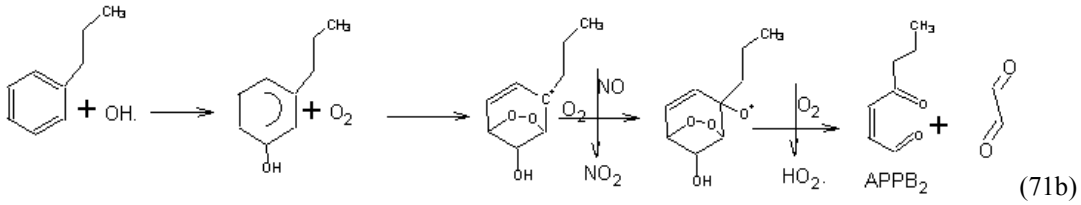

(71b)

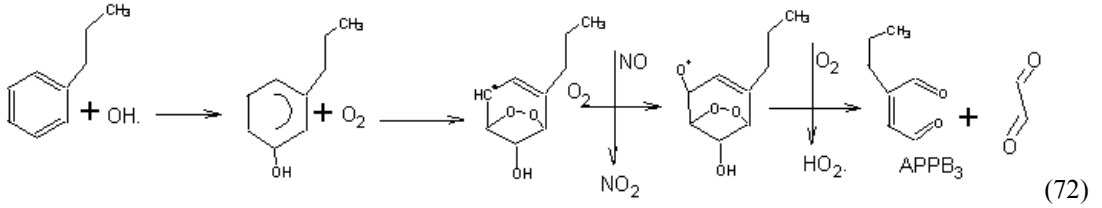

(72)

N-C3-BEN + OH. = 0.167APPB1 + 0.167MGLY + 0.167(2XC) + 0.158APPB2 + 0.079APPB3 + 0.238GLY + 0.404RO2R **Reaction 64**

Net: N-C3-BEN + OH. = 0.11BALD + 0.06CO2 + 0.06HCHO – 0.12OH. + 0.19CRES + 0.19HO2. + 0.296NBEN - 0.296NO2 +0.167APPB1 + 0.158APPB2 + 0.079APPB3 + 0.238GLY + 0.634RO2R + 0.476H2O + 1.702XC + 0.167MGLY **Reaction 65**

Aerosol precursors (APPB1-APPB3) react further with OH radical to form two types of condensable products (PBPM1 and PBPM2). PBPM1 is a product with organonitrate group, PBPM2 is product with hydroxy carbonyl groups. Reactions leading to formation of PBPM1 and PBPM2 from aerosol precursors are shown in

pathways 73-75. Yields of PBPM1 (25%) and PBPM2 (75%) were estimated from those for 1,3,5-trimethylbenzene, obtained from chamber experiments (Eusebi, 1996).

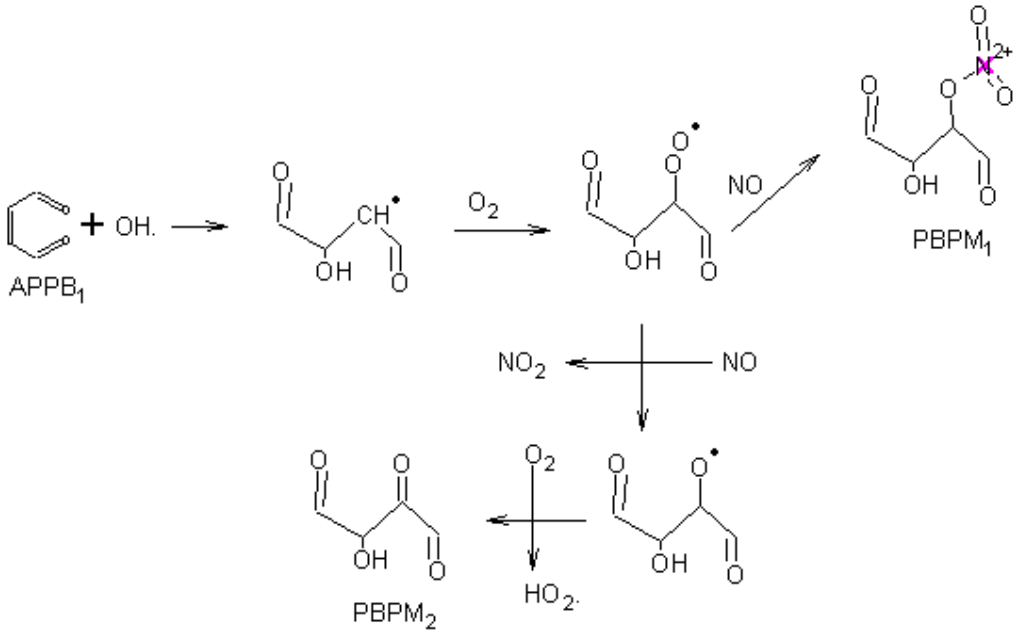

(73a)

(73b)

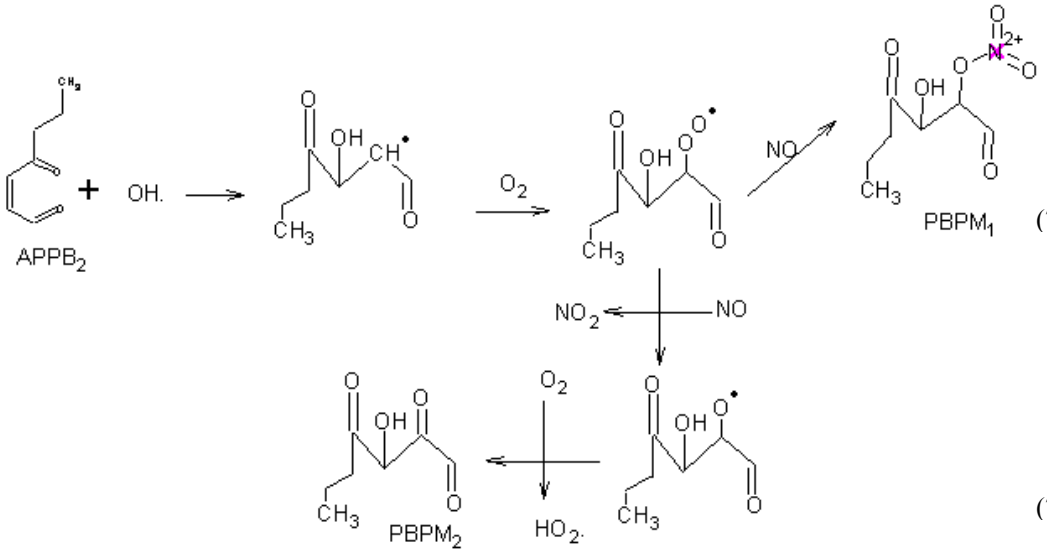

(74a)

(74b)

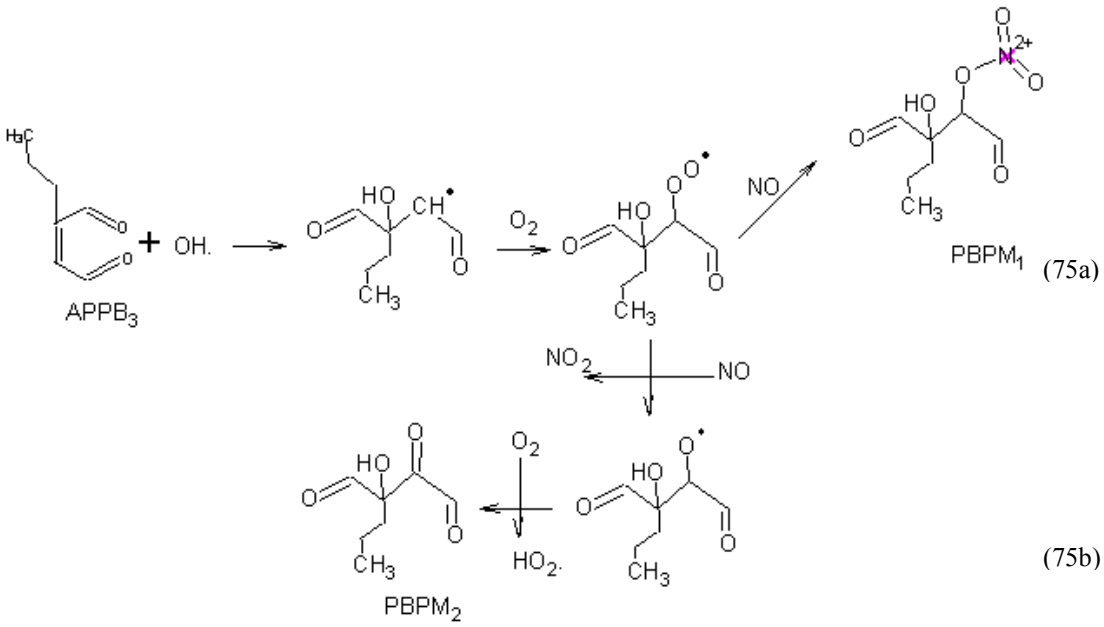

APPB1 +OH. = 0.25PBPM1 +0.75PBPM2 +0.25RO2N + 0.75RO2R **Reaction 66**

APPB2 +OH. = 0.25PBPM1 +0.75PBPM2 +0.25RO2N + 0.75RO2R **Reaction 67**

APPB3 +OH. = 0.25PBPM1 +0.75PBPM2 +0.25RO2N + 0.75RO2R **Reaction 68**

The stoichiometric coefficients and sources of the data in reactions 65-68 are summarized in Table 9.

Table C.9: Kinetic parameters of n-propylbenzene reactions with OH radical forming aerosol products and their source

Notations	Descriptions	Stoichiometric Coefficients (SC)	Source of SC
CRES	Cresol	0.19	SAPRC-99
BALD	Benzaldehyde	0.11	Estimated from toluene, Bandow, 1985
MGLY	Methylglyoxal	0.167	Estimated from product for toluene, Smith 1998
GLY	Glyoxal	0.238	Estimated from product for toluene, Smith 1998
HO2.	Hydroperoxy radical	0.19	SAPRC-99
H2O	Water	0.476	Estimated from product

			for toluene, Smith 1998
NBEN	Nitrobenzene	0.296	Estimated from product for toluene, Smith 1998
CO2	Carbon dioxide	0.06	Estimated from product for toluene, Smith 1998
HCHO	Formaldehyde	0.06	Estimated from product for toluene, Smith 1998
RO2R	Operator RO2R	0.634(reaction 65)	Estimated from product for toluene, Smith 1998
		0.75 (reaction 66-68)	Estimated from 1,3,5-trimethylbenzene
APPB1	Aerosol precursor APPB1	0.167	Estimated from product for toluene, Smith 1998
APPB2	Aerosol precursor APPB2	0.158	Estimated from product for toluene, Smith 1998
APPB3	Aerosol precursor APPB3	0.079	Estimated from product for toluene, Smith 1998
PBPM1	Aerosol product species 1	0.25	Estimated from product for 1,3,5-trimethylbenzene
PBPM2	Aerosol product species 2	0.75	Estimated from product for 1,3,5-trimethylbenzene
RO2N	Operator RO2N	0.25	Estimated from toluene, Eusebi 1996
XC	Balance carbon atom	1.702	SAPRC-99

Isopropylbenzene

Photochemical reactions of iso-propylbenzene leading to the formation of semivolatile products are similar to those for n-propylbenzene. The oxidation is initiated by OH radical. Reaction can either proceed through the addition of OH to aromatic ring or the abstraction of H atom by OH radical. The abstractions predominantly occur at either one of the methyl groups, then undergoes oxidation with the conversion of NO to NO_2 and formation of HO_2 radical forming $C_6H_5C_3H_5O$. The abstraction of H atom from the carbonyl group by OH radical occurs again. The

product from this reaction then proceeds through the consecutive reactions of decomposition generating CO_2, and oxidization in the presence of NO to produce NO_2, HO_2 radical, and benzaldehyde plus one extra carbon atom (BALD +1XC). Yield of this pathway (11%) was relatively estimated from that for toluene (Smith, 1998).

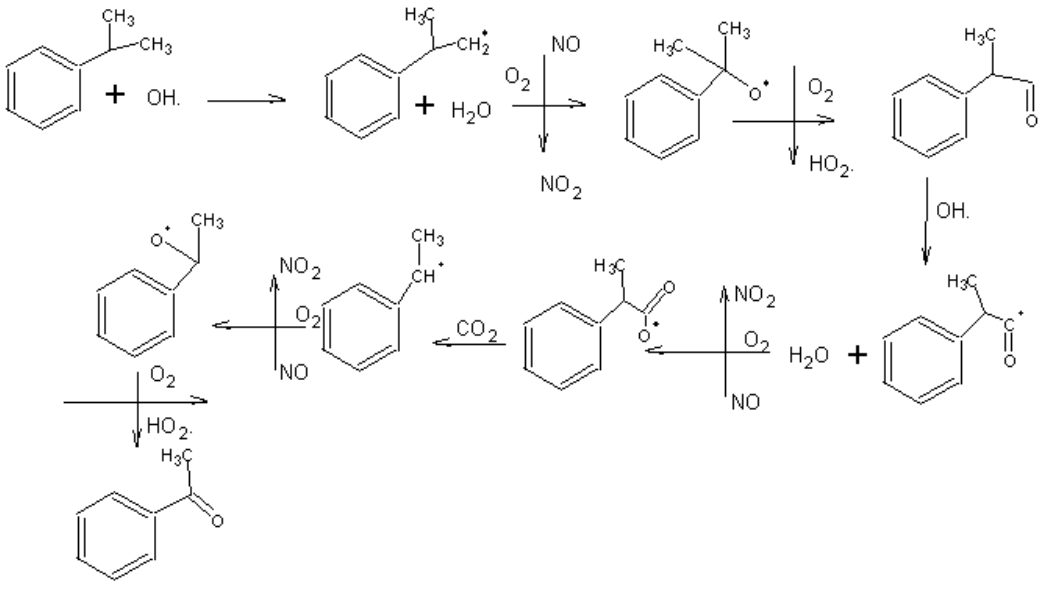

(76)

11%: I-C3-BEN + OH. = BALD + 1XC + 2RO2R + CO2 – OH. + 2H2O **Reaction 69**

The addition of OH radicals to the aromatic ring primirily occurs at the ortho position. Initial reaction of iso-propylbenzene with OH radical addition can produce cresol plus two extra carbon atoms (CRES + 2XC) or nitrobenzene plus three extra carbon atoms (NBEN + 3XC) which account for 19% (SAPRC-99) and 29.6% (estimated from toluene (Smith, 1998)), respectively.

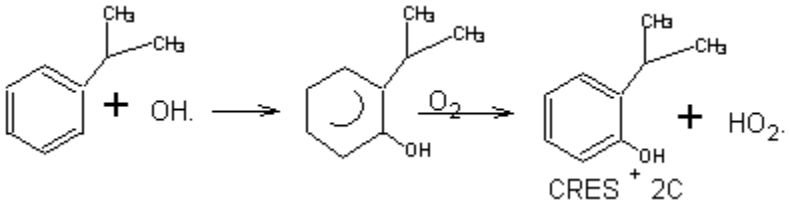

(77)

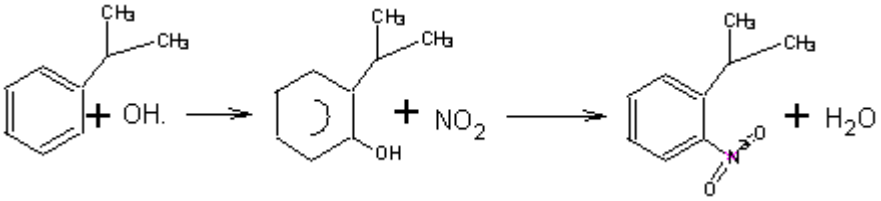

(78)

19%: I-C3-BEN + OH. = CRES + 2XC + HO2. **Reaction 70**

29.6%: I-C3-BEN + OH. = NBEN + 3XC + H2O – NO2 **Reaction 71**

Another reaction pathway that can occur following the formation of the OH-aromatic adduct is bridging of O_2 across the ring, leading to ring cleavage reactions. Ring-cleavage products are produced through four possible pathways (pathways 79-81). All of these four possible pathways proceed through two similar steps, the abstraction of O atom by NO forming NO_2, and the abstraction of H atom by O_2. The cleavage reactions produce 16.7% APB2 and MGLY + 2XC, 15.8% APB3, 7.9% APB4, and 23.7% GLY (estimated from toluene (Smith, 1998)).

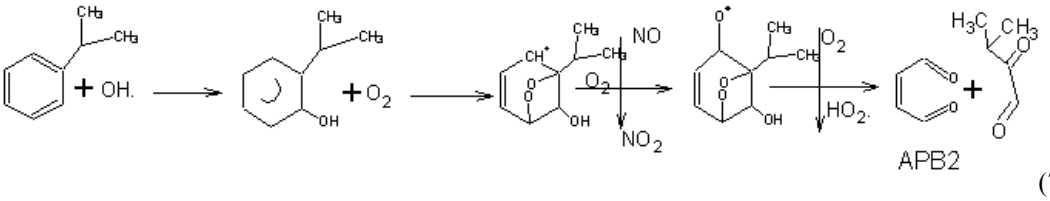

(79)

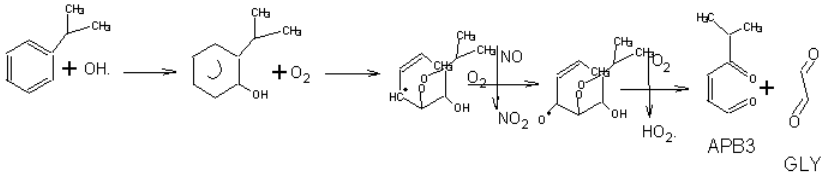

(80a)

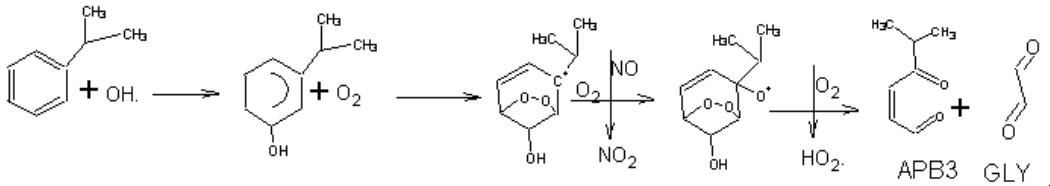

(80b)

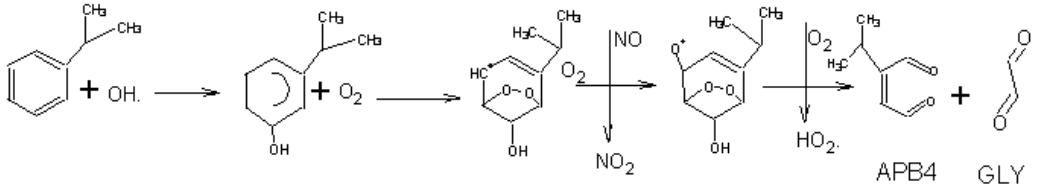

(81)

40.4 % I-C3-BEN + OH. = 0.167APB2 + 0.158APB3 + 0.079APB4 + 0.167MGLY + 0.334XC + 0.404RO2R **Reaction 72**

Net: I-C3-BEN + OH. = 0.11BALD + 0.11CO2 – 0.11OH. + 0.19CRES + 0.19HO2. + 0.167APB2 + 0.167MGLY +0.158APB3 + 0.079APB4 + 0.237GLY + 0.624RO2R – 0.296NO2 + 0.516H2O + 1.712XC + 0.296NBEN **Reaction 73**

Aerosol precursors (APB2-APB4) react further with OH radical to form two types of condensable products (BPM3 and BPM4). BPM3 is a product with an organonitrate group, BPM4 is product with hydroxy carbonyl groups. Reactions leading to formation of BPM3 and BPM4 from aerosol precursors are shown in pathways 82-84. Yields of PBPM1 (25%) and PBPM2 (75%) were relatively estimated from those for 1,3,5-trimethylbenzene, obtained from chamber experiments (Eusebi, 1996).

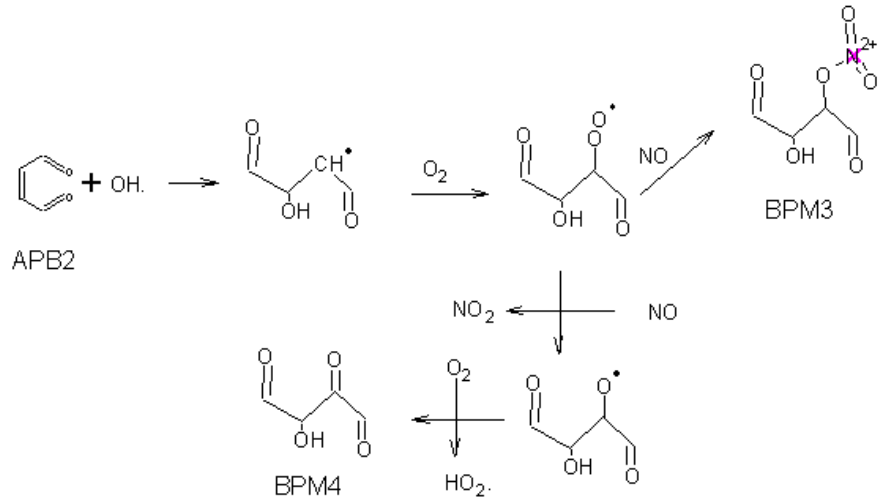

(82a)

(82b)

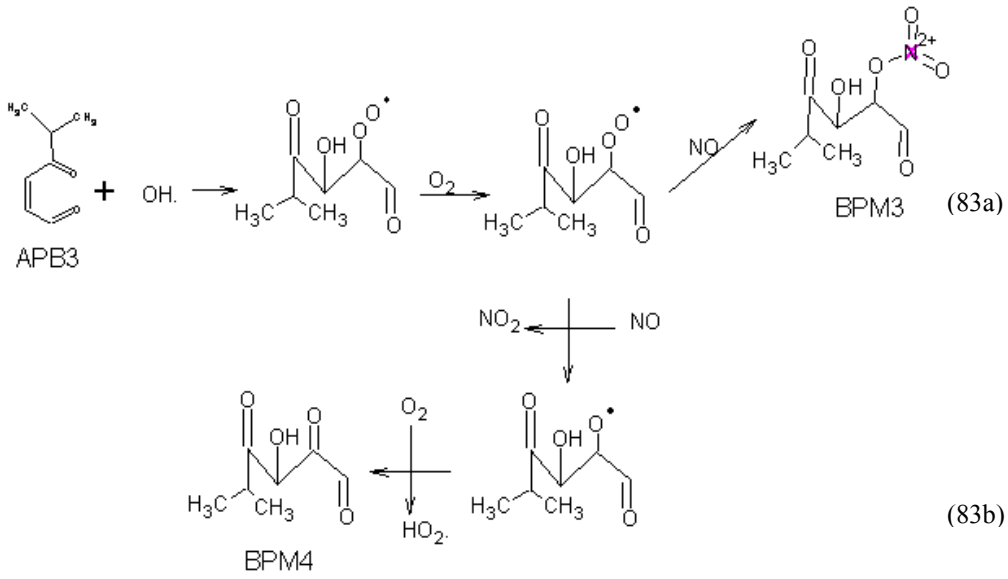

(83a)

(83b)

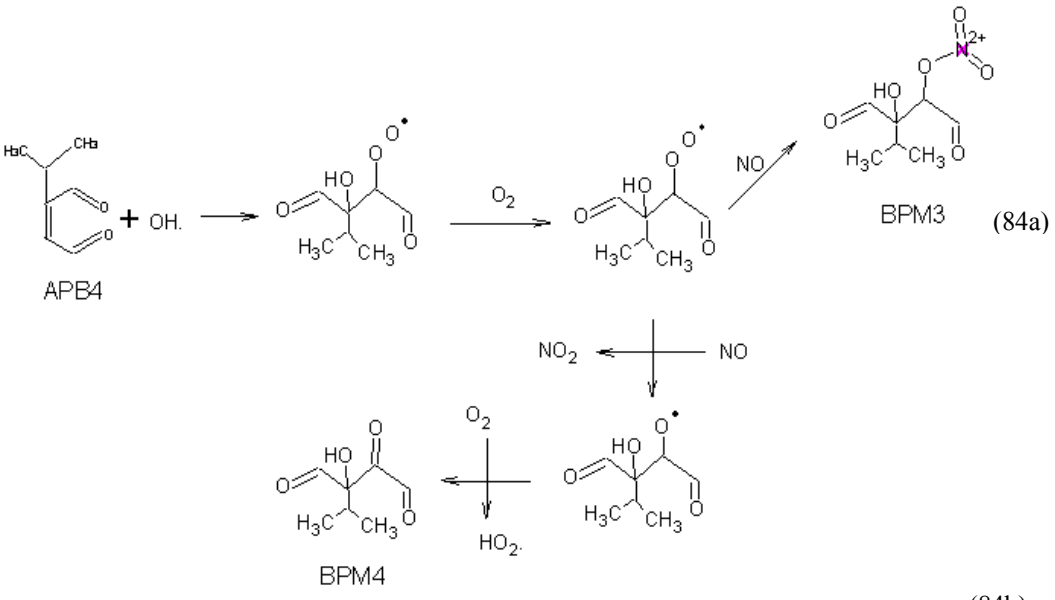

(84a)

(84b)

APB2 + OH. = 0.25BPM3 +0.75BPM4 +0.25RO2N + 0.75RO2R **Reaction 74**

APB3 + OH. = 0.25BPM3 +0.75BPM4 +0.25RO2N + 0.75RO2R **Reaction 75**

APB4 + OH. = 0.25BPM3 +0.75BPM4 +0.25RO2N + 0.75RO2R **Reaction 76**

Reactions 73-76 show the mechanistic models leading to SOA formation for iso-propylbenzene which proceed via two steps, similar to other aromatic precursors. Table C10 lists stoichiometric coefficients in reactions 73-76, and cite sources of the data.

Table C.10: Kinetic parameters of iso-propylbenzene reactions with OH radical forming aerosol products and their source

Notations	Descriptions	Stoichiometric Coefficients (SC)	Source of SC
CRES	Cresol	0.19	SAPRC-99
BALD	Benzaldehyde	0.11	Estimated from toluene, Bandow, 1985
MGLY	Methylglyoxal	0.167	Estimated from product for toluene, Smith 1998
GLY	Glyoxal	0.237	Estimated from product for toluene, Smith 1998

HO2.	Hydroperoxy radical	0.19	SAPRC-99
H2O	Water	0.516	Estimated from product for toluene, Smith 1998
NBEN	Nitrobenzene	0.296	Estimated from product for toluene, Smith 1998
CO2	Carbon dioxide	0.11	Estimated from product for toluene, Smith 1998
RO2R	Operator RO2R	0.624(reaction 73)	Estimated from product for toluene, Smith 1998
		0.75 (reaction 74-76)	Estimated from 1,3,5-trimethylbenzene
APB2	Aerosol precursor APB2	0.167	Estimated from product for toluene, Smith 1998
APB3	Aerosol precursor APB3	0.158	Estimated from product for toluene, Smith 1998
APB4	Aerosol precursor APB4	0.079	Estimated from product for toluene, Smith 1998
BPM3	Aerosol product species 1	0.25	Estimated from product for 1,3,5-trimethylbenzene
BPM4	Aerosol product species 2	0.75	Estimated from product for 1,3,5-trimethylbenzene
RO2N	Operator RO2N	0.25	Estimated from 1,3,5-trimethylbenzene
XC	Balance carbon atom	1.712	SAPRC-99

Sec-butylbenzene

Photooxidation reactions of sec-butylbenzene are initiated by OH radical. Reactions either occur via addition or abstraction. Abstraction of H atom by OH radical can proceed through two possible pathways. In the first pathway, H atom at one of the four of alkyl groups is abstracted by OH radical, then oxidation occurs with conversion of NO to NO_2 and formation of HO_2 radical forming $C_6H_5C_4H_7O$. The abstraction of H atom from carbonyl group of $C_6H_5C_4H_7O$ by OH radical occurs again. The product from this reaction then proceeds through consecutive reactions of

decomposition producing CO_2, and oxidization in the presence of NO to produce NO_2, HO_2 radical, and $C_6H_5C_3H_5O$. Consecutive reactions of H atom abstraction, decomposition, and oxidation are repeated again to produce benzaldehyde plus one extra carbon atom (BALD +1XC), pathway 85. Yield of this pathway (5%) was estimated from that for toluene (Smith, 1998).

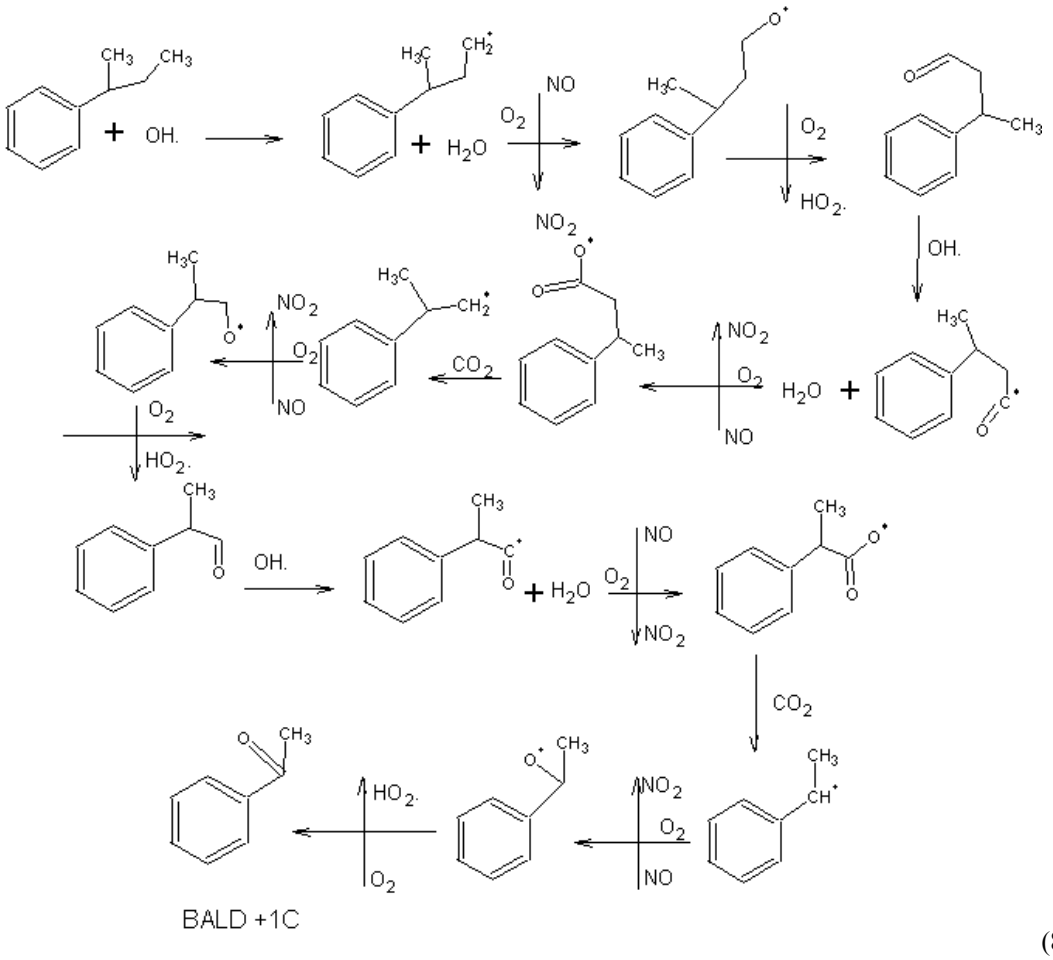

(85)

5%: S-C4-BEN + 3OH. = BALD + 1XC + 3RO2R + 3H2O + 2CO2

Reaction 77

In the second pathway, the abstraction of H atom occurs at position two (secondary carbon) of polysubstituent group (pathway 86). Proceeding through the similar consecutive reactions as in first pathway, benzaldehyde plus two extra carbon atoms, NO_2, and HO_2 radical are formed (pathway 86).

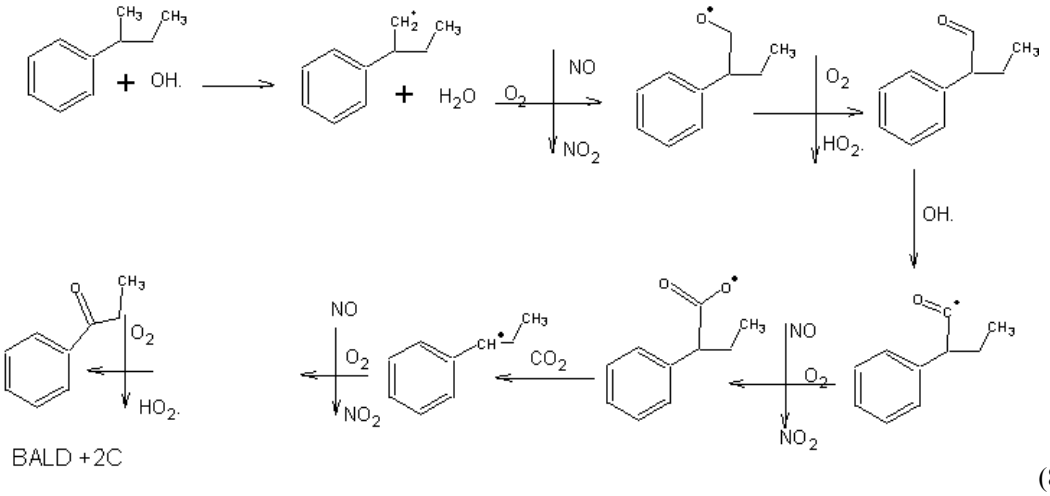

(86)

6%: S-C4-BEN + OH. = BALD + 2C + 2RO2R + CO2 – OH. + 2H2O

Reaction 78

The addition of OH radicals primarily occur at the othro position. Initial addtion of OH radical to sec-butylbenzene produces 19% cresol plus three extra carbon atoms (pathway 87, Smith, 1998), and 29.6% nitrobenzene plus four extra carbon atoms (pathway 88, Smith, 1998).

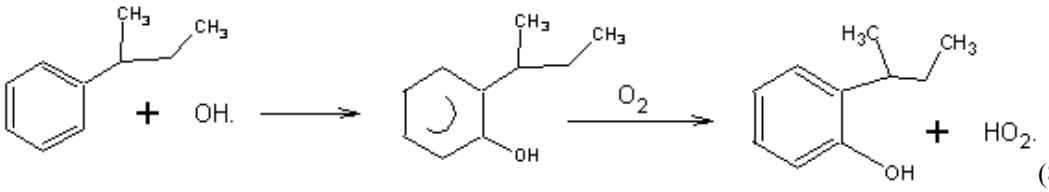

(87)

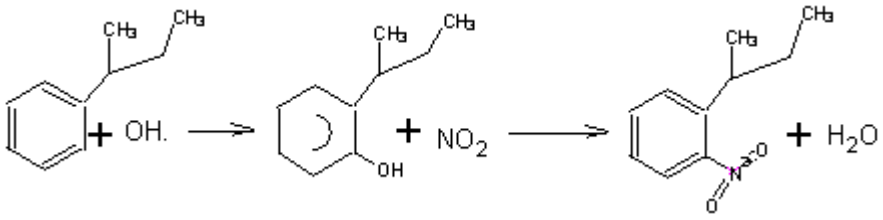

(88)

19%: S-C4-BEN + OH. = CRES + 3XC + HO2. **Reaction 79**

29.6%: S-C4-BEN + OH. = NBEN + 4XC + H2O – NO2 **Reaction 80**

The remainder of OH-aromatic adduct undergoes ring-cleavage reactions, which can proceed through six possible pathways (pathway 89-91). All of these six possible pathway occur via two steps, the abstraction of O atom by NO forming NO_2, and the abstraction of H atom by O_2. The cleavage reactions produce 16.7% APB5 and MGLY + 2XC, 11.9% APB6, 11.9% APB7, and 23.7% GLY (estimated from toluene (Smith, 1998)).

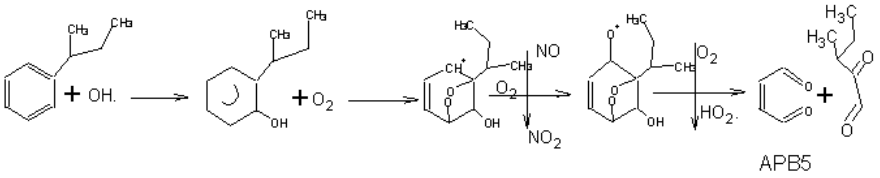

(89a)

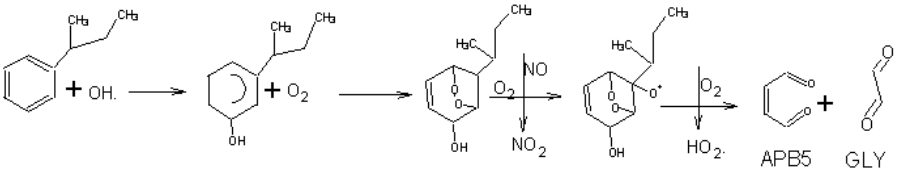

(89b)

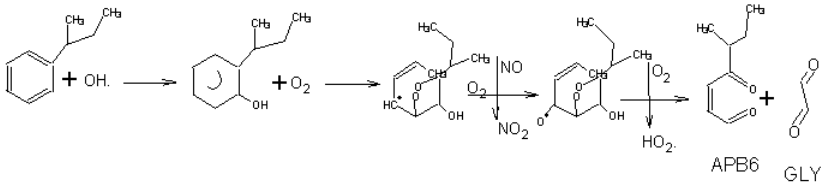

(90a)

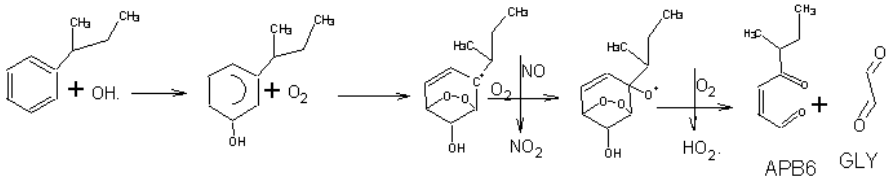

(90b)

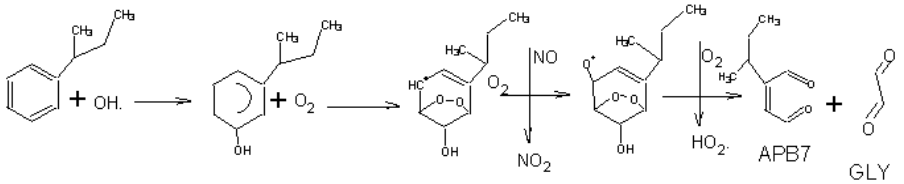

(91a)

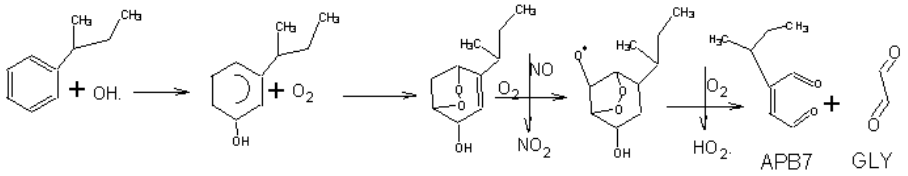

(91b)

40.5% S-C4-BEN + OH. = 0.167APB5 + 0.167MGLY + 0.167(3)XC +0.119APB6 + 0.119APB7 + 0.238GLY + 0.404RO2R **Reaction 81**

Net: S-C4-BEN + OH. = 0.19CRES + 0.19HO2. + 0.11BALD + 0.296NBEN – 0.296NO2 + 0.167APB5 + 0.119APB6 + 0.119APB7 + 0.167MGLY + 0.238GLY + 0.675RO2R + 0.566H2O – 0.16OH. + 2.425XC + 0.16CO2 **Reaction 82**

Aerosol precursors (APB5-APB7) further react with OH radical. OH radical adds to the carbon double bonds. Two types of semivolatile products (BPM5 and

BPM6) are produced from reactions of aerosol precursors. BPM5 is produced through the addition of NO to the O2-OH –aromatic adduct (pathways 92a-94a). BPM6 is generated via the abstraction of O atom by NO forming NO_2, and followed by the abstraction of H atom by O_2 producing HO_2 radical (pathways 92b – 94b). Yields of these two products, 25% for BPM5 and 75% for BPM6 were estimated from those for 1,3,5-trimethylbenzene (Eusebi, 1996).

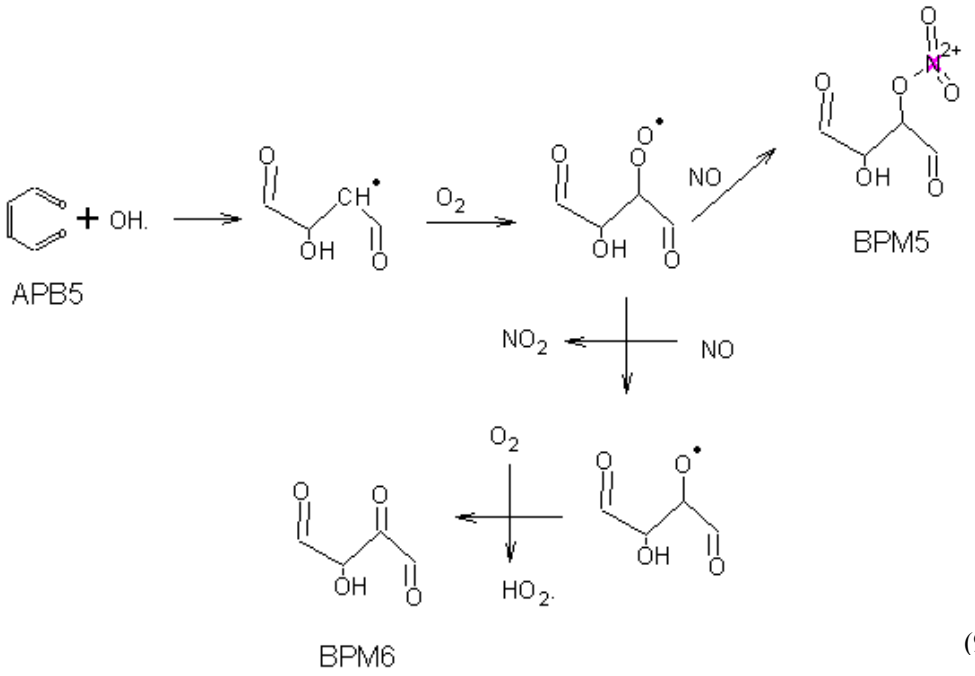

(92a)

(92b)

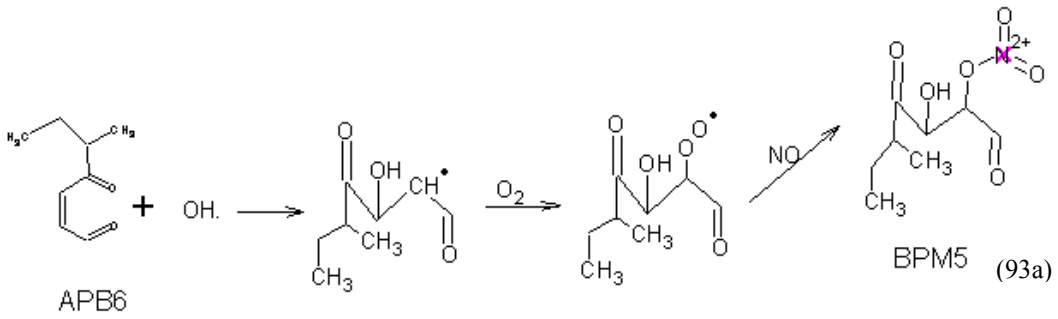

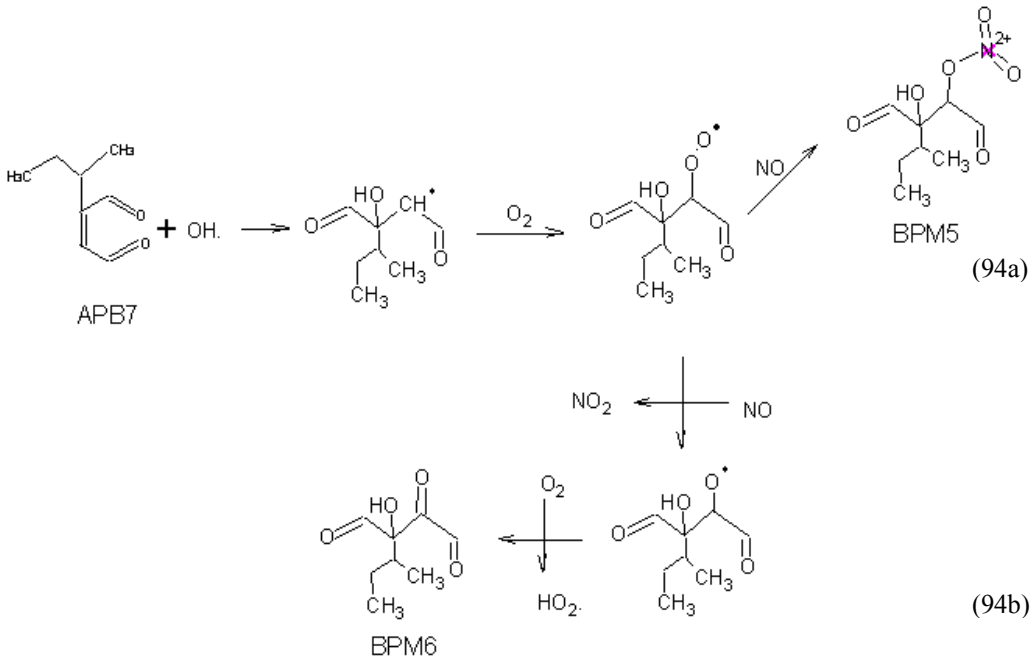

APB5 + OH. = 0.25BPM5 + 0.75BPM6 + 0.25RO2N +0.75RO2R **Reaction 83**

APB6 + OH. = 0.25BPM5 + 0.75BPM6 + 0.25RO2N +0.75RO2R **Reaction 84**

APB7 + OH. = 0.25BPM5 + 0.75BPM6 + 0.25RO2N +0.75RO2R **Reaction 85**

Reactions 82-85 describe the mechanistic models leading to SOA formation for iso-propylbenzene which proceed via two steps, similar to other aromatic precursors. Table 11 enumerates stoichiometric coefficients in reactions 82-85, and cites sources of the data.

Table C.11: Kinetic parameters of sec-butylbenzene reactions with OH radical forming aerosol products and their source

Notations	Descriptions	Stoichiometric Coefficients (SC)	Source of SC
CRES	Cresol	0.19	SAPRC-99
BALD	Benzaldehyde	0.11	Estimated from toluene, Bandow, 1985
MGLY	Methylglyoxal	0.167	Estimated from product for toluene, Smith 1998
GLY	Glyoxal	0.238	Estimated from product for toluene, Smith 1998
HO2.	Hydroperoxy radical	0.19	SAPRC-99
H2O	Water	0.566	Estimated from product for toluene, Smith 1998
NBEN	Nitrobenzene	0.296	Estimated from product for toluene, Smith 1998
CO2	Carbon dioxide	0.16	Estimated from product for toluene, Smith 1998
RO2R	Operator RO2R	0.675(reaction 82) 0.75 (reaction 83-85)	Estimated from product for toluene, Smith 1998 Estimated from 1,3,5-trimethylbenzene (Eusebi, 1996)
APB5	Aerosol precursor APB5	0.167	Estimated from product for toluene, Smith 1998
APB6	Aerosol precursor APB6	0.119	Estimated from product for toluene, Smith 1998
APB7	Aerosol precursor APB7	0.119	Estimated from product for toluene, Smith 1998
BPM5	Aerosol product species 1	0.25	Estimated from product for 1,3,5-trimethylbenzene, (Eusebi 1996)
BPM6	Aerosol product species 2	0.75	Estimated from product for 1,3,5-

			trimethylbenzene (Eusebi, 1996)
RO2N	Operator RO2N	0.25	Estimated from 1,3,5-trimethylbenzene, Eusebi 1996
XC	Balance carbon atom	2.425	SAPRC-99

p-ethyltoluene

Similar to photooxidation reactions of p-xylene, reactions of p-ethyltoluene are predominantly initiated by OH radical. Reactions with OH radical can either proceed through abstraction of H atom, or addition of OH. Abstraction by OH radical is likely to occur via two possible pathways. In the first pathway, H atom at the position terminal methyl group of the ethyl chain is abstracted by OH radical, then the oxidation occurs with the conversion of NO to NO_2 and formation of HO_2 radical, forming $C_6H_5C_2H_3OCH_3$ (pathway 95) . The abstraction of H atom from the carbonyl group of $C_6H_5C_2H_3OCH_3$ by OH radical occurs again. The product from this reaction then proceeds through the consecutive reactions of decomposition forming CO_2, and oxidization in the presence of NO to produce NO_2, HO_2 radical, and benzaldehyde plus one extra carbon atom (pathway 95). Yield of this pathway (4.2%) was estimated from p-xylene.

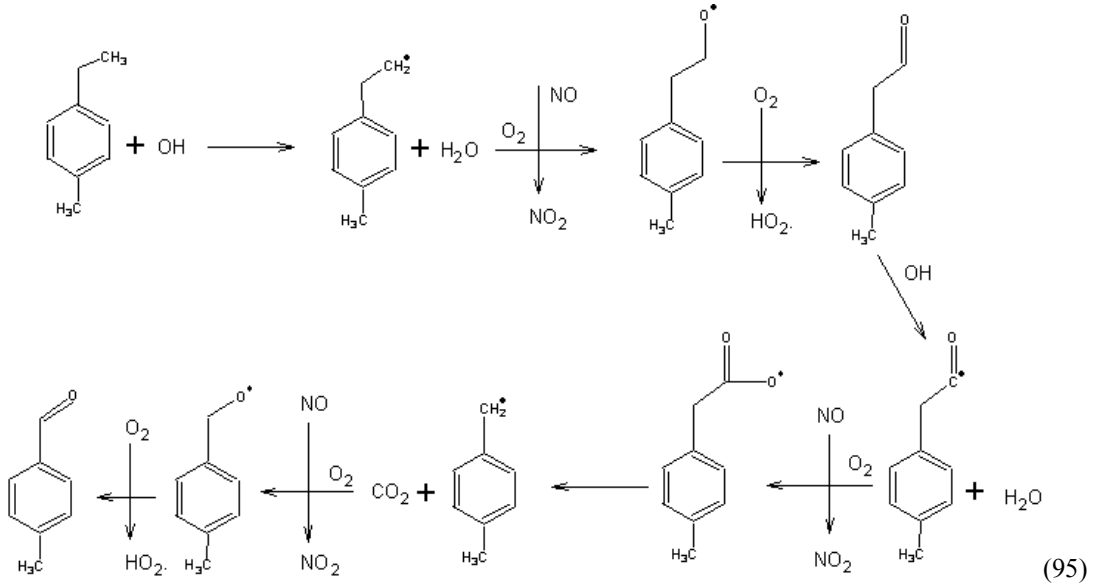

(95)

4.2%: P-C2-TOL + OH. = BALD + 1XC + CO2 + 2RO2R + 2H2O –OH.

Reaction 86

In another abstraction pathway, an H atom at the alpha position in the ethyl group is extracted. The structure with secondary radical is oxidized in the presence of NO generating NO_2, HO_2 radical, and benzaldehyde plus two extra carbon atoms (pathway 96). This pathway accounts for 4.2% of all reactions (relatively estiamted from p-xylene).

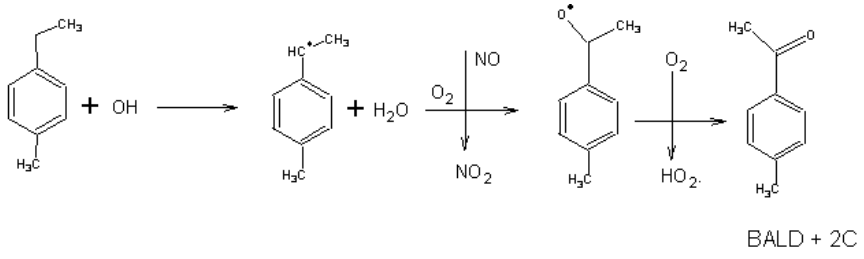

(96)

4.2%: P-C2-TOL + OH. = BALD + 2XC + RO2R **Reaction 87**

Addition of the OH radical to the p-ethyltoluene ring can occur at multiple ring positions, but predominantly adds at the aromatic ring carbon ortho to one of the cabons attached to the methyl group (Grovenstein, 1970; Atkinson et al., 1980). The initial addition of OH radical to p-ethyltoluene partially results in cresol with two extra carbon atoms and HO_2 radical (pathway 97). This pathway acounts for 18.8% of all reaction (estimated from p-xylene).

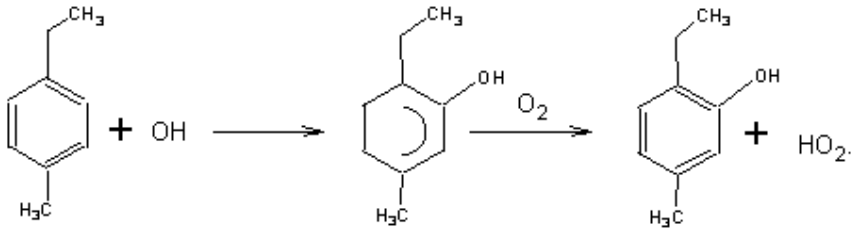

CRES + 2C

(97)

18.8%: P-C2-TOL + OH. = CRES + 2XC + HO2. **Reaction 88**

The remainder of the OH-aromatic adduct reacts further forming ring-cleavage products. Ring-cleavage reactions can proceed through five likely pathways, each undergoes two steps. The first step is the addition of O_2 to the OH-aromatic radical, and the abstraction of O atom by NO forming NO_2. The second step is the abstraction of H atom by O_2 to produce HO_2 radical and ring-cleavage products (unsaturated dicarbonyl species denoted as aerosol precursors). Estimates of yields of products for p-xylene suggest that 49% of all reactions produce aerosol precursor species APET1, 20% result in APET2, and 4% form APET3 (pathways 98-100).

Methylglyoxal and glyoxal are also generated with the yields of 24% and 49%, respectively (pathways 98-100).

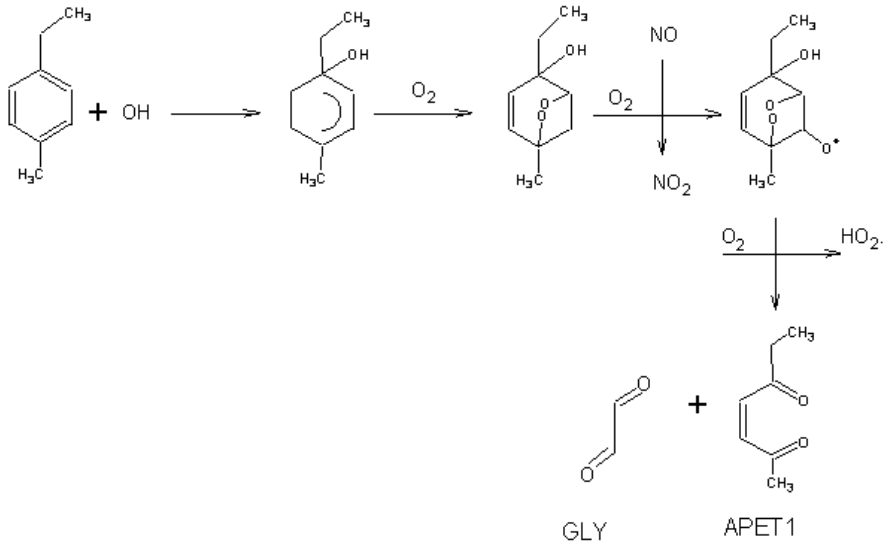

(98a)

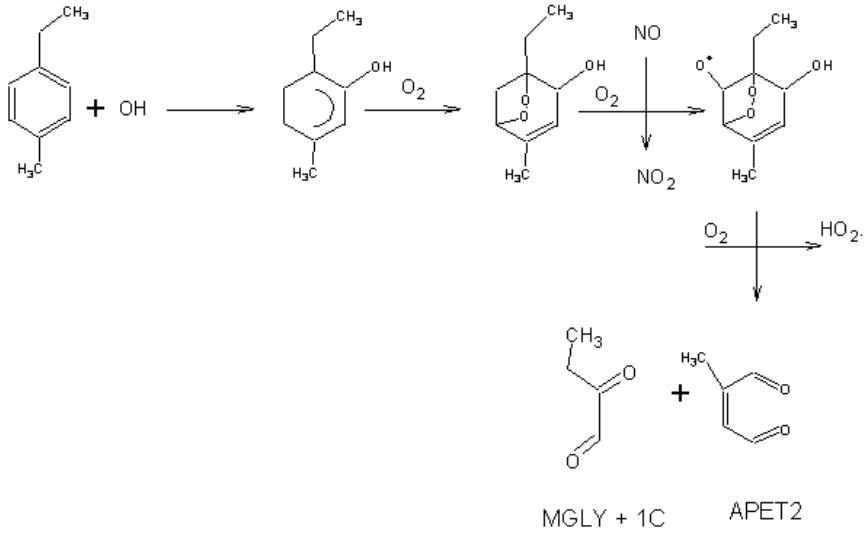

(99a)

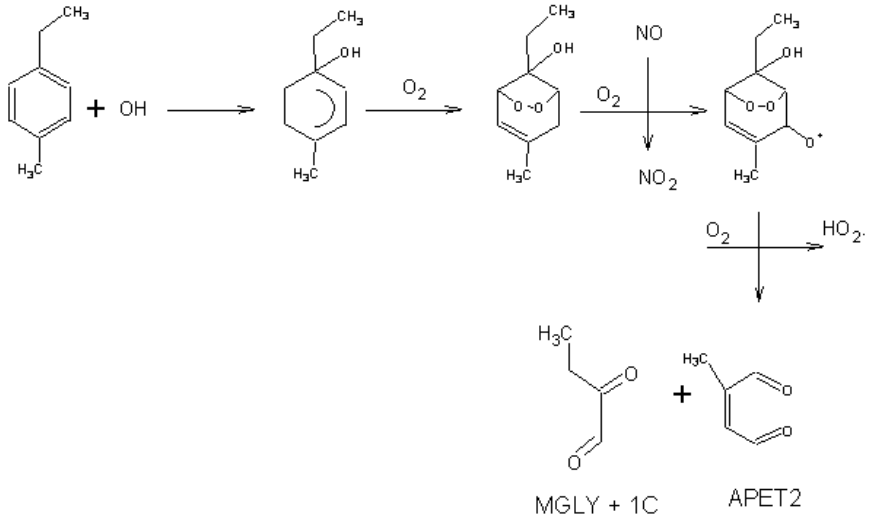

(99b)

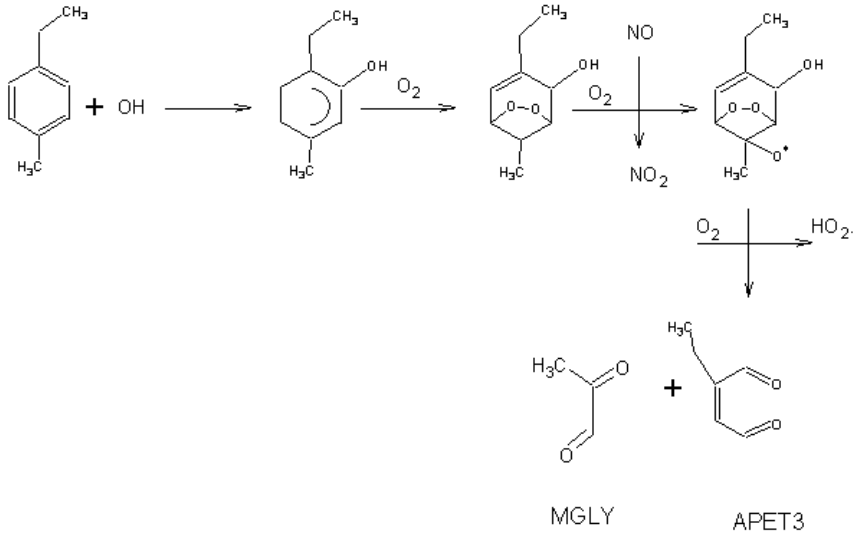

(100)

73.0% P-C2-TOL + OH. = 0.49APET1 + 0.2APET2 +0.04APET3 + 0.24MGLY + 0.49GLY + 0.73RO2R + 0.2XC **Reaction 89**

Net: P-C2-TOL + OH. = 0.188CRES + 0.188HO2. + 0.084BALD + 0.042CO2 + 0.084H2O + 0.49APET1 + 0.2APET2 + 0.04APET3 + 0.24MGLY + 0.49GLY + 0.702C + 0.856RO2R –0.0402OH. **Reaction 90**

Aerorol precursors (APET1-APET3) further react with OH radical in the presence of O_2 and NO_2 to form two types of condensable products (ETPM1 and ETPM2).

ETPM1, aerosol products with organonitrate, is produced through first the addition of OH to carbon double bonds, then the addition of O_2 and NO_2 to the radical (pathways 101a – 103a). This pathway accounts for 25% (estimated from o-xylene). The remainder of the OH-ring clevage adduct (75%) further oxidizes in the presence of NO forming NO_2, HO_2 radical, and ETPM2 (pathways 101b-103b).

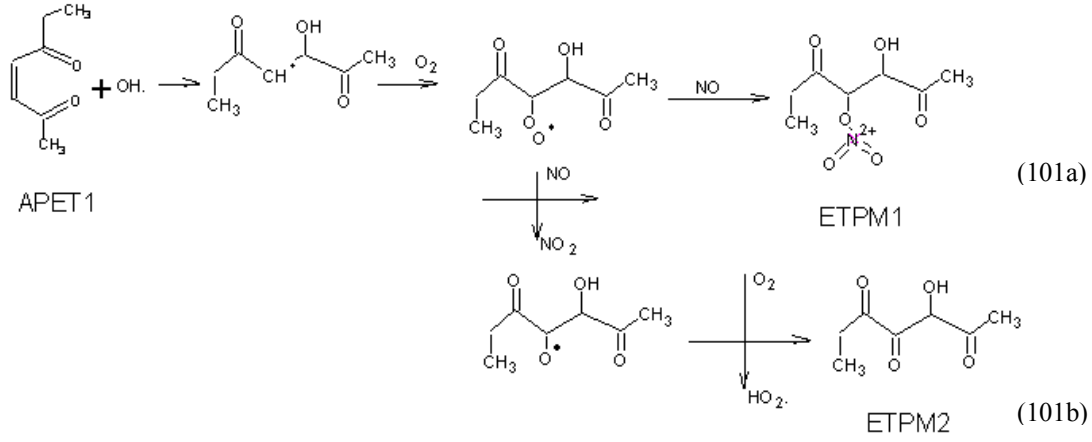

(101a)

(101b)

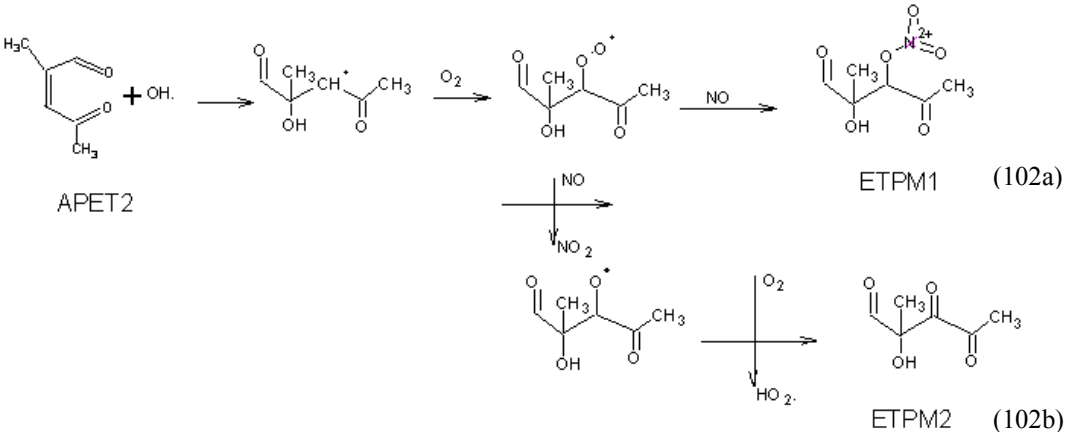

(102a)

(102b)

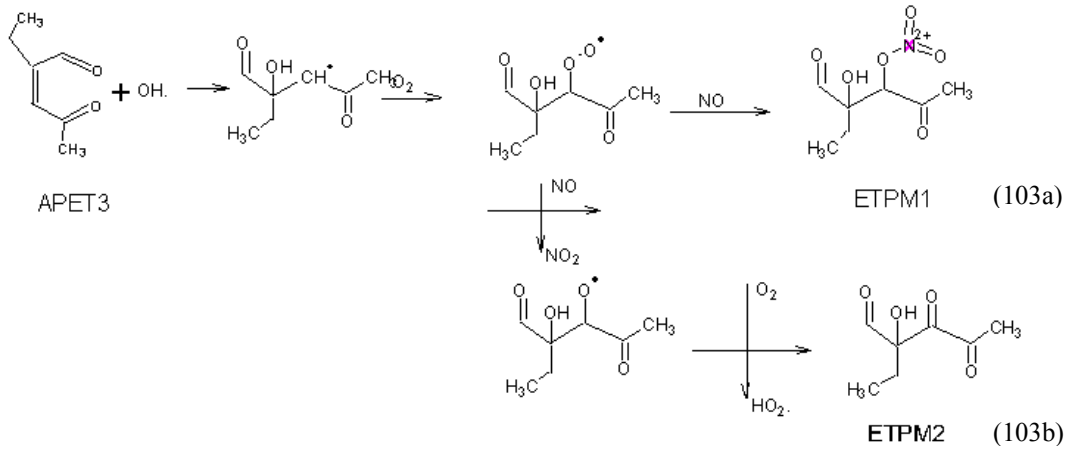

APET1 + OH. = 0.25ETPM1 +0.75ETPM2 +0.25RO2N +0.75RO2R **Reaction 91**

APET2 + OH. = 0.25ETPM1 +0.75ETPM2 +0.25RO2N +0.75RO2R **Reaction 92**

APET3 + OH. = 0.25ETPM1 +0.75ETPM2 +0.25RO2N +0.75RO2R **Reaction 93**

Reactions 90-93 describe condensed mechanisms of p-ethyltoluene with OH radical leading to SOA formation. The stoichiometric coefficients are summarized in Table C12.

Table C.12: Kinetic parameters of p-ethyltoluene reactions with OH radical forming aerosol products and their source

Notations	Descriptions	Stoichiometric Coefficients (SC)	Source of SC
CRES	Cresol	0.188	Estimated from p-xylene (Eusebi, 1996)
BALD	Benzaldehyde	0.084	Estimated from p-xylene (Eusebi, 1996)
MGLY	Methylglyoxal	0.24	Estimated from p-xylene (Eusebi, 1996)
GLY	Glyoxal	0.49	Estimated from p-xylene (Eusebi, 1996)
HO2.	Hydroperoxy radical	0.188	Estimated from p-xylene (Eusebi, 1996)
RO2R	Operator RO2R	0.856(reaction 90)	Estimated from p-xylene (Eusebi, 1996)
		0.75 (reaction 91-93)	Estimated from o-xylene (Eusebi, 1996)

APET1	Aerosol precursor APET1	0.49	Estimated from p-xylene (Eusebi, 1996)
APET2	Aerosol precursor APEt2	0.20	Estimated from p-xylene (Eusebi, 1996)
APET3	Aerosol precursor APET3	0.04	Estimated from p-xylene (Eusebi, 1996)
ETPM1	Aerosol product species 1	0.25	Estimated from products from o-xylene (Eusebi, 1996)
ETPM2	Aerosol product species 2	0.75	Estimated from products from o-xylene (Eusebi, 1996)
RO2N	Operator RO2N	0.25	Estimated from products from o-xylene (Eusebi, 1996)
XC	Balance extra carbon	0.702	SAPRC-99, estimated from p-xylene, (Eusebi, 1996)
CO2	Carbon dioxide	0.042	Estimated from p-xylene (Eusebi, 1996)
H2O	Water	0.084	Estimated from p-xylene (Eusebi, 1996)

o-ethyltoluene

Condensed mechanisms describing SOA formation from o-ethyltoluene were developed analogous to those of other aromatics. Reactions of o-ethyltoluene with OH radical can either proceed through the abstraction of H atom, or the addition of OH radical to aromatic ring. Abstraction of H atom by OH radical is likely to occur via two possible pathways. The first pathway, H atom at position terminal methyl group in the ethyl chain is abstracted by OH radical, then the oxidation occurs with the conversion of NO to NO_2 and formation of HO_2 radical forming $C_6H_5C_2H_3OCH_3$ (pathway 104) . The abstraction of H atom from the carbonyl group of $C_6H_5C_2H_3OCH_3$ by OH radical occurs again. The product from this reaction then proceeds through the consecutive reactions of decomposition producing CO_2, and

oxidization in the presence of NO to produce NO_2, HO_2 radical, and benzaldehyde plus one extra carbon atom (pathway 104). Yield of this pathway (3.25%) was estimated from o-xylene.

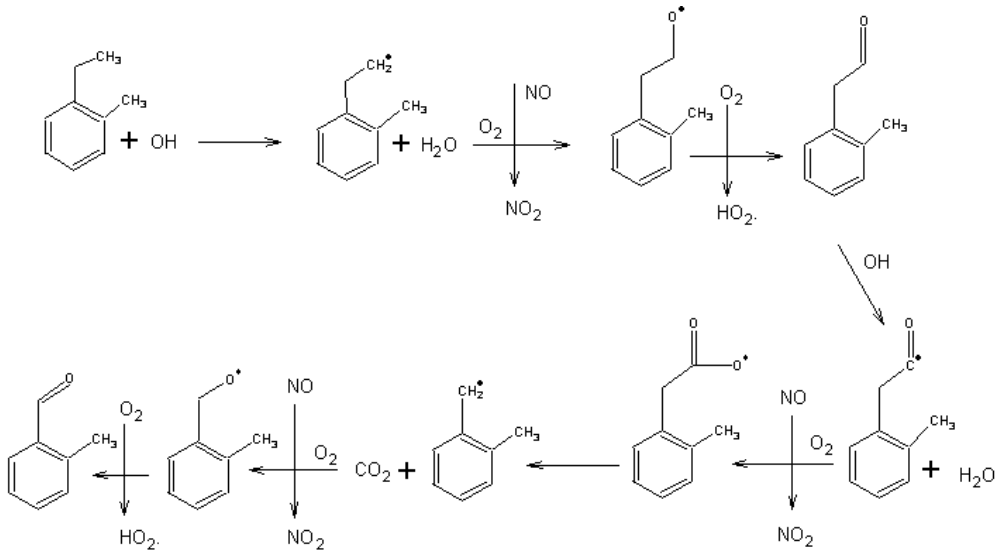

3.25%: O-C2-TOL + OH. = BALD + 1XC + CO2 + 2RO2R + 2H2O – OH.

Reaction 94

The second pathway involves abstraction of H atom at the alpha-carbon in the ethyl chain. The radical is oxidized in the presence of NO generating NO_2, HO_2 radical, and benzaldehyde plus two extra carbon atoms (pathway 105). This pathway accounts for 3.25% of all reactions (estiamted from o-xylene).

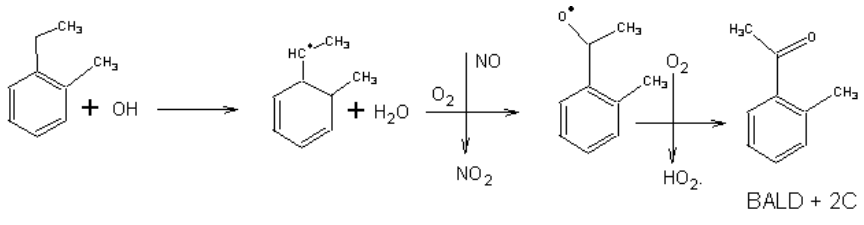

(105)

3.25%: O-C2-TOL + OH. = BALD + 2XC + RO2R **Reaction 95**

Addition of OH radical predominantly occurs at the aromatic carbon ortho to the carbon attached to the methyl group. The initial addition of OH radical to o-ethyltoluene results in cresol with two extra carbon atoms and HO_2 radical (pathway 106). This pathway acounts for 18% of all reaction (estimated from o-xylene).

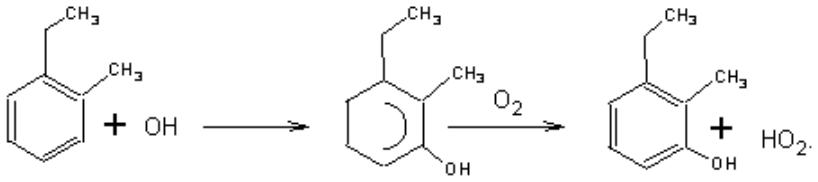

CRES + 2C

(106)

18.8%: O-C2-TOL + OH. = CRES + 2XC + HO2. **Reaction 96**

Another reaction pathway that can occur following the formation of the OH-aromatic adduct is bridging of O_2 atom across the ring. This reaction then leads to the formation of ring-cleavage products. Ring-cleavage reactions can proceed through 14 likely pathways, each of them undergoes two similar steps. The first step is the addition of O_2 to the OH-aromatic radical, and the abstraction of O atom by NO forming NO_2. The second step is the abstraction of H atom by O_2 to produce HO_2 radical and ring-cleavage products (unsaturated dicarbonyl species denoted as aerosol precursors). The yield of aerosol precursor species APET4 is 32.9%, APET5 is 8.5%, APET6 is 2.6%, APET7 is 5.1%, APET8 is 18.6%, and APET9 is 6.6%. These yields were estimated from yields of products for o-xylene. Along with the production of

aerosol precursors, methylglyoxal, biacetyl, and glyoxal are also generated with the yields of 39.5, 18.6, and 16.2%, respectively (pathways 107-112).

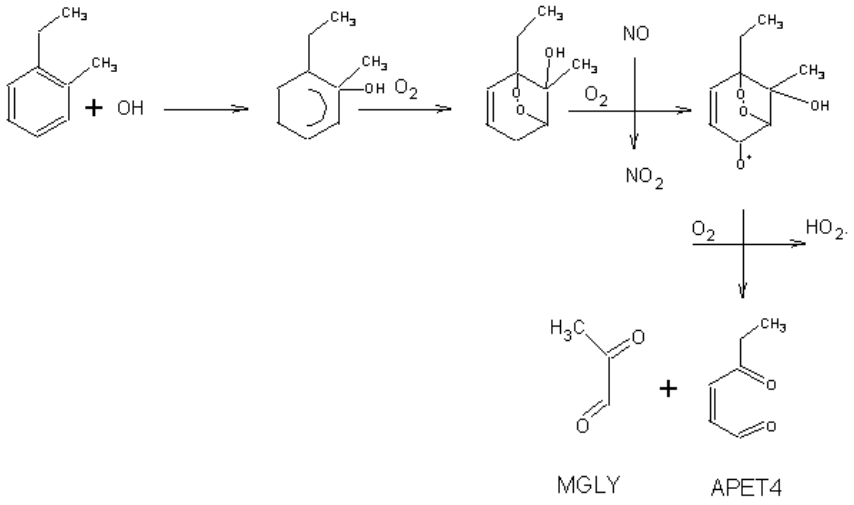

(107a)

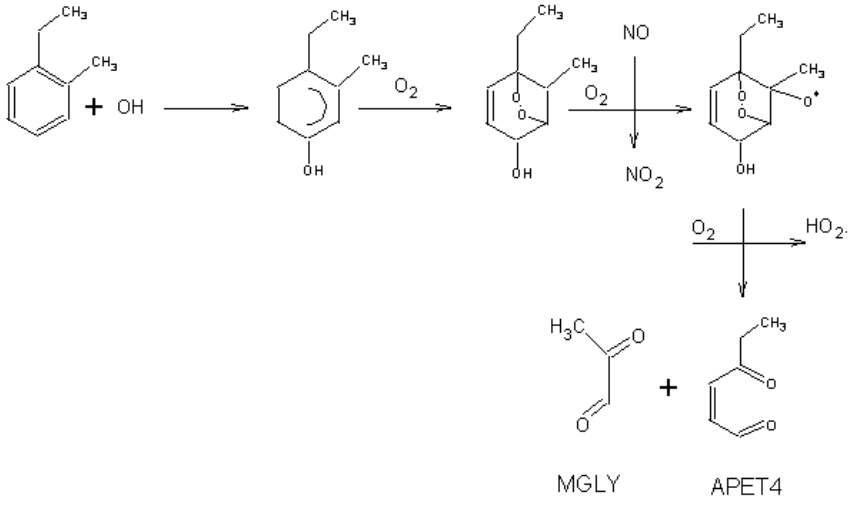

(107b)

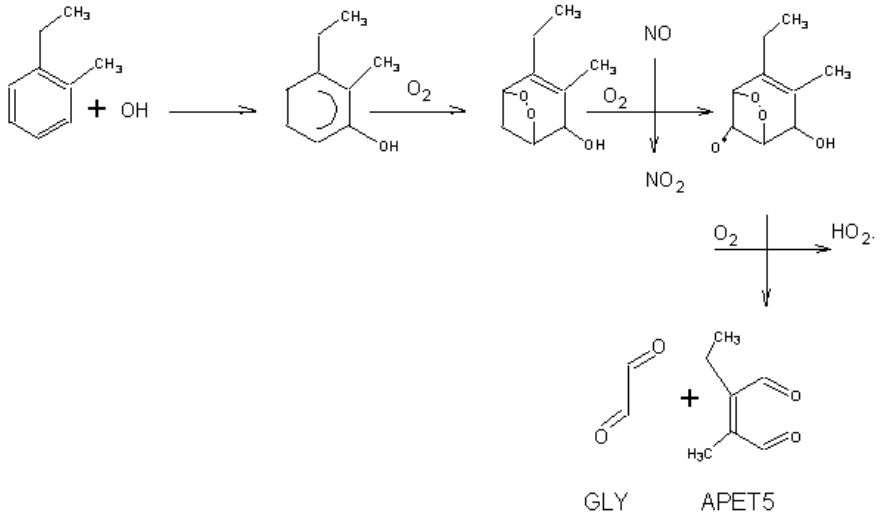
CH3
OH
O2
NO
NO2
HO2·
O
H3C
GLY
APET5

(108a)

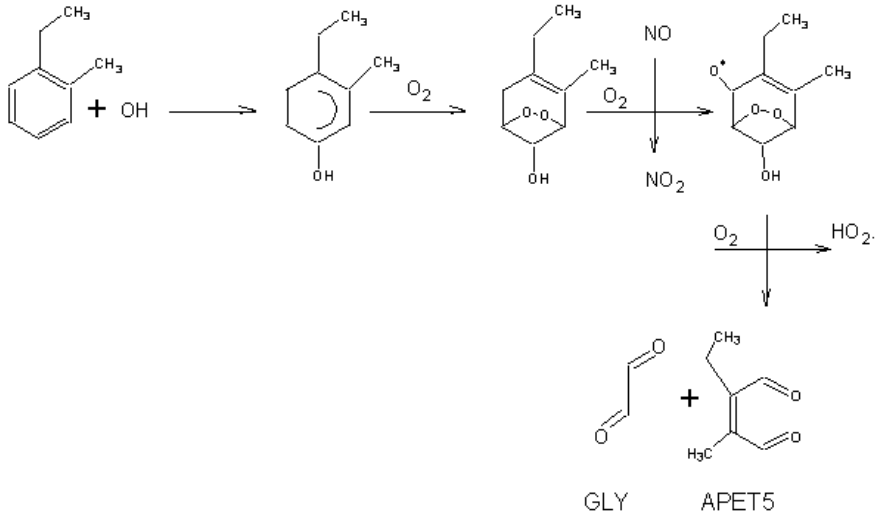
CH3
OH
O2
NO
NO2
HO2·
O
H3C
GLY
APET5

(108b)

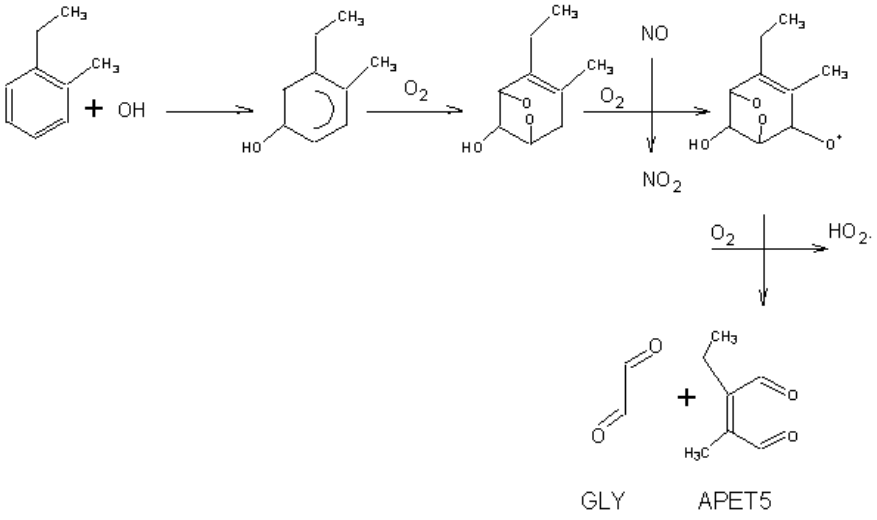
CH3
OH
HO
O2
NO
NO2
HO2·
O
H3C
GLY
APET5

(108c)

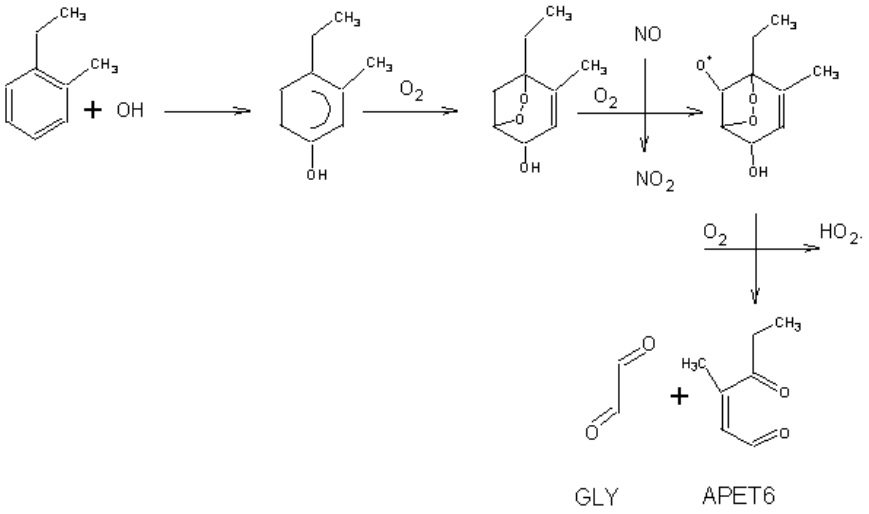
CH3
OH
O2
NO
NO2
HO2·
O
H3C
GLY
APET6

(109a)

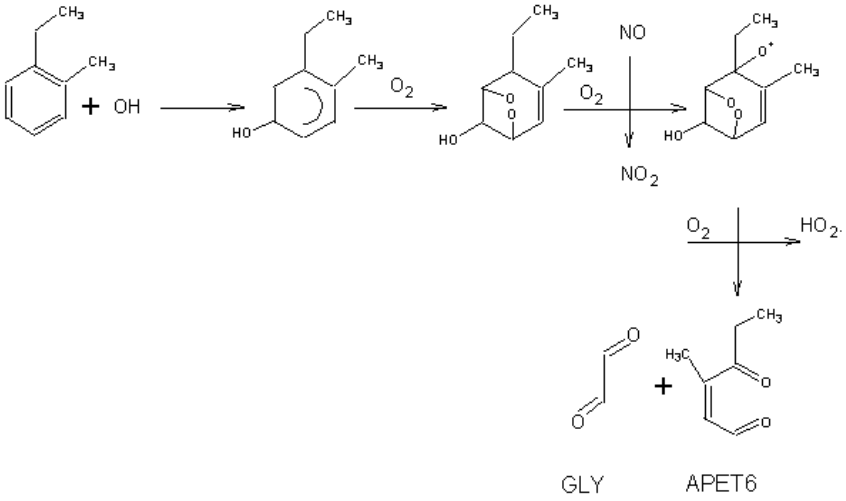

(109b)

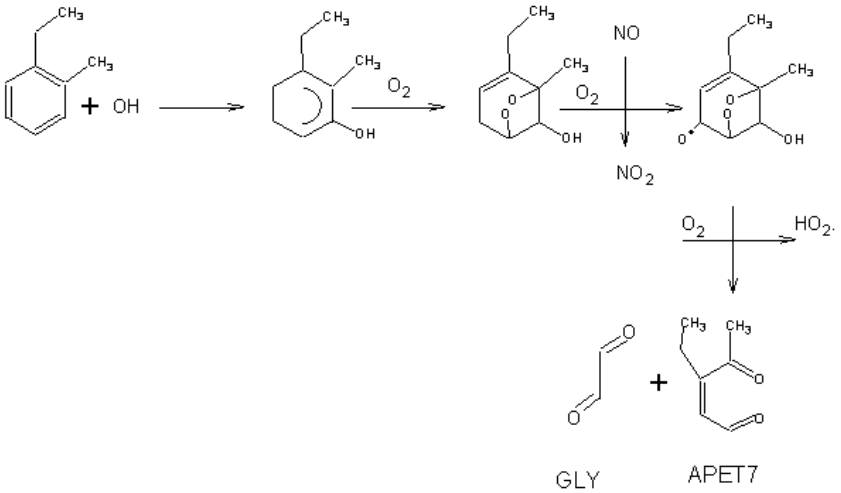

(110a)

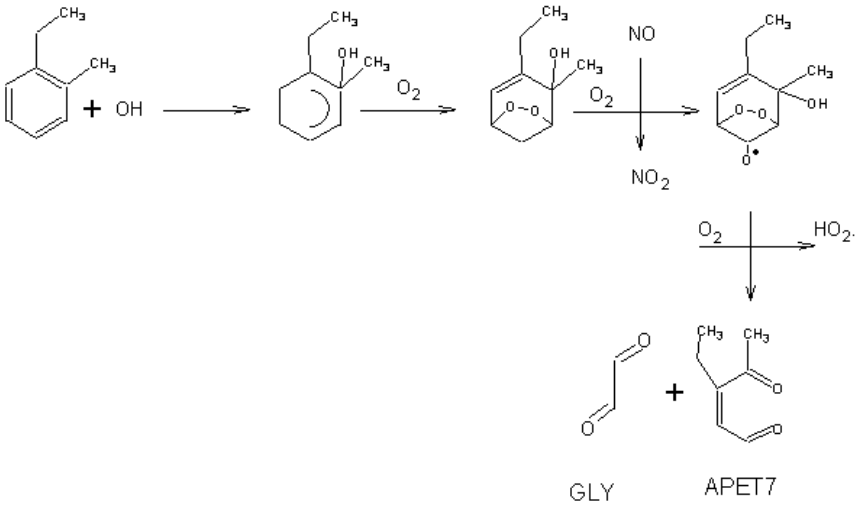

(110b)

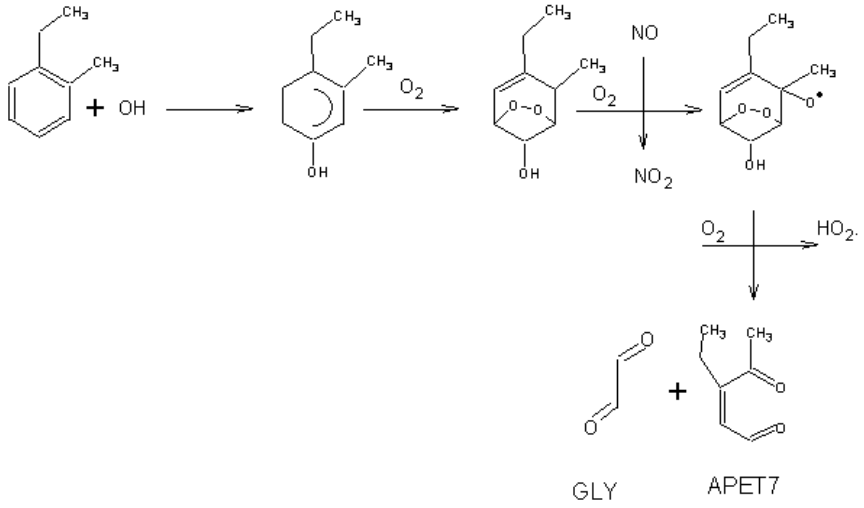
CH3
OH
O2
NO
NO2
HO2·
O
GLY
APET7

(110c)

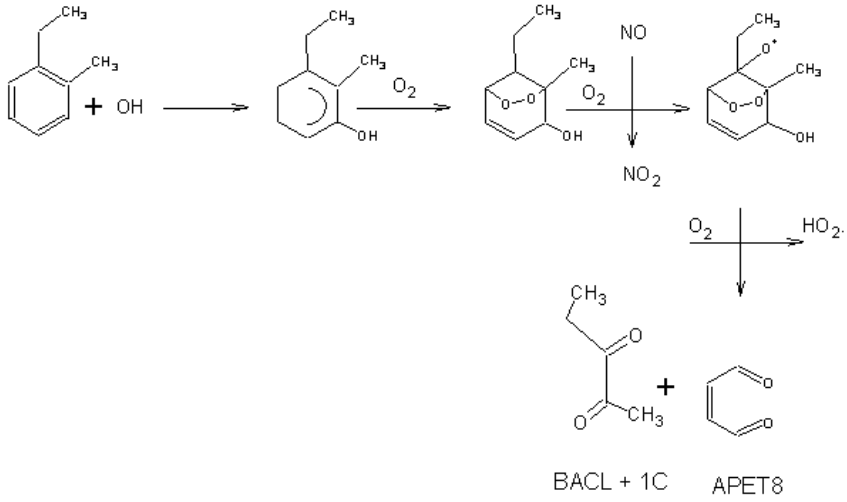
CH3
OH
O2
NO
NO2
HO2·
O
BACL + 1C
APET8

(111a)

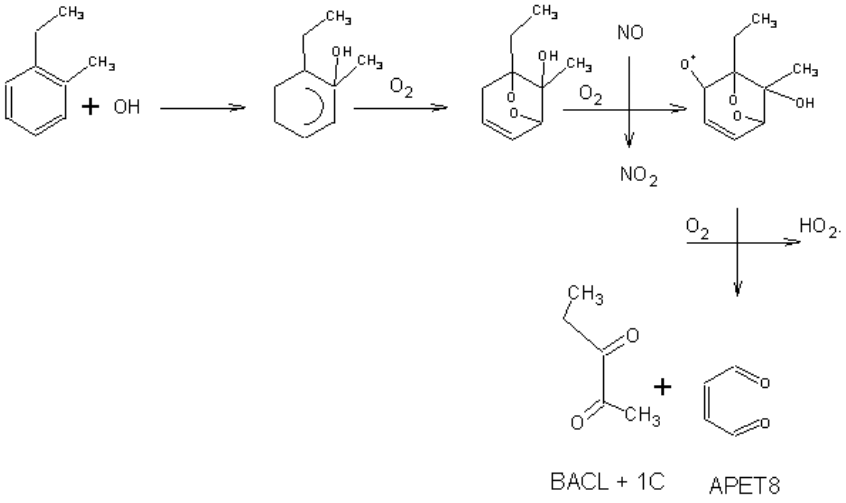
CH3
OH
O2
NO
NO2
HO2.
O
BACL + 1C
APET8

(111b)

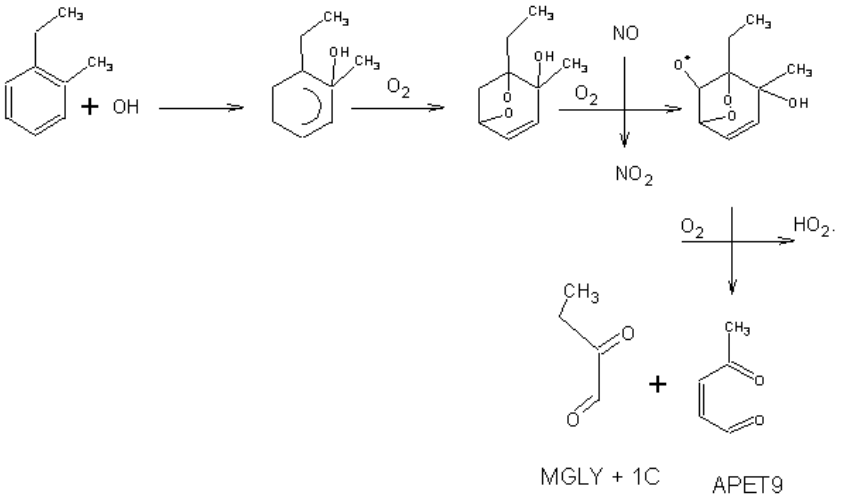
CH3
OH
O2
NO
NO2
HO2.
O
MGLY + 1C
APET9

(112a)

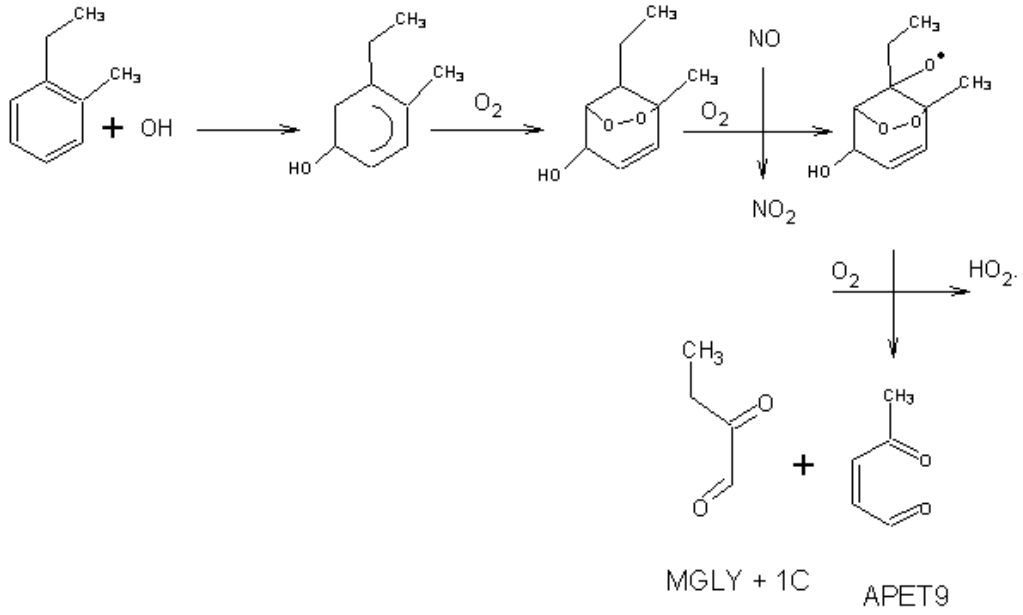

(112b)

74.29% O-C2-TOL + OH. = 0.329APET4 + 0.085APET5 +0.026APET6 +0.051APET7 +0.186APET8 +0.0659APET9 + 0.395MGLY + 0.186BACL +0.162GLY + 0.7429RO2R + 0.252XC **Reaction 97**

Net: O-C2-TOL + OH. = 0.188CRES + 0.188HO2. + 0.065BALD + 0.0325CO2 + 0.065H2O + 0.329APET4 + 0.085APET5 +0.026APET6 +0.051APET7 +0.186APET8 +0.0659APET9 + 0.395MGLY + 0.186BACL +0.162GLY + 0.7255XC + 0.8404RO2R – 0.0325HO. **Reaction 98**

Aerorol precursors (APET4-APET9) further react with OH radical in the presence of O_2 and NO_2 to form two types of condensable products (ETPM3 and ETPM4). ETPM3, containing organonitrate, is produced through the addition of OH to carbon double bonds, then the addition of O_2 and NO_2 to the radical (pathways 113a – 118a). This pathway accounts for 25% (estimated from o-xylene) of the products. The

remainder of the OH-ring clevage adduct (75%) further oxidizes in the presence of NO forming NO_2, HO_2 radical, and ETPM4 (pathways 113b-118b).

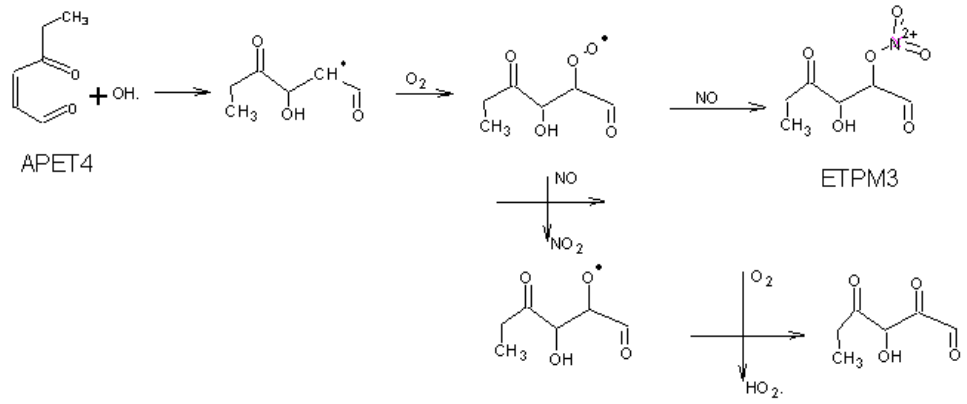

(113a)

(113b)

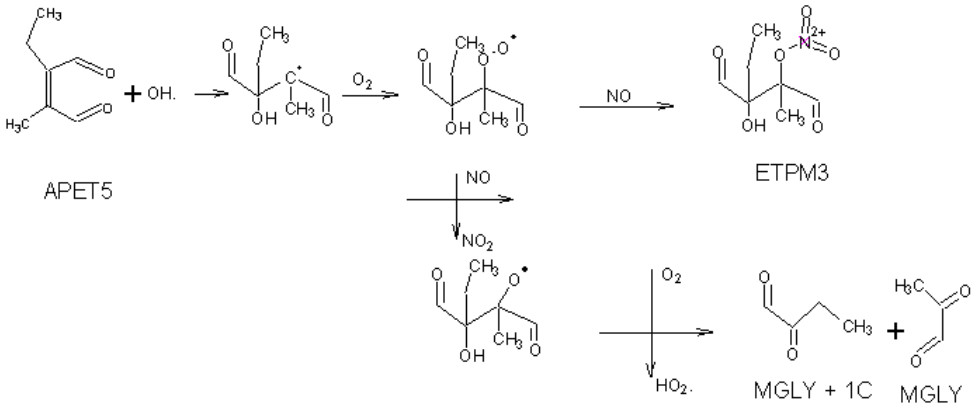

(113b)

(114a)

(114b)

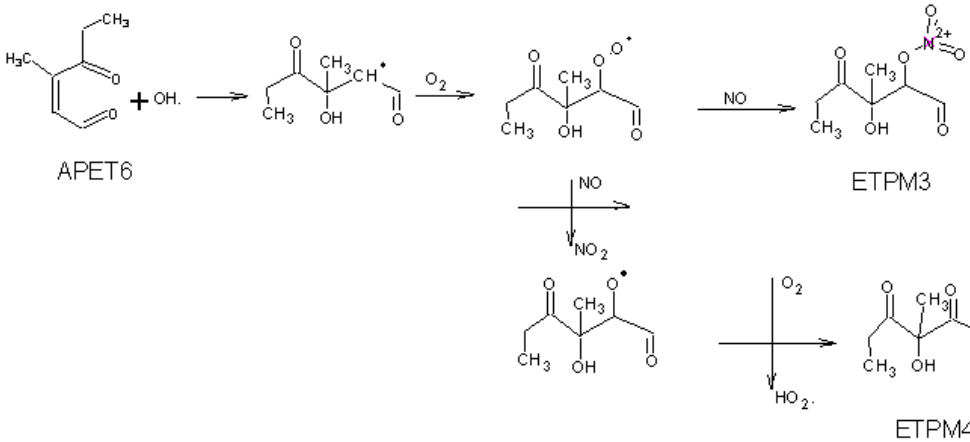

(115a)

(115b)

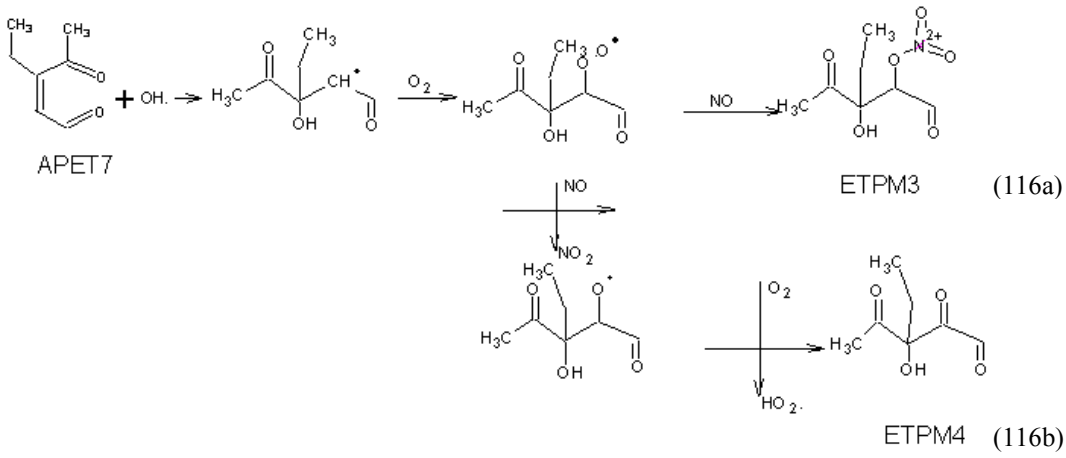

(116a)

(116b)

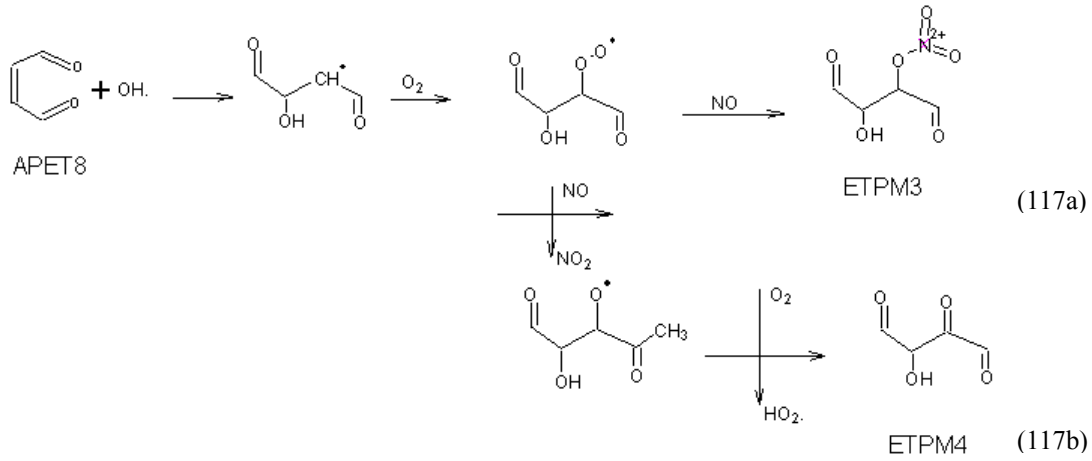

(117a)

(117b)

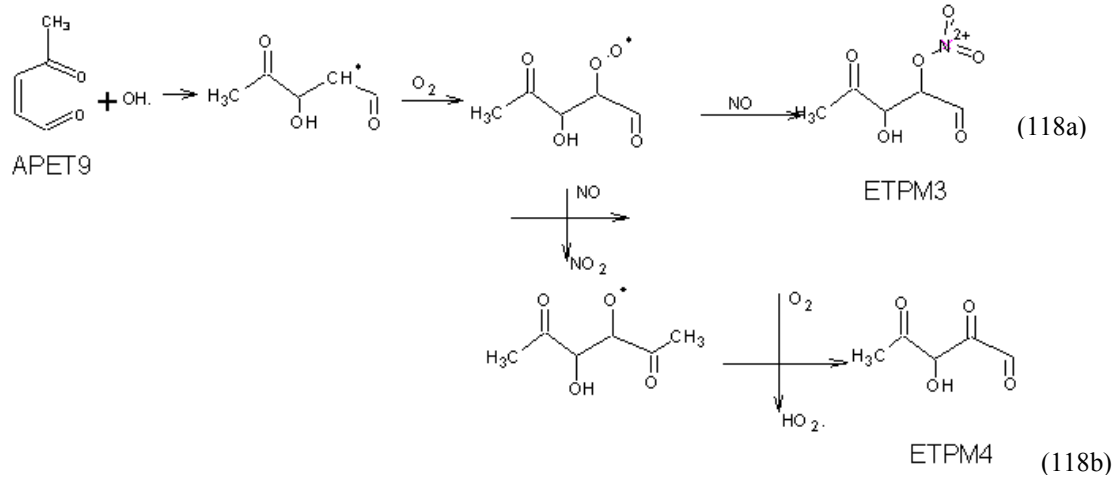

(118a)

(118b)

APET4 + OH. = 0.25ETPM3 +0.75ETPM4 +0.25RO2N +0.75RO2R **Reaction 99**

APET5 + OH. = 0.25ETPM3 +0.75(2MGLY + 1C) +0.25RO2N +0.75RO2R **Reaction 100**

APET6 + OH. = 0.25ETPM3 +0.75ETPM4 +0.25RO2N +0.75RO2R **Reaction 101**

APET7 + OH. = 0.25ETPM3 +0.75ETPM4 +0.25RO2N +0.75RO2R **Reaction 102**

APET8 + OH. = 0.25ETPM3 +0.75ETPM4 +0.25RO2N +0.75RO2R **Reaction 103**

APET9 + OH. = 0.25ETPM3 +0.75ETPM4 +0.25RO2N +0.75RO2R **Reaction 104**

Reactions 98-104 describe condensed mechanisms of o-ethyltoluene with OH radical leading to SOA formation. The stoichiometric coefficients are summarized in Table 13.

Table C.13: Kinetic parameters of o-ethyltoluene reactions with OH radical forming aerosol products and their source

Notations	Descriptions	Stoichiometric Coefficients (SC)	Source of SC
CRES	Cresol	0.188	Estimated from o-xylene (Eusebi, 1996)
BALD	Benzaldehyde	0.065	Estimated from o-xylene (Eusebi, 1996)
MGLY	Methylglyoxal	0.395	Estimated from o-xylene (Eusebi, 1996)
BACL	Biacetyl	0.186	Estimated from o-xylene (Eusebi, 1996)
GLY	Glyoxal	0.162	Estimated from o-xylene (Eusebi, 1996)
HO2.	Hydroperoxy radical	0.188	Estimated from o-xylene (Eusebi, 1996)
RO2R	Operator RO2R	0.8404(reaction 98)	Estimated from o-xylene (Eusebi, 1996)
		0.75 (reaction 99-104)	Estimated from o-xylene (Eusebi, 1996)
APET4	Aerosol precursor APET4	0.329	Estimated from o-xylene (Eusebi, 1996)
APET5	Aerosol precursor APET5	0.085	Estimated from o-xylene (Eusebi, 1996)
APET6	Aerosol precursor APET6	0.026	Estimated from o-xylene (Eusebi, 1996)
APET7	Aerosol precursor APET7	0.051	Estimated from o-xylene (Eusebi, 1996)

APET8	Aerosol precursor APET8	0.186	Estimated from o-xylene (Eusebi, 1996)
APET9	Aerosol precursor APET9	0.066	Estimated from o-xylene (Eusebi, 1996)
ETPM3	Aerosol product species 1	0.25	Estimated from products from o-xylene (Eusebi, 1996)
ETPM4	Aerosol product species 2	0.75	Estimated from products from o-xylene (Eusebi, 1996)
RO2N	Operator RO2N	0.25	Estimated from products from o-xylene (Eusebi, 1996)
XC	Balance extra carbon	0.7255	SAPRC-99, estimated from o-xylene (Eusebi, 1996)
CO2	Carbon dioxide	0.0325	Estimated from o-xylene (Eusebi, 1996)
H2O	Water	0.065	Estimated from o-xylene (Eusebi, 1996)

m-ethyltoluene

Condensed mechanisms describing SOA formation of m-ethyltoluene were developed analogous to those used for other aromatics. Reactions of m-ethyltoluene with OH radical can either proceed through abstraction, or addition. Similar ring to p-and o-ethyltoluene, abstraction of H atom by OH radical is likely to occur via two possible pathways. In the first pathway, H atom from the methyl group in the ethyl chain is abstracted by OH radical, then the oxidation occurs with the conversion of NO to NO_2 and formation of HO_2 radical forming $C_6H_5C_2H_3OCH_3$ (pathway 119). The abstraction of H atom from the carbonyl group of $C_6H_5C_2H_3OCH_3$ by OH radical occurs. The product from this reaction then proceeds through the consecutive reactions of decomposition producing CO_2, and oxidization in the presence of NO to

produce NO_2, HO_2 radical, and benzaldehyde plus one extra carbon atom (pathway 119). Yield of this pathway (1.85%) was estimated from m-xylene.

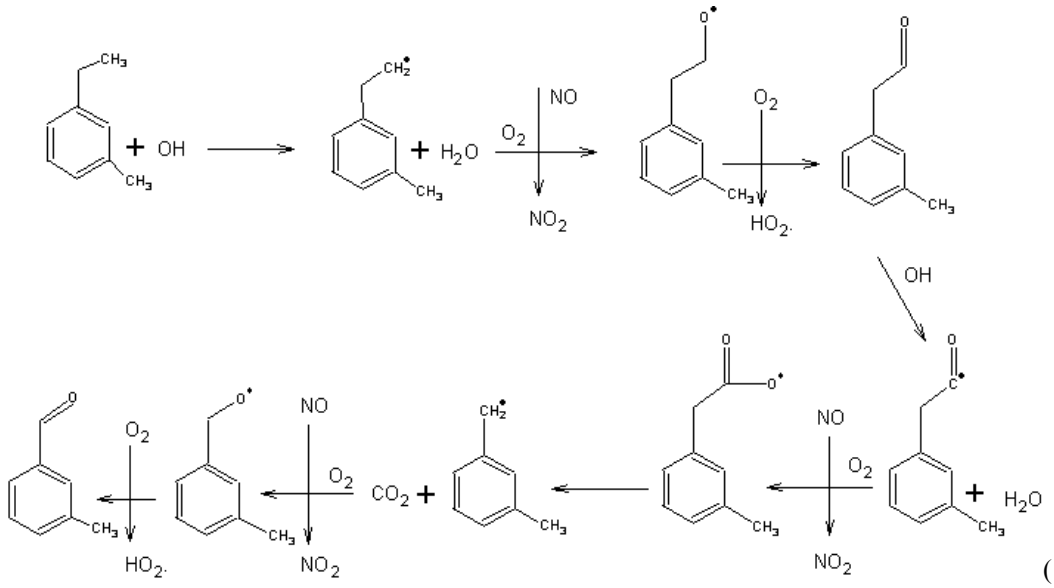

(119)

1.85%:M-C2-TOL + OH. = BALD + 1XC + CO2 + 2RO2R + 2H2O – OH.

Reaction 105

The second pathway involves abstraction of H. The aromatic-radical reacts with O_2 in the presence of NO generating NO_2, HO_2 radical, and benzaldehyde plus two extra carbon atoms (pathway 120). This pathway accounts for 1.85% of all reactions (estimated from m-xylene).

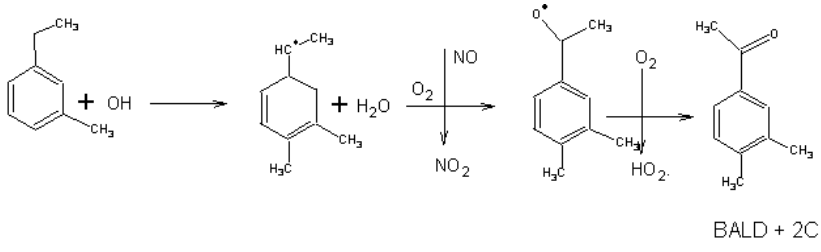

(120)

1.85%: M-C2-TOL + OH. = BALD + 2XC + RO2R **Reaction 106**

Addition of OH radical occurspredominantly adds at the aromatic carbon ortho to the methyl group. The initial addition of OH radical to o-ethyltoluene results in cresol with two extra carbon atoms and HO_2 radical (pathway 121). This pathway acounts for 21% of all reactions (estimated from m-xylene).

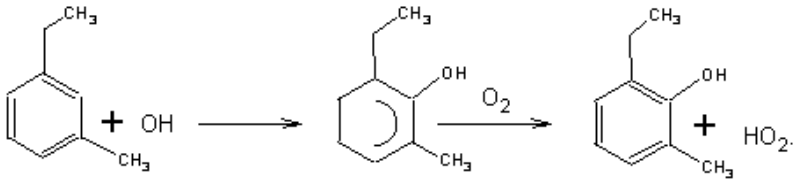

CRES + 2C

(121)

21%: M-C2-TOL + OH. = CRES + 2XC + HO2. **Reaction 107**

Another reaction pathway that can occur following the formation of the OH-aromatic adduct is bridging of O_2 across the ring, leading to the formation of ring-cleavage products. Ring-cleavage reactions proceed through 12 pathways, each of them undergoes two steps. The first step is the addition of O_2 to the OH-aromatic radical, and the abstraction of O atom by NO forming NO_2. The second step is the abstraction of H atom by O_2 to produce HO_2 radical and ring-cleavage products (unsaturated dicarbonyl species denoted as aerosol precursors). The yield of aerosol precursor species APET10 is 5.4%, APET11 is 13.4%, APET12 is 8%, APET13 is 10.6%, APET14 is 22.6%, and APET15 is 15.3%. These yields were estimated from yields of products for m-xylene. Ring-cleavage reactions also produce

methylglyoxal, and glyoxal with the yields of 57.7 and 18.6%, respectively (pathways 122-127).

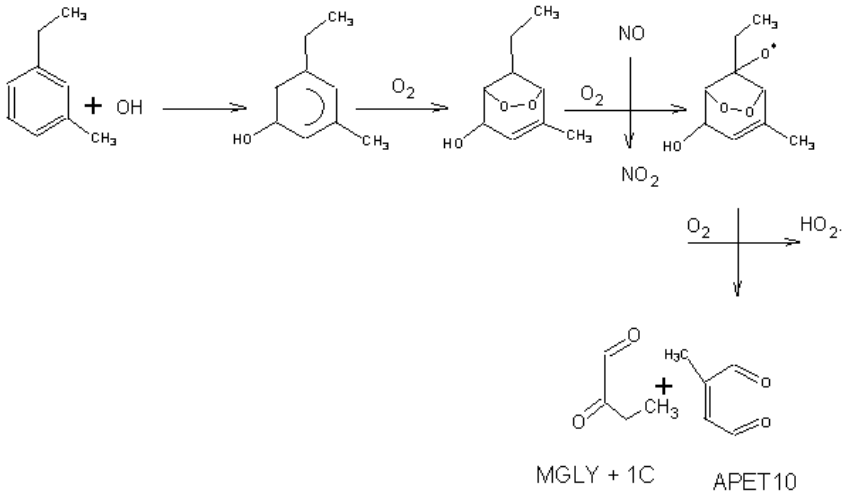

(122a)

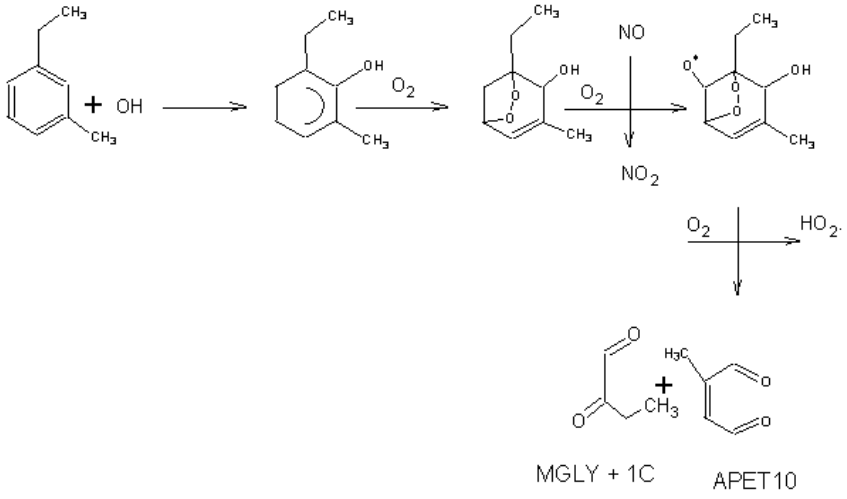

(122b)

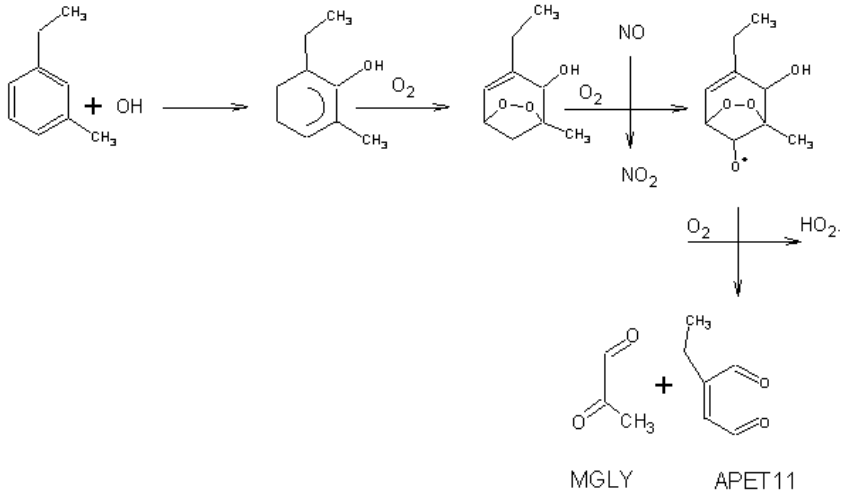
CH3
OH
O2
NO
NO2
HO2.
MGLY
APET11

(123a)

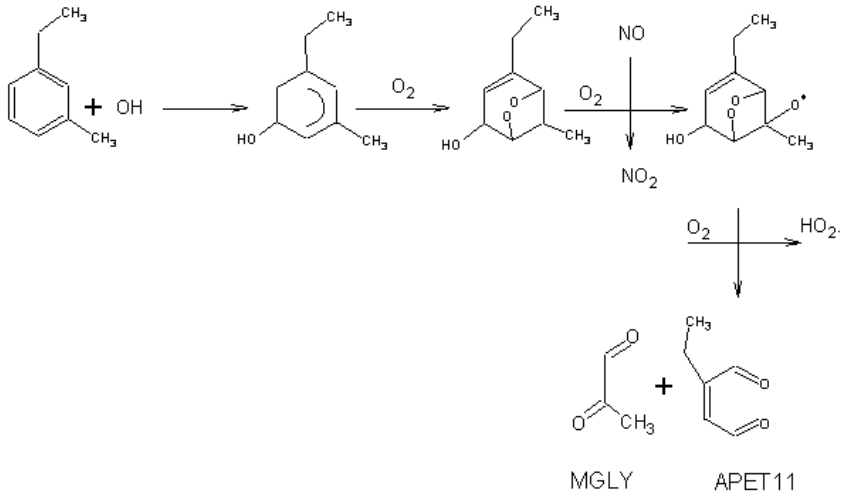
CH3
OH
HO
O2
NO
NO2
HO2.
MGLY
APET11

(123b)

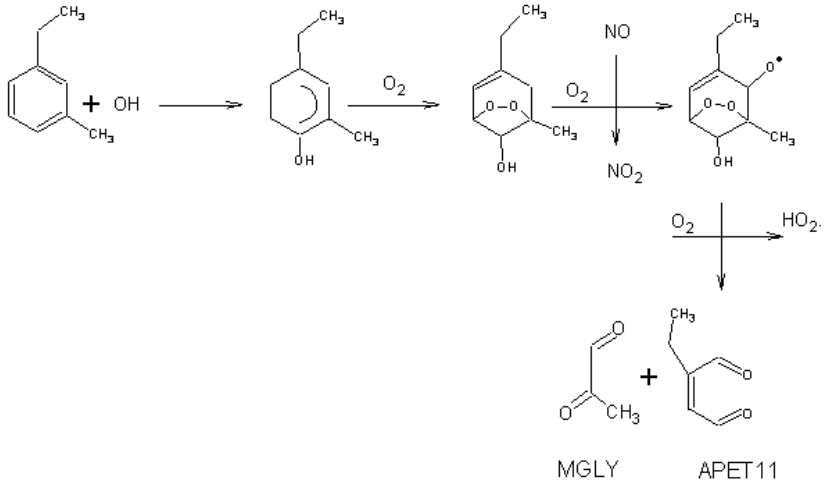

(123c)

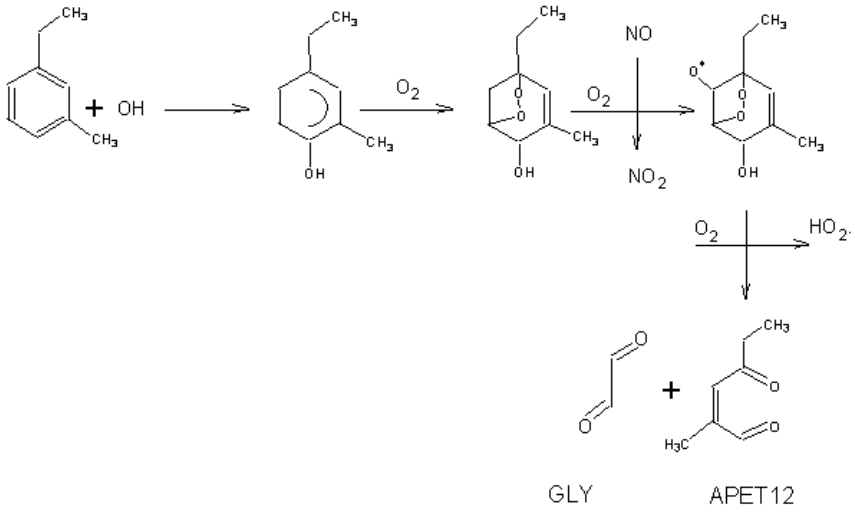

(124a)

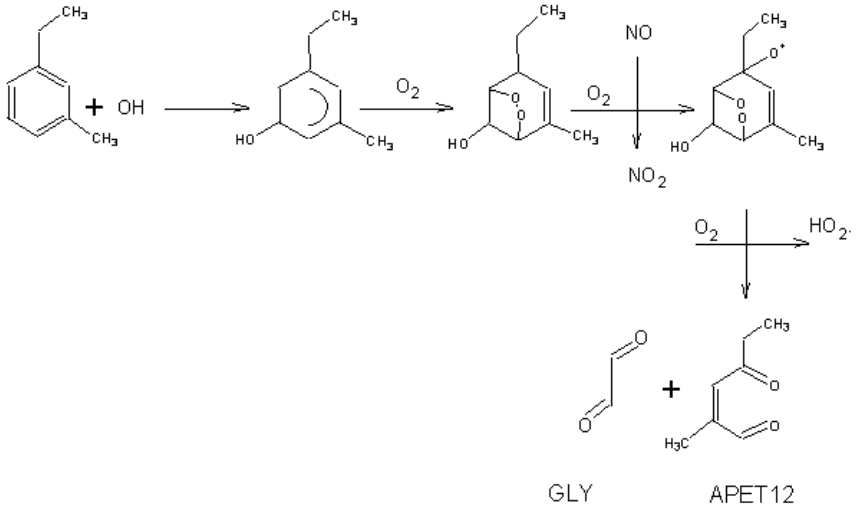
CH3
OH
HO
O2
NO
NO2
HO2·
O
H3C
GLY
APET12

(124b)

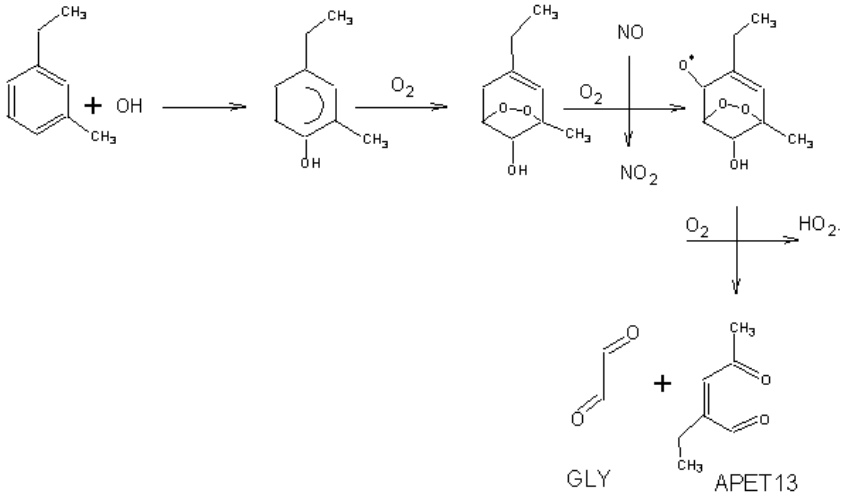
CH3
OH
O2
NO
NO2
HO2·
O
GLY
APET13

(125a)

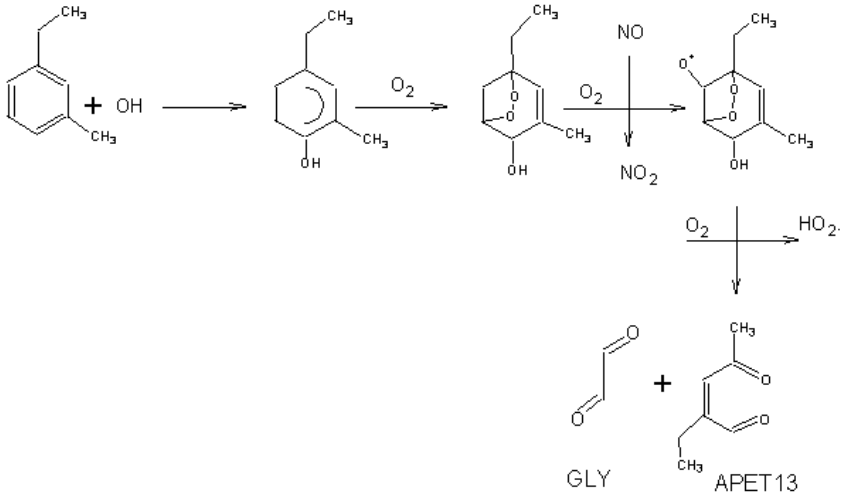

(125b)

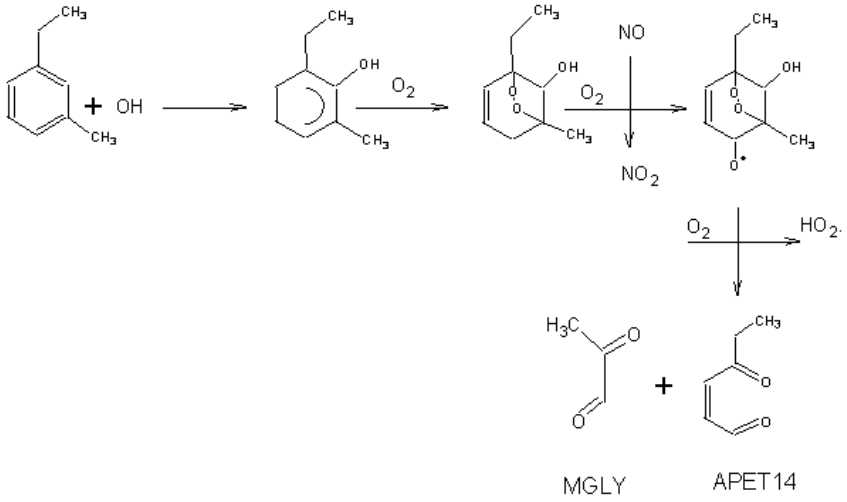

(126a)

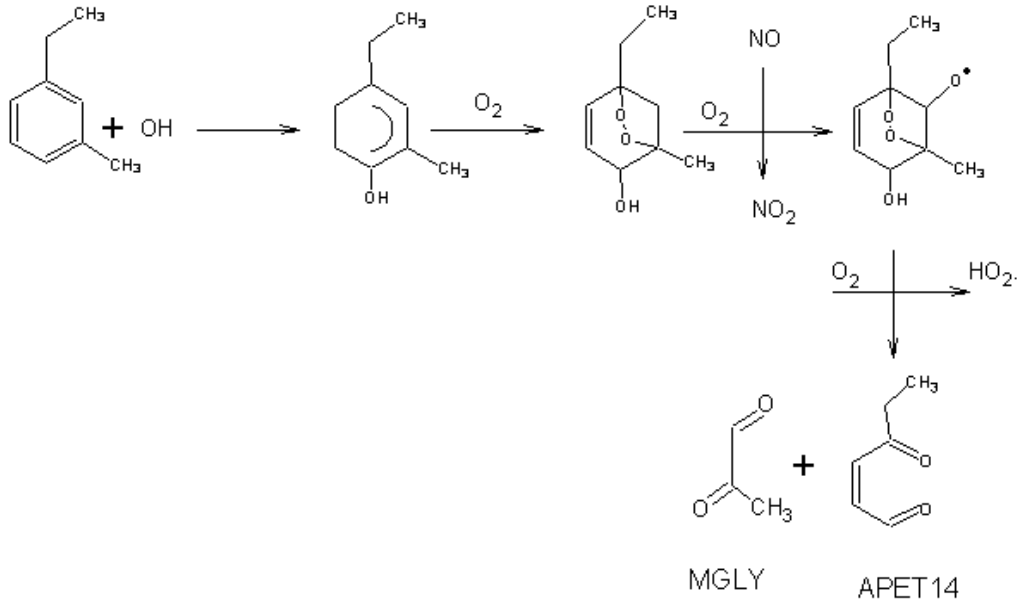

(126b)

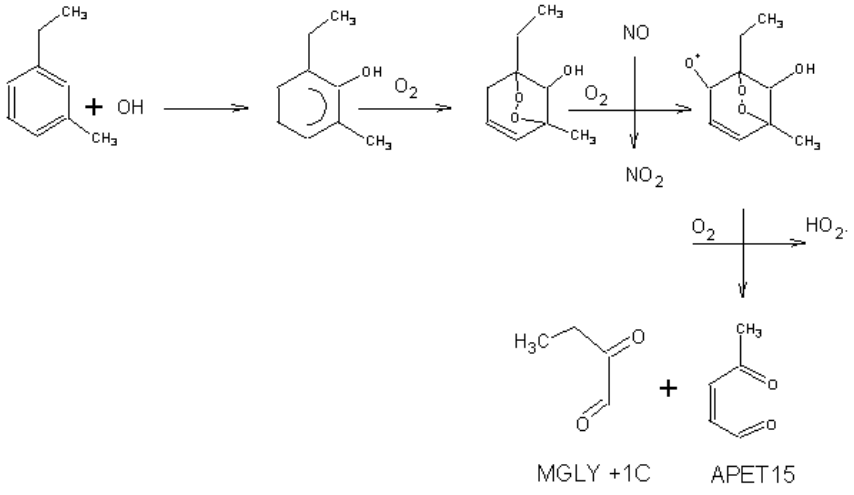

(127)

75.3% M-C2-TOL + OH. = 0.054APET10 + 0.134APET11 +0.08APET12 +0.106APET13 +0.226APET14 +0.153APET15 + 0.567MGLY +0.186GLY + 0.753RO2R + 0.207XC **Reaction 108**

Net: M-C2-TOL + OH. = 0.21CRES + 0.21HO2. + 0.037BALD +
0.0185CO2 + 0.037H2O + 0.054APET10 + 0.134APET11 +0.08APET12
+0.106APET13 +0.226APET14 +0.153APET15 + 0.567MGLY +0.186GLY
+ 0.6825XC + 0.8085RO2R – 0.0185OH.. **Reaction 109**

Aerorol precursors (APET10-APET15) further react with OH radical in the presence of O_2 and NO_2 to form two types of condensable products (ETPM5 and ETPM6). ETPM5, with organonitrate, is produced through the consecutive reactions: first the addition of OH to carbon double bonds, then the addition of O_2 and NO_2 to the radical (pathways 128a – 133a). This pathway accounts for 25% of the products(estimated from o-xylene). The remainder of the OH-ring clevage adduct (75%) further oxidizes in the presence of NO forming NO_2, HO_2 radical, and ETPM6 (product without organonitrate group), pathways 128b-133b.

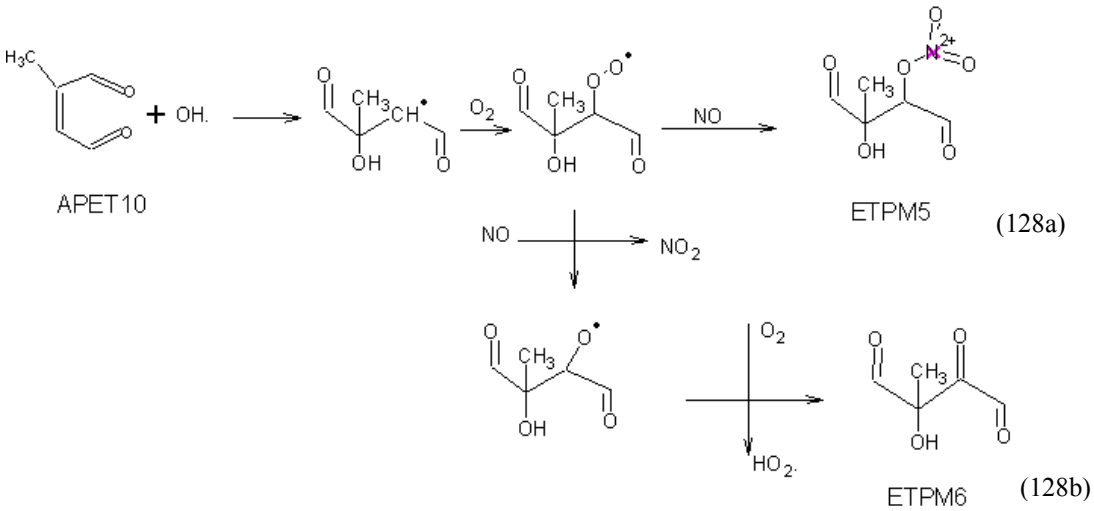

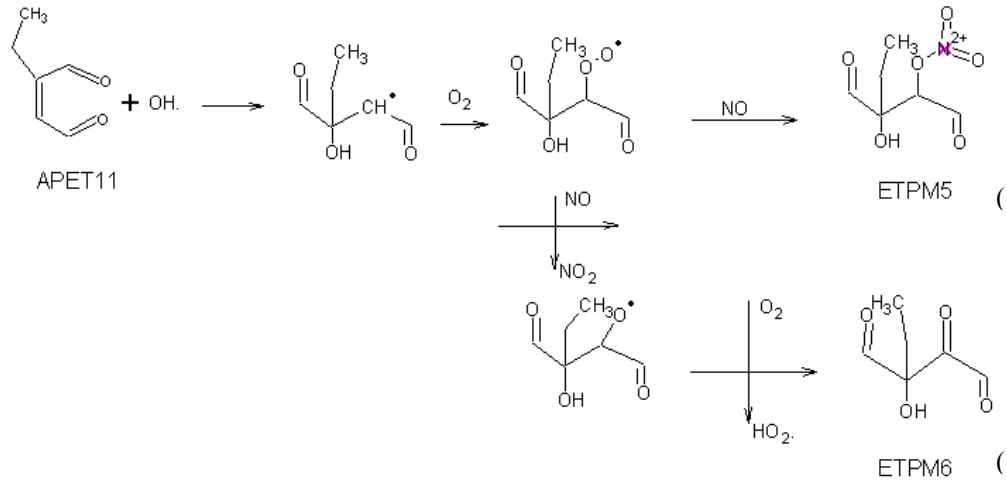

(129a)

(129b)

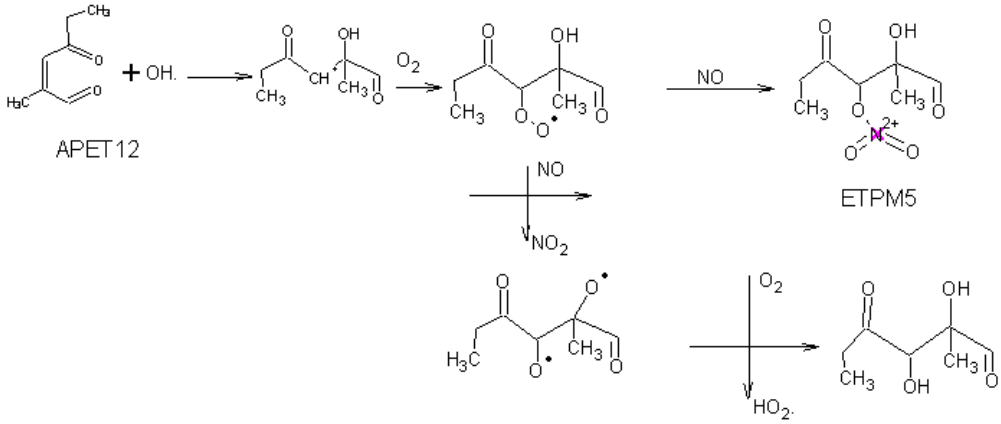

(130a)

(130b)

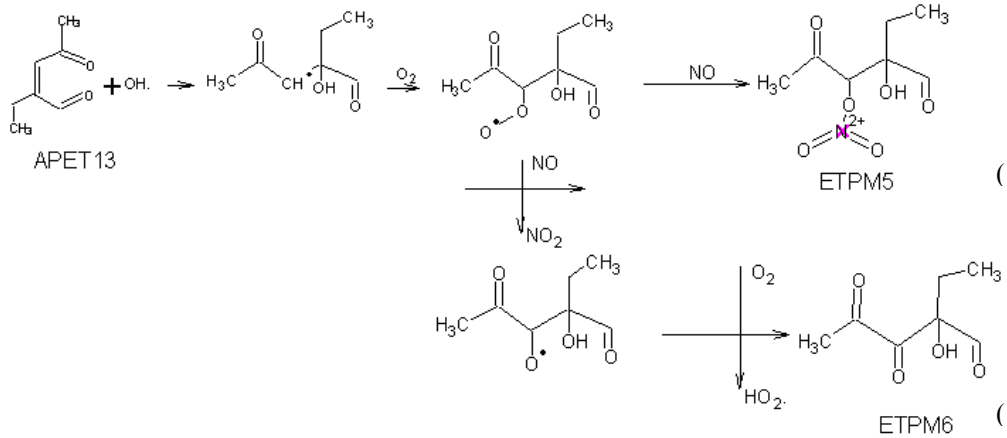

(131a)

(131b)

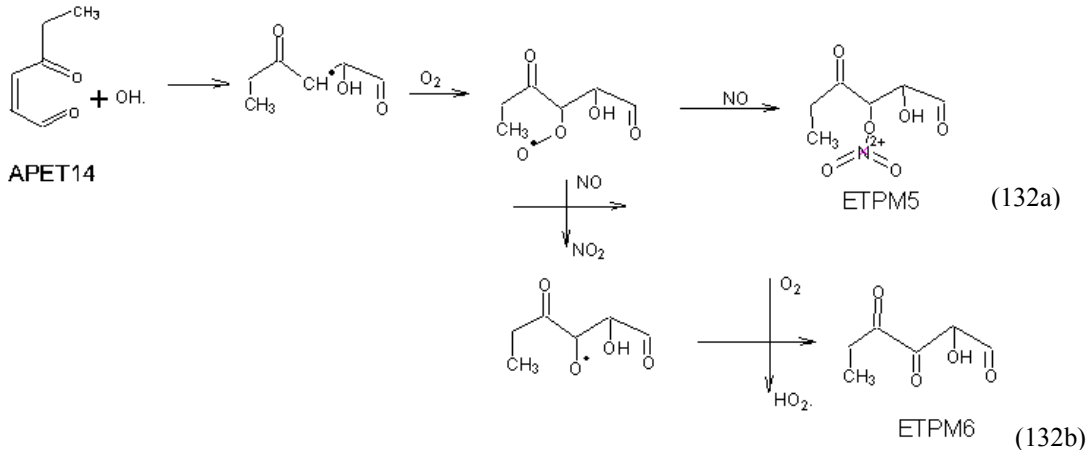

(132a)

(132b)

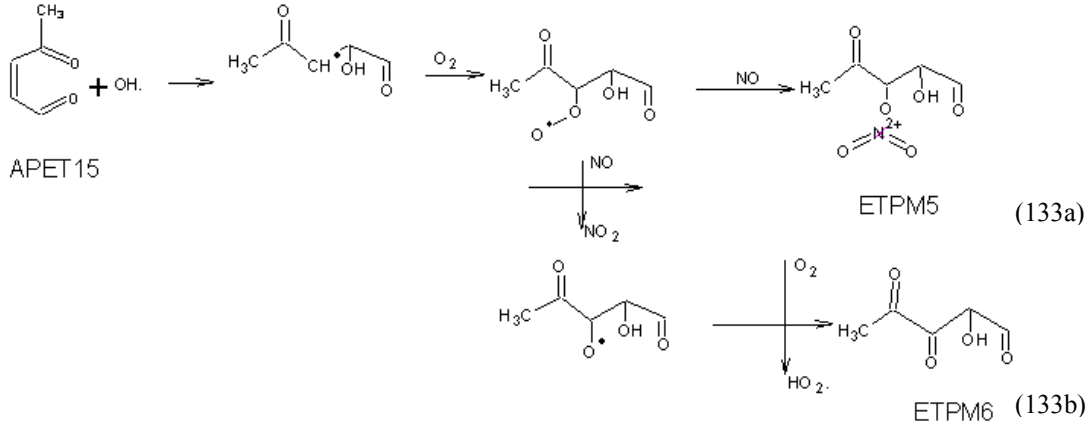

(133a)

(133b)

APET10 + OH. = 0.25ETPM5 +0.75ETPM6 +0.25RO2N +0.75RO2R **Reaction 110**

APET11 + OH. = 0.25ETPM5 +0.75ETPM6 +0.25RO2N +0.75RO2R **Reaction 111**

APET12 + OH. = 0.25ETPM5 +0.75ETPM6 +0.25RO2N +0.75RO2R **Reaction 112**

APET13 + OH. = 0.25ETPM5 +0.75ETPM6 +0.25RO2N +0.75RO2R **Reaction 113**

APET14 + OH. = 0.25ETPM5 +0.75ETPM6 +0.25RO2N +0.75RO2R **Reaction 114**

APET15 + OH. = 0.25ETPM5 +0.75ETPM6 +0.25RO2N +0.75RO2R **Reaction 115**

Reactions 109-115 describe condensed mechanisms of m-ethyltoluene with OH radical leading to SOA formation. Table 14 summarizes the stoichiometric coefficients in reactions 109-115, and cites sources of the data.

Table C.14: Kinetic parameters of m-ethyltoluene reactions with OH radical forming aerosol products and their source

Notations	Descriptions	Stoichiometric Coefficients (SC)	Source of SC
CRES	Cresol	0.21	Estimated from m-xylene (Eusebi, 1996)
BALD	Benzaldehyde	0.037	Estimated from m-xylene (Eusebi, 1996)
MGLY	Methylglyoxal	0.567	Estimated from m-xylene (Eusebi, 1996)
GLY	Glyoxal	0.186	Estimated from m-xylene (Eusebi, 1996)
HO2.	Hydroperoxy radical	0.21	Estimated from m-xylene (Eusebi, 1996)
RO2R	Operator RO2R	0.8085(reaction 109)	Estimated from m-xylene (Eusebi, 1996)
		0.75 (reaction 110-115)	Estimated from o-xylene (Eusebi, 1996)
APET10	Aerosol precursor APET10	0.054	Estimated from m-xylene (Eusebi, 1996)
APET11	Aerosol precursor APET11	0.134	Estimated from m-xylene (Eusebi, 1996)
APET12	Aerosol precursor APET12	0.08	Estimated from m-xylene (Eusebi, 1996)
APET13	Aerosol precursor APET13	0.106	Estimated from m-xylene (Eusebi, 1996)
APET14	Aerosol precursor APET14	0.226	Estimated from m-xylene (Eusebi, 1996)
APET15	Aerosol precursor APET15	0.153	Estimated from m-xylene (Eusebi, 1996)
ETPM3	Aerosol product species 1	0.25	Estimated from products from o-xylene (Eusebi, 1996)
ETPM4	Aerosol product species 2	0.75	Estimated from products from o-xylene (Eusebi, 1996)
RO2N	Operator RO2N	0.25	Estimated from products from o-xylene (Eusebi, 1996)
XC	Balance extra carbon	0.6825	SAPRC-99, estimated from m-xylene (Eusebi, 1996)
CO2	Carbon dioxide	0.0185	Estimated from m-xylene

			(Eusebi, 1996)
H2O	Water	0.037	Estimated from m-xylene (Eusebi, 1996)

Appendix D : Conditions used for SAPRC simulation for case study of aromatic precursors

Table D1: Simulation conditions for aromatic precursors, obtained from Odum's experiments

Species	Date	ROGo (μg/m3)	ΔROG (μg/m3)	ΔMo (μg/m3)	NO (ppb)	NO_2 (ppb)	Tavg (K)	Y (%)
m-ethyltoluene	06/06a	2141	1927	208	510	240	307	0.108
	06/12b	1091	971	66	265	97	304	0.068
	06/17b	415	334	13	96	47	306	0.039
p-ethyltoluene	07/08a	998	708	38	166	110	308	0.054
o-ethyltoluene	07/08b	1131	789	49	166	113	308	0.062
m-xylene	06/06b	2017	1891	106	415	185	307	0.056
	06/19a	1596	1571	46	306	136	304	0.029
	06/19b	1596	1528	48	287	127	304	0.031
p-xylene	06/28b	1163	823	16	228	142	303	0.019
	07/01b	1399	1063	32	210	171	315	0.030
o-xylene	09/09	1403	1117	35	368	188	312	0.031
	09/11	1779	1082	23	511	266	310	0.021
1,3,5-trimethylbenzene	06/12a	1029	1029	31	280	105	304	0.031
ethylbenzene	06/17a	4011	434	13	989	460	306	0.030
	06/21a	6733	3176	394	484	260	301	0.124
	06/24b	3696	1872	185	255	167	302	0.099
	07/10a	3514	1169	104	185	119	307	0.089
n-propylbenzene	07/05b	4314	1314	103	507	316	312	0.078
	07/17a	1862	657	39	260	158	307	0.059
	07/19a	5398	1790	190	409	259	312	0.106
toluene	06/28a	2560	1413	133	443	242	303	0.094
	07/01a	2415	1268	111	200	145	315	0.088
	07/05a	2656	1710	171	488	305	312	0.100
	07/10b	3065	923	68	149	104	307	0.074

Note: 1.Simulations were performed using temperature as given in the above table plus extra 10 K for smog chamber

2. Light intensities were multiplied by factor of 2 to obtain the desirable amount of ΔROG within simulating time of 10 hours

Where:

ROGo is initial concentration of hydrocarbon precursors (e.g., 1,2,4-trimethylbenzene)

ΔROG is amount of hydrocarbon that reacts

Mo is amount of secondary organic aerosol formed

Y is secondary organic aerosol yield (Mo/ΔROG)

Appendix E : Aerosol mass changes of PM3-PM8 from lumped APR2-APR4

Lumped aerosol precursors APR2-APR4 produce secondary organic aerosol species PM3-PM8. Figure E.1 demonstrates amount of PM3-PM8 produced from precursor reactions and partitions into particulate phase.

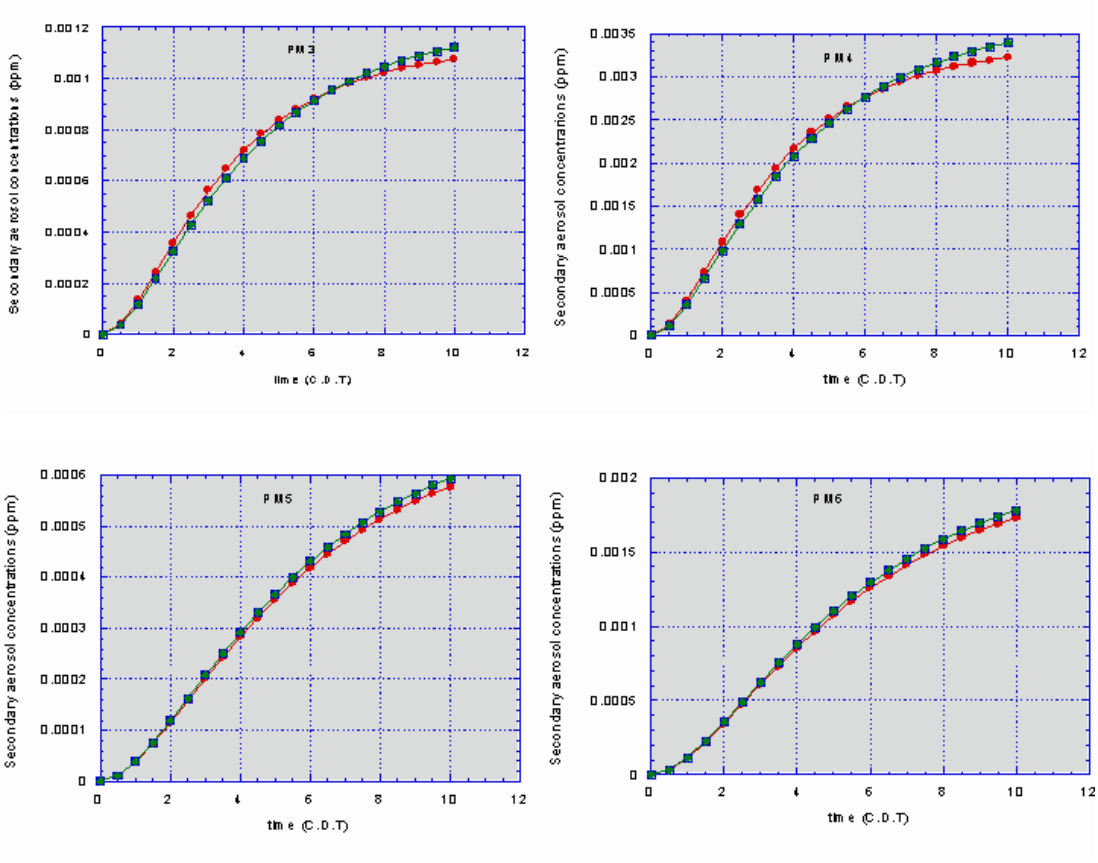

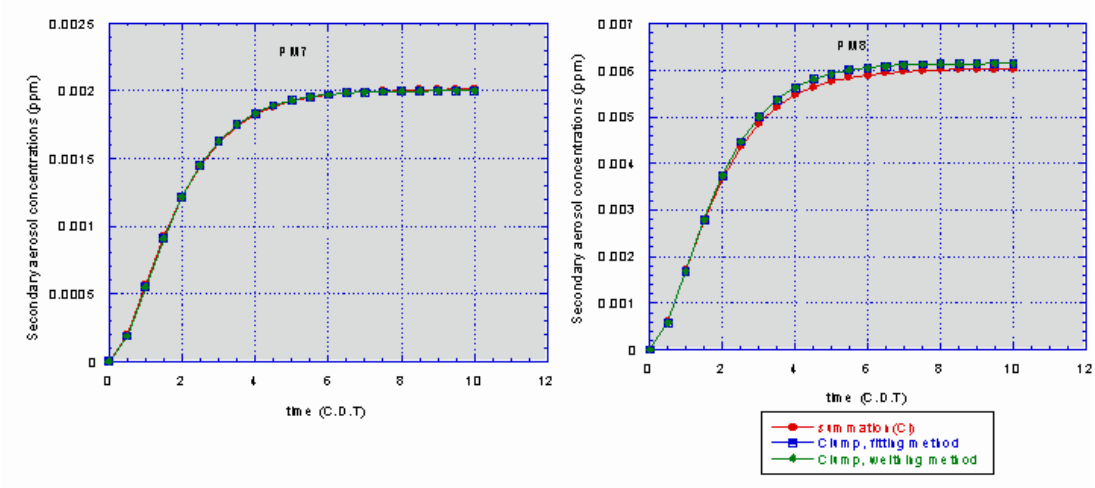

Figure E1: amount of PM3-PM8 produced and partition into particulate phase as a function of time

Bibliography

Atkinson et al., "Evaluated Kinetic, Photochemical and Heterogeneous Data for Atmosphere" 11, 45, 1997

Atkinson, "Gas Phase Tropospheric Chemistry of Organic Compounds" *J. Phys. Chem. Ref. Data*, **Monograph no. 2**, 1994

Atkinson et al., "Formation of Ring-Retaining Products from the OH Radical-Initiated Reactions of o-,m-, and p-Xylene", *Int. J. Chem. Kint*., **23**, 77, 1991

Atkinson, "Gas-Phase Tropospheric Chemistry of Organic Compounds: A Review", *Atmos. Envion*., **24A**, 1-41, 1990

Atkinson et al., "Kinetics of the Reactions of Acenaphthalene and Acecnaphthylene and Structurally-Related Aromatic Compounds with OH and NO_3 Radicals, N_2O_5 and O_3 at 296 $\pm$ 2 K", *Int. J. Chem. Kinet*., **20**, 513, 1988

Atkinson et al., "Kinetics of Gas Phase Reactions of Alkylnaphthalenes with O_3, N_2O_5, and OH radicals at 298± 2 K" *Atmos. Environ*, **21**, 2323, 1987

Atkinson et al., “Kinetic of the Reactions of Naphthalene, 2-Methylnaphthalene, and 2,3-Dimehtylnephthalene with OH radicals, and with O_3 at 295 $\pm$ 1K”, *Int. J. Chem. Kint*, **18**, 569, 1986

Atkinson et al., “Atmospheric Gas Phase Loss Processes for Chlorobenzene, Benzotrifluoride, and 4-Chlorobenzotrifluoride, and Generalization of Predictive Techniques for Atmospheric Lifetimes of Aromatic Compounds” *Arch Environ. Contamin. Toxical*. **14**, 417, 1985

Atkinson and Carter, “Kinetic and Mechanisms of the Gas-Phase Reactions of Ozone with Organic Compounds under Atmospheric Conditions”, *Chem. Rev*., **84,** 437-470, 1984

Atkinson, Carter, “A Smog Chamber and Modeling Study of the Gas Phase NO-Air Photooxidation of Toluene and the Cresols” *Int. J.Chem. Kin*., **12**, 779-836, 1980

Bandow, “Ring-Clevage Reactions of Aromatic Hydrocarbons Studied by FT-IR Spectroscopy. I. Photooxidation of Toluene and Benzene in the NOx-Air System”, *Bull. Chem.Soc. Jpn*., **58**, 2531-2540, 1985,

Bandow Hiroshi, Washida Nobuaki, “Ring-cleavage Reactions of Aromatic Hydrocarbons Studies by FT-IR Spectroscopy. II. Photooxidation of o-, m-, and p-

Xylene in the NOx-Air System", *The Chemical Society of Japan*, **58**, 2541-2548 (1985)

Bandow Hiroshi, Washida Nobuaki, "Ring-cleavage Reactions of Aromatic Hydrocarbons Studies by FT-IR Spectroscopy. III. Photooxidation of 1,2,3-,1,2,4-, and 1,3,5-Trimethybenzene in the NOx-Air System", *The chemical Society of Japan*, **58**, 2549-2555 (1985)

Barthelmie, R. J., Pyor, S. C., "Secondary Organic Aerosols: Formation Potential and Ambient Data", *The Science of the Total Environment*, **205**, 167-178, 1997

Biermann et al., "Kinetics of the Gas-Phase Reactions of the Hydroxyl Radical with Baogtgakebe, Phenanthrene, and Anthracecne", *Environ. Sci*., **19**, 244-248, 1985

Binkowski and Shankar, "The Regional Particulate Matter Model", 1: Model Description and Preliminary Results, *J. Geophy. Res*., **100**, 26, 191-209, 1995

Bowman, F. M., Standley, I. J., "Natural and Anthropogenic Organic Compounds in the Global Atmosphere", *Atmospheric Acidity*, Elsevier Applied Science, 313-381, 1992

Carter P. L., “Documentation of the SAPRC-99 Chemical Mechanism for VOC Reactivity Assessment” Report to California Air Resources Board Contract 92-329, 95-308, 2000

Carter, P. L., “Development and Application of an Up-To-Date Photochemical Mechanism for Airshed Modeling and Reactivity Assessment”, Air Resources Board Research Division, Final Report Contract No. A932-094, 1998

Carter, P. L., “Development of Ozone Reactivity Scales for Volatile Organic Compounds”, *Journal of Air and Waste Management Assoc.*, **44**, 881-899, 1994

Carter, P. L., “Computer modeling of environmental chamber studies of maximum incremental reactivities of volatile organic compounds, *Atmos. Environ*., **29**, 2, 513-2, 527, 1995

Carter, P. L., “A Detailed Mechanism of the Gas Phase Atmospheric Reactions of Organic Compounds”, *Atmospheric Environment*, **24A**, 481-518, 1990

Carter, P. L., “Documentation for the SAPRC Atmospheric Photochemical Mechanism Preparation and Emissions Processing Programs for Implementation in Airshed Models”, California Air Resources Board, Contact No. A5-122-32, 1988

Dekermenjian M., Allen, D. T., Atkinson R., Arey J., "FTIR Analysis of Aerosol Formed in the Photooxidation of Naphthalene", *Aerosol Science and Technology*, 1997

Environ, user's guide, "Comprehensive Air Quality Model with Extensive (CAMx) version 2, 2000

Eusebi A., "Composition of Aerosol Formed by the Reactions of Hydrocarbons in Urban Atmospheres: Smog Chamber and Field Measurements", University of California, 1996

Fujiwara M., Mishima K., Tamai K., Tanimoto Y., "Spectroscopic Studies on Photochemical of o-Xylene in Solution", *Journal of Chem*. **101**, 4912-4915, 1997

Gery et al., "A Photochemcial Kinetics Mechanism for Urban and Regional Scale Computer Modeling" *J. Geophys,. Res*., **94**, 12, 925-12, 956, 1989

Golikeri and Luss, "Aggregation of Many Coupled Consecutive First Order Reactions", *Chem. Engineering Sci*., **29**, 845-855, 1974

Griffin, R. J., Cocker, D. R., "Organic Aerosol Formation from the Oxidation of Biogenic Hydrocarbons", *Journal of Geo*., **104**, 3555-3567, 1999

Grosjean D., and Seinfeld, J. H., "Parametrization of the Formation Potential of Secondary Organic Aerosols", *Atmos Environ.* **23**. 1733-1747 (1989)

Grosjean D., "In Situ Organic Aerosol Formation During a Smog Episode Estimated Production and Chemical Functionality", *Atmos. Environ.* **26A**. 953-963 (1992)

Grovenstein et al., "Reaction of Atomic Oxygen with Atomic Hydrocarbons", *J. Amer. Chem. Soc*., **92**, 3810-3812, 1970

Heintzenberg J., "The Life Cycle of the Atmospheric Aerosol", Topics in Atmospheric and Interstellar Physics and Chemistry, 251-270, 1994

Holes A., Eusebi A., Allen D.T., "FTIR Analysis of Aerosol Formed in the Photooxidation of 1,3,5-Trimethybenzene", *Aerosol Science and Technology*, 1997

Isidorov V.A., "Organic Chemistry of the Earths Atmosphere", 215, 1990

Jacobson, "Developing, Couple and Applying a Gas, Aerosol, Transport and Radiation Model to Study Urban and Regional Air Pollution, PhD. Thesis,

Department of Atmospheric Sciences, University of California, Los Angeles, California, 1994

Jacobson, "Development and Application of a New Air Pollution Modeling System, part II: Aerosol Module Structure and Design", *Atmos. Environ*., **31**, 131-144, 1997

Kumar, "Development and Application of a Three-Dimensional Aerosol Model, Sonoma Technology, Inc., Santa Rosa, California, 1996

Kwok, "Rate Constants for the Gas-Phase Reaction of Selected Carbamates and Lactates", *Environ. Sci. Tchono*., **30**, 329-334, 1996

Kwok and Atkinson, "Estimation of Hydroxyl Radical Reaction Rate Constants for Gas-Phase Organic Compounds Using a Structure-Reactivity Relationship: and Update.", *Atmos. Environ*., **29**, 1685-1695, 1995

Kwok et al., "Gas Phase Atmospheric Chemistry of Selected Thiocarbamates", *Environ. Sci. Techno*., **26**, 1798-1807, 1992

McMurry and Grosjean, "Photochemical Formation of Organic Arosols: Growth Laws and Mechanisms", *Atmos. Environ*., **19**, 1, 445-1, 451, 1985

Meylan “Atmospheric Oxidation Program, Group Rate Constants and Substituent Values”, Syracuse Research Corporation, 1998

Meylan, “User’s Guide for MPBPVP version 1.2” Syracuse Research Corporation, 1996

Meng et al., “Gas/Aerosol Distribution of Formic and Acetic Acids, *Aerosol Sci. Technol*., **23**, 561-578, 1997

Moucheron and Milford, “Development and Testing of a Process Model for Secondary Organic Aerosol, Air & Waste Management Association Annual Meeting, Paper 96-FA1308.03, Nashville, Tennessee, 1997

MPBPWIN programming software, developed by Syracuse Research Corporation, 1996

Mylonas, T. D., Allen, D. T., Ehrman, S. H., and Pratsinis, S. E., “The Sources and Size Distributions of Organonitrates in Los Angeles”, *Atmos. Envir*. **25A**. *12*, 2855-2861 (1991)

The National Research Council, "Ozone-Forming Potential of Reformulated Gasoline", National Academic Press, Washington D. C., 1999

Noakov T., Penner J.E., "Large Contribution of Organic Aerosols to Cloud-Condensation Nuclei Concentration", *Nature*, **365**, 823-826, 1993

Odum et al., "The Atmospheric Aerosol-Forming Potential of Whole Gasoline Vapor", *Science*, **276**, 96-99, 1997

Odum et al, "Gas'Particle Partitioning and Secondary Organic Aerosol Yields", *Environ. Sci. Technol*., **30**, 2,580-2,585, 1996

Pandis, S. N., and Seinfeld, J. H., "Atmospheric Photochemical Oxidation of 1-Octene: OH, O_3, and $O(^3P)$ Reactions", *Environ. Sci. Technol.*, 26, 1165-1173 (1992).

Pankow, "An Absorption Model of Gas/Particle Partitioning of Organic Compounds in the Atmosphere, *Atmos. Environ*., **28**, 185-188, 1994

Perry R. A., Atkinson R., and Pitts J. N., Jr., "Kinetics and Mechanisms of the Gas Phase Reactions of OH Radicals with Aromatic Hydrocarbons Over the Temperature Range 296 – 473 K", *J. Phys. Chem*., **81**, 296-304 (1977)

Pickle T. and Allen D. T., "The Sources and Size Distributions of Aliphatic and Carbonyl Carbon in Los Angeles Aerosol", *Atmos. Envir*. **24A**, *8*, 2221-2228 (1990)

Saxena P., Hildemann L. M., McMurry P.H., Seinfeid J. H., "Organics Alter Hygroscopic Behavior of Atmospheric Particles", *Journal of Geophysic Research*, **100**, 18-755, 1995

Schwartz J., Dockery D.W., Neas L.M., "Is Daily Mortality Associated Specifically with Fine Particles", *J. Air & Waste Management Association*, **46**, 927-939, 1996

Siegneur et al.,, "Review of Air Quality models for Particulate Matter" Document Number CP015-97-1b, 1997

Seinfeld J.M., Bowman F.M., Andino J.M., "Tropospheric Chemistry Advances in Chemical Engineering", J. Wei, ed., **19**, 325-407, 1994

Stockwell et al., "The Second-Generation Regional Acid Deposition Model Chemical Mechanism for Regional Air Quality Modeling, *J. Geophys. Res*., **95D**, 16, 343-16, 367, 1990

Sun and Wexler, “Am implicit-Explicit Hybrid Solver for a System of Stiff Kinetic Equations, Air & Waste management. Assoc. 87th Annual Meeting, Cincinnati, Ohio, 1997

Tropp, R. J., Kohl, S. D., Chow, J. C., and Frazier, C. A., “Final Report for the Texas PM2.5 Sampling and Analysis Study”, prepared for Bureau of Air Quality Control, City of Houston, TX, 1998

Turpin B. J., and Huntzicker J. J., “Secondary Formation of Organic Aerosol in the Los Angeles Basin: A Descriptive Analysis of Organic and Elemental Carbon Concentrations”, *Atmos. Envir.*, **25A**, *2*, 207-215 (1991)

U.S. Environmental Protection Agency, “Summary of Model-Adjusted Estimates of Fine Particulate Matter for 2020 Base and Control Cases”, 1999

U.S. Environmental Protection Agency, http://www.epa.gov/oar/aqtrnd97/chapter2.pdf”, 1997

U.S. Environmental Protection Agency, “National Ambient Air Quality Standard for Particulate matter: Proposed Decision”, 40 CFR Part 50, 1996

U.S. Environmental Protection Agency, User's guide for the industrial source complex dispersion models, Vol.1, User Instruction, EPA-450/14-92-008, 1992

Venkatram, "The Development of a Model to Examine Source-Receptor Relationships for Visibility on the Colorado Plateau, *J. Air & Waste Manage*. *Assoc*., **47**, 286-301, 1997

Wei and Kuo, *Ind. Eng. Chem. Fundamentals*, **8**, 114-124, 1969

VITA

Wipawee Dechapanya was born in Bangkok, Thailand. She is the youngest sister of her family. She has one twin sister, Wipada Dechapanya, who is currently a graduate student in the Department of Civil and Environmental Engineering at Michigan Technological University (MTU). She attended the primary school and high school in Bangkok, Thailand. After graduating from high school, she became an undergraduate student in the Department of Chemical Engineering at Khonkean University, Khonkean, Thailand. On the senior year of her undergraduate study, she applied to be a lecturer in the faculty of Engineering at Ubon-Ratchathani University, Thailand. While she was working as a lecturer, she passed the qualified examination, held by the Royal Thai Government, and received the Royal Thai Scholarship for studying abroad.

She had become a graduate student in the Department of Chemical Engineering at MTU since September 1996, and received the degree of Master of Science in July 1998. She has pursued her doctoral study at the University of Texas at Austin in the Fall, 1998. She is going to finish her Ph.D in May 2002. Once she receives her doctoral degree, she will return to Thailand and become a faculty member at Ubon-Ratchathani University, Thailand.

Permanent Address: 15/2 Moo.1 Tonsai Bangyao, Pharpradang Samutprakarn 10130, Thailand

This dissertation was typed by Wipawee Dechapanya.